1st PI Annual Research Partnership Workshop

Petroleum Institute
Abu Dhabi, UAE
January, 6 & 7, 2010

Table of Contents Page

1st PI Annual Research Partnership Workshop
The Petroleum Institute, Abu Dhabi, United Arab Emirates
January 6 – 7, 2010

Agenda

Wednesday, January 6, 2010

8:00 – 8:30 Registration and refreshments

8:30 – 8:40 **Welcome and Opening Remarks**
Dr. M. Ohadi, *Provost and Acting President, The Petroleum Institute*
Dr. K. Berteussen, *Director of Research, The Petroleum Institute*
Dr. I. Economou, *Associate Provost for Graduate Studies, The Petroleum Institute*

8:40 – 9:00 **Opening Remarks by ADNOC Group Representative** (Name to be confirmed)
Representation of ADNOC group, Oil subcommittee, Gas subcommittee

9:00 – 9:30 **Overview of the Collaborative Activities**
Dr. N. Middleton, *Senior Vice President for Strategic Enterprises, Colorado School of Mines*
Dr. A. Bar-Cohen, *Chairman, Department of Mechanical Engineering, University of Maryland, College Park*
Dr. J. Derby, *Executive Officer, Department of Chemical Engineering and Materials Science, University of Minnesota*

9:30 – 11:00 **Energy Recovery and Conversions – I**
Chair: E. Al Hajri (PI), A. Nazeri (UMD)
9:30 – 10:00 Waste Heat Utilization in the Petroleum Industry
R. Radermacher (UMD), Y. Hwang (UMD), S. Al Hashimi (PI), P. Rodgers (PI)
10:00 – 10:30 Hybrid Solar Cooling/Heating System
R. Radermacher (UMD), Y. Hwang (UMD), I. Kubo (PI)
10:30 – 11:00 Synthesis and Catalytic Performance of Hierarchically Ordered Micro/Mesoporous Catalysts
A. Bhan (UMN), S. Al Hashimi (PI), M. Tsapatsis (UMN), R. Vladea (PI), P. Lee (UMN), D. Liu (UMN), A. Malek (PI-UMN), O. Muraza (PI), X. Zhang (UMN)

11:00 – 11:30 Coffee break

11:30 – 13:00 Energy Recovery and Conversions – II (Parallel Session I)
Chair: A. Abdala (PI), Y. Hwang (UMD)
11:30 – 12:00 Understanding of Chemical Kinetics in the Thermal Stage of Claus Process
A.K. Gupta (UMD), A. Al Shoaibi (PI), N. Al Amoodi (PI)
12:00 – 12:30 Selection and Optimization of Miscible and Immiscible Displacement to Improve Production from Fractured Carbonate Reservoirs of Abu Dhabi
R. Graves (CSM), H. Kazemi (CSM), E. Ozkan (CSM), S. Ghedan (PI)
12:30 – 13:00 Solid Oxide Fuel Cells for CO_2 Capture and Enhanced Oil Recovery
G. Jackson (UMD), B. Eichhorn (UMD), A. Almansoori (PI), K. Nandakumar, V. Eveloy

11:30 – 13:00 Process Intensification and Advanced Heat / Mass Transfer (Parallel Session II)
Chair: M. Haroun (PI), M. Tsapatsis (UMN)
11:30 – 12:00 Multidisciplinary Design and Characterization of Polymer Composite Seawater Heat Exchanger Module
P. Rodgers (PI), A. Bar-Cohen (UMD), S.K. Gupta (UMD), D. Bigio (UMD)
12:00 – 12:30 Study on Microchannel-Based Absorber/Stripper and Electrostatic Precipitators for CO_2 Separation from Flue Gas
S. Dessiatoun (UMD), A. Shooshtari (UMD), M. Ohadi (PI), A. Goharzadeh, M. Al Shehhi (PI)
12:30 – 13:00 Microreactors for Oil and Gas Processes Using Microchannel Technologies
S. Dessiatoun (UMD), A. Shooshtari (UMD), M. Ohadi (PI), A. Goharzadeh (PI), E. Al-Hajri (PI)

13:00 – 14:00 Lunch break

14:00 – 15:30 Mathematical Modeling and Optimization in Oil and Gas Industry (Parallel Session I)
Chair: P. Rogers (PI), M. Hillmyer (UMN)
14:00 – 14:30 Assessment of the Integrity of Pipelines subject to corrosion-Fatigue, Pitting Corrosion, Creep and Stress Corrosion
M. Modarres (UMD), A. Seibi (PI)
14:30 – 15:00 Robust Optimization of Engineering-Business Decisions for Petrochemical Systems
S. Azarm (UMD), P.K. Kannan (UMD), A. Almansoori (PI), S. Al Hashimi (PI)
15:00 – 15:30 Simulation, Optimization and Control of Solid Oxide Fuel Cell System
P. Daoutidis (UMN), J. Derby (UMN), A. Almansoori (PI)

14:00 – 15:30 Management and Control of Energy Systems (Parallel Session II)
Chair: G. Bassioni (PI), S. Ainane (UMD/PI)
14:00 – 14:30 Dynamics and Control of Drill Strings
B. Balachandran (UMD), H. Karki (PI), Y. Abdelmagid (PI)
14:30 – 15:00 Studies on Mobile Sensor Platforms
B. Balachandran (UMD), N. Chopra (UMD), H. Karki (PI), S. Fok (PI)
15:00 – 15:30 Use of Horizontal Wells to Improve Pattern Waterfloods In Fractured Carbonate Reservoirs
R. Graves (CSM), H. Kazemi (CSM), E. Ozkan (CSM), S. Ghedan (PI)

15:30 – 16:00 *Coffee break*

16:00 – 17:00 Meetings with PI Senior and Graduate Students

19:00 *Dinner*

Thursday, January 7, 2010

8:30 – 10:00 **Catalytic Processes (Parallel Session I)**
Chair: H. Karki (PI), J. Derby (UMN)

8:30 – 9:00 Development of I. Zeolite Catalysts for Alkane Metathesis and II. Adsorbents for H_2S Removal
A. Bhan (UMN), M. Cococcioni (UMN), S. Al Hashimi (PI), M. Tsapatsis (UMN), R. Vladea (PI), P. Kumar (UMN), A. McCormick (UMN), N. Katabathini (PI), C.-Y. Sung (UMN)

9:00 – 9:30 Coatings for Catalytic and Separation Processes
L. Francis (UMN), S. Al Hashimi (PI), M. Tsapatsis (UMN), R. Vladea (PI), O. Muraza (PI), W.J. Suszynski (UMN), K. Varoon (UMN), H. Zhang (UMN)

9:30 – 10:00 Atomic-Resolution Quantitative Electron Microscopy
K.A. Mkhoyan (UMN), J. Derby (UMN), W. Gerberich (UMN), C. Macosko (UMN), K. Liao (UMN), A. Mittal (UMN), A. Wagner (UMN)

8:30 – 10:00 **Materials Development and Characterization for Upstream Processes (Parallel Session II)**
Chair: I. Economou (PI), M. Modarres (UMD)

8:30 – 8:45 Development of High Interstitial Stainless Steel for Use in Down Hole Drilling Applications
D. Olson (CSM), B. Mishra (CSM)

8:45 – 9:00 SCC Susceptibility for High Strength Low Alloy Steels in CO_2 Containing Corrosive Oil and Gas Well Environments
D. Olson (CSM), B. Mishra (CSM), A.B. Gavanluei (CSM)

9:00 – 9:15 Investigation of Microbiologically Influenced Corrosion (MIC) in Ethanol Fuel Environments
D. Olson (CSM), B. Mishra (CSM), J. Spear (CSM), L. Jain (CSM),S. Bhola (CSM), C. Williamson (CSM)

9:15 – 9:30 Understanding the Role of Alternating Current on Corrosion of Pipeline Steels Under Sacrificial Anode Cathotic Protection
D. Olson (CSM), B. Mishra (CSM), T. Reyes (CSM), S. Bhola (CSM)

10:00 – 10:30 *Coffee break*

10:30 – 12:00 Advanced Materials for Industrial Applications (Parallel Session I)
Chair: S. Vukušić (PI), A. Bar-Cohen (UMD)
10:30 – 11:00 Synthesis and Processing of Functionalized Polyolefins
C. Macosko (UMN), M. Hillmyer (UMN), A. Abdala (PI), S. Vukusic (PI)
11:00 – 11:30 Graphene Reinforced Polyolefin Nanocomposites
C. Macosko (UMN), F. Bates (UMN), A. Abdala (PI), H. Kim (UMN)
11:30 – 12:00 Polymeric Membranes for Advanced Process Engineering
F. Bates (UMN), E. Cussler (UMN), M. Hillmyer (UMN), T. Lodge (UMN), A. Abdala (PI), I. Economou (PI), S. Vukusic (PI)

10:30 – 12:00 Reservoir Characterization and Simulation (Parallel Session II)
Chair: S. Ghedan (PI), M. Haroun (PI)
10:30 – 11:00 Characterization and Simulation of Abu Dhabi Fractured Carbonate Reservoirs
H. Kazemi (CSM), E. Ozkan (CSM), R. Graves (CSM), J. Miskimins (CSM), S. Ghedan (PI)
11:00 – 11:30 Fluid Sensitivity of Seismic Properties in Carbonate Reservoirs
R. Graves (CSM), M. Batzle (CSM), M. Prasad (CSM), S. Vega (PI)
11:30 – 12:00 Integrated Carbonate Reservoir Characterization
R. Graves (CSM), Sarg (CSM), S. Lokier (PI), T. Steuber (PI), S. Vega (PI)

12:00 – 13:00 Lunch break

13:00 – 15:00 Future Directions in R & D and our Research Collaborations
Chair: M. Ohadi (PI), K. Berteussen (PI)
Round table discussions between representatives from partner schools, sponsors and the PI faculty (by invitation)

15:00 Closing remarks – End of the workshop

Overview of the Collaborative Activities

Overview of Collaboration Activities

Colorado School of Mines

Dr. Nigel T. Middleton
Senior VP, Strategic Enterprises

1st Annual PI Partner Schools Research Workshop
The Petroleum Institute, Abu Dhabi, U.A.E.
January 6-7, 2010

PI Partners

PI Sponsors

CSM – PI Chronology

- 1999 – PI concept (ADNOC); solicitation; RFP
- 2000 – Proposal; Phase 0, Phase 1 responses
- 2001 – Construction; staffing; students; long-term agreement
- 2001 – PI opening
- 2001 to 2007 – Curriculum; administration; initial hiring; undergraduate program focus
- 2008 to 2009 – Realignment of agreement: research focus; amended agreement

Current CSM – PI Partnership Areas

- Membership on PI Governing Board
- Research – upstream engineering and science
  - Reservoir characterization
  - Materials corrosion
  - Center for Wave Phenomena
- Education
  - Undergraduate engineering design
  - Center for Teaching Excellence
- UAE students at CSM

CSM's Energy Agenda

- Reservoir simulation
  - Faculty expertise
  - High performance computing
- Unconventional reserves
  - Natural gas
  - Oil shale
  - Hydrates
- Geology
  - Includes upcoming carbonates workshop at PI
- Environment
  - Carbon sequestration
  - Water
- Alternative energy technologies
  - Solar, biofuels; wind; fuel cells; nuclear; materials …

Energy Education and Research Collaboration EERCC

Securing the Path, Achieving the Promise

Provost Farvardin, **Prof. Bar-Cohen**

1st Annual PI Partner Schools Research Workshop
The Petroleum Institute, Abu Dhabi, U.A.E.
January 6-7, 2010

PI Partners

PI Sponsors

Presentation Outline

- History
- Goals
- Education
- Research
- Achievements

EERC History

- ***March 2006***: His Excellency Mr. Yousef Omeir Bin Yousef, visited the University of Maryland to meet with administrators and faculty
- ***March 2006***: Petroleum Institute and UMD sign MOU on Education and Research in Energy Sciences and Engineering
- ***October 2006***: PI/UMD sign contract initiating energy research and education effort
- ***Jan 2008:*** EERC 1st Workshop & Commencement Participation
- ***Nov 2008:*** EERC 2nd Workshop & President Mote as Commencement speaker
- ***April 2009***: Phase II EERC contract is signed

Long Term EERC Goals

- Joint UMD-PI EERC **Center of Excellence** in energy systems research and education.
- PI-UMD Co-Leadership of joint EERC.
- Administrative and technical infrastructure for world-class research and education.
- Broadly based academic excellence in energy systems engineering.
- Regional, later international, leadership in conventional and alternative energy research.

Multi-phase Path to Joint EERC

- ***Phase I***: Initiation Projects
- ***Phase II***: Co-leadership & Outcome parity
- ***Phase III+***: Sustainable Joint Center of Excellence

EERC – Educational Goals

Excellence in Energy System Education

- Educate next-generation, technology and academic Emirate leaders
- Transfer Educational "Best Practices" To Enrich Undergraduate Programs
- Support development of graduate programs

ADNOC Scholars and New PI Faculty

- **Dr. Ebrahim Al –Hajri**
- **PhD Topic:** Prediction of Heat transfer and Pressure Drop of Condensing Refrigerant Flow in a High Aspect Ratio Microchannels
- **Joined ME Department at PI : Fall 2009**

- **Dr. Mohamed Al Shehhi**
- **Ph D Topic:** Electrostatic Gas-Liquid Separation-Application to Advanced On-Line/On-Demand Separation Techniques
- **Joined ME Department at PI: Spring 2010**

ADNOC Scholars and New PI Faculty

- **Dr. Mohamed Chooka**
- **PhD Topic:** Structuring a Probabilistic Model for Reliability Evaluation of Piping Subject to Corrosion Fatigue Degradation
- **Current Position:** Director of Licensing, Emirates Nuclear Energy Corporation.

EERC --Summer Internship 2008

EERC – Summer Internship 2009

Transfer of "Best Practices"

- ***Dr. Ohadi as Director of ME, Provost and Acting President at PI***

Education and Transfer of "Best Practices"

- ***ABET***

Dr. Sami Ainane

- **Director of ME Student Affairs at UMD**
- **Assigned to PI for one year to help with the ABET accreditation process.**

- ***Sabbatical***

Prof. Mikahel Anisimov

- **Professor of Chemical Engineering UMD**
- **Built a state-of-the-art dynamic light scattering lab**
- **Taught 3 courses, Served on two committees**

EERC – Research Goals

Leadership in energy Research

- Establish significant research programs on critical energy engineering issues
- Successfully apply research outcomes to the Energy Industry
- Stimulate an intellectual environment for collaborative research

EERC – Research Thrust 1

Energy Recovery and Conversion

- **Sulfur Recovery from Gas Stream using Flameless and Flame Combustion Reactor** **A. Al Shoaibi, A.K. Gupta,**

Solid Oxide Fuel Cells for CO2 Capture and Enhanced Oil Recovery **A. Almansoori, V. Eveloy, G. Jackson, B. Eichhorn,**

- **Separate Sensible and Latent Cooling with Solar Energy** **I. Kubo, R. Radermacher, Y. Hwang,**
- **Waste Heat Utilization in the Petroleum Industry** **P. Rodgers, S. Al Hashimi, R. Radermacher, Y. Hwang,**

EERC – Research Thrust 2

Energy-Efficient Transport Processes

- **Multidisciplinary Design and Characterization of Polymer Composite Seawater Heat Exchanger Module** **P. Rodgers, A. Bar-Cohen, S.K. Gupta, D. Bigio**
- **Study on Microchannel-Based Absorber/Stripper and Electrostatic Precipitators for CO2 Separation from Flue Gas** **M. Ohadi, A. Goharzadeh, S. Dessiatoun, A. Shooshtari**
- **Microreactors for Oil and Gas Processes Using Microchannel Technologies** **M. Ohadi, A. Goharzadeh, E. Al-Hajri, S. Dessiatoun, A. Shooshtari**

EERC – Research Thrust 3

Energy System Management

- **Integration of Engineering and Business Decisions for Robust Optimization of Petrochemical Systems** **A. Almansoori, S. Al Hashimi, S. Azarm, P.K. Kannan,**

- **Dynamics and Control of Drill Strings** **H. Karki, Y. Abdelmagid, B. Balachandran,**

- **Studies on Mobile Sensor Platforms** **H. Karki, B. Balachandran, N. Chopra,**
- **Development of a Probabilistic Model for Degradation Effects of Corrosion-Fatigue Cracking in Oil and Gas Pipelines** **A. Seibi, M. Modarres,**

EERC – A Bridge between Research & Industry

- **Presentations of the UMD/PI research to ADNOC and its Operating Companies**
- **PI and UMD collaborators visited the following OpCo's in the past year:**
  - **ADGAS,** (January 2009, May 2009 & August 2009, Ahmad Abbas)
  - **GASCO,** (May 2990, Abdulla Al Minhali)
  - **ADCO,** (Nov 2009, Ali Noor Moosavi & August 2009,Dr. Shaheen)
  - **ZADCO, (**August 2009)
  - **Takreer** (August 2009, Fareed Mohamed Al Jaberi, Dr. Haitem Hasan-Beck, Mansoor Mohamed Al-Mehairbi)
  - **Borouge** (January 2009, August 2009)
  - **NDC** (Nov 2009, Saleh Khalifa)

EERC - Achievements

Education & Knowledge Transfer

- **3 ADNOC Scholars Complete PhDs in 2009**
  - **2 ADNOC Scholar return as PI faculty**
  - **1 ADNOC Scholar returns as an Executive in the Emirates Nuclear Energy Corporation**
- Visits of UMD President Mote and Dean Pines
- UMD Faculty assignment/sabbatical – Ohadi, Ainane , Anisimov
- More than 40 visits between UMD and PI
- 15 students completing MS/Ph D at UMD through EERC support
- Internships/Research at PI by EERC graduate students
- Summer internship of 16 PI students at UMD
- Distance Delivery of several Clark School Engineering Courses

EERC - Achievements

Achieving Project's Milestones

- Significant progress in 3 Research Thrusts (10 research projects in Phase I, and 11 in Phase II)
- Organizing **two EERC Workshops**, Jan 2008, Nov 2008

Publications (2007-2009)

- More than **60 publications** in Archival journals and Conference Proceedings

International Visibility

- **Organized two Energy 2030 International Conferences**
- UMD President Mote – 2008 PI Commencement Speaker
- UMD Provost Farvardin – PI Institutional Advisory Board Member
- UMD Faculty attend 2 PI Commencements

Meeting ADNOC's Needs

- Visiting and Presenting PI/UMD collaborative research to OpCos
- Research initiated/modified to meet ADNOC needs
- Professor Amir Riaz hired in Reservoir Modeling at UMD

EERC – Work in Progress

- Continue 11Research Projects
- Develop Joint UMD-PI Ph D Program
  - Work with Dr. Economou to recruit students for MS and PhD at PI who are jointly advised by UMD and PI faculty
- Help Develop the Graduate Program of Health, Safety and Environmental (HSE) at PI
  - Work with Dr. Clarence Rodrigues at PI on developing a graduate program with help from Fire Protection, and Civil Engineering at UMD

Abu Dhabi–Minnesota Institute for Research Excellence, ADMIRE

UMN Team: Department of Chemical Engineering and Materials Science
PI Team: Chemical Engineering Program

1st Annual PI Partner Schools Research Workshop
The Petroleum Institute, Abu Dhabi, U.A.E.
January 6-7, 2010

PI Partners

PI Sponsors

ADMIRE is an inter-institutional collaboration whose mission is...

- To promote research excellence through inter-institutional research groups (IRGs), especially in fields relevant to petroleum and energy
- To promote educational opportunities between the PI and UMN
- To promote the development of best practices as the PI evolves to a world-class academic institution
- To promote wider exchanges between Abu Dhabi and Minnesota

The primary participants of ADMIRE are...

PI Chemical Engineering Program

PI ADMIRE Point-Of-Contact:
Professor Saleh Al Hashimi

UMN ADMIRE Director:
Professor Jeffrey J. Derby

UMN Department of Chemical Engineering and Materials Science

The research groups within ADMIRE are...

Projects	***UMN Faculty***	***PI Faculty***
<u>IRG 1: Hydrocarbon processing</u> IRG 1.1 Catalytic Removal of Sulfur from Process Gas Streams without Hydrogen IRG 1.2 Catalytic Alkane Metathesis IRG 1.3 Coatings for Catalytic and Photo-catalytic Processes	Aditya Bhan Matteo Cococcioni Lorraine F. Francis Michael Tsapatsis	Saleh Al Hashimi Radu V. Vladea
<u>IRG 2: Simulation and optimization</u> IRG2.1 Simulation, Optimization and Control of Solid Oxide Fuel Cell System	Prodromos Daoutidis Jeffrey J. Derby	Ali S. Almansoori
<u>IRG 3: Polymer processing</u> IRG 3.1 Polymeric Membranes for Advanced Process Engineering IRG 3.2 Graphene/Polymer Composites IRG 3.3 Synthesis and Processing of Functionalized Polyolefins	Frank S. Bates Edward L. Cussler Marc A. Hillmyer Timothy P. Lodge Chris Macosko	Ahmed Abdala Ioannis G. Economou Sulafudin Vukusic
<u>IRG 4: Materials Science and Engineering (SEED)</u> IRG 4.1 Processing Improved Microstructures for the Energy Industry	Jeffrey J. Derby William W. Gerberich K. Andre Mkhoyan	To be determined

ADMIRE is structured to receive input from a variety of sources...

Prof. Frank Bates
CEMS Head

Prof. Steven Crouch
IT Dean

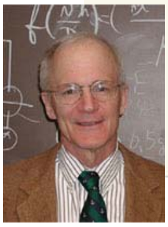

Prof. Ed Cussler
AAB Chair

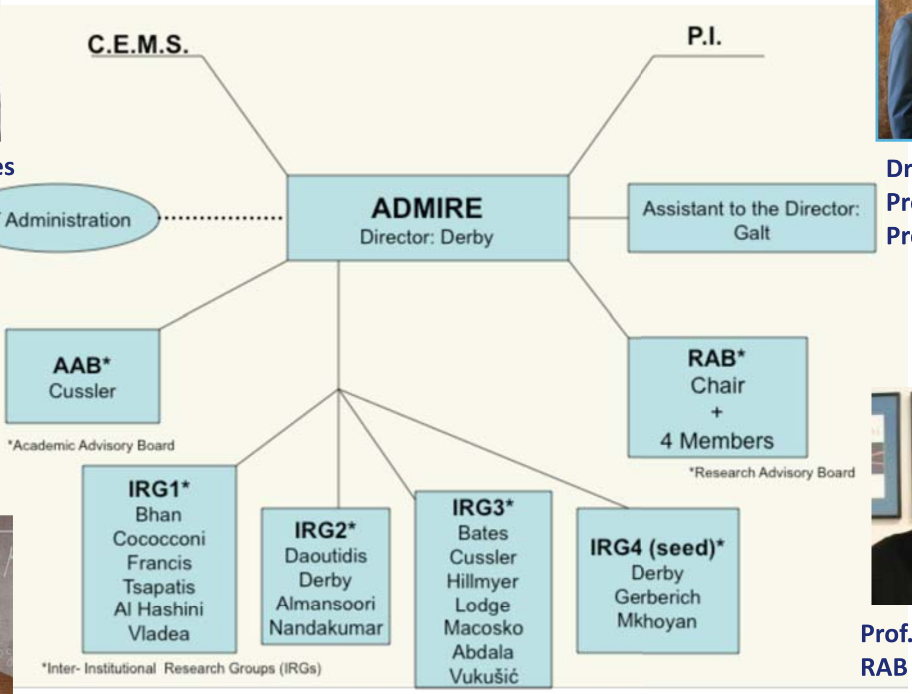

C.E.M.S.

P.I.

IT Administration

ADMIRE
Director: Derby

Assistant to the Director: Galt

AAB*
Cussler

*Academic Advisory Board

RAB*
Chair
+
4 Members

*Research Advisory Board

IRG1*
Bhan
Cococconi
Francis
Tsapatis
Al Hashini
Vladea

IRG2*
Daoutidis
Derby
Almansoori
Nandakumar

IRG3*
Bates
Cussler
Hillmyer
Lodge
Macosko
Abdala
Vukušić

IRG4 (seed)*
Derby
Gerberich
Mkhoyan

*Inter- Institutional Research Groups (IRGs)

Dr. Michael Ohadi
Provost and Acting
President

Prof. Michael Tsapatsis
RAB Chair

Additional ADMIRE activities include...

- Collaboration in departmental activities, including advisory board membership, curriculum development, accreditation.
- Exchange programs, including undergraduate summer internships and semester-abroad programs, graduate research, faculty sabbaticals.
- Workshops, short courses, cultural exchanges.
- More, as opportunities present themselves...

Examples of other ADMIRE activities...

Web page for visibility and repository of information...

UNIVERSITY OF MINNESOTA

CEMS | IT | U of MN

ADMIRE

Abu Dhabi – Minnesota Institute for Research Excellence

admire home

- home
  - more news
- about ADMIRE
- people
- research
- publications
- media
- restricted

links:

University of Minnesota
Petroleum Institute Abu Dhabi
CEMS at the U of MN

Welcome to the ADMIRE homepage!

The **A**bu **D**habi-**M**innesota **I**nstitute for **R**esearch **E**xcellence (ADMIRE) is a partnership between the Chemical Engineering Program and the soon-to-be established Materials Science and Engineering Program of the Petroleum Institute (PI) of Abu Dhabi, and the Department of Chemical Engineering and Materials Science (CEMS) of the University of Minnesota (UMN). ADMIRE has been founded to promote joint research projects between the two institutions and to foster the continued development of academic programs of the Petroleum Institute. For graduates from both programs, this collaboration will provide an intellectually rich environment conducive to the kind of education and development demanded of future world leaders in engineering, science, and technology. read more...

news and events

- **21 Apr 09** ADMIRE site online.
- **29 Feb 2009** Professor Chris Macosko visited the Chemical engineering Program at the PI and delivered a seminar (See photo.).

Examples of other ADMIRE activities...

Emerati achievement program...

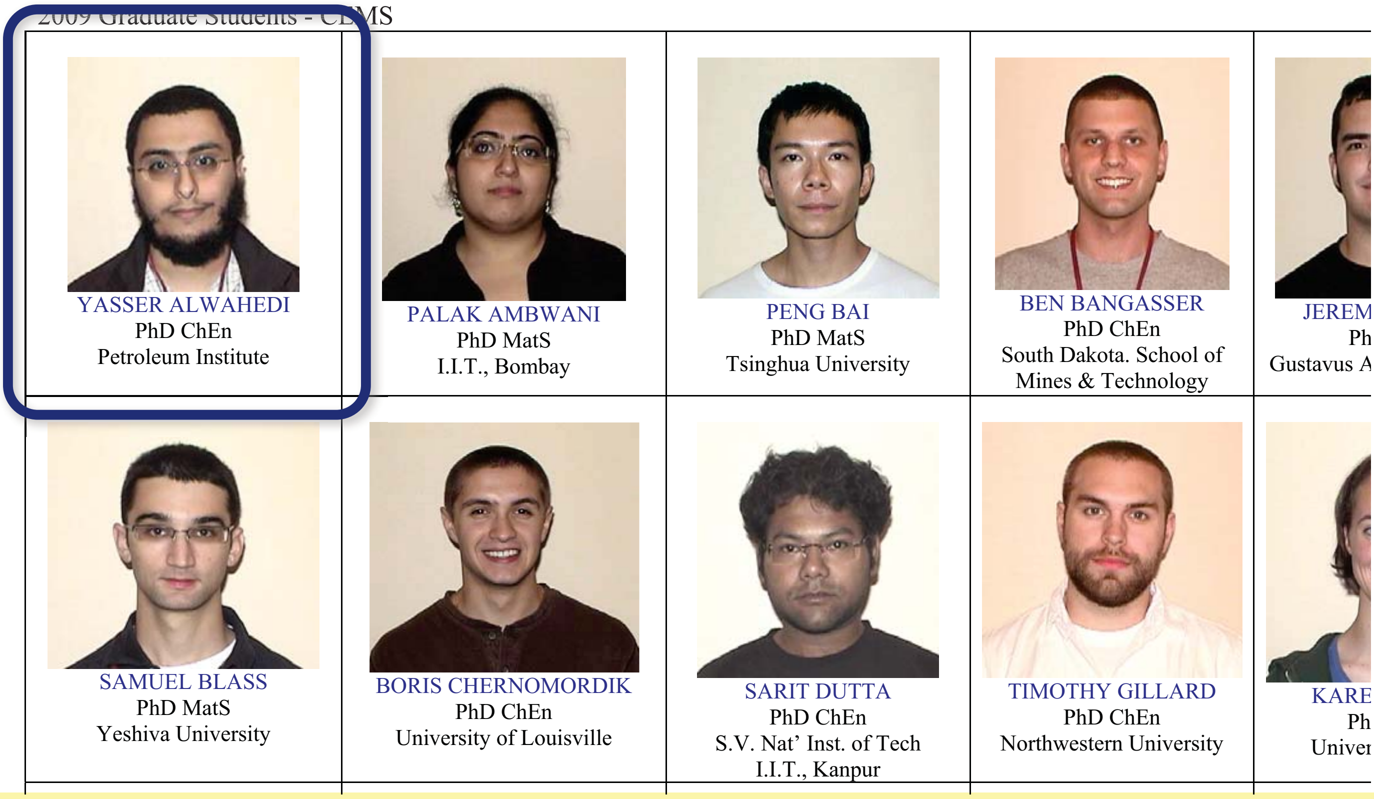

2009 Graduate Students - CEMS

YASSER ALWAHEDI PhD ChEn Petroleum Institute	PALAK AMBWANI PhD MatS I.I.T., Bombay	PENG BAI PhD MatS Tsinghua University	BEN BANGASSER PhD ChEn South Dakota. School of Mines & Technology	JEREM Ph Gustavus A
SAMUEL BLASS PhD MatS Yeshiva University	BORIS CHERNOMORDIK PhD ChEn University of Louisville	SARIT DUTTA PhD ChEn S.V. Nat' Inst. of Tech I.I.T., Kanpur	TIMOTHY GILLARD PhD ChEn Northwestern University	KARE Ph Univer

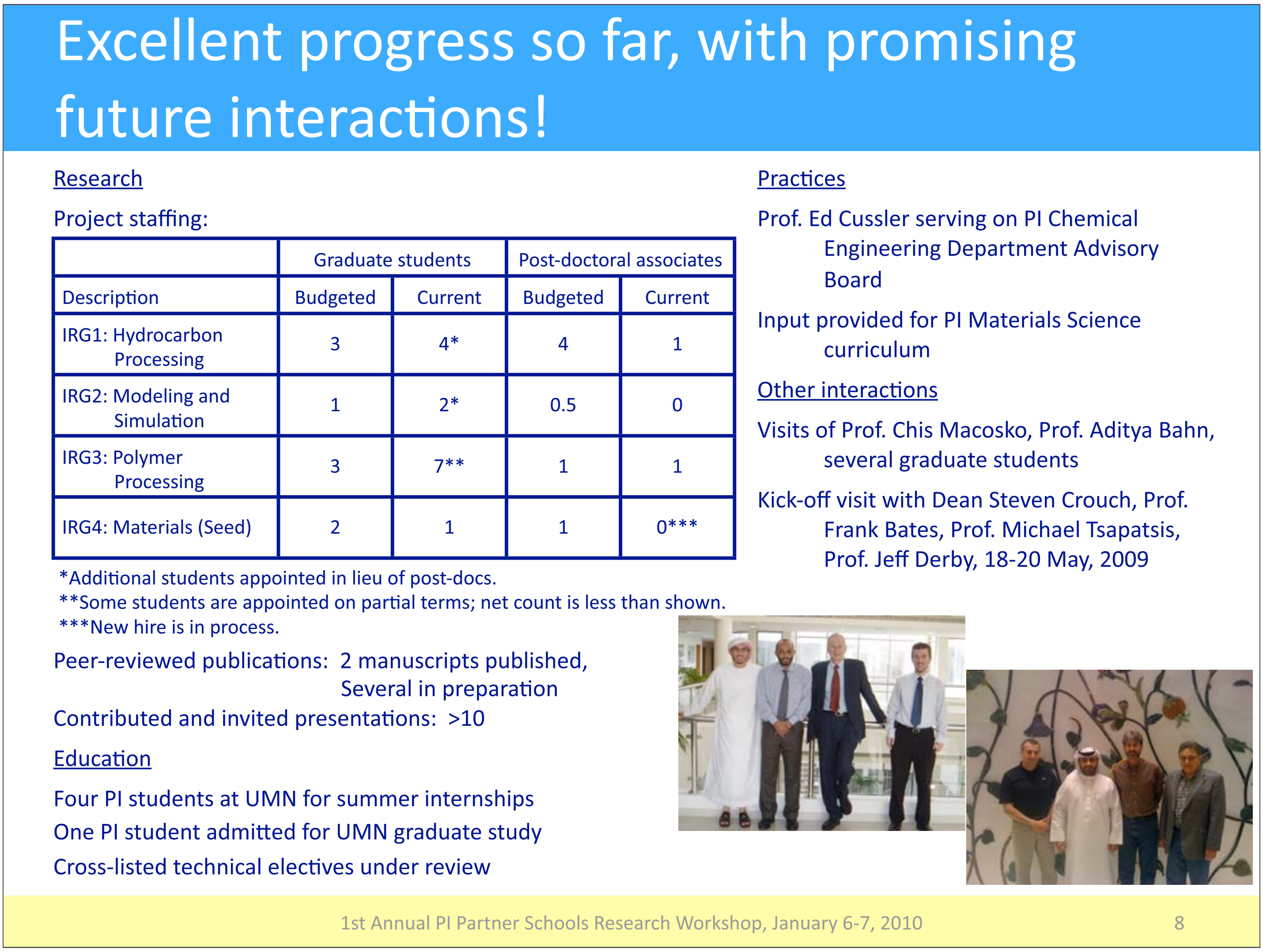

Excellent progress so far, with promising future interactions!

Research

Project staffing:

	Graduate students		Post-doctoral associates	
Description	Budgeted	Current	Budgeted	Current
IRG1: Hydrocarbon Processing	3	4*	4	1
IRG2: Modeling and Simulation	1	2*	0.5	0
IRG3: Polymer Processing	3	7**	1	1
IRG4: Materials (Seed)	2	1	1	0***

*Additional students appointed in lieu of post-docs.
**Some students are appointed on partial terms; net count is less than shown.
***New hire is in process.

Peer-reviewed publications: 2 manuscripts published,
Several in preparation

Contributed and invited presentations: >10

Education

Four PI students at UMN for summer internships

One PI student admitted for UMN graduate study

Cross-listed technical electives under review

Practices

Prof. Ed Cussler serving on PI Chemical Engineering Department Advisory Board

Input provided for PI Materials Science curriculum

Other interactions

Visits of Prof. Chis Macosko, Prof. Aditya Bahn, several graduate students

Kick-off visit with Dean Steven Crouch, Prof. Frank Bates, Prof. Michael Tsapatsis, Prof. Jeff Derby, 18-20 May, 2009

Energy Recovery and Conversions I

Waste Heat Utilization in the Oil & Gas Industry

UMD Team: Amir Mortazavi, Abdullah Alabdulkarem,
Yunho Hwang, Reinhard Radermacher
PI Team: Peter Rodgers, Saleh Al-Hashimi,
Sahil Popli, Alyas ALShehhi

1st Annual PI Partner Schools Research Workshop
The Petroleum Institute, Abu Dhabi, U.A.E.
January 6-7, 2010

PI Partners

PI Sponsors

Outline

- Introduction
- Project overview and approach
- Investigation of potential sources of waste heat and utilization at GASCO ASAB LNG site
- APCI LNG plant modeling and enhancement:
  - Integrating gas turbine drivers to LNG plant ASPEN model
  - Utilizing LNG plant gas turbine driver waste heat by absorption chillers
- Current status and future work

Introduction

Motivation

- Oil and Gas industry is a big energy consumer.
- Opportunities for energy usage improvement are abundant:
  - Energy efficiency audit
  - Improved plant design through system integration

Objectives

- Maximize energy efficiency in oil and gas plants
- Reduce particulate and greenhouse gas emissions
- De-bottleneck oil and gas production
- Increase production capacity

Project Overview and Approach

Project Overview and Approach

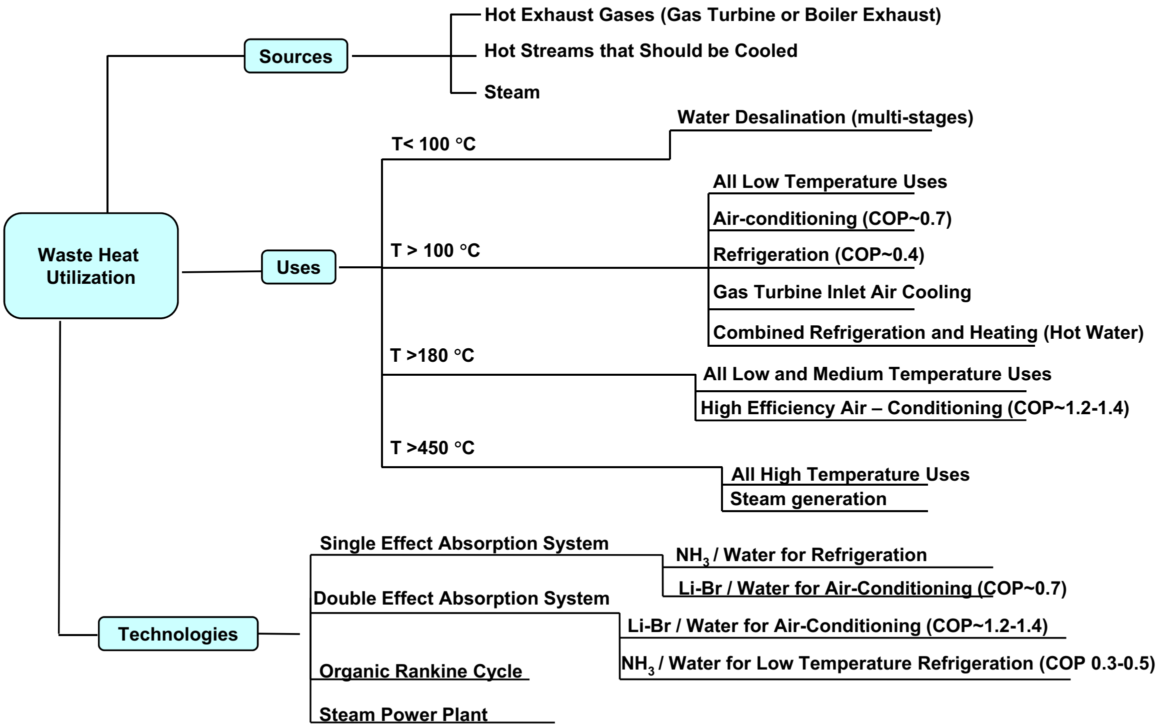

Waste Heat Utilization

Sources
- Hot Exhaust Gases (Gas Turbine or Boiler Exhaust)
- Hot Streams that Should be Cooled
- Steam

Uses
- T< 100 °C
  - Water Desalination (multi-stages)
- T > 100 °C
  - All Low Temperature Uses
  - Air-conditioning (COP~0.7)
  - Refrigeration (COP~0.4)
  - Gas Turbine Inlet Air Cooling
  - Combined Refrigeration and Heating (Hot Water)
- T >180 °C
  - All Low and Medium Temperature Uses
  - High Efficiency Air – Conditioning (COP~1.2-1.4)
- T >450 °C
  - All High Temperature Uses
  - Steam generation

Technologies
- Single Effect Absorption System
  - NH_3 / Water for Refrigeration
  - Li-Br / Water for Air-Conditioning (COP~0.7)
- Double Effect Absorption System
  - Li-Br / Water for Air-Conditioning (COP~1.2-1.4)
  - NH_3 / Water for Low Temperature Refrigeration (COP 0.3-0.5)
- Organic Rankine Cycle
- Steam Power Plant

Project Overview and Approach (Cont'd)

- Energy efficiency audit:
  - Assess waste heat sources
  - Assess waste heat conversion processes
  - Assess utility requirements
  - Match waste heat sources/processes and utility requirements
- Improved plant design through system integration approach:
  - Create a series of models for relevant systems
  - Create a "library of options" for cycle improvement
  - Produce a final recommendation considering all options evaluated to date

Investigation of Potential Sources of Waste Heat and Utilization at GASCO ASAB LNG Site

---

Integrated Model Proposal for Waste Recovery Opportunities at GASCO ASAB0 and ASAB1 LNG Plants

- Energy efficiency audit previously conducted at ADGAS, Das Island facility
- Ongoing analysis at GASCO ASAB LNG Plant.

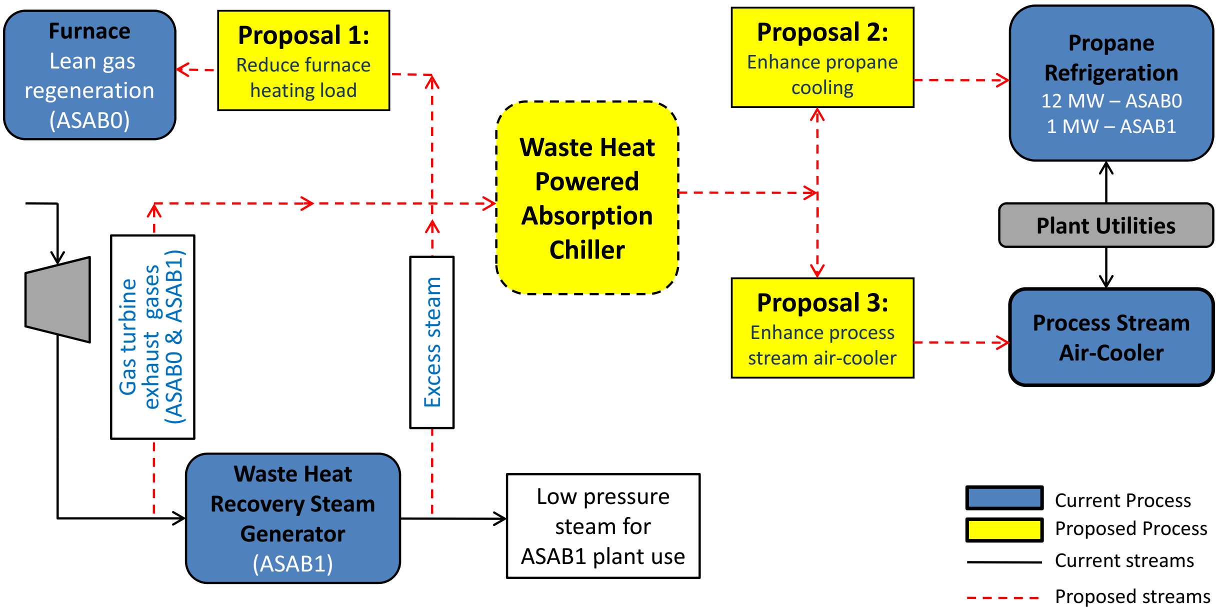

Furnace
Lean gas regeneration
(ASAB0)

Proposal 1:
Reduce furnace heating load

Proposal 2:
Enhance propane cooling

Propane Refrigeration
12 MW – ASAB0
1 MW – ASAB1

Waste Heat Powered Absorption Chiller

Plant Utilities

Gas turbine exhaust gases (ASAB0 & ASAB1)

Excess steam

Proposal 3:
Enhance process stream air-cooler

Process Stream Air-Cooler

Waste Heat Recovery Steam Generator
(ASAB1)

Low pressure steam for ASAB1 plant use

🟦 Current Process
🟨 Proposed Process
— Current streams
- - - Proposed streams

Integrated Model Proposal for Waste Recovery Opportunities at GASCO ASAB0 and ASAB1 LNG Plants (Cont'd)

Reduce Furnace Heating Load:

- **Proposal 1:** Utilization of waste heat from both turbine exhaust gases (ASAB0 & ASAB1) and excess low pressure process steam (ASAB1) for lean gas regeneration at ASAB0.

Absorption Chillers for Enhanced Cooling:

- **Proposal 2:** Enhance propane cooling using waste heat from both turbine exhaust gases (ASAB0 & ASAB1) and excess low pressure process steam (ASAB1).
- **Proposal 3:** Enhance process stream air-cooling using waste heat from both turbine exhaust gases (ASAB0 & ASAB1) and excess low pressure process steam (ASAB1).

APCI LNG Plant Modeling and Enhancement

Project Overview and Approach

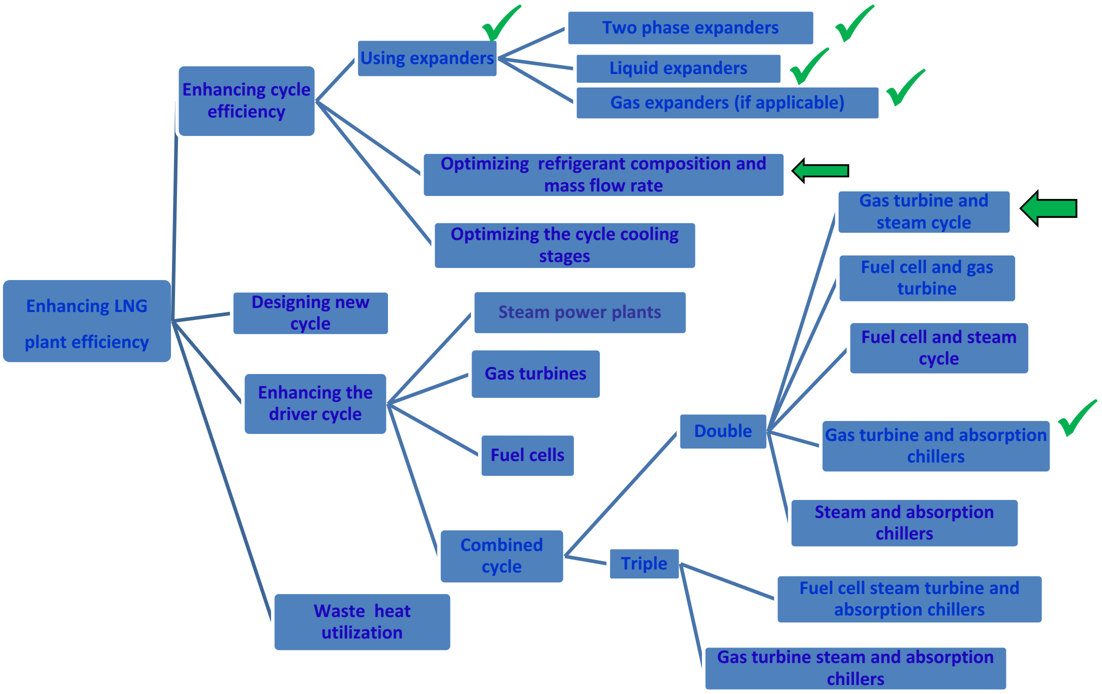

- Enhancing LNG plant efficiency
  - Enhancing cycle efficiency
    - Using expanders ✓
      - Two phase expanders ✓
      - Liquid expanders ✓
      - Gas expanders (if applicable) ✓
    - Optimizing refrigerant composition and mass flow rate ←
    - Optimizing the cycle cooling stages
  - Designing new cycle
  - Enhancing the driver cycle
    - Steam power plants
    - Gas turbines
    - Fuel cells
    - Combined cycle
      - Double
        - Gas turbine and steam cycle ←
        - Fuel cell and gas turbine
        - Fuel cell and steam cycle
        - Gas turbine and absorption chillers ✓
        - Steam and absorption chillers
      - Triple
        - Fuel cell steam turbine and absorption chillers
        - Gas turbine steam and absorption chillers
  - Waste heat utilization

APCI Liquefaction Cycle

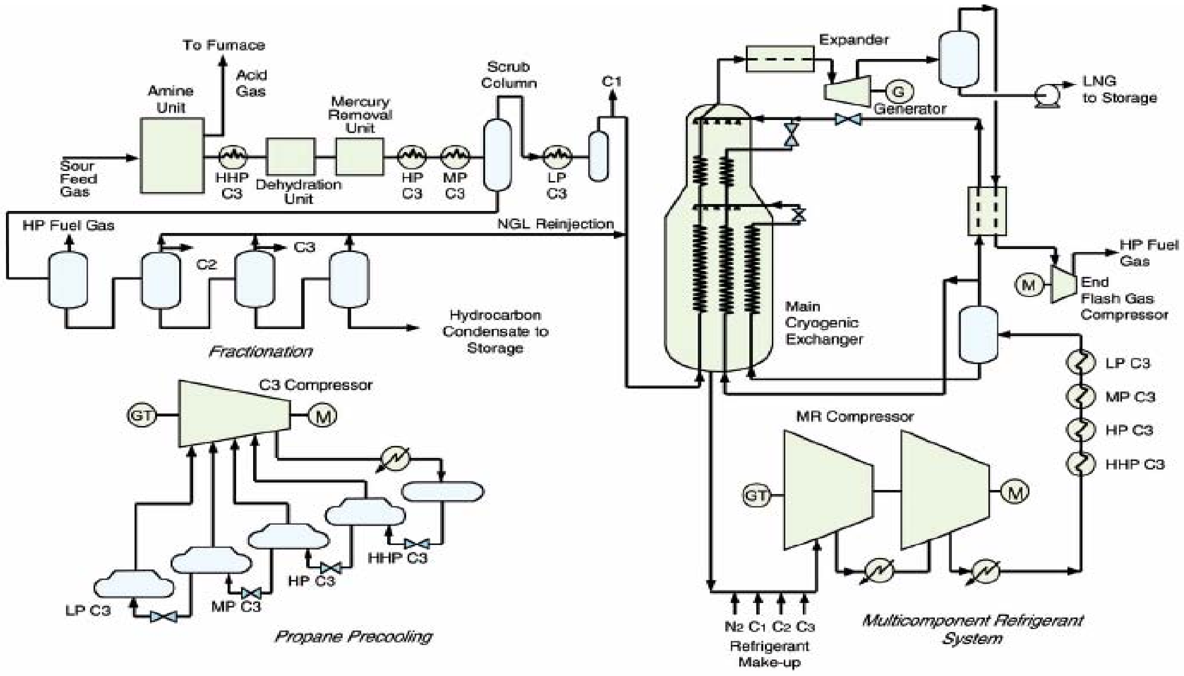

Utilizing LNG Plant Gas Turbine Driver Waste Heat by Absorption Chillers

---

Enhancement Options

- **Option 1: replacing 22°C propane cycle evaporators with absorption chillers**
- **Option 2: Replacing 22°C propane cycle evaporators and cooling the inlet of gas turbine with absorption chillers**
- **Option 3: Replacing 22°C and 9°C propane cycle evaporators with absorption chillers**
- **Option 4: Replacing 22°C and 9°C propane cycle evaporators cooling the inlet of gas turbine with absorption chillers**

Enhancement Options (Cont’d)

- **Option 5: Replacing 22^{o}C and 9^{o}C evaporators and cooling the condenser of propane cycle at 27^{o}C with absorption chillers**
- **Option 6: Replacing 22^{o}C and 9^{o}C evaporators and cooling the condenser of propane at 27^{o}C cycle and turbine inlet with absorption chillers**
- **Option 7: Replacing 22^{o}C and 9^{o}C evaporators and cooling the condenser of propane cycle at 14^{o}C with absorption chillers**
- **Option 8: Replacing 22^{o}C and 9^{o}C evaporators and cooling the condenser of propane at 14^{o}C cycle and inter cooling the compressor of mixed refrigerant cycle with absorption chillers**

Modeling Results

	Compressor Power [MW]	Power Reduction [MW]	Required Amount of Waste Heat [MW]	Fraction of Available Amount of Waste Heat [%] Scaled	Fraction of Available Amount of Waste Heat [%] Unscaled	Fuel Consumption [MW] Scaled (% saving)	Fuel Consumption [MW] Unscaled (% saving)
APCI base cycle	110.185	-----	-----	-----	-----	329.448	329.448
Option 1	107.510	2.675 (2.43%)	8.613	5.779	5.788	321.444 (2.43)	322.754 (2.03)
Option 2	107.510	2.675 (2.43%)	12.215	8.730	8.836	314.002 (4.69)	318.175 (3.42)
Option 3	100.334	9.851 (8.94%)	33.538	24.112	24.255	299.999 (8.94)	304.859 (7.46)
Option 4	100.334	9.851 (8.94%)	39.840	32.134	33.550	287.624 (12.70)	296.482 (10.01)
Option 5	94.043	16.142 (14.65%)	95.048	72.910	73.610	281.186 (14.65)	289.482 (12.21)
Option 6	94.043	16.142 (14.65%)	100.954	86.87	91.799	269.598 (18.17)	281.006 (14.70)
Option 7	88.420	21.765 (19.75%)	99.833	81.446	82.501	264.378 (19.75)	275.340 (16.42)
Option 8	86.696	23.489 (21.32%)	110.058	91.575	92.852	259.217 (21.32)	271.086 (17.715)

ASPEN Model of Best Chiller Configuration

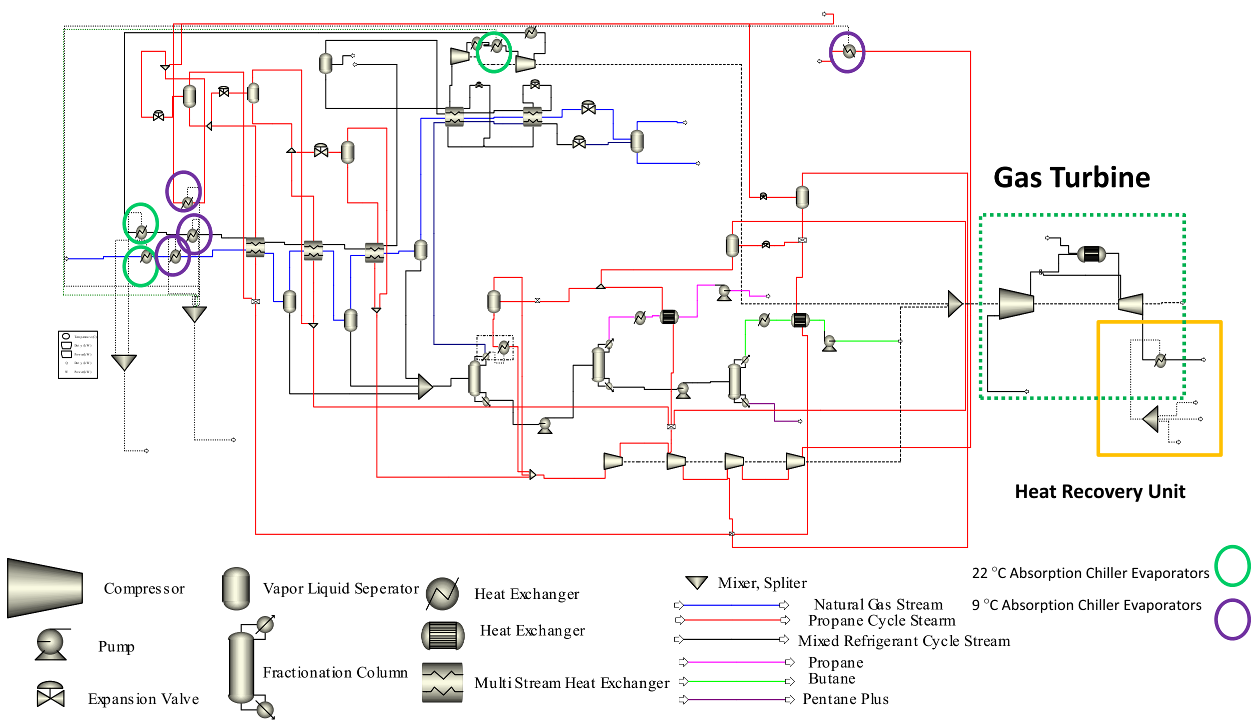

APCI and Gas Turbine Optimization (On-going)

HYSYS-Matlab Optimization

- Matlab is a powerful optimization tool
  - It can do multi-objective, multi-variable optimization
  - It has the Genetic Algorithm (Global optimal is guaranteed)
- Matlab has been coupled with HYSYS
  - HYSYS Object is created in Matlab
  - Reading and writing variables is automated

HYSYS Model

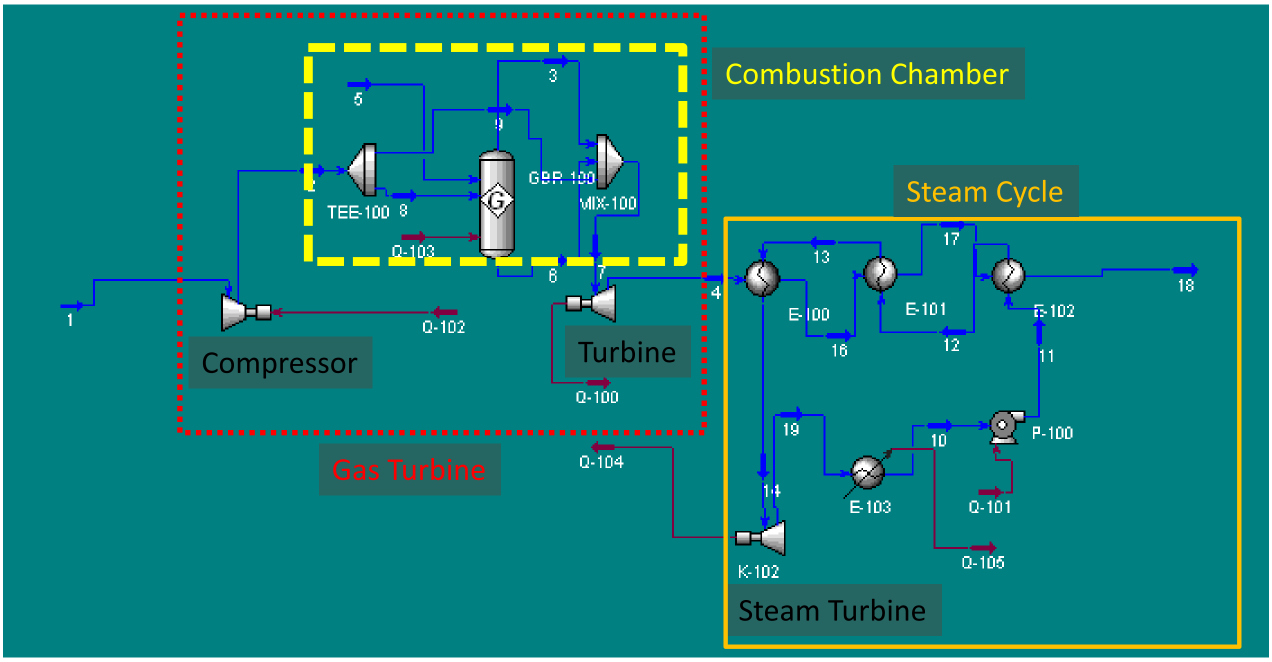

Results

Steam Mass Flow Rate [kg/s]	Steam Boiler Pressure [kPa]	Super Heater Temperature [C]	Total Power [kW]
54.44	8969	552.0	181805
54.44	8969	552.0	181805
55.65	6190	506.5	178726
54.44	8969	552.0	181805
54.44	8969	552.0	181805
54.44	8969	552.0	181805
54.44	8969	552.0	181805
54.44	8969	552.0	181805
54.12	7383	551.9	180779
54.44	8969	552.0	181805
54.44	8969	552.0	181805
54.44	8969	552.0	181805
54.44	8969	552.0	181805
54.44	8969	552.0	181805
54.44	8969	552.0	181805
54.44	8969	552.0	181805
54.44	8969	552.0	181805
54.44	8969	552.0	181805
54.44	8969	552.0	181805
54.44	8969	552.0	181805

Current Status and Future Work

Current Status

The following options have been modeled in ASPEN:

- APCI base plants
- Enhanced APCI LNG plants
- Ammonia/water absorption chillers
- Water/LiBr absorption chillers
- LNG plant gas turbine driver
- LNG plant gas turbine driver waste heat utilization with water/LiBr absorption chillers

Current Status (Cont'd)

The following options were modeled in HYSYS:

- The base APCI LNG plant cycle
- Gas turbine driver cycle
- APCI enhanced by combined gas turbine absorption chiller cycle
- Coupling Matlab with HYSYS to optimize the cycle

Future Work

- Modeling gas turbine combined cycles for waste heat utilization
- Modeling gas turbine, steam cycle and absorption chiller-triple combined cycle for waste heat utilization
- Using Matlab optimization package for the selection of the best driver configuration
- Optimizing the mixed refrigerant composition by Matlab

Publications

- **Published Paper:**
  - **Application of Waste Heat Powered Absorption Refrigeration System to the LNG Recovery Process, P. Kalinowski, Y. Hwang, R. Radermacher, S.A. Hashimi, P. Rogers, Int. J. Refrigeration, 2009**
- **Submitted Papers:**
  - **Mortazavi, A., Hwang, Y., Radermacher, R., S. Al-Hashimi, and P. Rodgers , *Performance Enhancement of APCI LNG Plant*, APEN, 2009.**
  - **Mortazavi, A., Hwang, Y., Radermacher, R., S. Al-Hashimi, and P. Rodgers, *Enhancement of LNG Propane Cycle through Waste Heat Powered Absorption Cooling*, APEN, 2009.**
  - **Somers, C., Mortazavi, A., Hwang, Y., Radermacher, R., Al-Hashimi, S., and Rodgers, P., *Modeling Absorption Chillers in ASPEN*, APEN, 2009.**
  - **Mortazavi, A., Alabdulkarem, A., Somers, C., Hwang, Y., Radermacher, R., Al-Hashimi, S., and Rodgers, P., Enhancement of APCI Cycle Efficiency with Absorption Chillers, Energy Journal, 2009.**

Hybrid Solar Cooling/Heating System

UMD Team: Ali Al-Alili, Yunho Hwang,
Reinhard Radermacher
PI Team: Isoroku Kubo

1st Annual PI Partner Schools Research Workshop
The Petroleum Institute, Abu Dhabi, U.A.E.
January 6-7, 2010

PI Partners

PI Sponsors

Presentation Outline

- Background
- Objectives
- Experimental Setup
- Results and Discussions
- Project Status
- Conclusions and Summary

Background

- In hot and humid regions, removal of moisture from the air represents a major portion of the air conditioning load.
- Flat solar collectors require large fields
- The current available solar cooling cycles have low overall efficiency, less than unity.

Project Objectives

- Design and fabricate a solar cooling/heating system with the highest overall COP value.
- Fabricate and test the solar cooling system at UMD.
- Perform a field test in the UAE.

Weather Data

Madison, WI
Lat: 43.13 °N
Long: 89.33 °W
Ele = 262 m

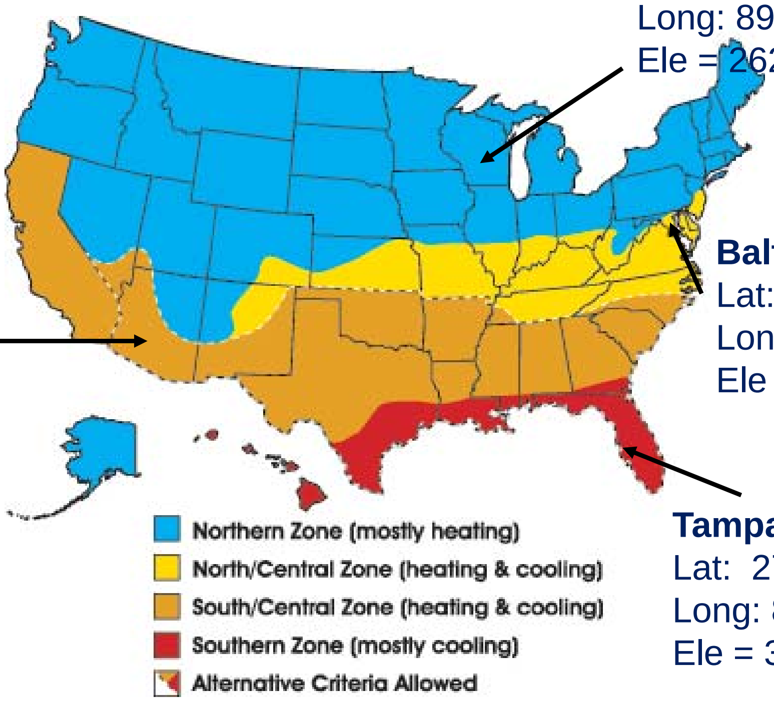

Phoenix, AZ
Lat: 33.43 °N
Long: 112.02 °W
Ele = 339 m

Baltimore, MD
Lat: 39.18 °N
Long: 76.67 °W
Ele = 47 m

Tampa, FL
Lat: 27.97 °N
Long: 82.53 °W
Ele = 3 m

Sub-Systems Schematics

Solar Sub-System

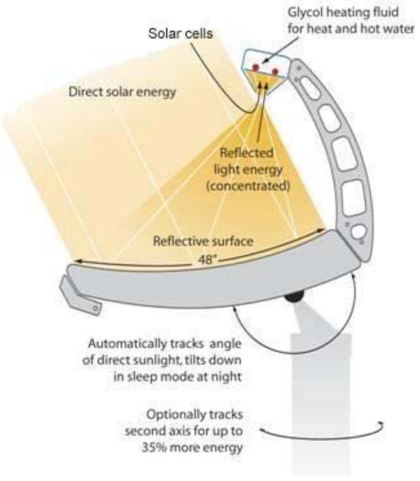

[1]

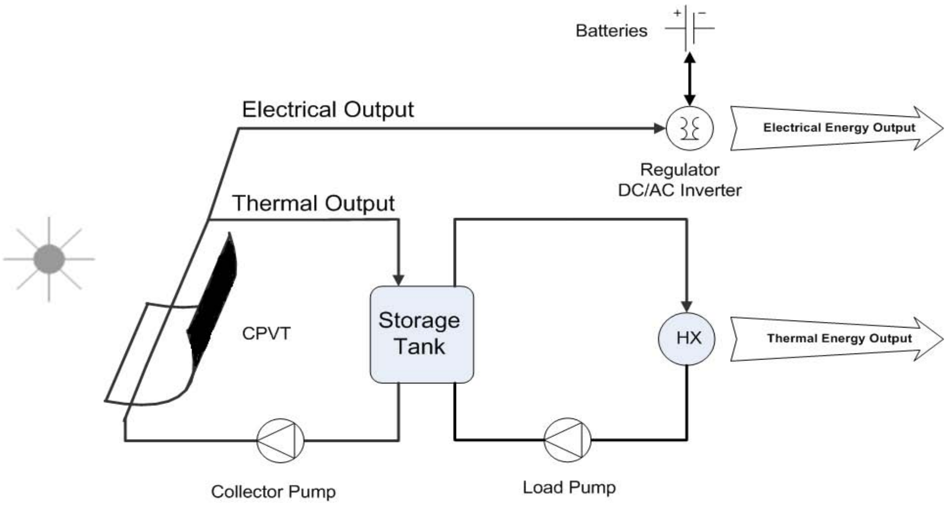

[1] http://www.power-spar.com

Sub-Systems Schematics

Cooling Sub-System

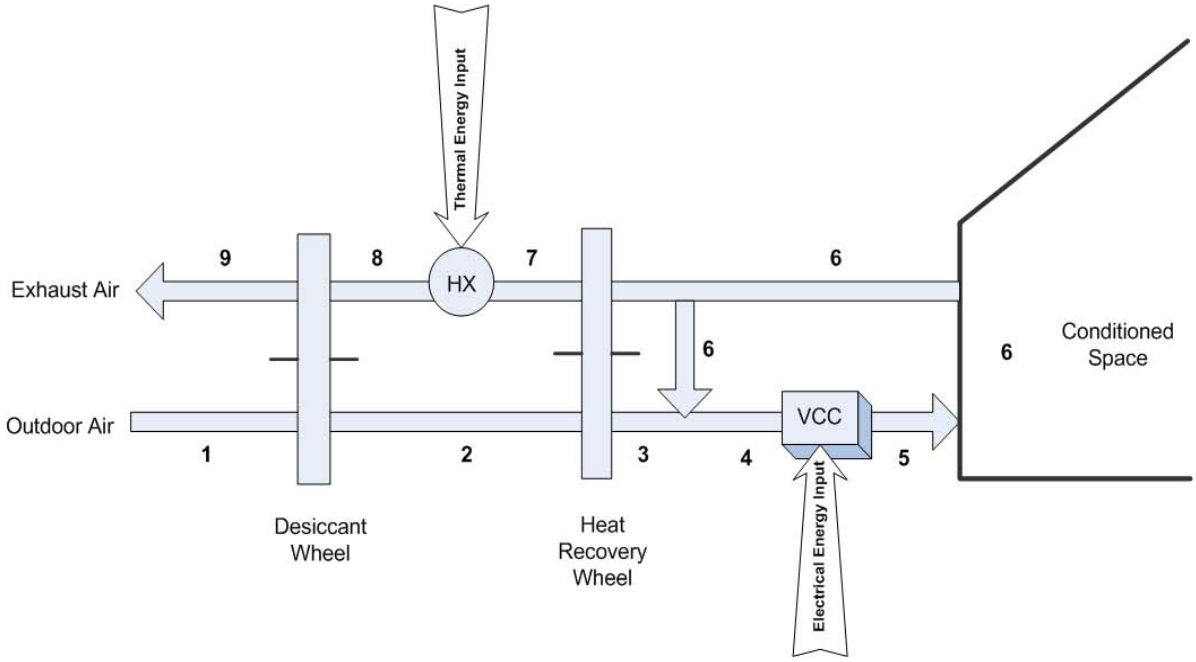

Complete System Schematic

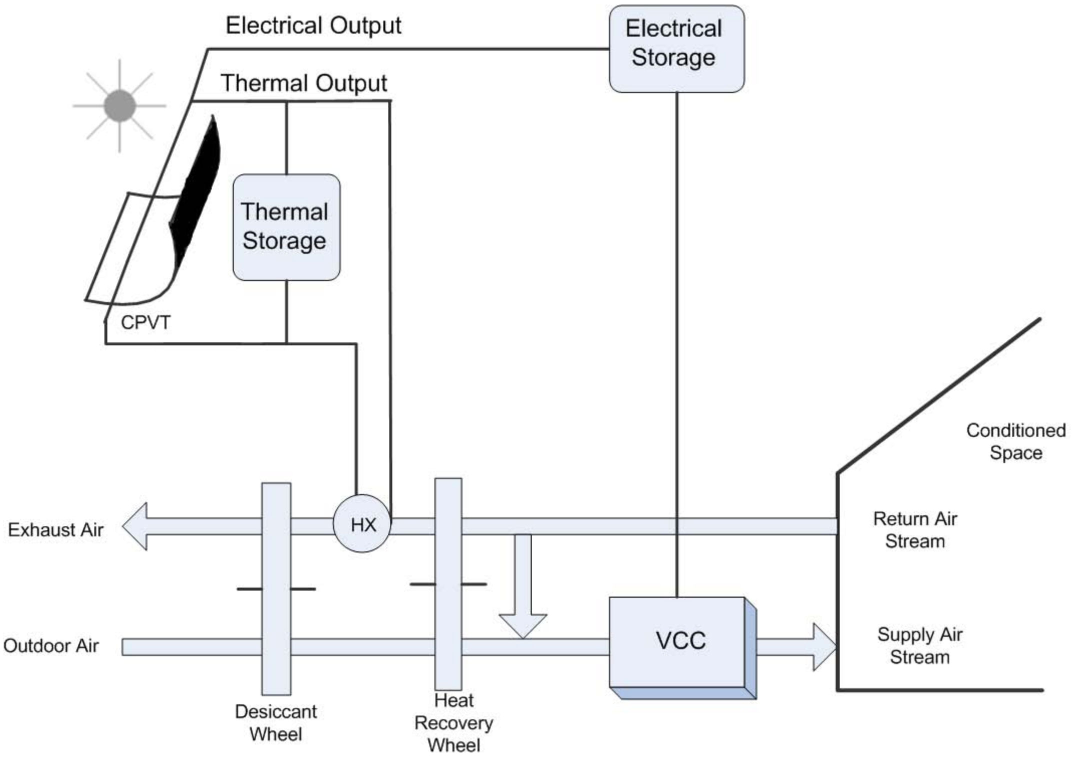

Design Methodology

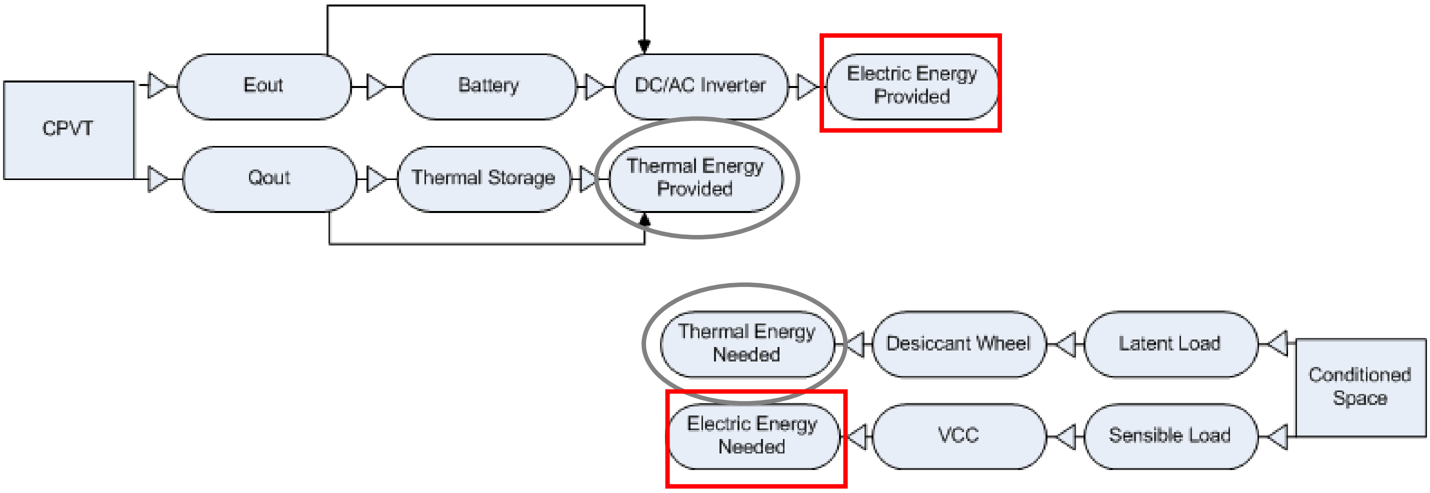
CPVT
Eout
Battery
DC/AC Inverter
Electric Energy Provided
Qout
Thermal Storage
Thermal Energy Provided
Thermal Energy Needed
Desiccant Wheel
Latent Load
Conditioned Space
Electric Energy Needed
VCC
Sensible Load

Thermal solar fraction = $Q_{provided}$ / $Q_{required}$

Electrical solar fraction = $E_{provided}$ / $E_{required}$

System Flow Diagram in TRNSYS

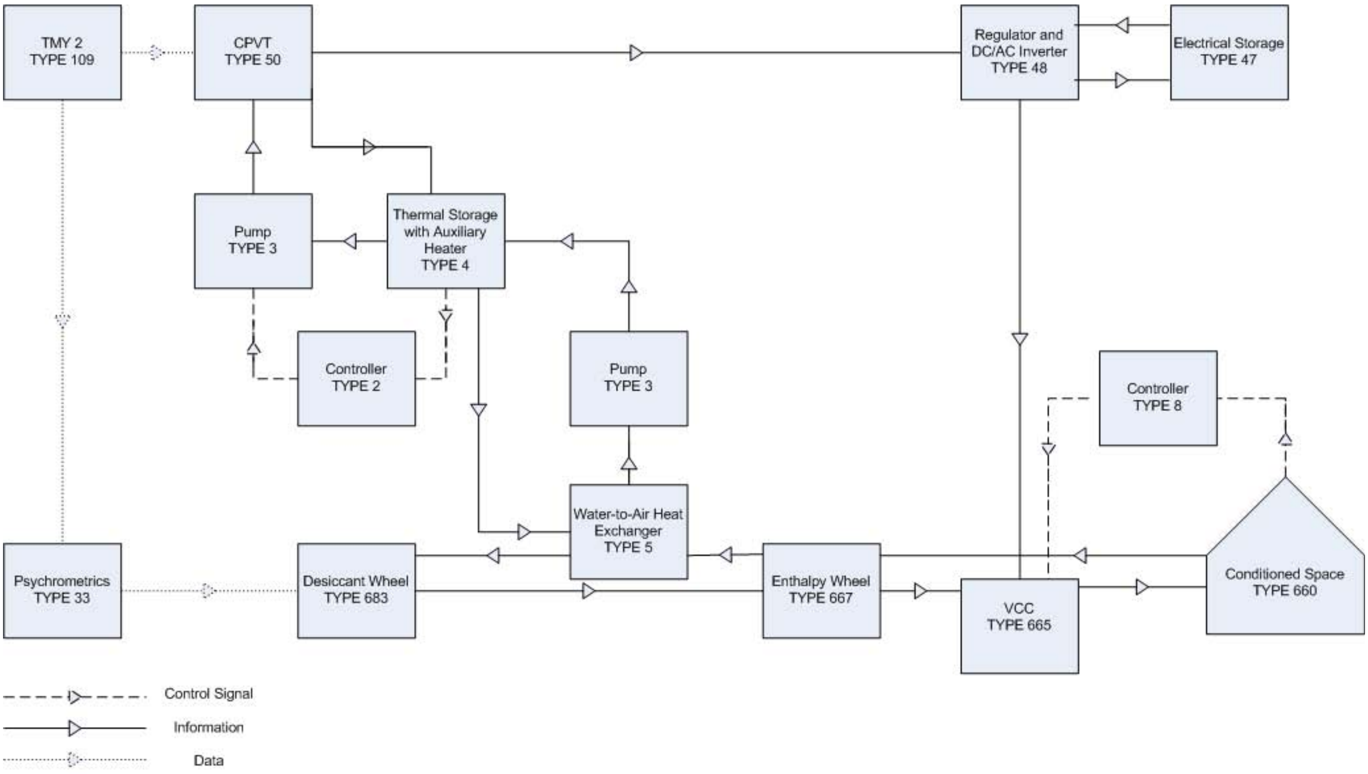
TMY 2 TYPE 109
CPVT TYPE 50
Regulator and DC/AC Inverter TYPE 48
Electrical Storage TYPE 47
Pump TYPE 3
Thermal Storage with Auxiliary Heater TYPE 4
Controller TYPE 2
Pump TYPE 3
Controller TYPE 8
Water-to-Air Heat Exchanger TYPE 5
Psychrometrics TYPE 33
Desiccant Wheel TYPE 683
Enthalpy Wheel TYPE 667
VCC TYPE 665
Conditioned Space TYPE 660
Control Signal
Information
Data

Solar Cooling System- TRNSYS

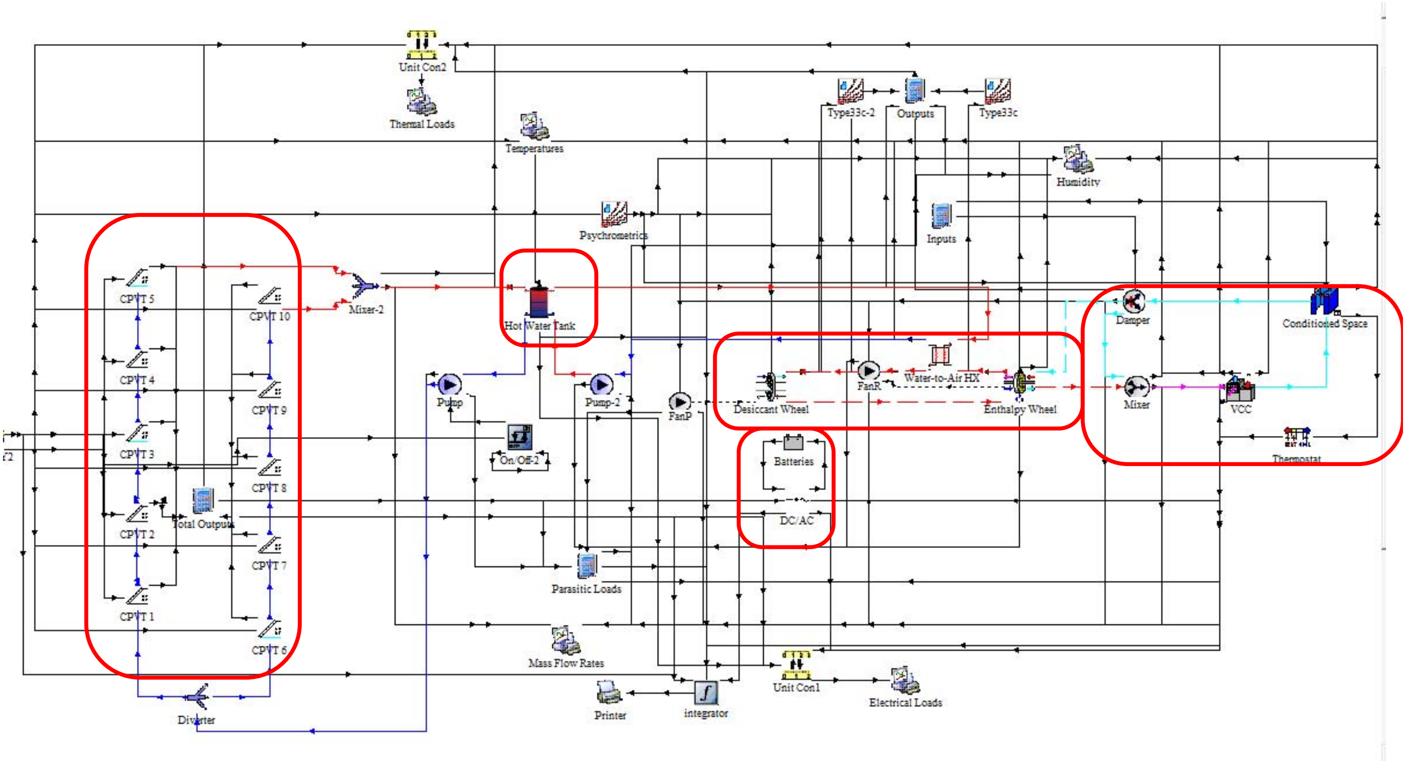

Performance Investigation

Sensible VCC

- ASHRAE 1% design conditions for AD
    - T_{amb} = 42.5°C
    - RH_{amb} = 19%
- Conditioned space
    - T_{space} = 25°C
    - RH_{space} = 50%

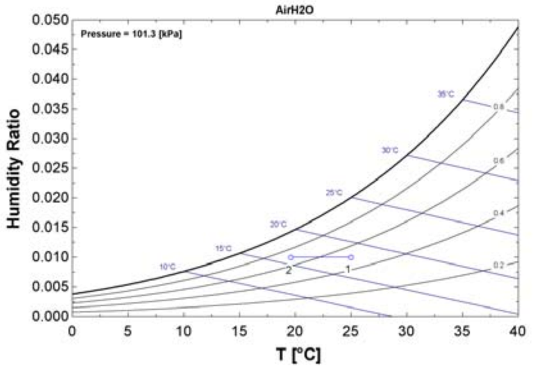

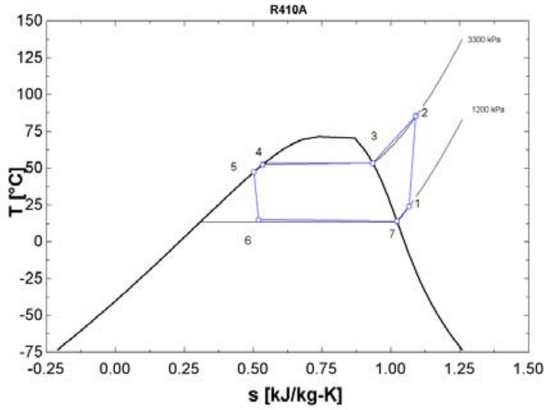

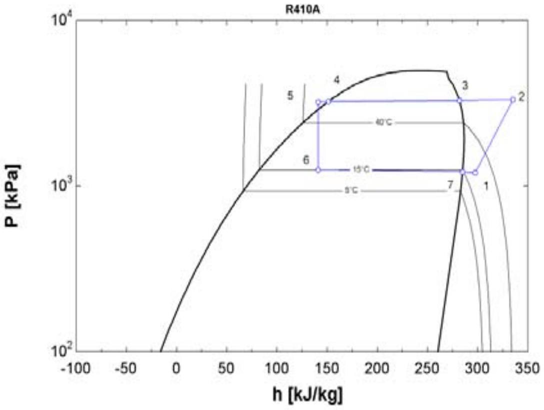

Performance Investigation

Abu Dhabi, UAE

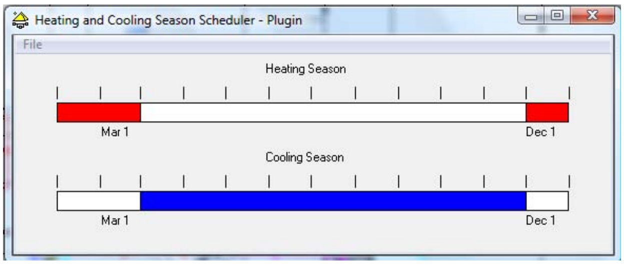

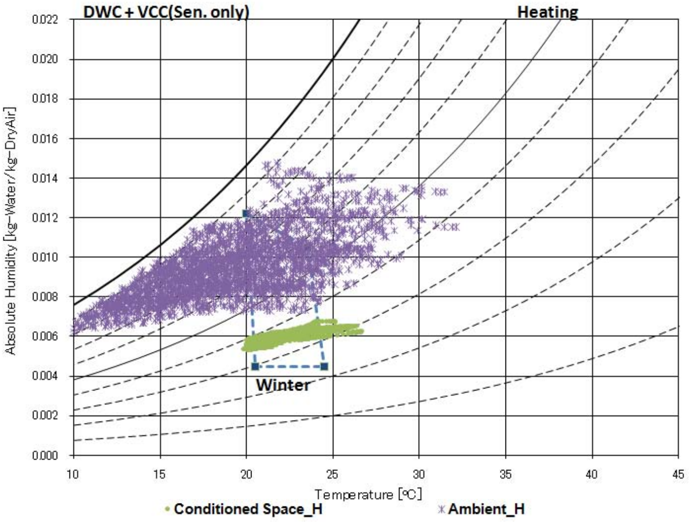

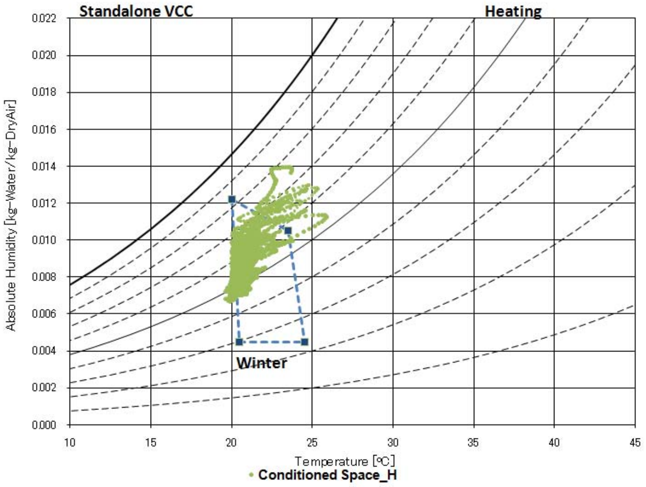

Performance Investigation

Abu Dhabi, UAE

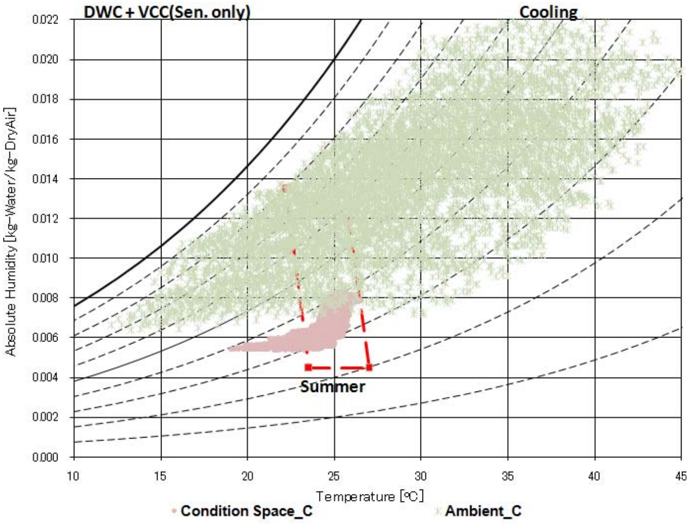

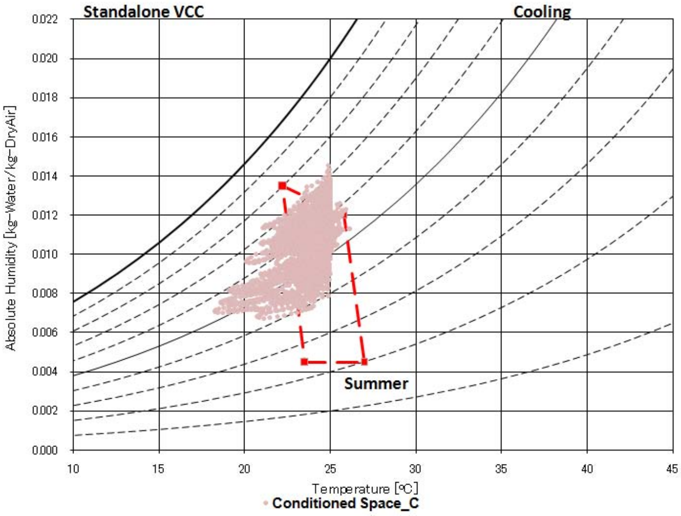

Performance Investigation

Tampa, Florida

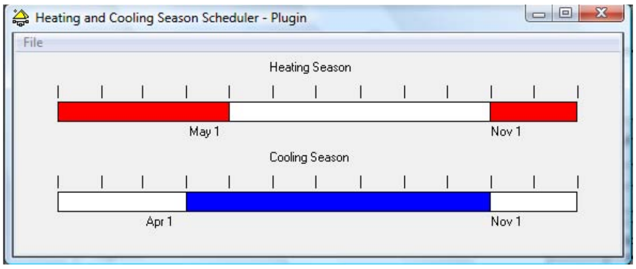

Heating Season
May 1
Nov 1

Cooling Season
Apr 1
Nov 1

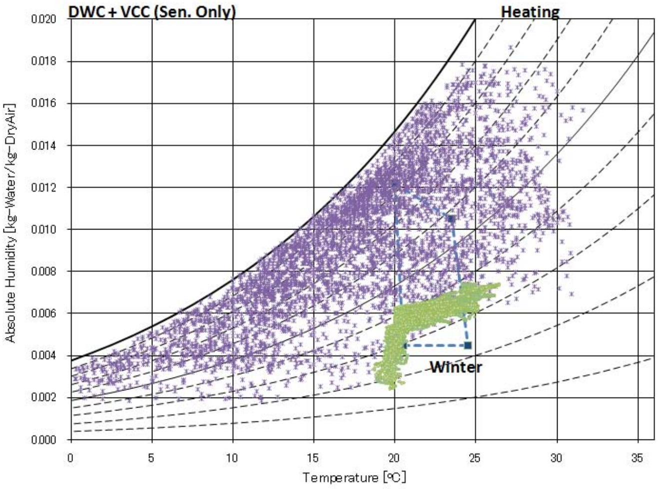

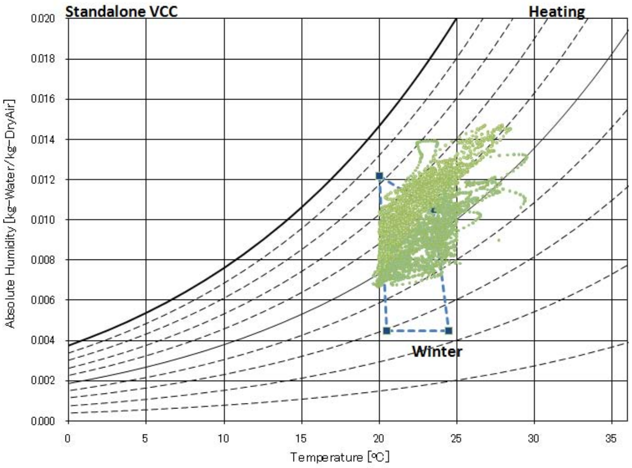

Performance Investigation

Tampa, Florida

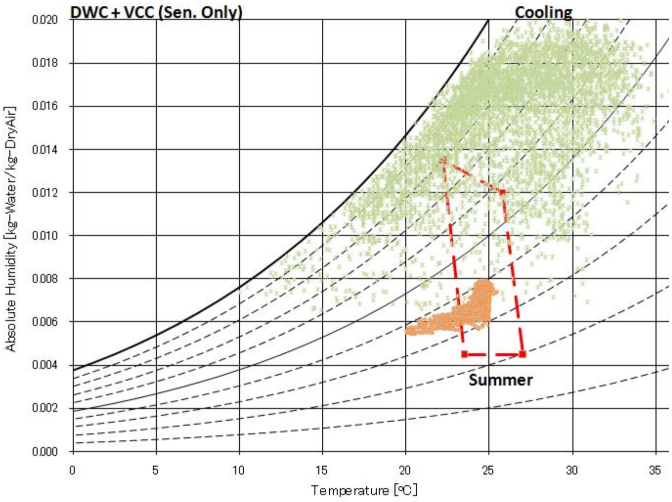

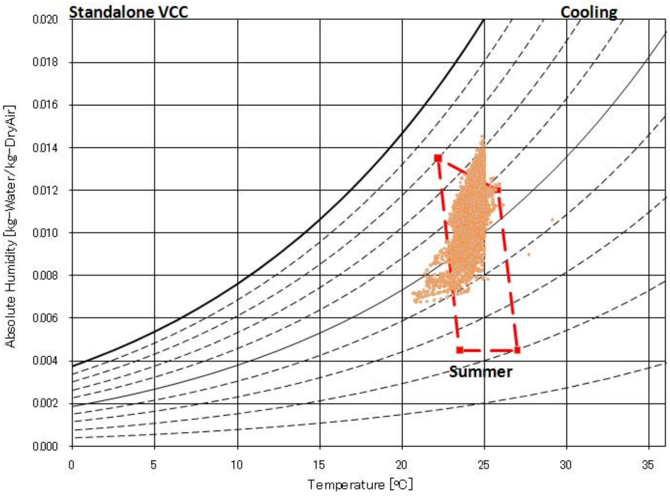

Performance Investigation

- The hybrid solar cooling system performance is compared to:
  - PV + electrically driven VCC
  - Evacuated tube thermal collector + Absorption cycle

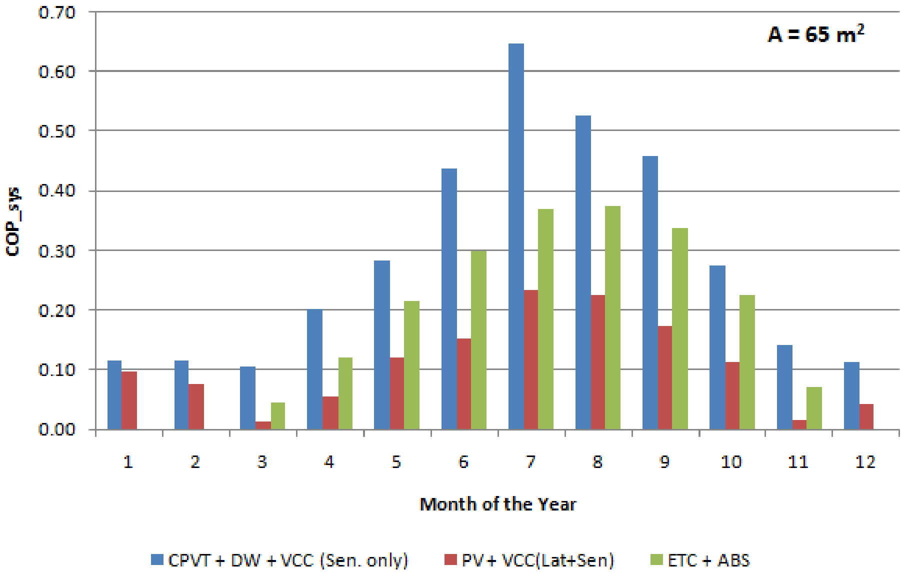

Performance Investigation

- The simulated system performance using 1% ASHRAE design conditions for Abu Dhabi.

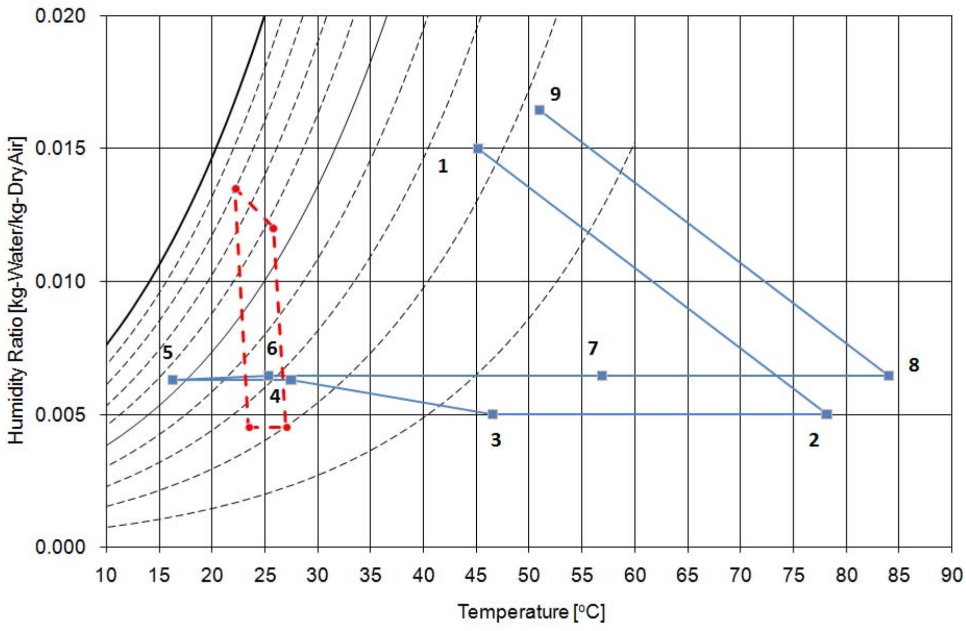

Optimization Approach

GenOpt TRNOPT TRNSYS

MATLAB Tool Box Interface TRNSYS

Approximation Assisted Optimization Interface TRNSYS

Optimization Example

A test problem, minimizing the electric heater consumption for a solar absorption cycle, was used to compare various optimization algorithms.

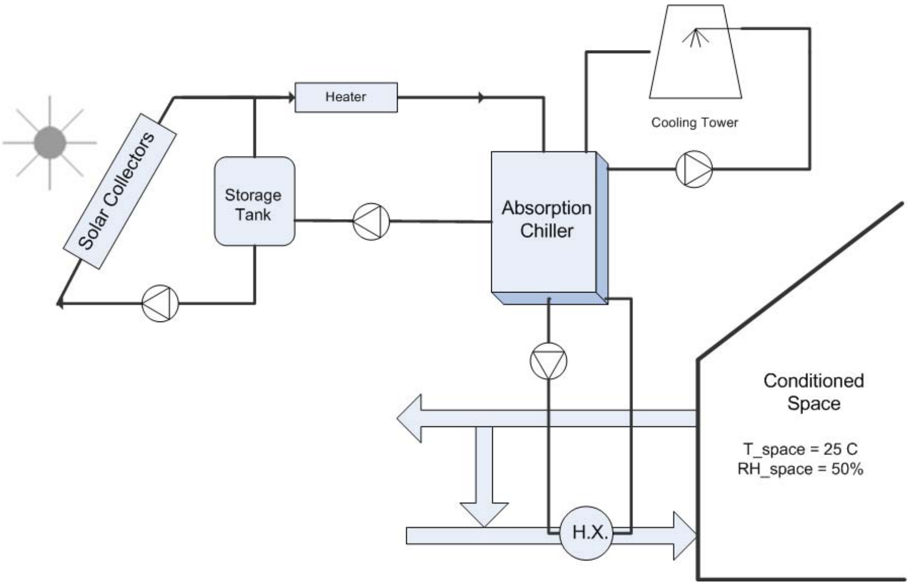

Optimization Example

Variables	Description
x_1	Collector Area [m^2]
x_2	Storage Tank Volume [m^3]
x_3	Collector Mass Flow Rate [kg/hr]
x_4	Collector Slop [deg.]

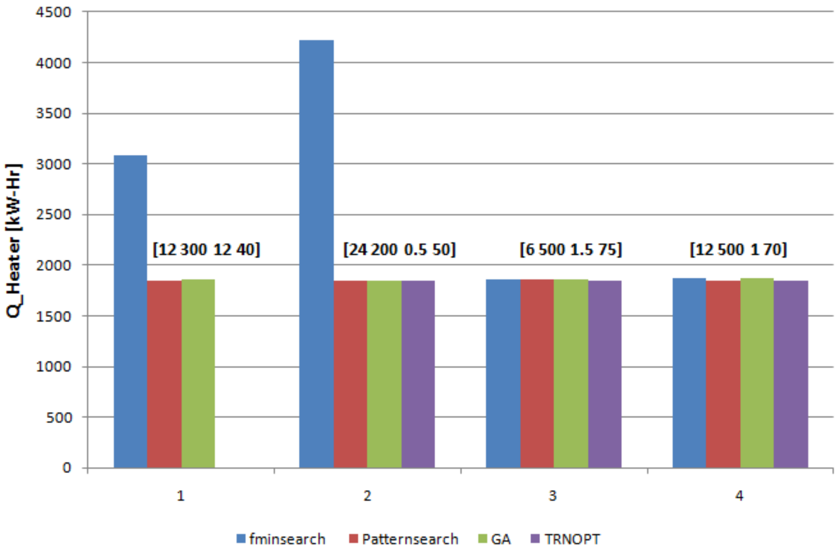

Experimental Setup

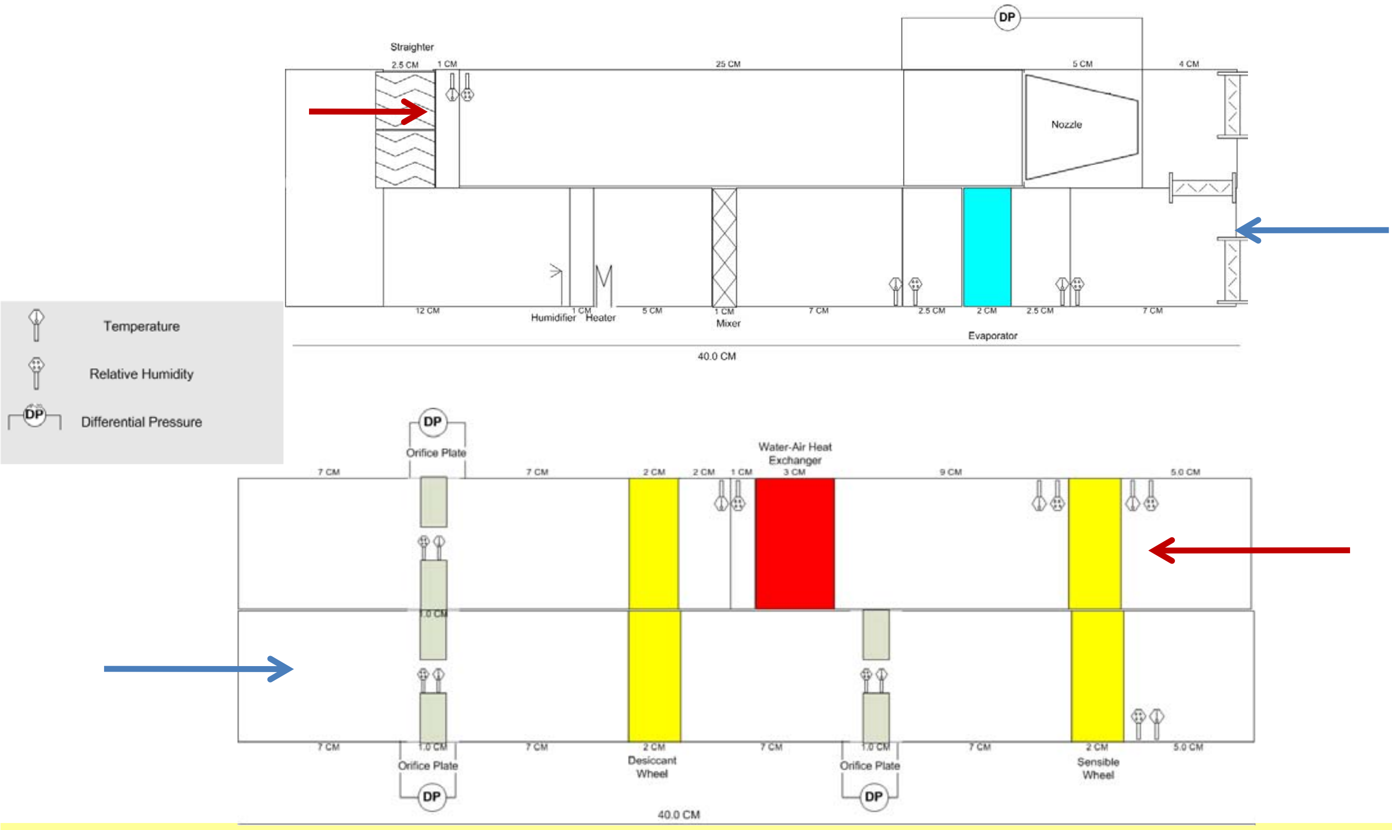

Conclusions

- A novel application for a hybrid photovoltaic/thermal (CPVT) collector was investigated.
- The system performance was modeled using Transient Systems Simulation (TRNSYS) program.
- The system performance was also compared to the performance of the standalone VCC which is widely used in the UAE .
- To provide the same cooling capacity, the proposed system reduces the electrical energy required to drive the standalone VCC by 50%.

Conclusions

- Simulation results show that decoupling of latent and sensible load is very effective in meeting the humidity and temperature requirements of buildings.
- TRNSYS program was successfully linked to MATLAB in order to expand its optimization capabilities.
- The design of experimental set up was finalized.

Future Work

- Experimentally evaluate the performance of the desiccant subsystem to ensure its operation at low regeneration temperature.
- Build the complete system in the laboratory and record all relevant operating parameters.
- Verify the TRNSYS model based on the measured data.
- Optimize the system and its controls based on measured data.
- Develop installation and operation guidelines for the hybrid solar cooling/heating system.

Publications

- Published Paper:
  - Y. Hwang, R. Radermacher, A. Al-Alili, and I. Kubo, *Review of Solar Cooling Technologies*, Int. Journal of HVAC&R Research, Vol. 14, No. 3, pp. 507-528, 2008.,

- Submitted Papers:
  - A. Al-Alili, Y. Hwang, R. Radermacher, and I. Kubo, *A High Efficiency Solar Cooling Technique*, APEN, 2009.
  - A. Mortazavi, Y. Hwang, R. Radermacher, and I. Kubo, *Optimization of a Solar Powered Absorption Cycle under Abu Dhabi's Weather Conditions*, Solar Energy, 2009.

Synthesis and Catalytic Performance of Hierarchically Ordered Micro/Mesoporous Catalysts

UMN Team: ***Aditya Bhan*** ***M. Tsapatsis***, ***Pyoongsoo Lee, Dongxia Liu, Xueyi Zhang***
PI Team: ***S. Al Hashimi, Radu Vladea, Abdulla Malek, Oki Muraza***

1st Annual PI Partner Schools Research Workshop
The Petroleum Institute, Abu Dhabi, U.A.E.
January 6-7, 2010

PI Partners

PI Sponsors

Presentation Outline

- Background
- Objectives
- Experimental Setup
- Results and Discussion
- Project Status
- Conclusions and Summary

Objectives: ADMIRE IRG 1.1.

One of the **objectives** of ADMIRE IRG1.1 is to develop new catalyst designs for hydrodefurization (HDS) over noble metals supported on zeolites.
A design currently investigated is based on micro/mesoporous zeolites.

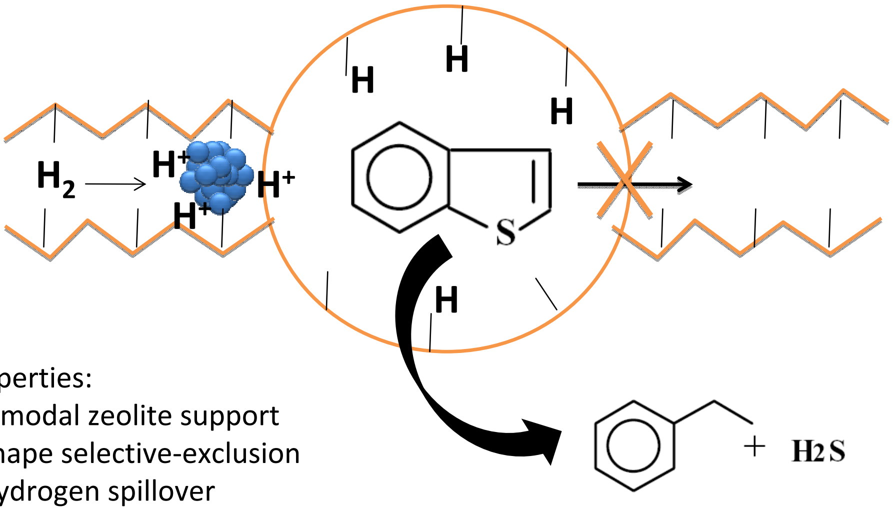

Properties:
1.Bimodal zeolite support
2.Shape selective-exclusion
3.Hydrogen spillover
4.Sulfur-tolerant catalyst

Background: typical miroporous molecular sieves (zeolites)

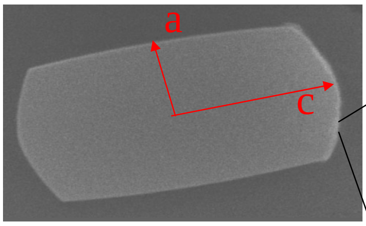

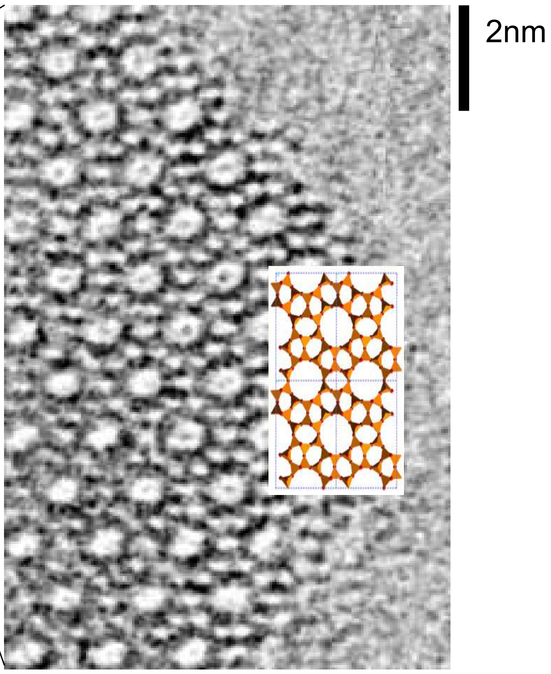

The SEM and TEM images show a typical micrometer sized ZSM-5 catalyst particle with uniform 5.5Angstrom pores

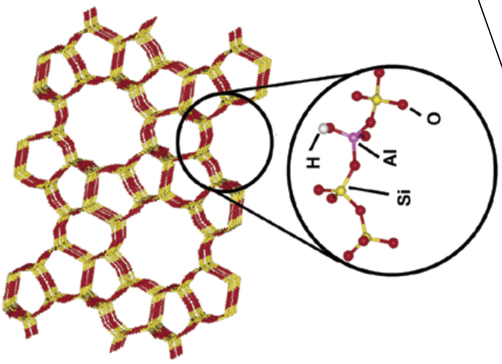

Background

Recent Progress on Synthesis of Micro/Mesoporous Zeolites

- I. Pillaring of Layered Zeolites

- Layered Zeolites

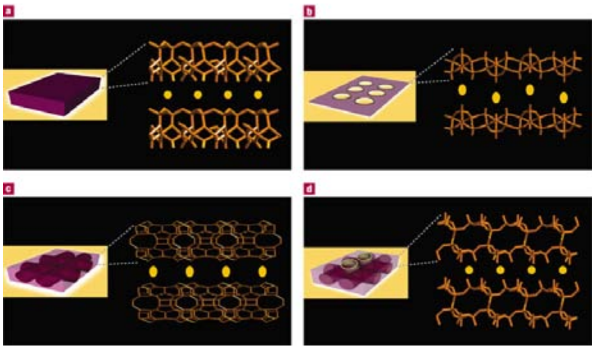

AlPO: Gao et al., **J. Solid State Chem** 129, 37 (1997)

MCM-22: Corma et al., **Nature** 396, 353-356 (1998)
Leonowicz et al.**Science** 264, 1910-1913 (1994)

AMH-3: Jeong et al., **Nature Materials** 2:(1), 53-58 (2003)

Tsapatsis et al.
U.S. Patent 6,863,983 B2 (2006)
U.S. Patent 7,087,288 B2 (2006)

- Pillaring of Layered Zeolites

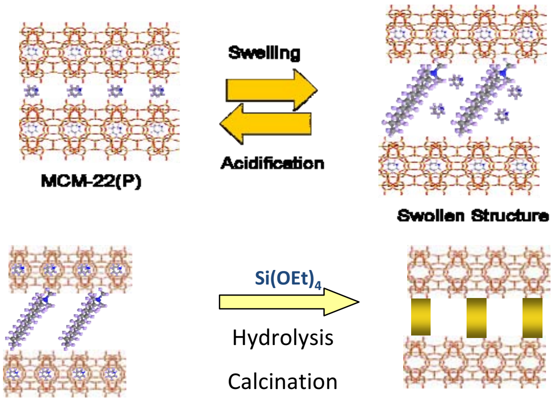

$Si(OEt)_4$

Hydrolysis

Calcination

Swollen Structure

MCM-36:
Material
Pillared with
silica

*Rubin and Chu, US Patent 4954325, **1990***

Background

Recent Progress on Synthesis of Micro/Mesoporous Zeolites

-I. Pillaring of Layered Zeolites: Preserving the structure of the zeolite layer during pillaring is very important for ensuring high catalytic activity (Maheshwari et. al., Journal of the American Chemical Society, **2008**, 230, p1507; "Layered Zeolite materials and Methods Related Thereto" Tsapatsis, M., Maheshwari S., Koros W. and Bates F.S. PCT/US2008/012455; WO2009108166)

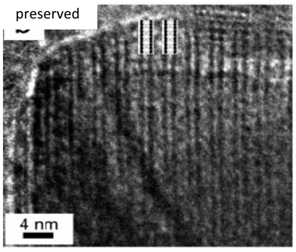

New Material (UMN) ●

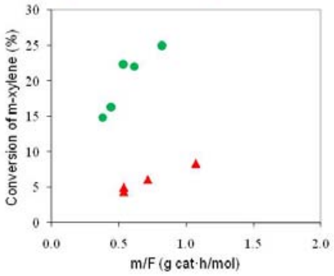

Xylene isomerization

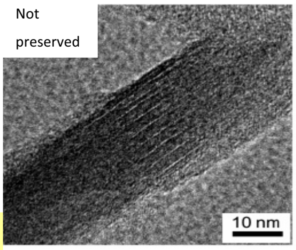

MCM-36 ▲ (ExxonMobil)

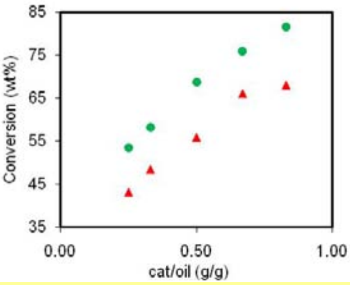

Cracking of gasoil

Background

Recent Progress on Synthesis of Micro/Mesoporous Zeolites

- **II. Three-Dimensionally Ordered Zeolites** (W. Fan, M.A. Snyder, S. Kumar, PS Lee, W. C. Yoo, A. V. McCormick, R. L. Penn, A. Stein and M. Tsapatsis, ***Nature Materials***, **7(12), 984-991(2008))**

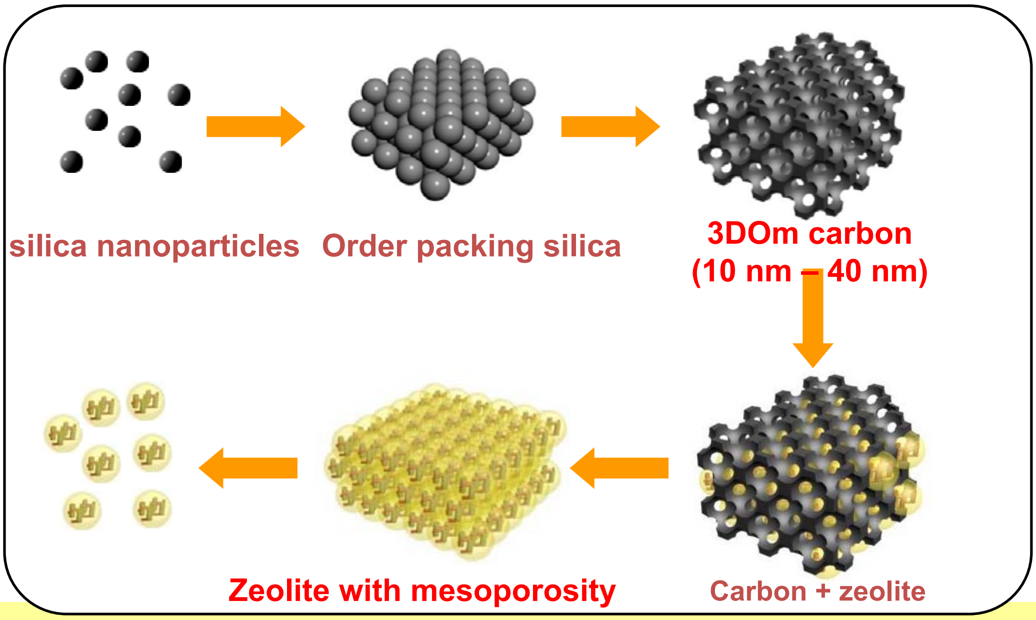

Background: 3DOm Silicalite-1: nm and Angstrom resolution

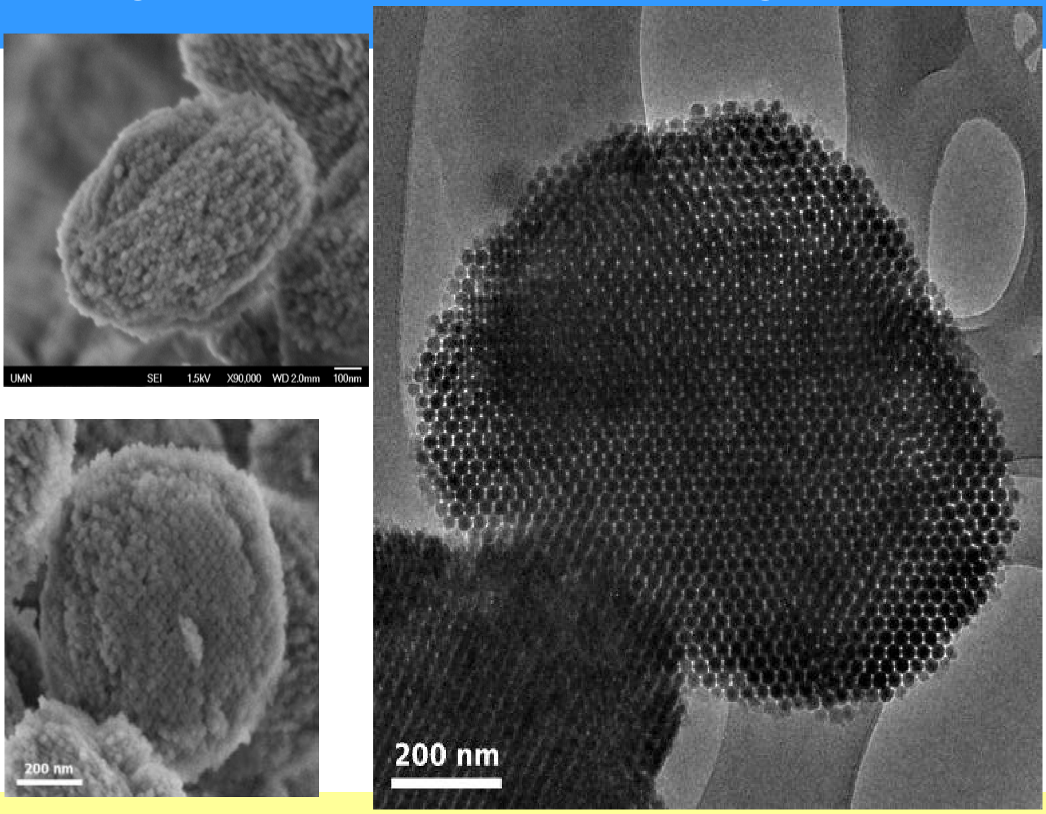

Project Objectives

Synthesize and characterize highly ordered microporous/mesoporous materials with interconnected porosity.

Perform catalytic tests to assess the intrinsic catalytic activity and compare with conventional microporous zeolites

Prepare multifunctional catalysts by placing metal nanoparticles in zeolitic pores

Perform desulfurization reactions using hydrogen and hydrocarbons

Experimental Setup: Reactor Unit

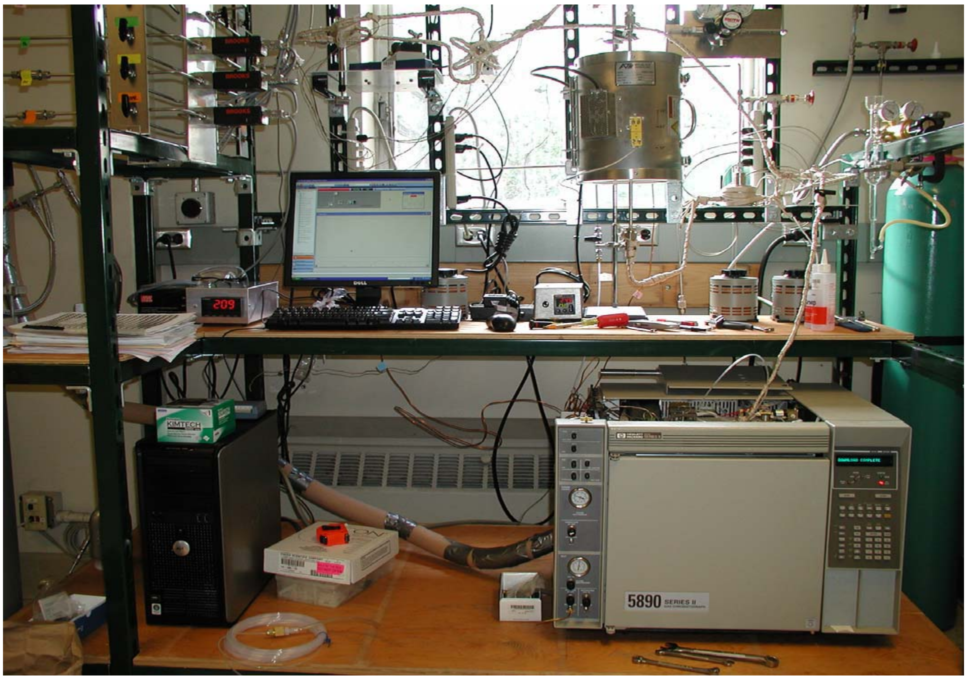

Experimental Setup: Characterization

Results and discussion

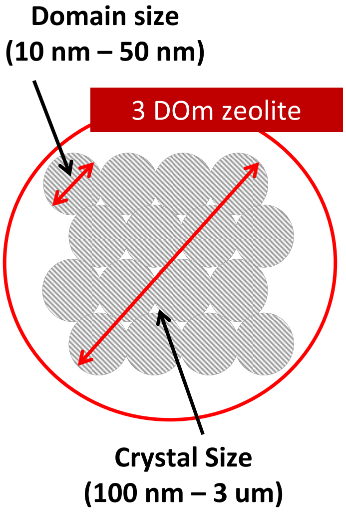

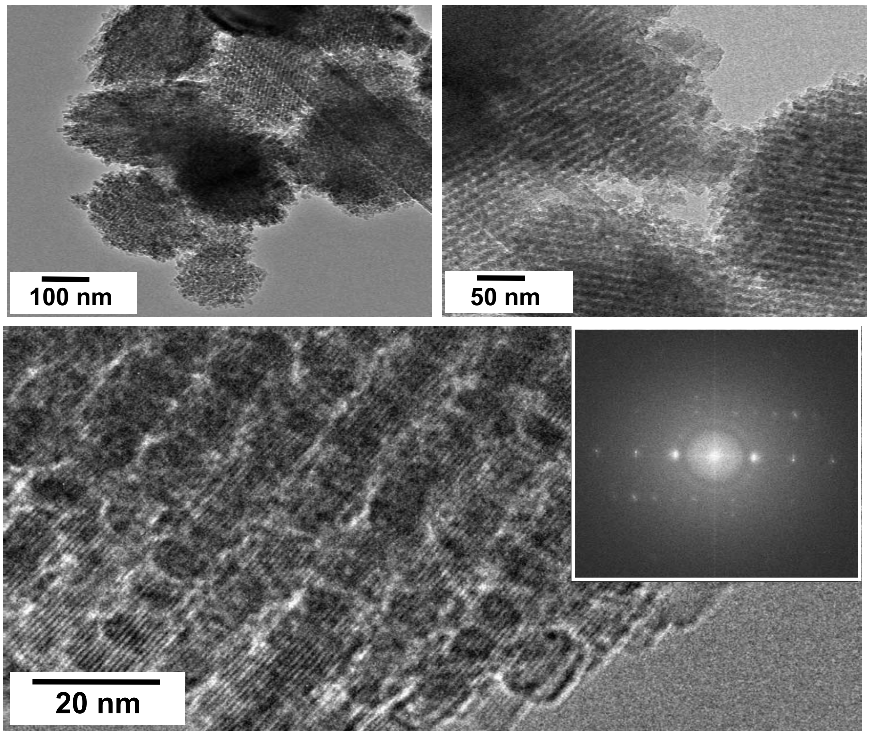

Results and discussion

3 DOm zeolite of 20 nm domains with different crystal size

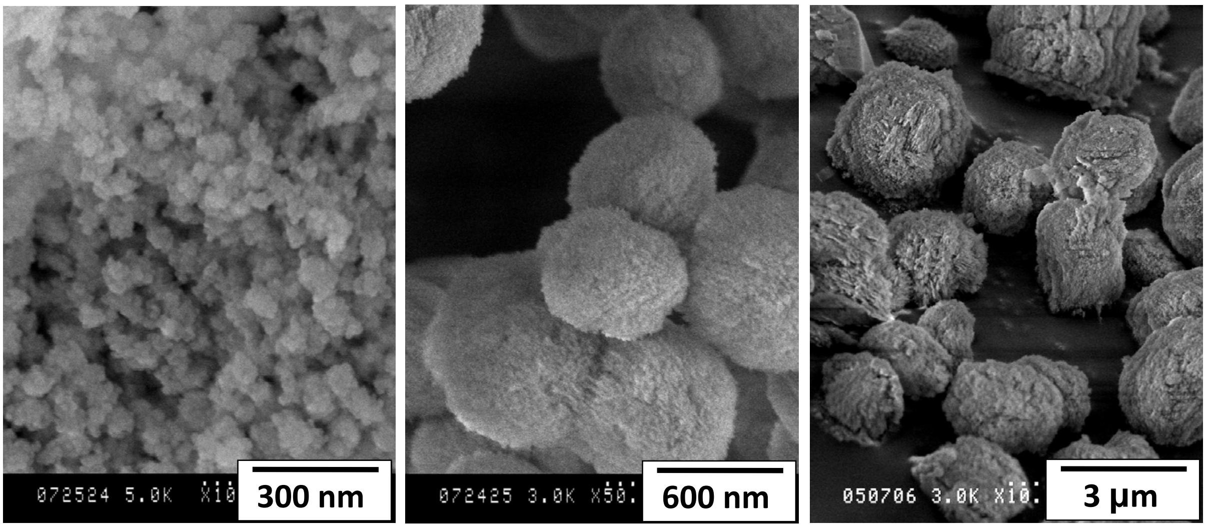

Results and discussion

3 DOm zeolite of similar crystal size with different domains

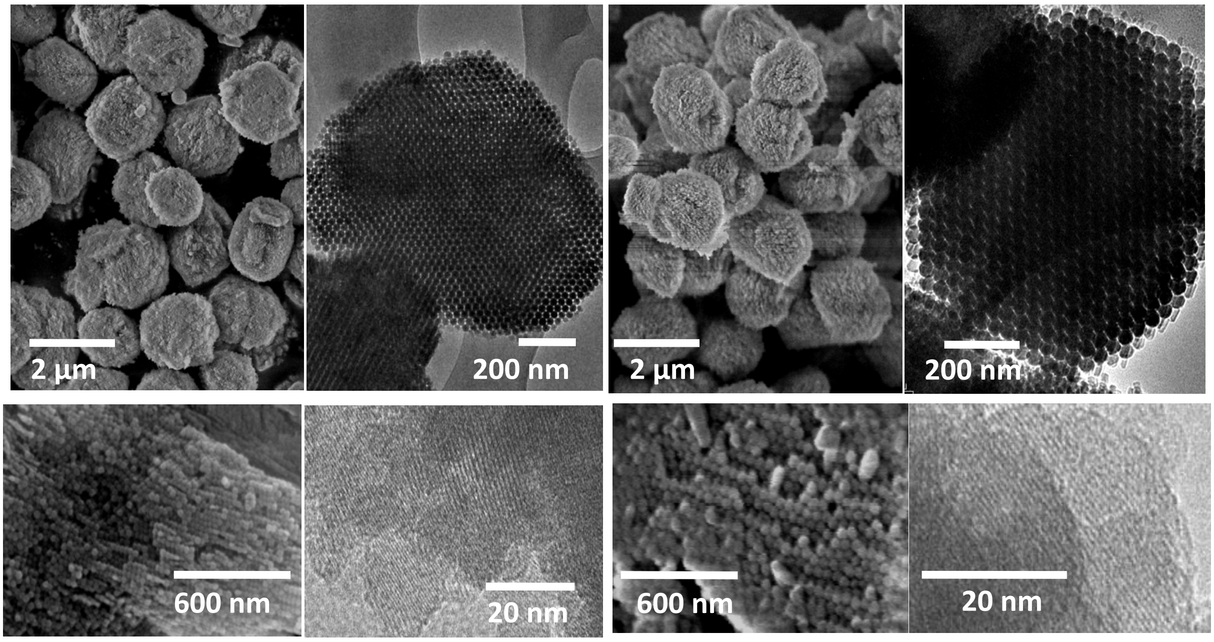

Results and discussion

X-ray diffraction pattrens of 3 DOm zeolites

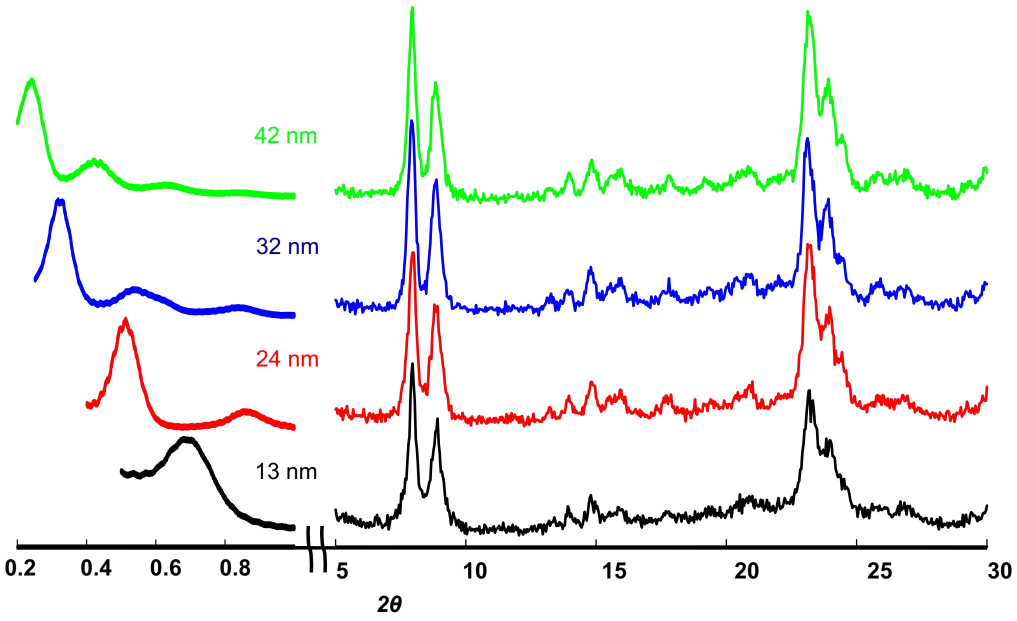

3 DOm zeolite of similar crystal size with different domains

Results and discussions

Nitrogen adsorption isotherm

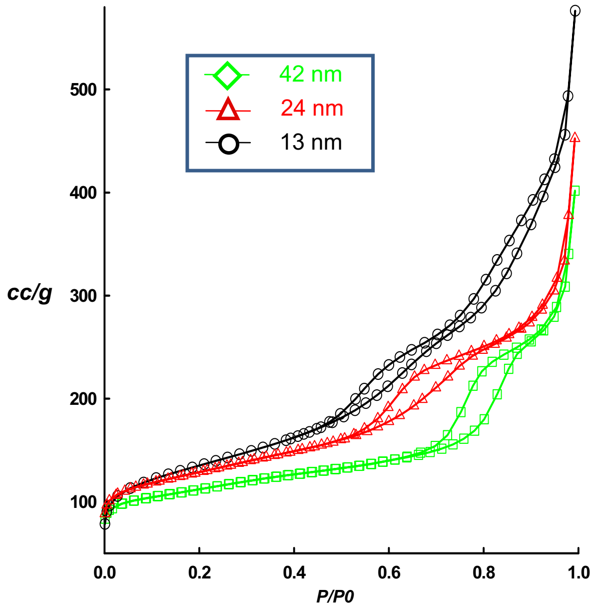

Texture properties of 3 DOm zeolites

domain dia.	*Crystal size*	*Micropore area(m^2/g)*	*BET surf. Area(m^2/g)*	*Ext. surf. Area (m^2/g)*	*Mesopore dia. (nm)*
13 nm	200-300 nm	153.4	508.4	354.9	5.5
24 nm	200-300 nm	186.8	459.7	272.9	6.5
32 nm	500-600 nm	206.4	406.3	214.4	8.0
42 nm	300-400 nm	193.3	406.3	213.0	15.5

Tunable mesoporosity by changing domain sizes of 3 DOm zeolite

Results and discussion

Solid State NMR

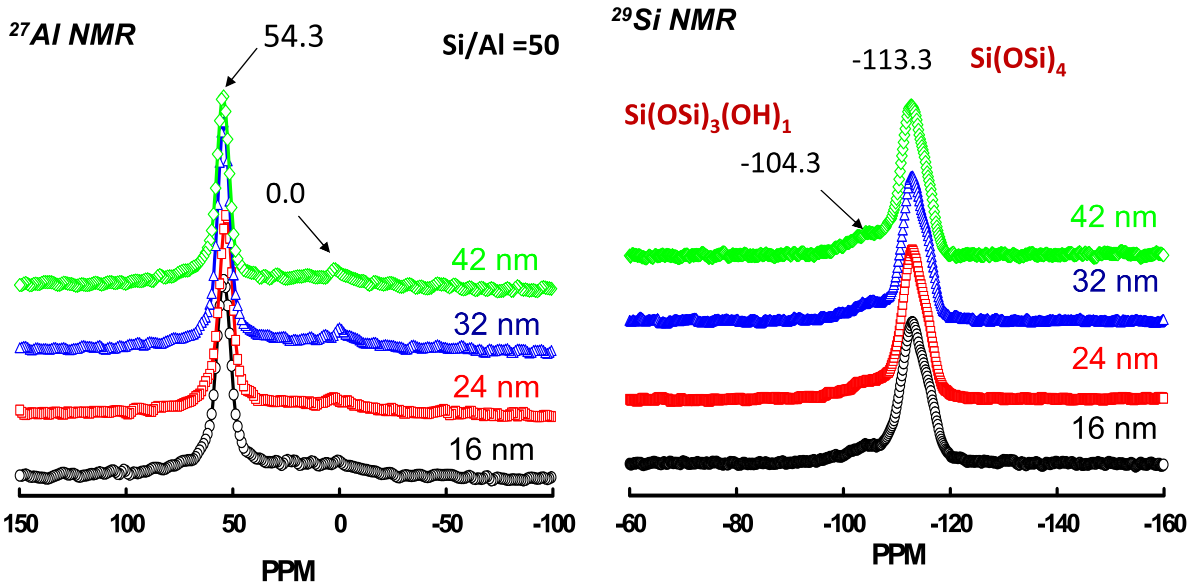

Successful Al incorporation into zeolite frameworks and good crystalline structure

Results and discussion

Synthesis of Meso/Microporous MCM-36 Catalyst

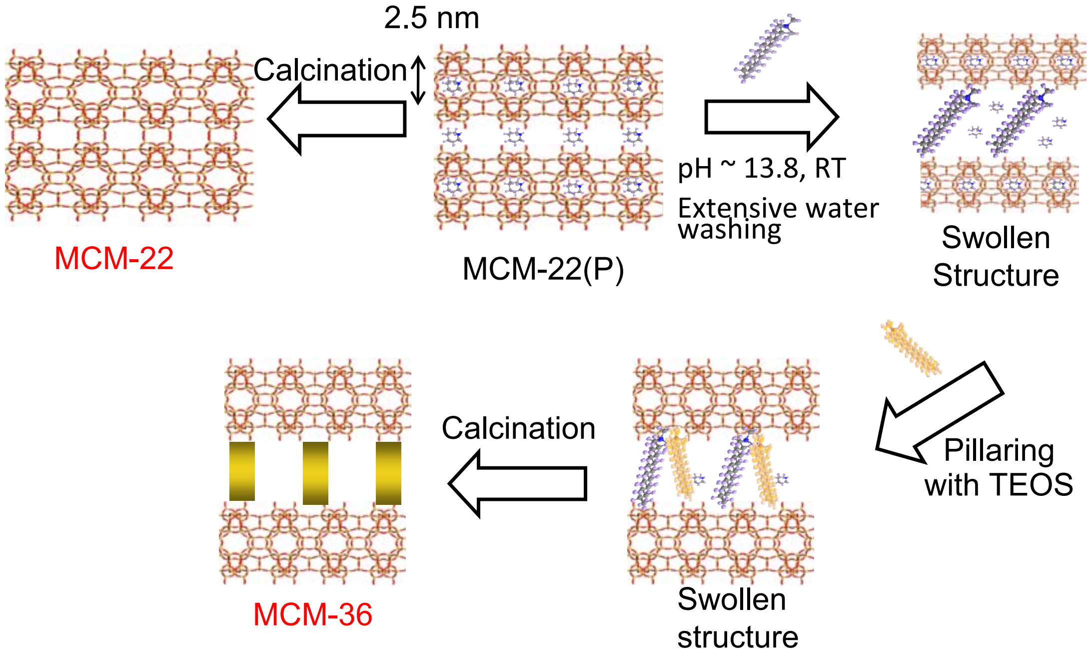

Results and discussion

XRD of Meso/Microporous MCM-36 Catalyst

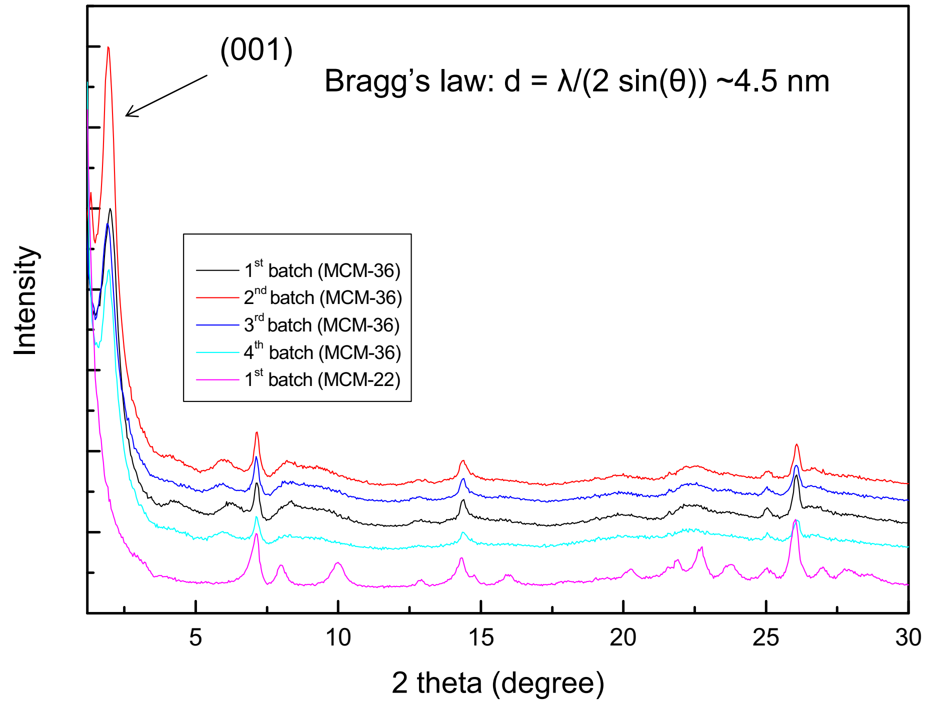

Results and discussion

BET Analysis of Meso/Microporous MCM-36 Catalyst

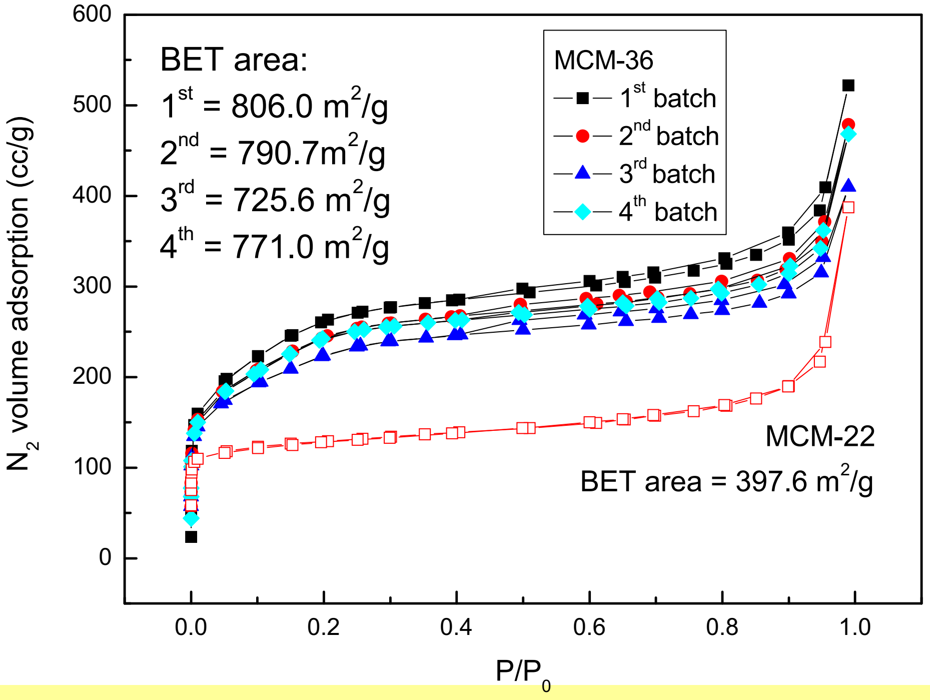

Mechanism of Ethanol Activation on Zeolites

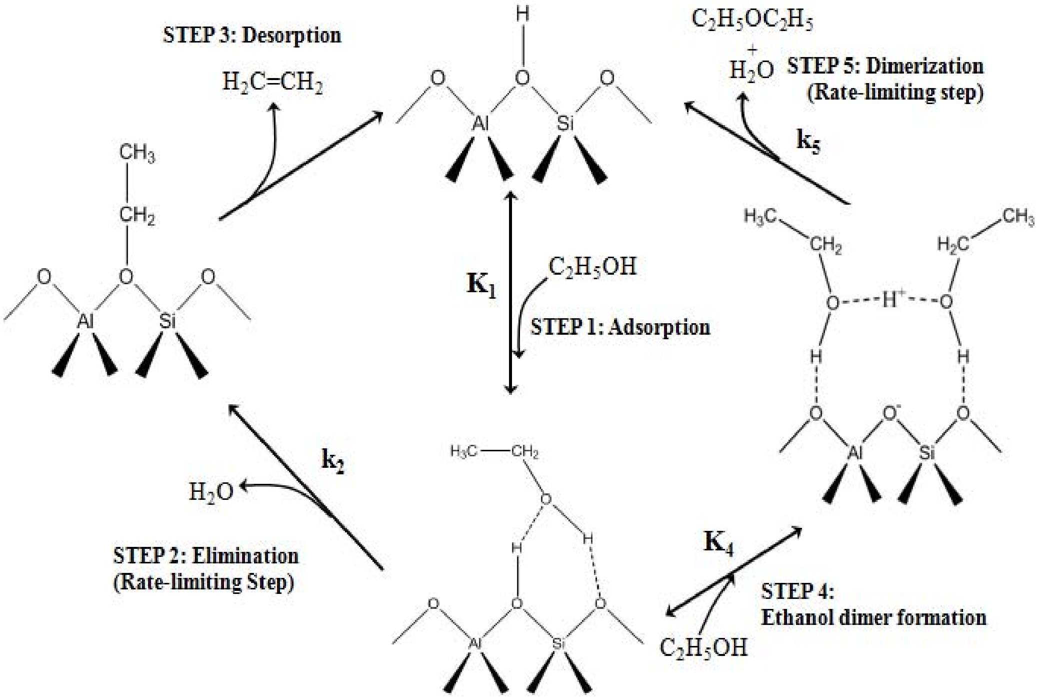

Ethanol Activation over Synthesized Zeolites

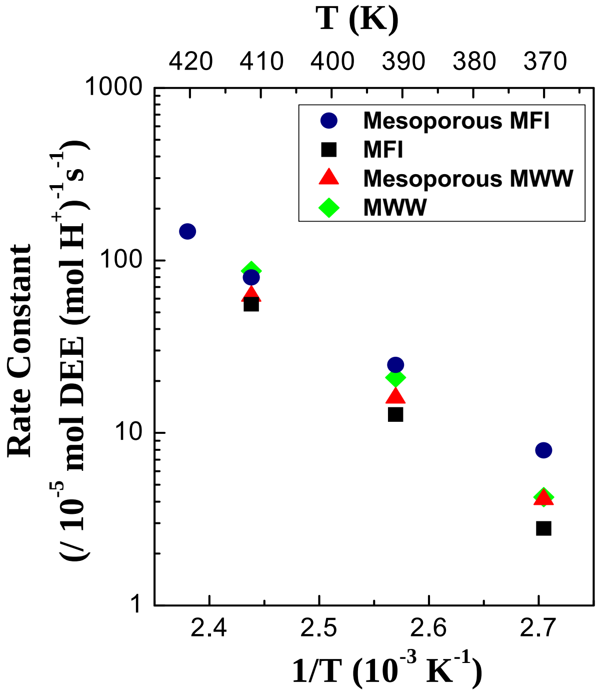

Mechanism of Propane Activation on Zeolites

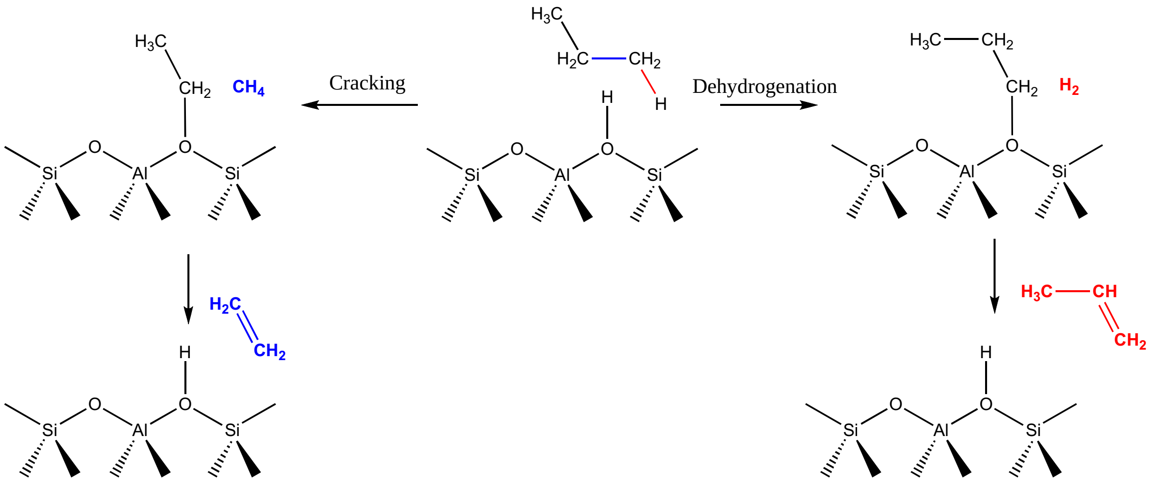

Cracking: $C_3H_8 \longrightarrow CH_4 + C_2H_4$

Dehydrogenation: $C_3H_8 \longrightarrow H_2 + C_3H_6$

Conversion of Propane over MFI

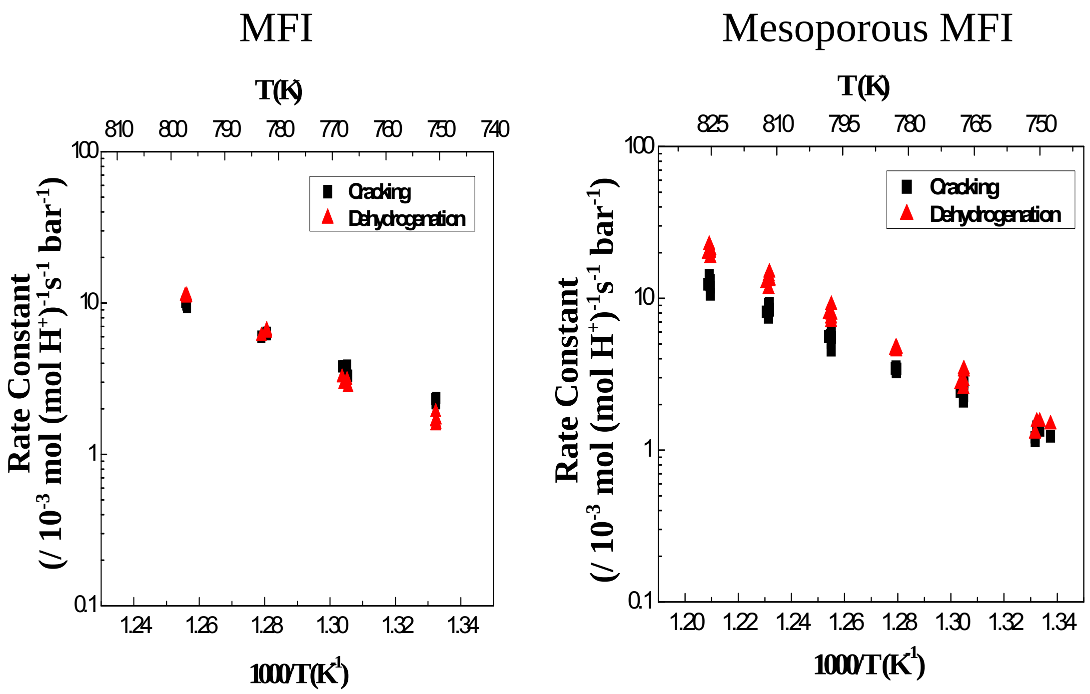
MFI

Mesoporous MFI

Cracking/Dehydrogenation Ratio

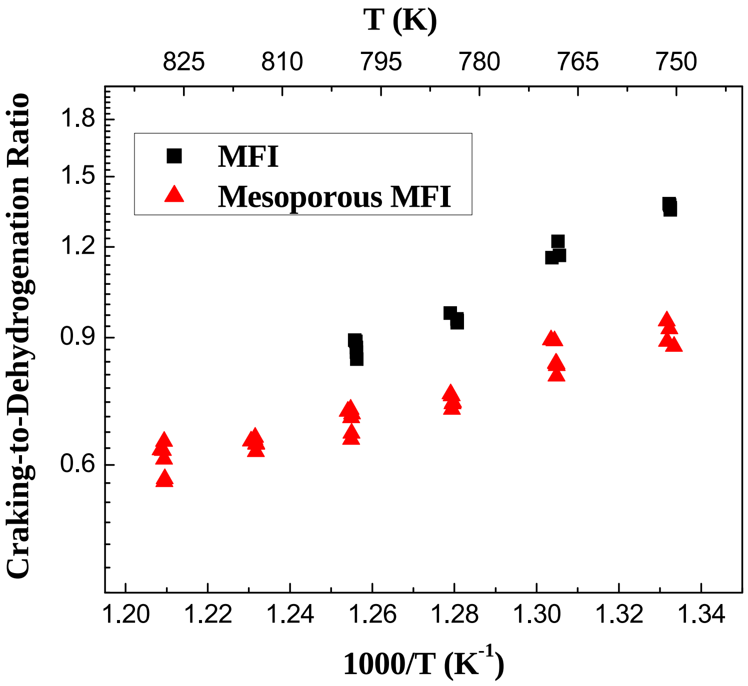

Project Status

The project progresses as planned

Experimental set up was completed

Microporous/mesoporous zeolites were synthesized and characterized by SEM, TEM, NMR, porosimetry and catalytic activity for ethanol dehydration and propane activation

Metal supported catalysts and bifunctional catalysis are the next target

A new graduate student from PI joined the team at UMN:
Mr. Yasser AlWahedi will be jointly advised by Tsapatsis and Bhan

An undergraduate student from PI (Mr. A. Malek) worked with the UMN team last summer.

Several publications and conference presentations are in preparation

1st Annual PI Partner Schools Research Workshop, January 6-7, 2010

Conclusions and Summary

- Micro/mesoporous zeolites with precisely controlled micro and mesoporosity at the Angstrom and nanometer levels respectively can be prepared
- The materials exhibit high intrinsic catalytic activity comparable to that of microporous zeolites
- They will be further developed for hydrodesulfurization and for diffusion limited reactions:

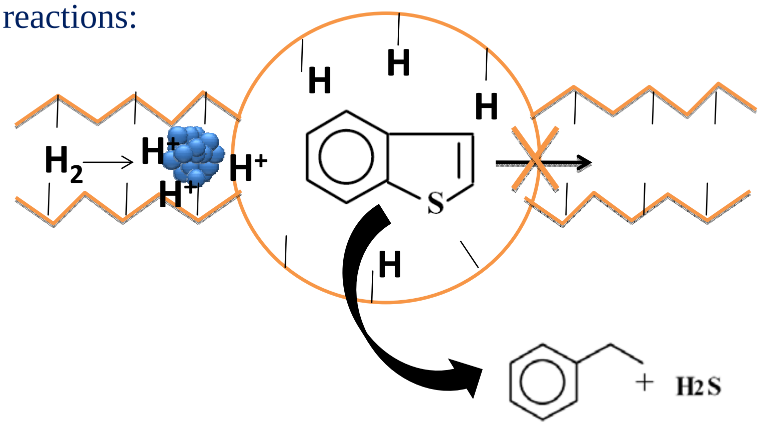

Energy Recovery and Conversions II

Understanding of Chemical Kinetics in the Thermal Stage of Claus Process

UMD Team: **Prof. Ashwani Gupta, Hatem Selim**

PI Team: **Dr. Ahmed Al Shoaibi, Nahla Al Amoodi**

1st Annual PI Partner Schools Research Workshop
The Petroleum Institute, Abu Dhabi, U.A.E.
January 6-7, 2010

PI Partners

PI Sponsors

Presentation Outline

- Background
- Objectives
- Approach
- Results and Discussions
- Project Status
- Conclusions

Background: Claus Process

- Claus process is the most widely used process for sulfur recovery from hydrogen sulfide
- Overall Main process reactions:

$H_2S + 3/2\ O_2 \rightarrow SO_2 + H_2O\quad \Delta H_r = -518\ kJ/mol \qquad (1)$

$2H_2S + SO_2 \rightarrow 3/2\ S_2 + 2H_2O \qquad \Delta H_r = \ 47kJ/mol \qquad (2)$

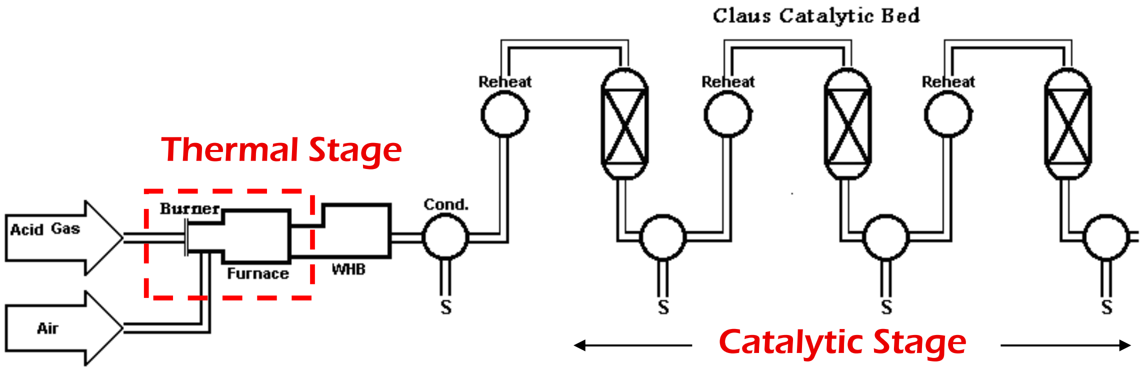

Project Objectives

- Hydrogen sulfide is a colorless, toxic, highly corrosive and flammable gas.
- Hydrogen sulfide is a valuable source of sulfur and hydrogen.
- Understanding Claus thermal stage kinetics identifies:
  - Optimum operating conditions which leads to high sulfur conditions such as temperature and residence time.
  - Important reactions to reduce mechanism. Using the reduced mechanism in CFD codes facilitate convergence.
- **Understand effects of contaminants (CO_2 and H_2O) on kinetics of sulfur recovery in Claus furnace.**

Approach

- Detailed kinetic analysis is performed on adiabatic runs of different contaminants compositions using CHEMKIN program.
- The kinetic model consists of 111 reactions and 41 species[1]
- The Claus furnace is modeled as a Plug Flow reactor
- Axial velocity at the inlet is specified at 1 cm/s
- The inlet temperature is 1650 K
- Reactor operate at atmospheric pressure
- Residence time 0.5 s

Test Matrix

Feed compositions of simulated runs:

Run	Mole %			
	H_2S	CO_2	H_2O	N_2
1	75	15	5	5
2	55	10	30	5
3	50	40	5	5
4	35	30	30	5

Results and Discussions

Run	Total Contaminants Feed Composition (%)	Exit Composition (%)	
		S_2	SO_2
1	20	15.5	13.7
2	40	13.3	15.4
3	45	10.9	16.9
4	60	8.7	17.5

- ❖ Sulfur composition decreases by 45% as the contaminants composition increase from 20 to 60 mol %.
- ❖ To explain the decrease of S_2, analyzing competing reactions to the production of S_2 is essential.

Thus, the focus of the analysis will be on pathways which produce byproducts, mainly SO_2.

SO_2 Production/Consumption profile

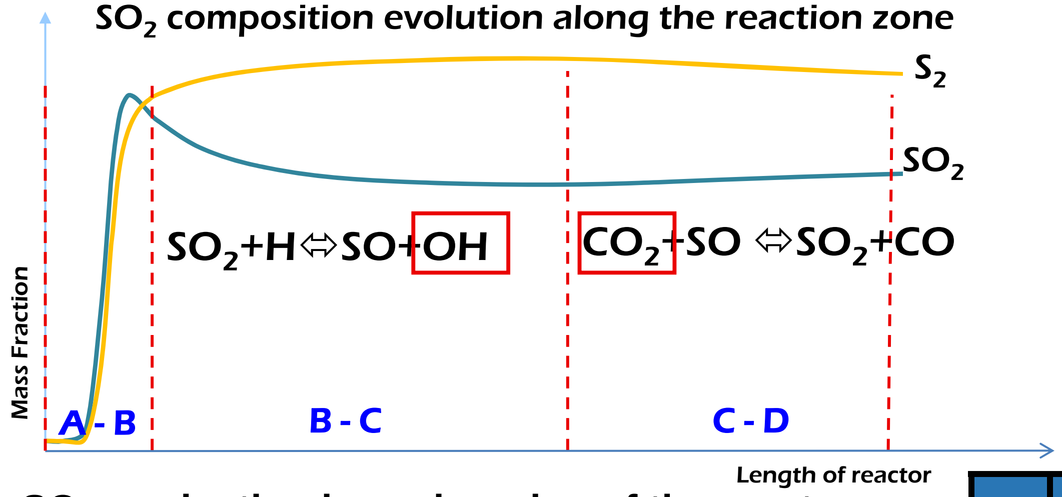

SO_2 composition evolution along the reaction zone

SO_2 production in each region of the reactor

Run	A-B	B-C	C-D
1	+	-	
2	+		+
3	+	-	+
4	+		+

Test Matrix

Run	Mole %			
	H_2S	CO_2	H_2O	N_2
1	75	15	5	5
2	55	10	30	5
3	50	40	5	5
4	35	30	30	5

OH Effect

Region B-C

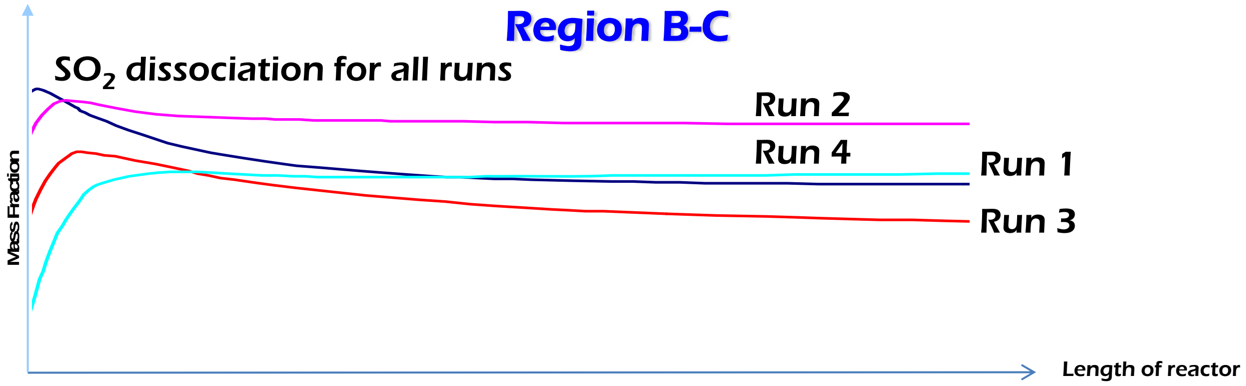

- The most significant reaction for dissociation of SO_2 is SO_2+H⇔SO+OH
- SO_2 dissociation in runs 1 and 3 is more significant compared to that of runs 2 and 4. Thus the excess availability of OH in runs 2 and 4 prevents the dissociation of SO_2.

Run	H_2O Feed Composition (%)	SO_2 Production
1	5	-
2	30	
3	5	-
4	30	

CO_2 Effect

Region C-D

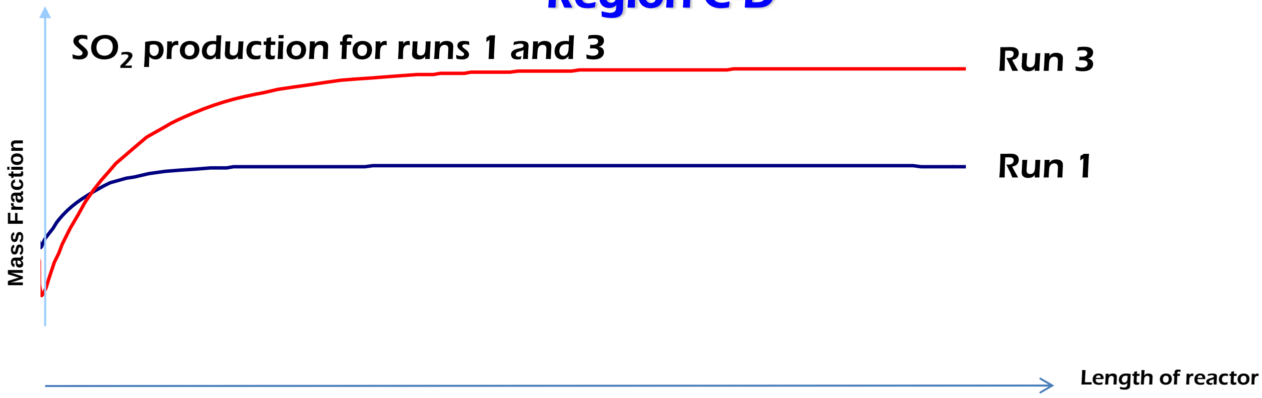

- The comparison is made between run 1 and 3
- The most significant reaction for production of SO_2 is CO_2+SO⇔SO_2+CO
- SO_2 production in runs 3 is more significant compared to that of run 1. Thus the excess availability of CO_2 in runs 3 promotes the production of SO_2.

Run	CO_2 Feed Composition (%)	SO_2 Production
1	15	
3	40	+

Summary

Run	Contaminant Feed Composition (%)	Exit Composition (%)	
		S_2	SO_2
1	20	15.5	13.7
2	40	13.3	15.4
3	45	10.9	16.9
4	60	8.56	17.5

❖ Higher total concentration of H_2O and CO_2 results in higher SO_2 concentrations.

Project Status

It is an ongoing project and we are starting year 2 of the project

Year 2 objectives:

- ❖ Perform detailed simulations using the Fluent (PI) and CHEMKIN (UMD) computer codes with special emphasis on the role of uniform and controlled thermal fields in the reactor on sulfur recovery.
- ❖ Assemble a flameless oxidation furnace reactor that can also operate in the normal combustion mode (PI and UMD).
- ❖ Conduct experiments using flameless and flame combustion over a range of dynamic conditions determined in the numerical study (UMD).
- ❖ Provide a preliminary design of the reactor for enhanced sulfur recovery. Determine the extent of sulfur recovery from different concentrations in the gas stream (PI and UMD).

Conclusions

- ❖ Higher total concentration of H_2O and CO_2 results in higher SO_2 concentrations.
- ❖ Availability of CO_2 provides an additional pathway to the production of SO_2.
- ❖ The reaction $CO_2 + SO \Leftrightarrow SO_2 + CO$ contributes to producing more SO_2 if CO_2 concentration is high.
- ❖ Availability of OH (mainly from H_2O) prevents the dissociation of SO_2 through $SO + OH \Leftrightarrow SO_2 + H$
- ❖ Varying total contaminants concentration from 20 to 60 mol % reduces S_2 recovery by 45%.
- ❖ Detailed kinetic mechanisms are essential to capture effect of gas phase kinetics on the Claus furnace operation.

Thank you

?Questions?

Additional Slides

S_2 Dominant Reactions :

- **Region A-C**

$2SH \Leftrightarrow S_2 + H_2$ $HS_2 + OH \Leftrightarrow S_2 + H_2O$

$HS_2 + M \Leftrightarrow S_2 + H + M$ $HS_2 + S \Leftrightarrow S_2 + SH$

$SH + S \Leftrightarrow S_2 + H$

$HS_2 + H \Leftrightarrow S_2 + H_2$

$HS_2 + O \Leftrightarrow S_2 + OH$

- **Region C-D**

$HS_2 + M \Leftrightarrow S_2 + H + M$

$S_2 + H_2 \Leftrightarrow 2SH$

$HS_2 + S \Leftrightarrow S_2 + SH$

$S_2 + H_2 \Leftrightarrow HS_2 + H$

SO_2 Dominant Reactions in region A-B:

$SO + O_2 \Leftrightarrow SO_2 + O$

$2SO \Leftrightarrow SO_2 + S$

$HSO + O_2 \Leftrightarrow SO_2 + OH$

$SO + OH \Leftrightarrow SO_2 + H$

$HSO + O \Leftrightarrow SO_2 + H$

$HOSO(+M) \Leftrightarrow SO_2(+M) + H$

$HOSO + O_2 \Leftrightarrow SO_2 + HO_2$

CO_2 Concentration Profile

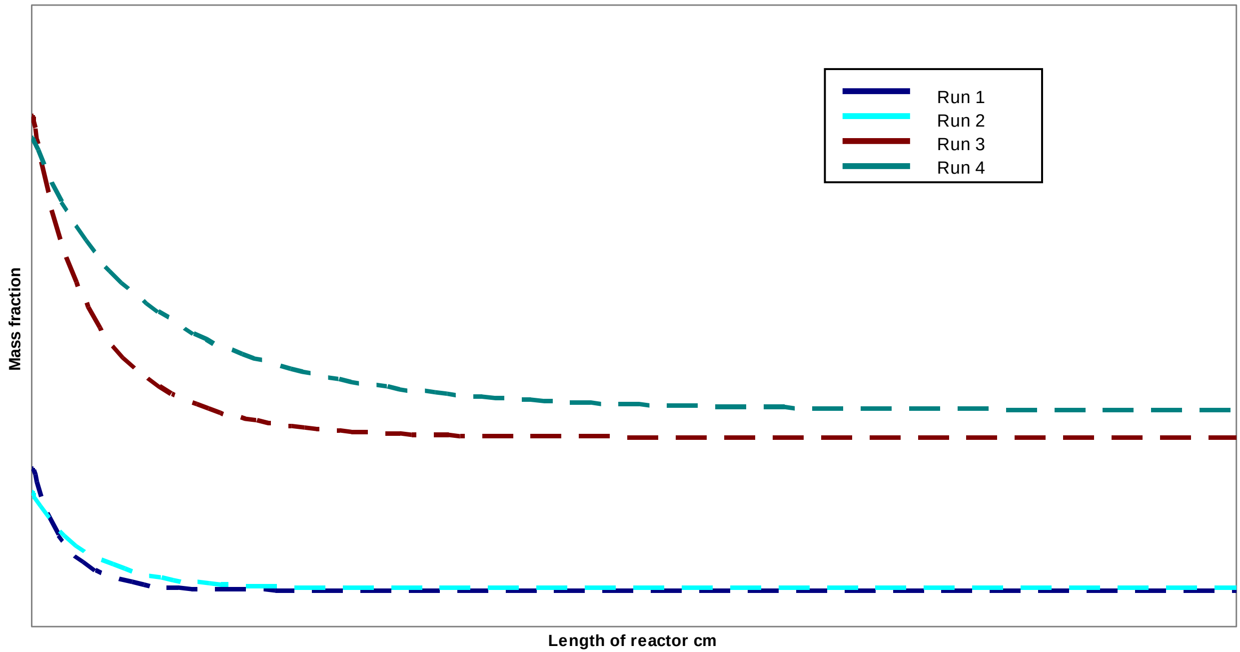

The rapid decrease of CO_2 in run 3 compared to 4 and run 1 compared to 2 is attributed to the high SO production in runs 1 and 3 (due to the longer reverse behavior of SO+OH⇔SO_2 + H and 2SO ⇔SO_2) thus more CO_2 reacts with SO through SO_2+CO⇔CO_2+SO.

Region C-D

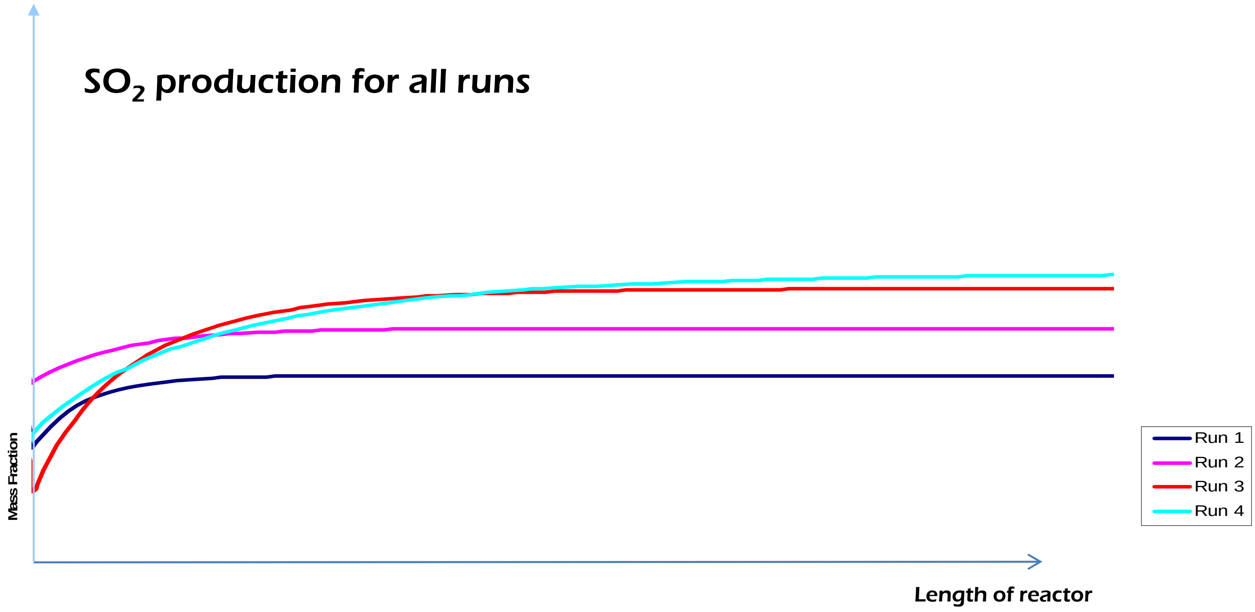

Selection and Optimization of Miscible and Immiscible Displacement to Improve Production from Fractured Carbonate Reservoirs of Abu Dhabi

CSM Team: Jeff Brown, PhD Candidate
Dr. M. Kazemi & Dr. E. Ozkan

PI Team: Dr. Ghedan

1st Annual PI Partner Schools Research Workshop
The Petroleum Institute, Abu Dhabi, U.A.E.
January 6-7, 2010

PI Partners

PI Sponsors

CSM GEOSCIENCE/ ENGINEERING TEAM

Dr. Rick Sarg (GE)

Dr. Hossein Kazemi (PE)

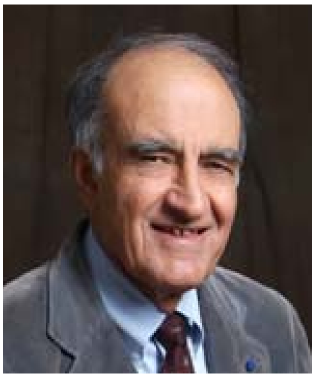

Dr. Manika Prasad (PE)

Dr. Mike Batzle (GP)

Dr. Ramona Graves (PE)

Dr. Erdal Ozkan (PE)

MISSION

- The research projects reported in the following slides were designed to produce the greatest amount of oil from **Zakum field**.

- In addition, these projects were designed as part of an educational process for the UAE graduate students studying at CSM, and a means for collaboration and technology transfer to the Petroleum Institute.

Background

- Thamama 1A Research Program consists of **FIVE** CSM/PI projects.

- The **research group** is an **integrated team** of petroleum engineers, geologists, petrophysicists, and geophysicists from CSM and PI.

Presentation Outline

- Background
- Objectives
- Results and Discussions
- Project Status
- Conclusions and Summary

Project Objectives

Selection and Optimization of Miscible and Immiscible Displacement to Improve Production from Fractured Carbonate Reservoirs of Abu Dhabi

(Kazemi, Ozkan, Ghedan)

Primary graduate student

Jeff Brown, PhD Candidate

"A physically based compositional simulation model for CO2 flooding"

Results and Discussions

- Numerical modeling - computer code being developed for compositional CO2.
- Finalized literature search and methodology.
- Working with Aramco’s technology reservoir modeling team on developing new computer code.

Project Status

- Code is being developed.
- Simulations cases are being developed.

Project Objectives

Special Project

New Developments in Numerical Modeling for Petroleum Reservoirs

(Kazemi)

Primary graduate students

Mohammed Al-Kobaisi (PI), PhD candidate

“Multiphysics multiscale simulation of water-oil flow in single & dual-porosity reservoirs”

Results and Discussions

Simulation Characteristics

- Full permeability tensor
- Permeability directionality in dual-porosity models

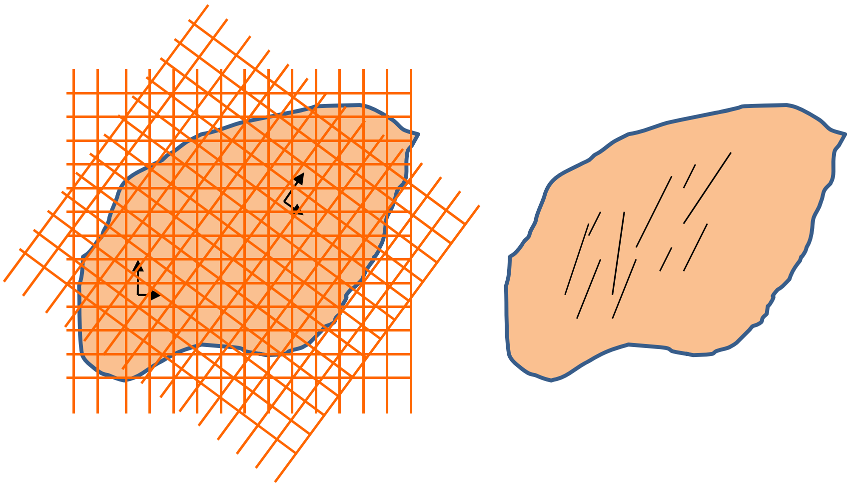

Results and Discussions

Finite-Difference : K_θ Approach

$$\boxed{\frac{1}{k_\theta}=\frac{\cos^2\theta}{k_{max}}+\frac{\sin^2\theta}{k_{min}}}$$

9-point Cartesian

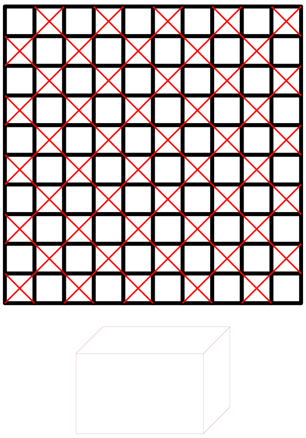

pebi grid

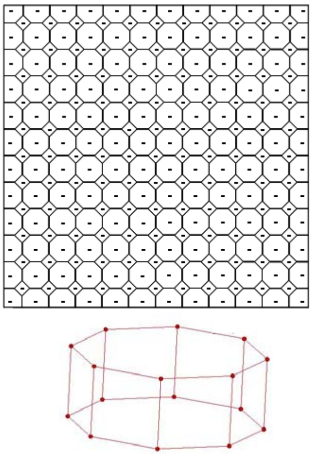

Results and Discussions

Control Volume Mixed Finite-Element

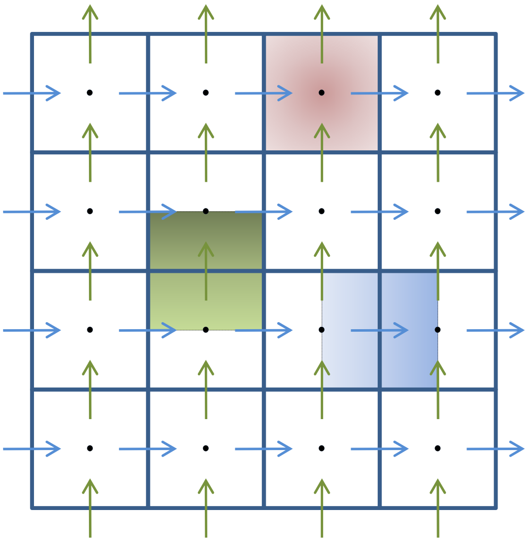

🟥 *p* equation

🟦 *u* equation

🟩 *v* equation

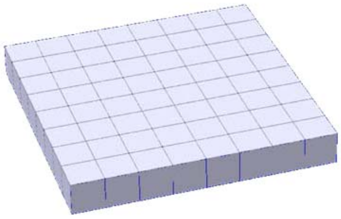

Results and Discussions

Incident Matrices

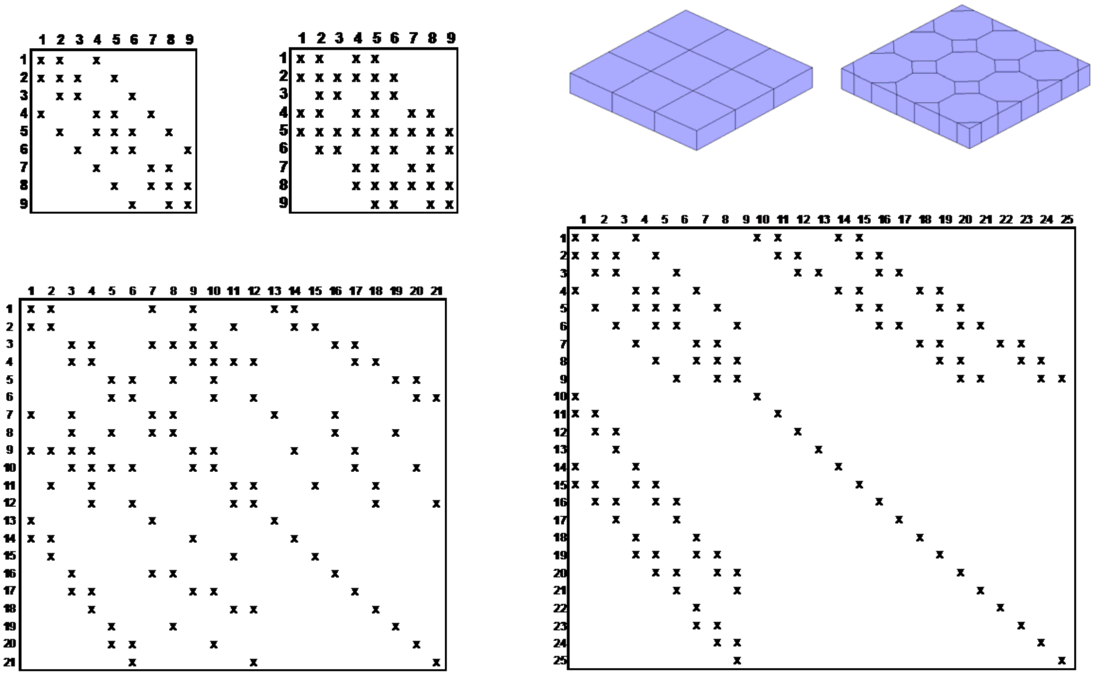

Results and Discussions

Waterflood in a homogeneous anisotropic reservoir: kmax=1000 md, kmin=10 md

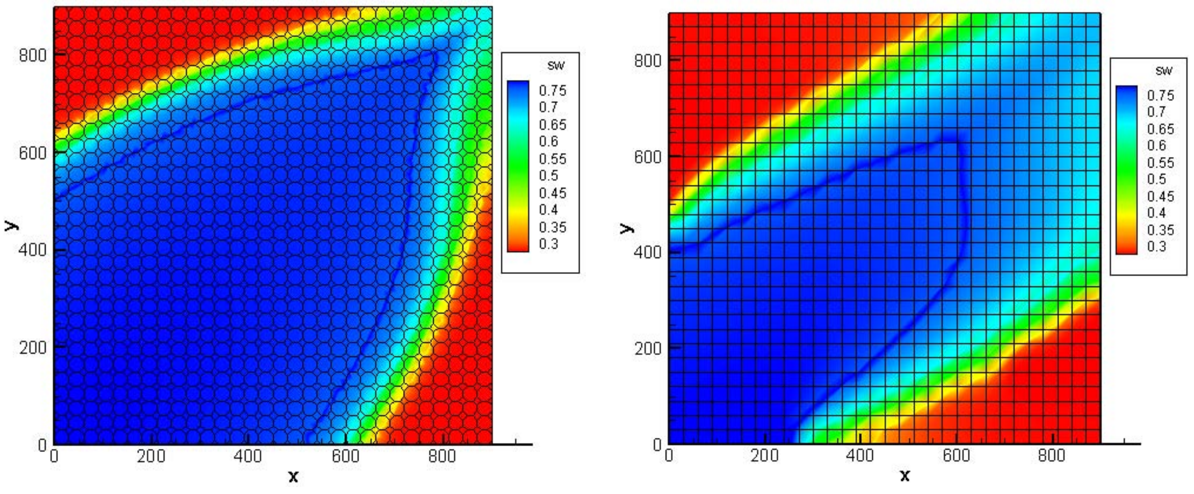

FD K_θ

CVMFEM

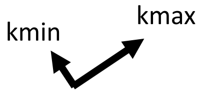

Results and Discussions

Waterflood in a heterogeneous reservoir

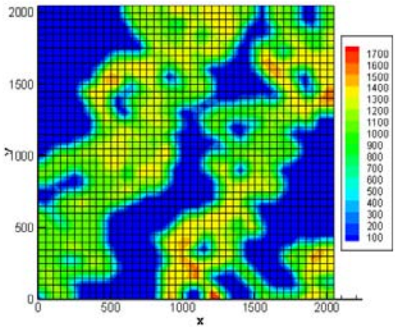

Permeability Distribution

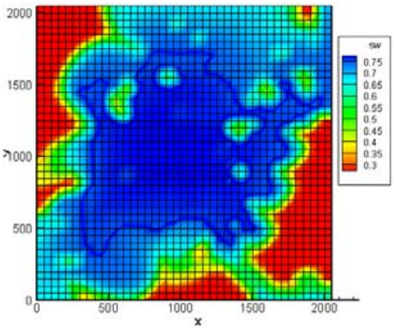

FD

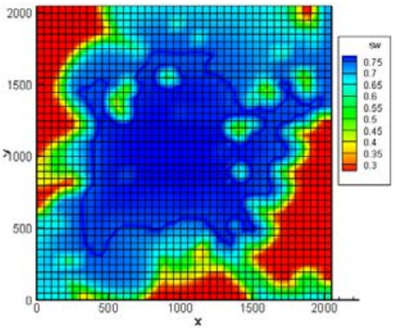

CVMFEM

Results and Discussions

Dual-porosity, CVMFEM

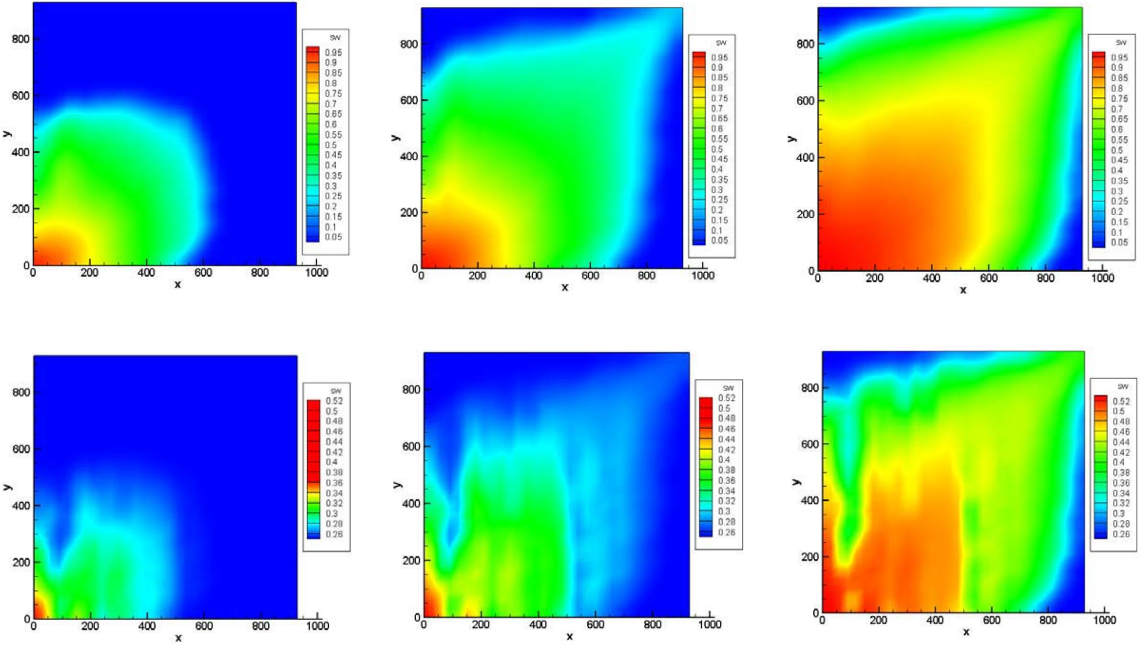

Fracture

Matrix

50 days

200 days

850 days

Results and Discussions

Multiscale Simulation

- **HR mesh: 99x99x1**
- **LR mesh: 33x33x1**

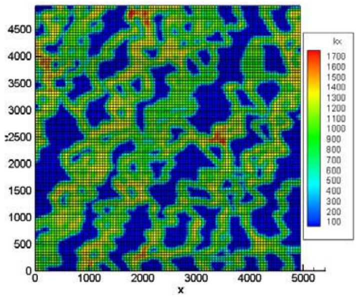

Permeability Distribution

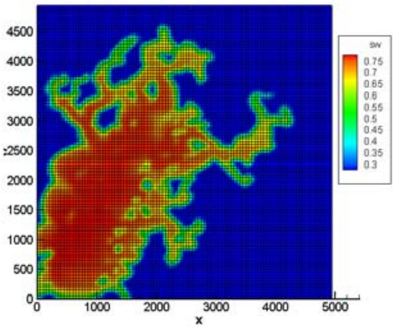

Reference FD

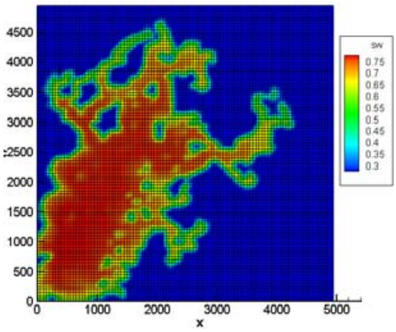

MSFD

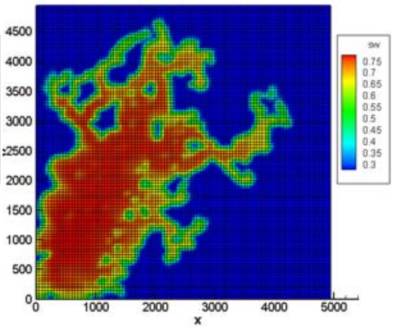

MSCVMFEM

Project Status

- Code for a new dual-porosity formulation
- using a *control-volume, mixed finite- element discretization technique was developed.*
- All simulations cases are completed
- Modeling, results, conclusions, and recommendations will be completed by June 2010. (Mohammed Al-Kobaisi dissertation written and defended).

Conclusions and Summary

The formulation is unique in the sense that it is capable of accurately computing flow at two scales —one at the fracture-matrix scale, and the second at the reservoir interwell scale. The computing requirement for this mixed finite-element technique is much greater than in an analogous *control-volume finite-difference formulation using directional permeability* concept to account for the permeability tensor anisotropy.

Solid Oxide Fuel Cells for CO_2 Capture and Enhanced Oil Recovery

UMD Team: Prof. Greg Jackson, Prof. Bryan Eichhorn,
Siddharth Patel, and Lei Wang
PI Team: Prof. Ali Almansoori and Ahmed Nafees

1st Annual PI Partner Schools Research Workshop
The Petroleum Institute, Abu Dhabi, U.A.E.
January 6-7, 2010

PI Partners

PI Sponsors

Presentation Outline

- Background
- Objectives
- Experimental Setup
- Results and Discussions
- Project Status
- Conclusions and Summary

Background

- Solid oxide fuel cells (SOFCs) can produce concentrated CO_2/H_2O in anode exhaust
  - Potential integration of carbon capture in large stationary plants
- Can SOFCs be developed for operating on hydrocarbon off-gases from petroleum processing for CO_2 capture and/or EOR?
- Current commercial SOFCs employ porous Ni/YSZ anodes which can provide steam reforming of carbon-based fuels
  - Carbonaceous and sulfur-containing fuels in Ni/YSZ anodes can lead to carbon deposition and/or irreversible loss in performance
- Ceria (CeO_2)-based anodes have potential to minimize carbon deposition and to operate stably with some sulfur in fuels (Gorte et al.)
- Can CeO_2-based SOFC anodes and SOFC stacks be developed for applications in petroleum processing for off-gas utilization?

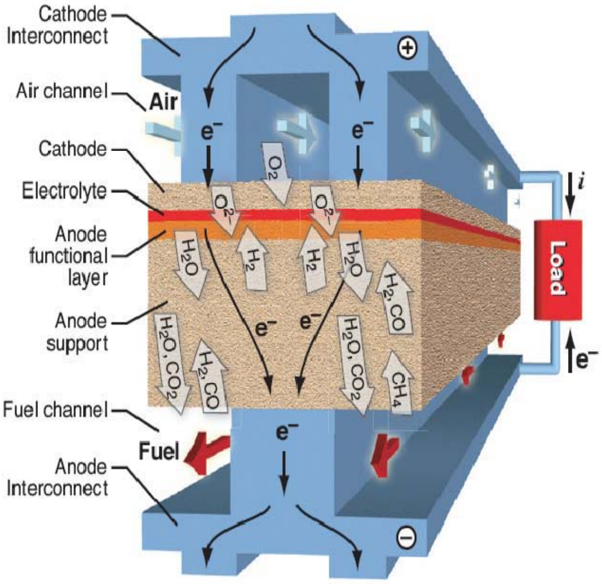

from Kee, Zhu, Sukeshini, and Jackson 2008

Project Objectives

- Establish single-cell SOFC performance to enhance and validate existing single-cell SOFC models to incorporate the effects of hydrocarbon composition and H_2S on SOFC performance.
- Translate single cell models to full stack evaluations in higher dimensions and incorporate into process-level plant models.
- Explore the impact of petroleum off-gas composition (direct hydrocarbon feeds vs. externally reformed feeds) and contaminants (H_2S and HCl) on SOFC performance/design.
- Evaluate the effectiveness of SOFC's for capturing energy from petroleum gases and for providing a means for possible CO_2 capture within a plant context.
- Garner interest from ADNOC partners to explore with the team possible design and challenges for a future SOFC systems operating on relevant petroleum gas streams.

Experimental Setup

- Performance (linear sweep voltammetry (LSV) and electrochemical impedance spectroscopy (EIS)) of SOFC's measured in button cells with effective area of 0.7 cm^2
- Stagnation flow feeds for anode-supported cells with set-up for re-using cells
- Porous Anode: Ni/YSZ, Ni/CeO$_2$/YSZ
  - CeO$_2$ co-fired with Ni/YSZ @ 1450°C to form ceria zirconates in anode support
  - Support layer: $\delta_{an,supp}$ = 1000 μm, $\varphi_{an,supp} \approx 0.57$
  - Functional layer: $\delta_{an,func} \approx$ 20 μm, $\varphi_{an,func} \approx 0.23$
- Dense YSZ electrolyte: δ_{elec} = 10 – 20 μm
- Porous Cathode: LSM/YSZ fired @1300°C
  - δ_{cath} = 30-50 μm with $\varphi_{cath} = 0.27$
- Ag mesh current collectors with Ag leads

from DeCaluwe, Zhu, Kee, and Jackson (2008)

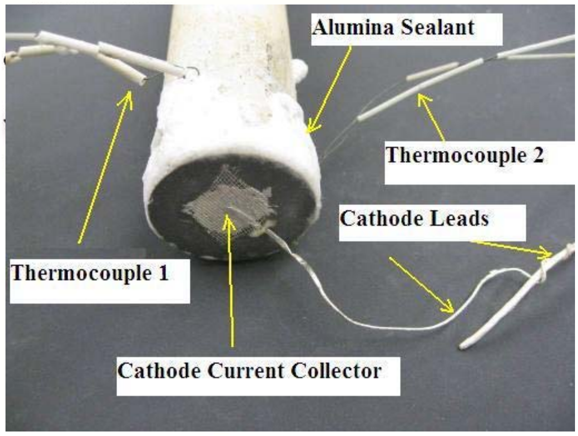

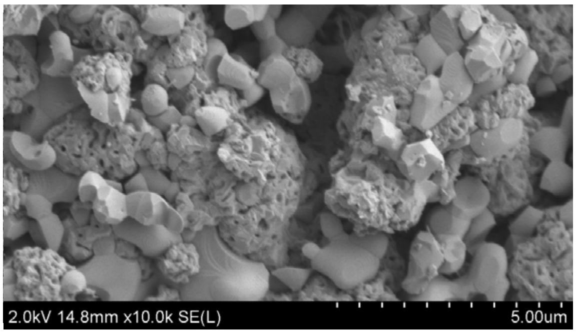

Experimental Setup

- Ni/YSZ & Ni/CeO$_2$/YSZ anode-supported cells tested for direct n-C$_4$H$_{10}$ + steam feeds and for reformate feeds at range of fuel conversions to represent down the channel performance in stacks
- Syngas compositions cover various fuel conversions to simulate different conditions down the channel of a flow-through cell

Anode Fuel Composition	P_{C4H10} (bar)	P_{H2} (bar)	P_{H2O} (bar)	P_{CO} (bar)	P_{CO2} (bar)	P_{Argon} (bar)
Butane S/C = 1.5	0.071	0.0	0.429	0.0	0.0	0.50
Butane S/C = 1.0	0.10	0.0	0.40	0.0	0.0	0.50
Syngas: 0% Conversion	0.0	0.651	0.082	0.215	0.052	0.0
Syngas: 25% Conversion	0.0	0.499	0.234	0.151	0.116	0.0
Syngas: 50% Conversion	0.0	0.328	0.405	0.105	0.162	0.0

Material Characterization: Ni/CeO_2/YSZ Anodes

- Formation of NiO due to leakage through electrolyte pinholes leading to irreversible cracking at high current densities (Menzler et al. 2007)
- Cerium zirconates (likely $Ce_2Zr_2O_7$) has thermo-mechanical stability in in redox cycles at temperatures in excess of 800 K (Trovarelli, 2002)
- XRD reveals formation of cerium zirconates in the anode after sintering
- Ceria addition reduces carbon buildup and cracking with hydrocarbon feeds

XRD of Ni/CeO_2/YSZ co-fired anodes

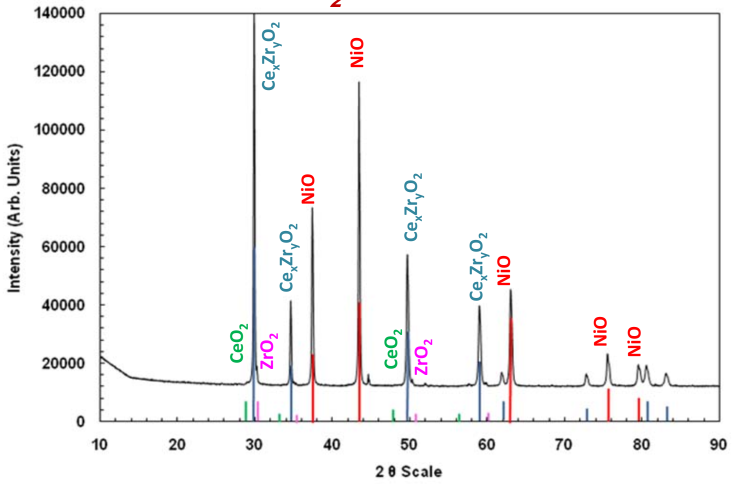

Images of button cell anodes after testing for days with C_4H_{10}/H_2O feeds

Electrochemical Characterization

- Linear sweep voltammetry (LSV) used to compare anodes to assess impact of ceria addition on cell performance
  - Initial testing of cells with 97% H_2/3% H_2O anode feeds followed by testing in syngas and then longer-term testing with direct C_4H_{10}/H_2O feeds
  - Evaluation of cathode and electrolyte overpotentials (η) to isotate η_{anode} due to carbonaceous feeds.
- Electrochemical impedance spectroscopy (EIS) shows impact of anodes and fuels
  - Low frequency process (associated with anode transport grows significantly with C_4H_{10}/H_2O feeds

Linear sweep voltammetry for Ni/YSZ and Ni/CeO_2/YSZ anodes

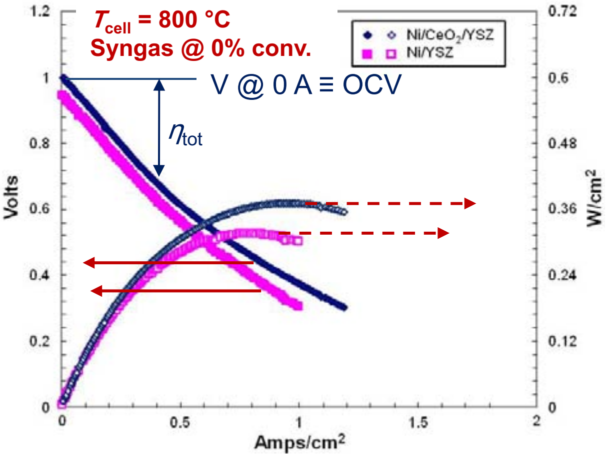

Electrochemical impedance spectra at 100 mV total cell overpotential for different anode/fuel compositions

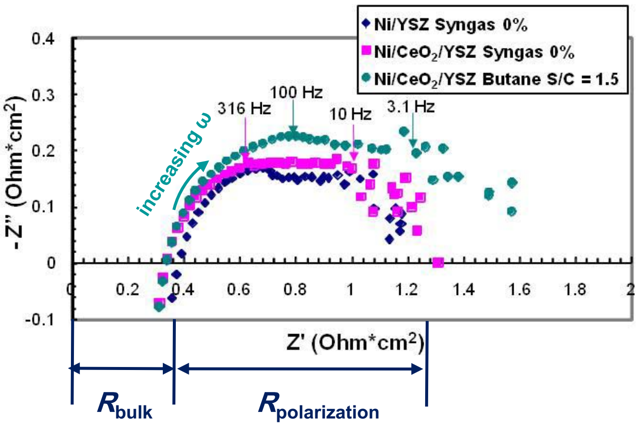

Performance of Ni/CeO_2/YSZ Anodes on Reformate (Syngas)

- Ni/CeO_2/YSZ with thin (10 µm) electrolyte provides performance of ~ 0.4 W/cm^2 at 0.75 V operating on syngas at 800 °C.
- Ni/CeO_2/YSZ anode performance show comparable performance for H_2 and syngas for syngas conversions up to 50%

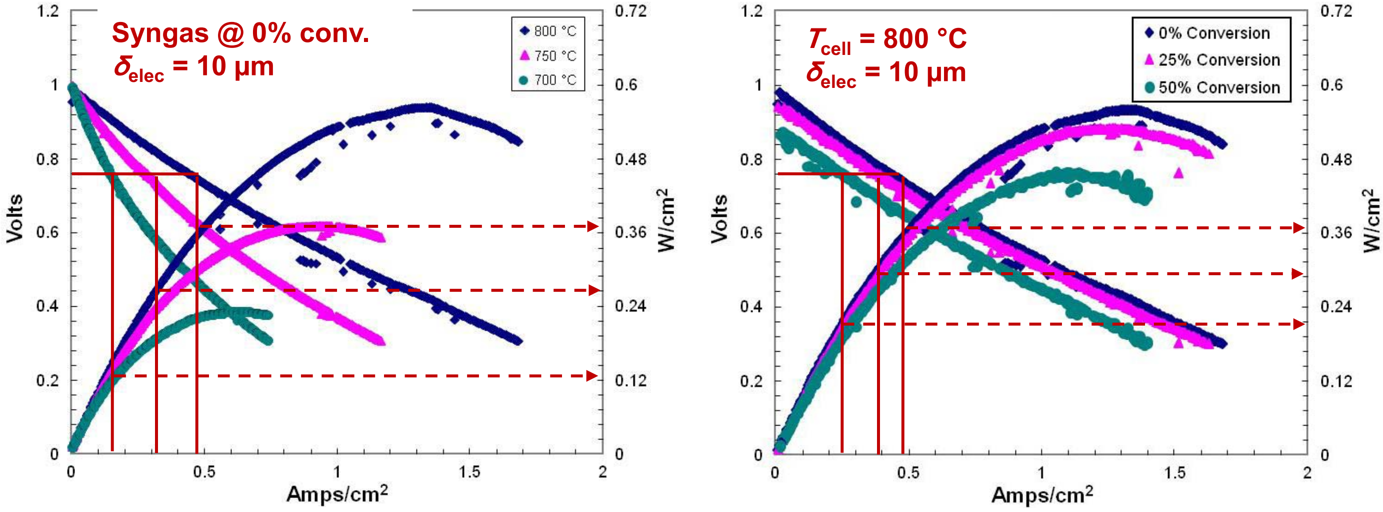

Performance Comparison between Ni/YSZ & Ni/CeO_2/YSZ for Direct Butane fFeeds

- Comparison of voltage and power density vs. current density curves for Ni/CeO_2/YSZ and Ni/YSZ anode supported MEA's: n-C_4H_{10} feeds with S/C = 1.0 and 1.5 (electrolyte: 20 µm)
- Improved performance (by 25% higher power density) most significant at $i > 0.3$ A/cm^2 due to reduction in R_{pol} (by about 15%)

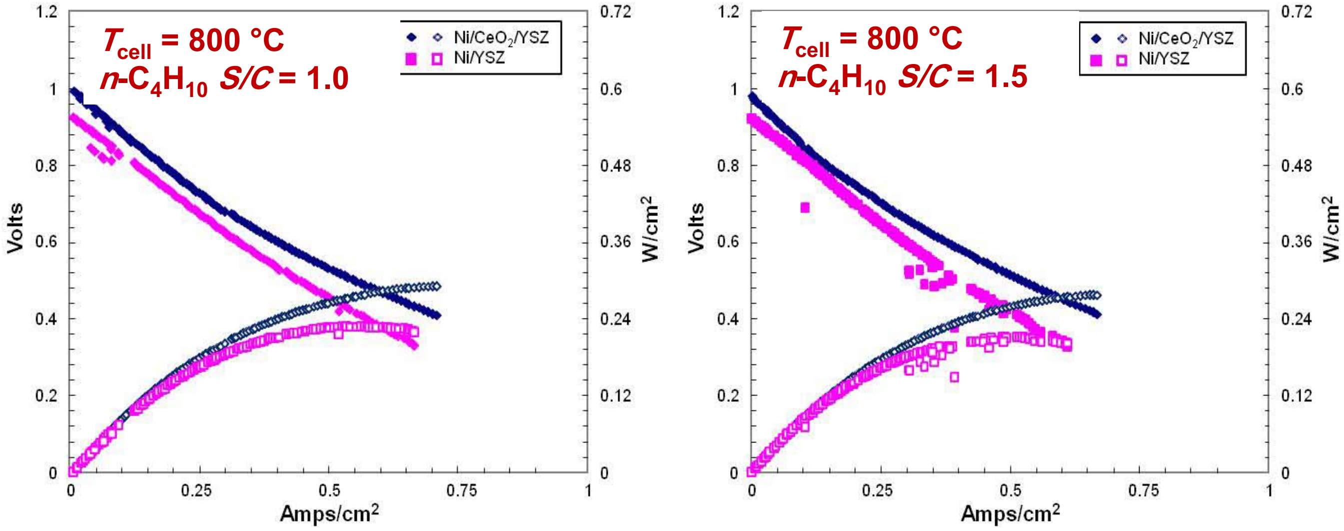

Stability of Ni/CeO$_2$/YSZ Operating with Butane

- Direct C_4H_{10} feeds doubles area-specific polarization resistance relative to H_2 feeds
- With δ_{elec} = 20 µm, stable ASR for operation with direct C_4H_{10} feeds at total overpotential (0.1-0.3 V) continuously for up to 6 days

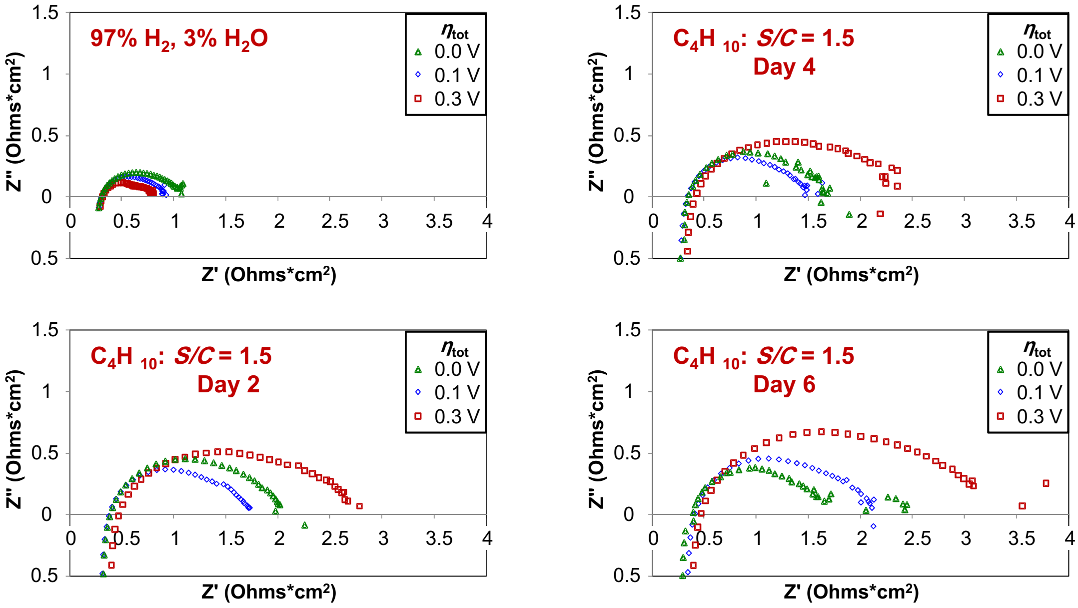

Stability of Ni/CeO$_2$/YSZ Operating with Butane

- *Ex-situ* Raman spectroscopy on Ni/YSZ & Ni/CeO$_2$/YSZ anode cross sections after multiple days of operating on direct C_4H_{10} feeds at 3 locations
  - Peak intensities are relative to NiO at 1122.5 cm^{-1}
- Graphite growth suppressed for Ni/CeO$_2$/YSZ at 'top' surface layer to the functional layer

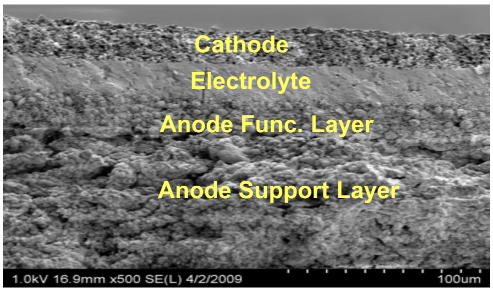

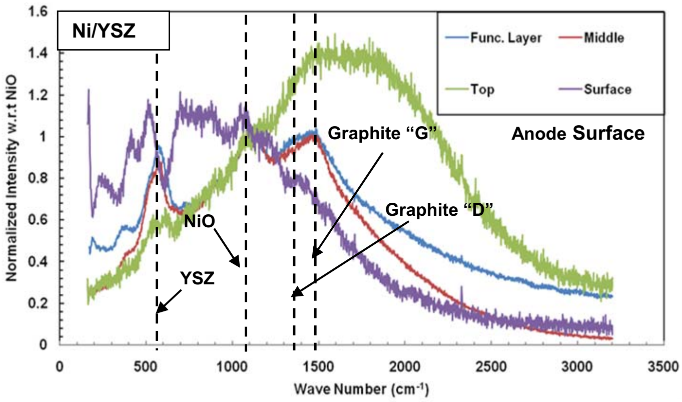

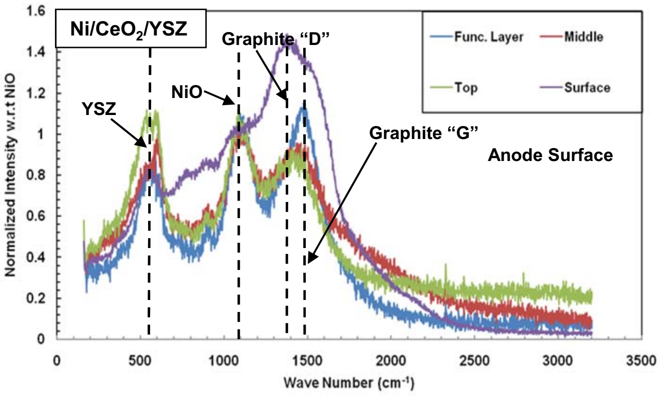

Detailed Models for SOFC’s: Exploring Down-the-Channel Performance with Syngas Operation

- Detailed MEA models explore SOFC performance with syngas or CH_4 fuel
- Results below are for Ni/YSZ anode-supported cell with 1020 μm thick anode, 10 μm thick YSZ electrolyte, and 50 μm thick LSM/YSZ cathode. Operating conditions – 800 °C and for range of H_2/CO feeds at different conversion
  - for two different micro-architectures to provide design guidance.

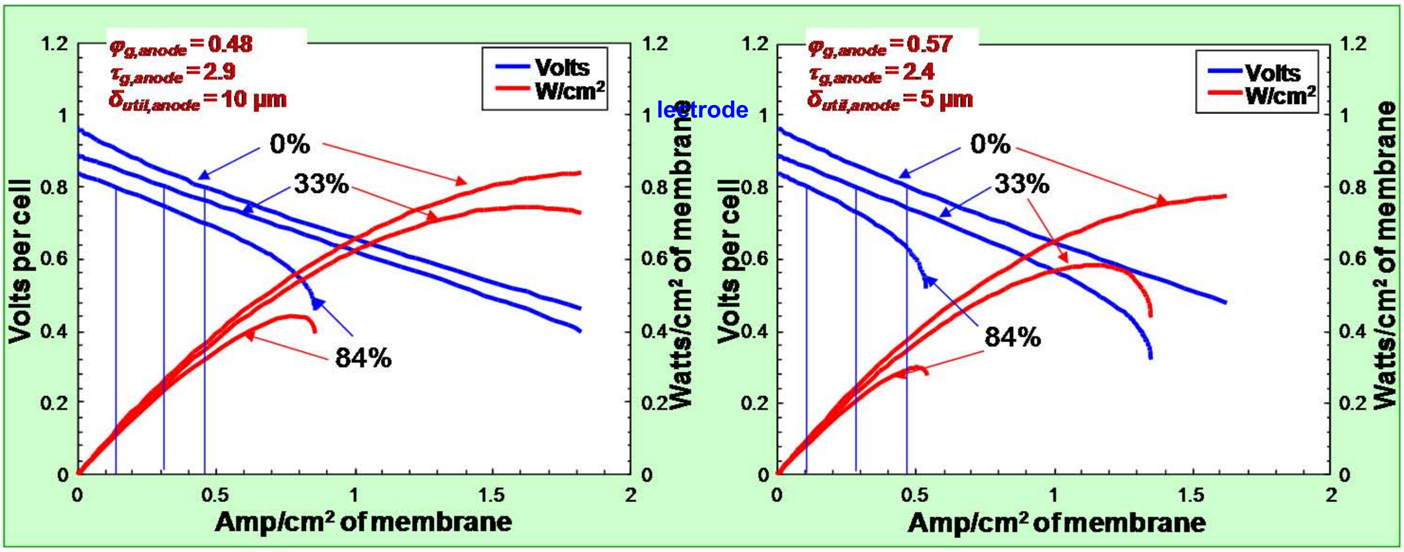

Using Detailed Models for Interpreting Experimental Results

- Using 97% H_2 anode feed data, detailed model used to determine overpotential contributions from cathode and O_2 gas leakage through electrolytes.
- Detailed model shows high sensitivity to key cathode and anode design parameters and these are used to fit results and derive anode overpotentials associated with fuel composition.

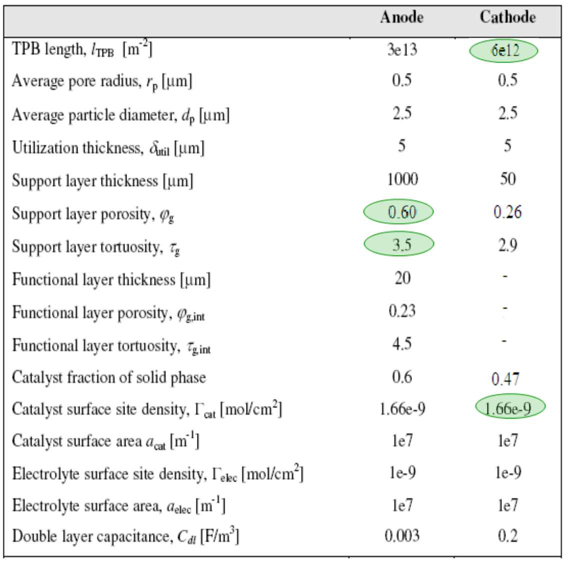

	Anode	Cathode
TPB length, l_{TPB} [m^{-2}]	3e13	6e12
Average pore radius, r_p [μm]	0.5	0.5
Average particle diameter, d_p [μm]	2.5	2.5
Utilization thickness, δ_{util} [μm]	5	5
Support layer thickness [μm]	1000	50
Support layer porosity, φ_g	0.60	0.26
Support layer tortuosity, τ_g	3.5	2.9
Functional layer thickness [μm]	20	-
Functional layer porosity, $\varphi_{g,int}$	0.23	-
Functional layer tortuosity, $\tau_{g,int}$	4.5	-
Catalyst fraction of solid phase	0.6	0.47
Catalyst surface site density, Γ_{cat} [mol/cm^2]	1.66e-9	1.66e-9
Catalyst surface area a_{cat} [m^{-1}]	1e7	1e7
Electrolyte surface site density, Γ_{elec} [mol/cm^2]	1e-9	1e-9
Electrolyte surface area, a_{elec} [m^{-1}]	1e7	1e7
Double layer capacitance, C_{dl} [F/m^3]	0.003	0.2

Anode overpotentials from fitting experimental data with detailed moels

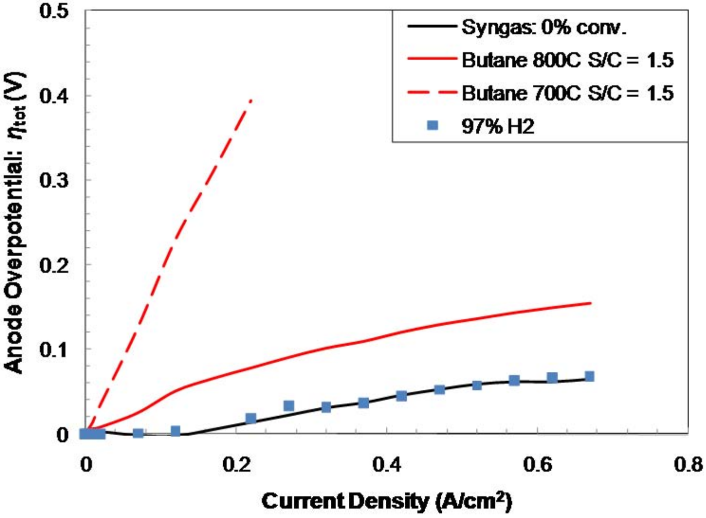

Detailed Model: Non-Isothermal Capabilities

- Detailed “through-the-MEA” model added energy equation to incorporate heating due to electrochemical oxidation and cooling due to endothermic reforming.
- Through-the-MEA model shows that solid-matrix conduction minimizes temperature gradients through the cell
- Only axial gradients in down-the-channel model will show significant gradients.

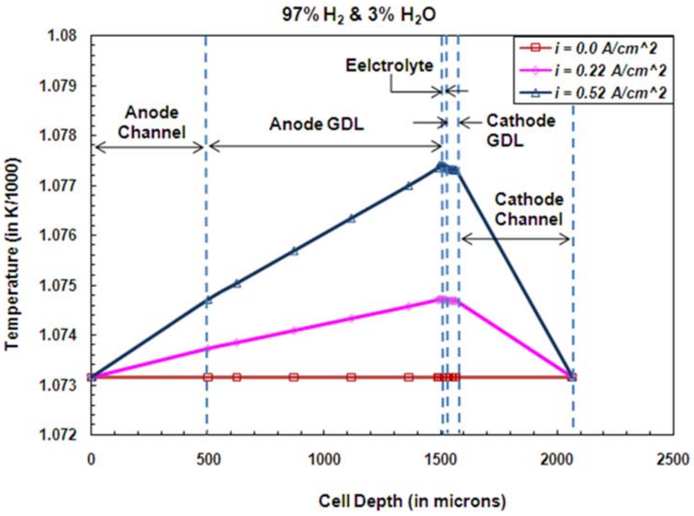

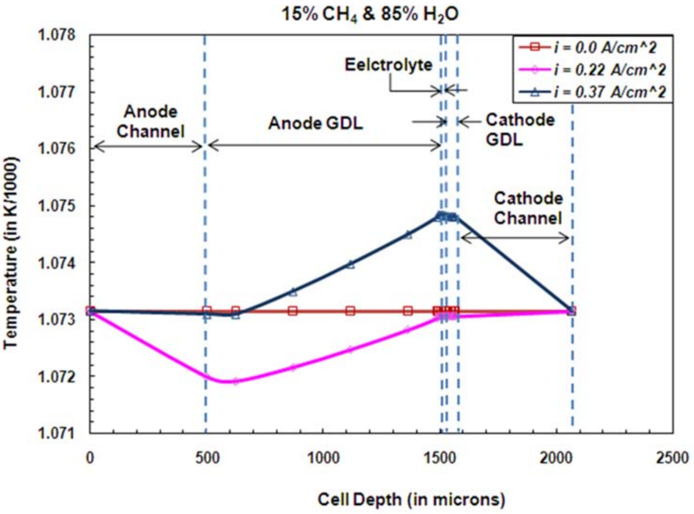

System Modeling in Aspen Hysys: Integrating SOFC Models into Plant Model

- PI/UMD working together to build Aspen/Hysys model based on detailed SOFC models.
- Selected plant for initial testing includes SOFC, pre-reformer of hydrocarbon fuels, anode exhaust combustor, and Brayton cycle

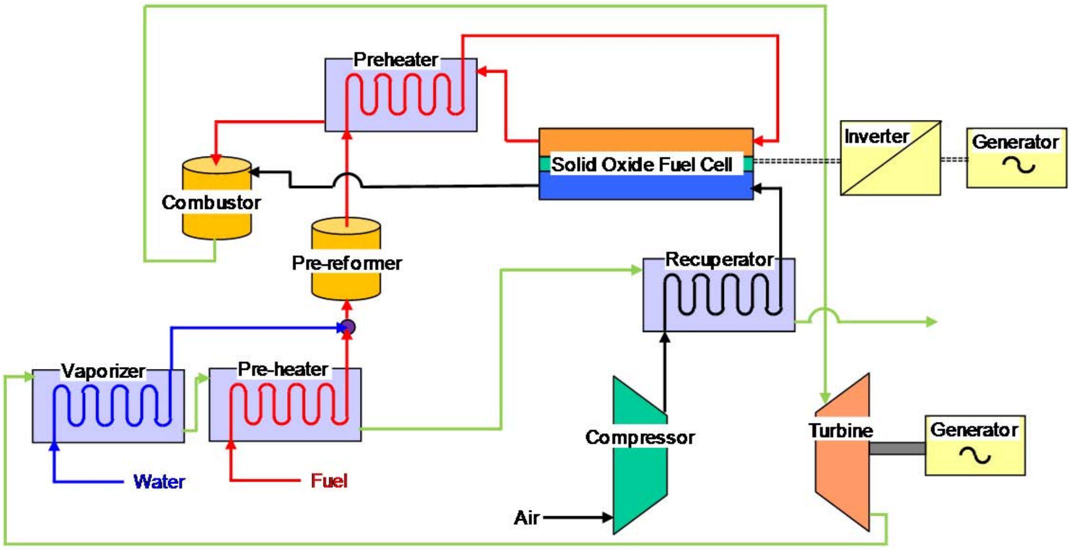

Project Status

- Experimental program
  - UMD has updated rig to handle contaminants and long-term durability testing with contaminant testing to begin in February 2010
  - Initial durability tests of direct butane feeds with Ni/CeO_2/YSZ anodes suggest that pre-reformer may be necessary
  - Further testing with CH_4 will be used to refine internal reforming model with Ni/CeO_2/YSZ anodes
- Modeling efforts
  - PI/UMD working to establish ASPEN modeling capabilities at PI for SOFC plant initially without CO_2 capture.
  - Detailed SOFC models will be updated to include impact of fuel composition (hydrocarbons and contaminants) on cell performance
- Publications
  - UMD/PI refining ASME Fuel Cell conference paper into joint journal publication

Conclusions and Summary

- Ni/CeO_2/YSZ has been identified as a potential hydrocarbon tolerant anode for SOFC applications for petroleum off-gas
  - Formation of cerium zirconates show resistance to cracking and coking
  - *Ex situ* MEA characterization
  - Improved performance with syngas and over direct n-C_4H_{10}/H_2O feeds
- Experimental rig at UMD redesigned for longer-term durability testing and for H_2S- and HCl-contaminated feeds
- Detailed SOFC model has been upgraded to handle CH_4, syngas, leakage through the electrolyte, and non-isothermal conditions.
- Aspen/Hysys model will employ results from detailed SOFC model to predict system level performance within petroleum plant applications.

Process Intensification and Advanced Heat / Mass Transfer

Multidisciplinary Design and Characterization of Polymer Composite Seawater Heat Exchanger Module

UMD Team: Avram Bar-Cohen, David Bigio, Hugh Bruck, S.K. Gupta, Juan Cevallos, Tim Hall, Patrick Luckow, William Pappas, and Frank Robinson
PI Team: Peter Rodgers and Mohammad Chowdhury

1st Annual PI Partner Schools Research Workshop
The Petroleum Institute, Abu Dhabi, U.A.E.
January 6-7, 2010

PI Partners

PI Sponsors

Presentation Outline

- Introduction
- Task #1: Study thermal characteristics of polymer composite HX
- Task #2: Study manufacturability of injection molded polymer composite HX
- Task #3: Study seawater effects on structural properties of polymer composite HX
- Task #4: Create and experimentally characterize a large polymer composite HX module
- Conclusions

Motivation

- Heat exchangers in seawater applications require use of exotic metals due to corrosion, scaling, and biofouling concerns
  - Usually Titanium alloys (Thermal conductivity around 20 W/m-K)
  - Require frequent maintenance due to scaling problems
- Advances in polymer composites have resulted in polymers with high thermal conductivities
- The cost of polymer heat exchangers and the energy investment in fabrication are expected to be considerably lower than their metal counterparts
- Polymer heat exchangers can be used in seawater applications
- Designing long lasting cost effective polymer heat exchangers presents many new challenges

Company	**Resin**	**Thermal Cond. (W/m-K)**
Cool Polymers	PPS	20
Sabic IP	PPS	7
PolyOne	PPS	10-11
PolyOne	LCP	18-20
PolyOne	PA 12	10
RTP	LCP	18
Ovation Polymers	PC	6.10

Goal

- Develop a systematic approach for designing polymer heat exchangers that accounts for all life cycle considerations:
  - Thermal Performance
  - Structural Performance
  - Manufacturability
  - Life Cycle Cost (e.g., Manufacturing, Installation, Operation, Maintenance)

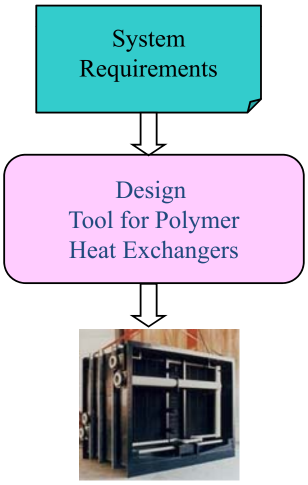

System Requirements

Design Tool for Polymer Heat Exchangers

Polymer Heat Exchanger with Optimal Geometry and Material

Approach

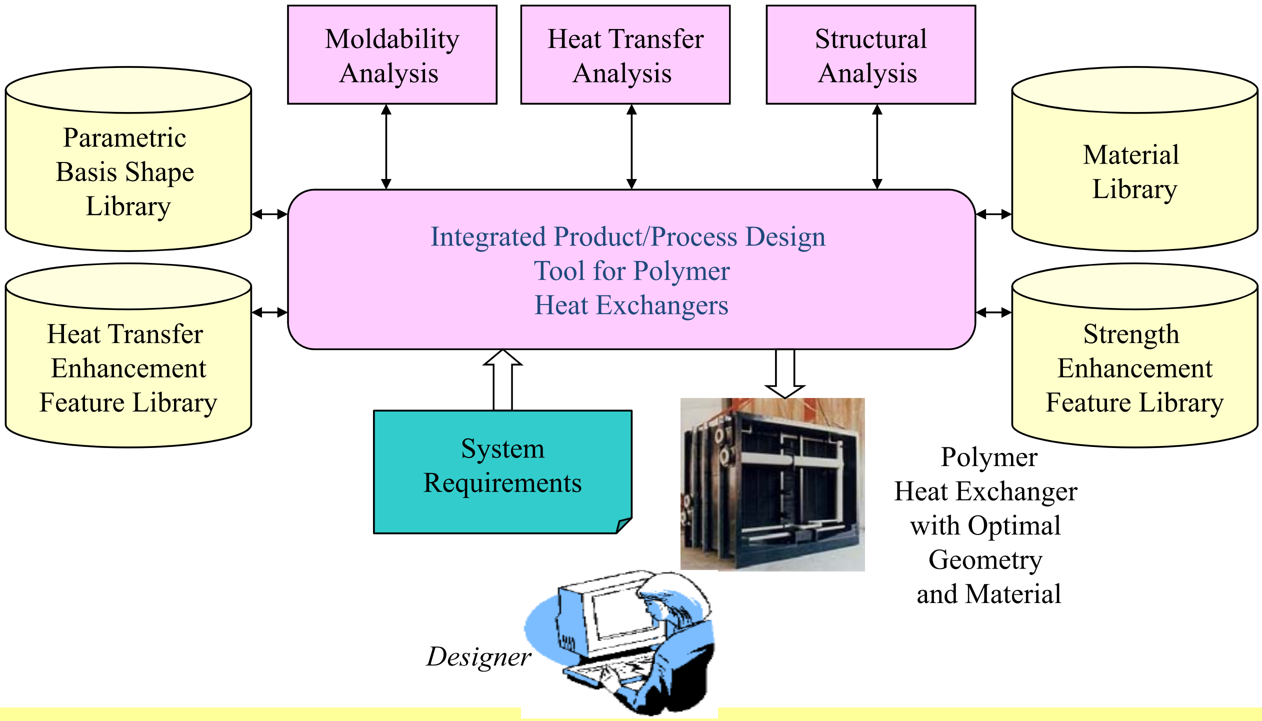

Moldability Analysis

Heat Transfer Analysis

Structural Analysis

Parametric Basis Shape Library

Heat Transfer Enhancement Feature Library

Integrated Product/Process Design Tool for Polymer Heat Exchangers

Material Library

Strength Enhancement Feature Library

System Requirements

Polymer Heat Exchanger with Optimal Geometry and Material

Designer

Task #1: Study thermal characteristics of polymer composite HX

Background

- Mechanical and thermal properties of fiber-filled composites can be highly anisotropic
- Fiber orientation in a part varies spatially depending on molding parameters
- Thermal conductivity of a composite varies according to orientation, leading to anisotropy

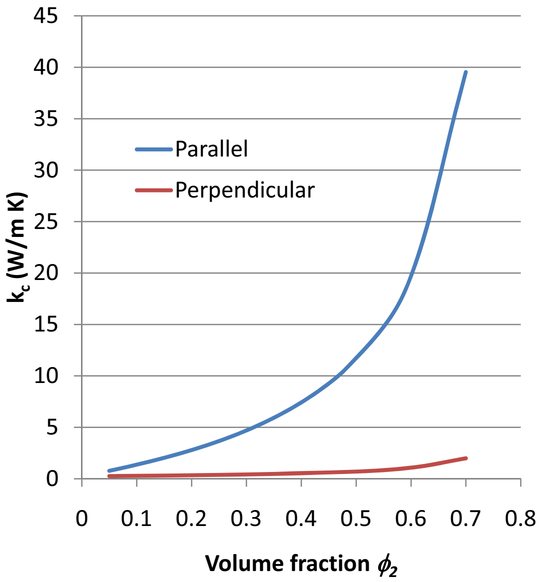

Uniaxially oriented fibers (Nielsen model 2002)
k_2 = 700 W/mK, k_1 = 0.25 W/mK, ϕ_m=0.82

Task Objectives

- Study thermal characteristics of polymer-composite geometries through an integrated molding-heat transfer modeling methodology
- Investigate the effect of fiber orientation on thermal conductivity
- Study the differences in heat transfer performance of anisotropic and isotropic materials in a representative heat exchanger geometry

Approach

- Numerical predictions of the fiber orientation in a representative geometry were obtained using a popular injection-molding software (Moldflow®) based on the Folgar-Tucker model
- These predictions are used, via the classic Nielsen model, to determine the anisotropic variation of thermal conductivity in the fin
- Thermal simulations are then performed to determine the effect of both global and local thermal anisotropy on the temperature distribution and heat transfer rate of the fin

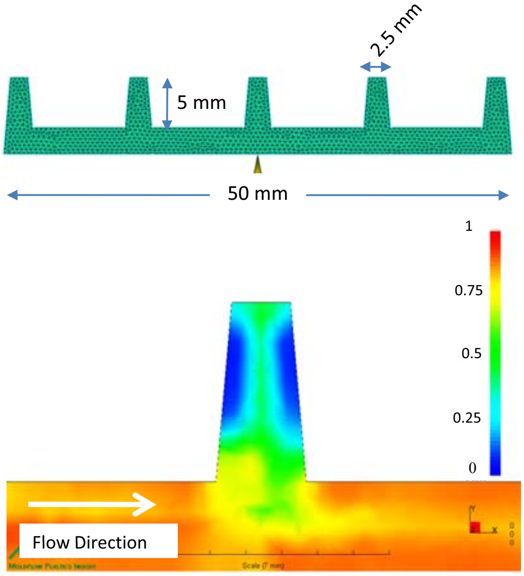

A_{xx} Fiber orientation in the x-direction (across the fin thickness)
Material used in study: Nylon 12 filled with carob fibers

Results: Converting Fiber Orientation Tensors to Thermal Conductivity

Orientation tensor values in x and y directions (as predicted by Moldflow®)

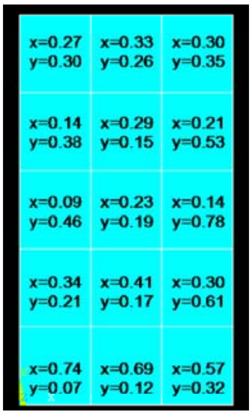

x=0.27 y=0.30	x=0.33 y=0.26	x=0.30 y=0.35
x=0.14 y=0.38	x=0.29 y=0.15	x=0.21 y=0.53
x=0.09 y=0.46	x=0.23 y=0.19	x=0.14 y=0.78
x=0.34 y=0.21	x=0.41 y=0.17	x=0.30 y=0.61
x=0.74 y=0.07	x=0.69 y=0.12	x=0.57 y=0.32

Using Nielsen's equations for thermal conductivity of composites

Anisotropic thermal conductivity values

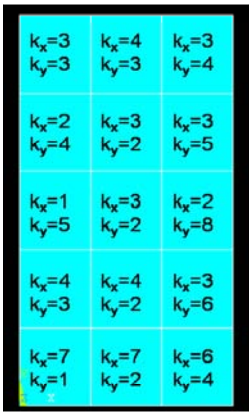

k_x=3 k_y=3	k_x=4 k_y=3	k_x=3 k_y=4
k_x=2 k_y=4	k_x=3 k_y=2	k_x=3 k_y=5
k_x=1 k_y=5	k_x=3 k_y=2	k_x=2 k_y=8
k_x=4 k_y=3	k_x=4 k_y=2	k_x=3 k_y=6
k_x=7 k_y=1	k_x=7 k_y=2	k_x=6 k_y=4

Results: Influence of Global Thermal Conductivity Anisotropy

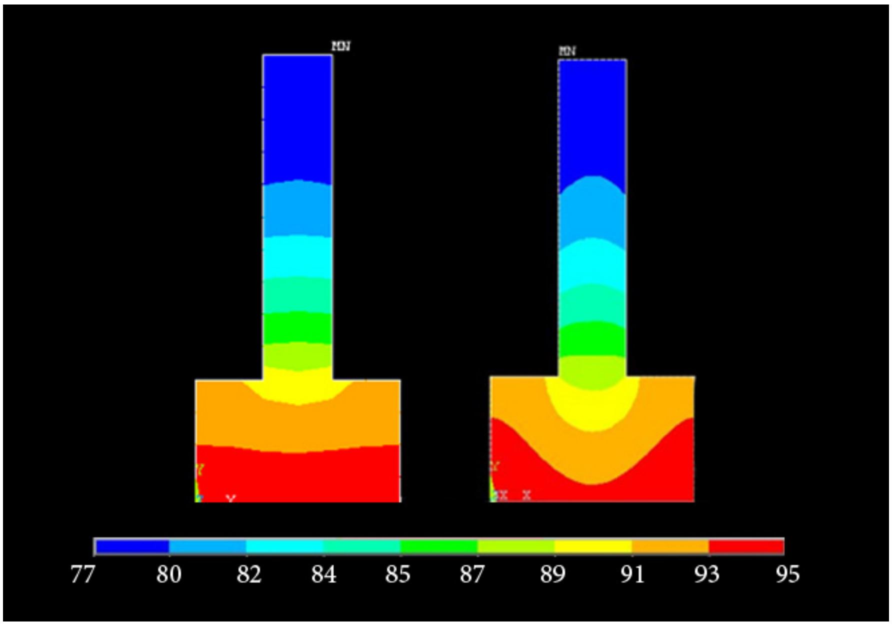

Temperature distribution in a rectangular plate fin, Isotropic fin (left) k_x= k_y=5 W/m·K, and Anisotropic fin (right) k_x=1 W/m·K, k_y=5 W/m·K, W=3mm, H=5mm, t_b=2mm,t_f=1mm,h=30 W/m^{2}K, Base heat flux 1000 W/m^{2}K

Results: Influence of Local Thermal Conductivity Anisotropy

heat transfer coefficient 40W/m^{2}K

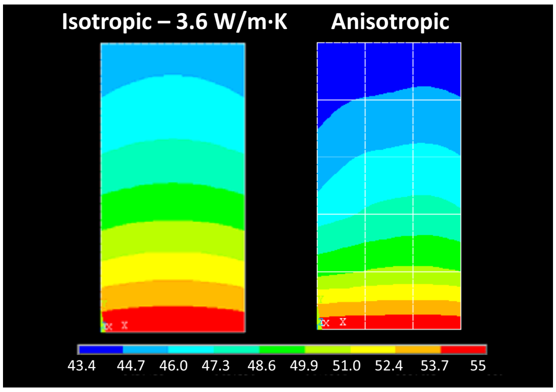

- Excess temperature at the tip of the anisotropic fin is 1.8K lower than the isotropic case
- Heat transfer rate through the base of the fin is also lower by 1W relative to the 30.1W for the isotropic fin
- Thru-thickness variation in anisotropic case up to 1K

heat transfer coefficient 1000W/m^{2}K

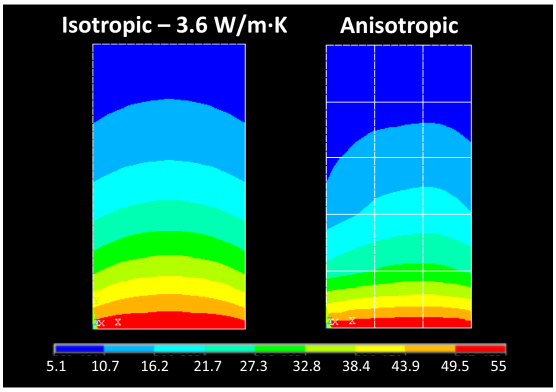

- Excess temperature at fin tip is 1.5K lower for the anisotropic case
- Poorer thermal dissipation of the anisotropic fin (186W to 224.7W)
- Thru-thickness temperature variations in the anisotropic case nearly 5K

Fin dimensions: 2. 5mm thick and 5mm high

Ambient temperature = 298K, Base excess temperature 55K

Results: Effective Isotropic Thermal Conductivity

Ways to determine a single, effective "isotropic" thermal conductivity to represent heat transfer in an anisotropic fin were explored using different "averages"

			Isotropic			
		Anisotropic Solution	Arithmetic Mean of k_y	Geometric Mean of k_y	RMS k_y	Harmonic Mean of k_y
50 W/m^2k	q (W/m)	29.1	30.1	29.7	30.5	29.3
	Error	-	3.6%	2.2%	4.8%	0.9%
200 W/m^2k	q (W/m)	81.6	90.0	87.0	92.8	84.1
	Error	-	10.3%	6.6%	13.7%	3.0%
400 W/m^2k	q (W/m)	121.0	139.1	133.0	145.0	127.2
	Error	-	14.9%	9.9%	19.8%	5.1%
800 W/m^2k	q (W/m)	168.6	201.4	191.0	211.5	181.4
	Error	-	19.5%	13.3%	25.5%	7.70%
1000 W/m^2k	q (W/m)	186.0	224.7	212.7	236.4	201.7
	Error	-	20.8%	14.4%	27.1%	8.5%

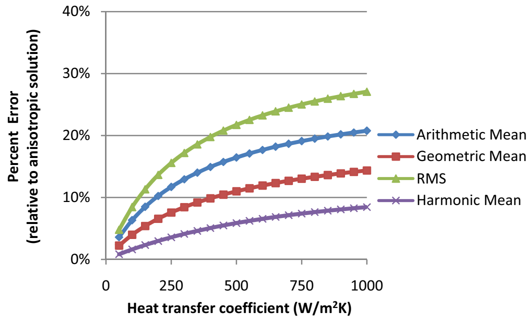

- Errors are small at low h values because the thermal resistance in the fluid dominates the heat dissipation rate
- Errors increase at high h because the conduction in the fin dominates the thermal performance

Summary

- Fiber orientation tensors can be successfully used to predict anisotropic thermal conductivities in heat exchanger geometries
- Global thermal anisotropy resulting from the flow direction can affect the temperature distribution and heat transfer rates from the fins
- Local anisotropy resulting from local variations in the fiber orientation can affect the heat transfer rate in the fins
- The harmonic mean performed best as a candidate for an effective isotropic conductivity
- Errors incurred by estimating an effective thermal conductivity increase whenever the relative magnitude of the thermal resistance due to conduction increases

Future Plans

- Study the thermal characteristics of other heat exchanger surface features (e.g. pin fins, plate coil heat exchangers) and compare the relative merits of each using the same heat transfer-molding modeling methodology
- Directly import information from Moldflow® simulations into ANSYS simulations to predict local anisotropic thermal conductivity in selected geometries and study thermal performance

Task #2: Study manufacturability of injection molded polymer composite HX

Task Objectives

- Characterize manufacturability of injection molded polymer composite HX geometries
- Characterize the influence of molding process parameters on fiber orientation
- Develop meta models for mold filling and fiber orientation for use in the heat exchanger design framework

---

Approach

- Characterize Moldflow® fiber orientation predictions as a function of molding process parameters
- Characterize manufacturability of typical HX features by conducting Moldflow® simulations
- Validate Moldflow® mold filling simulations using experimental data
- Validate Moldflow® fiber orientation predictions using experimental data
- Develop a meta model for fiber orientation predictions and integrate it with the PHX design framework
- Characterize manufacturability of typical HX features by conducting Moldflow® simulations

Results: Experimental Validation of Mold Filling

- Mold filling estimates from Moldflow® were experimentally verified using spiral mold testing
- Percent difference between Moldflow and average experimental results was less than 20%

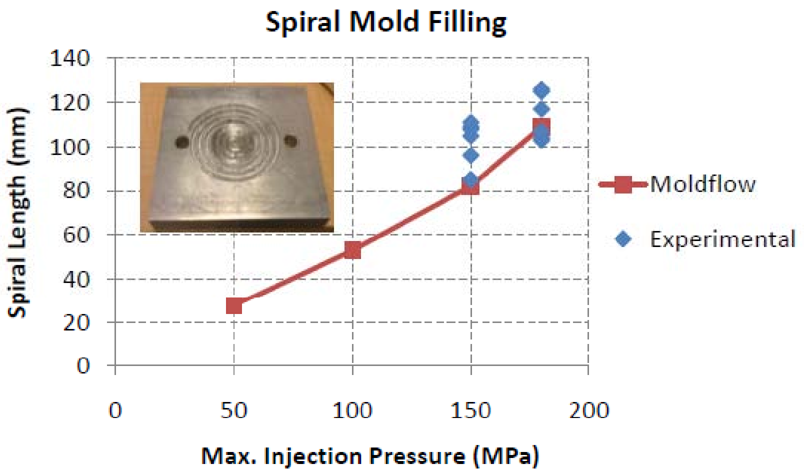
Spiral Mold Filling

Results: Mold Filling Meta Model

- Moldflow® filling analysis used to develop a set of data points within the parametric range selected
- Data points were used for creating a mold filling meta model for the chosen geometry

- The metamodel predicts the percentage of the mold cavity volume that is successfully filled

Finned Plate Geometry

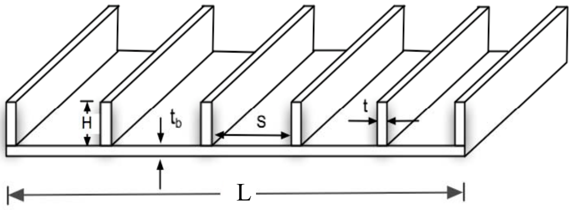

Design Variable	**Parametric Range**
Base length, L	200 mm – 1000 mm
Base thickness, t_b	1 mm – 4 mm
Fin spacing, S	3 mm – 20 mm
Fin thickness, t	1 mm – 5 mm

Sample metamodel plot

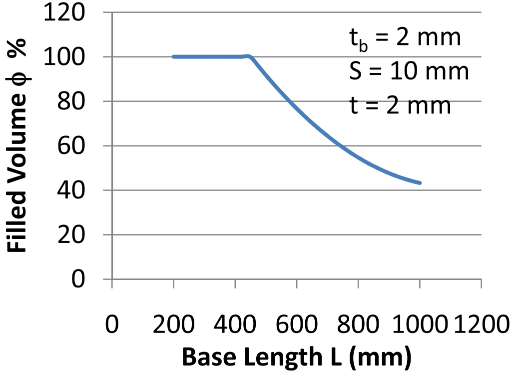

Results: Integrated Life-Cycle Cost Model

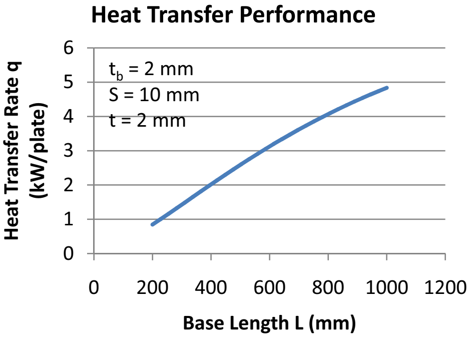
Heat Transfer Performance

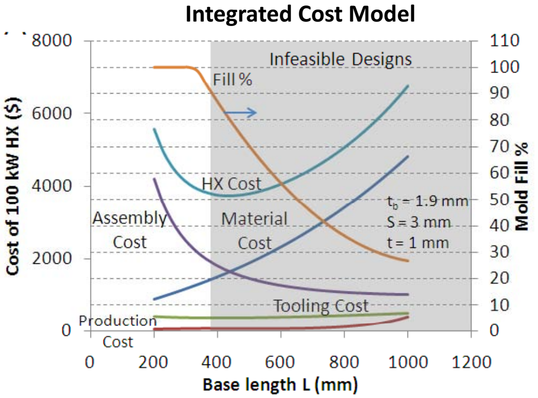
Integrated Cost Model

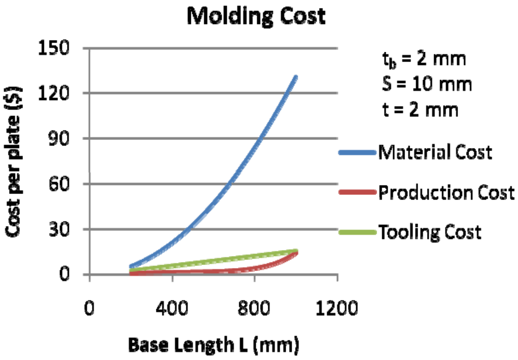
Molding Cost

Optimum Heat Exchanger Plate Geometry

Scenario	L (mm)	t_b (mm)	S (mm)	t (mm)	No. of plates	HX Cost ($)
Material price: $10/lb Assembly cost: $60/hr	382.4	1.9	3	1	62	3,800
Material price: $20/lb Assembly cost: $60/hr	313.6	1.7	3	1	78	5,060
Material price: $10/lb Assembly cost: $120/hr	454.4	2.2	3	1.2	52	5,500
Material price: $10/lb Assembly cost: $60/hr Lifetime:1 year (9.78 c/kWh)	649.6	3.0	3.5	1	42	8,180

Results: Fiber Orientation Prediction Using Moldflow Simulations

- Fiber orientation affects thermal and structural properties of the heat exchanger
- Study the effects of varying injection molding parameters and heat exchanger geometry

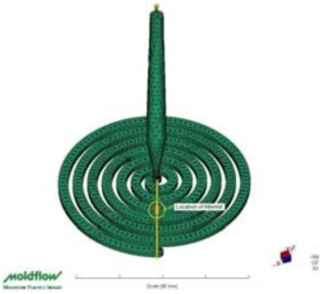
Spiral Mold

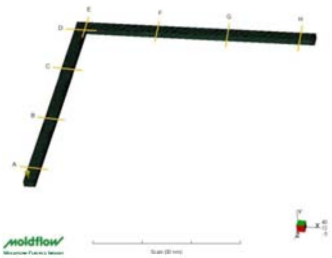
L-Channel Mold

Results: Influence of Fiber Concentration on Fiber Orientation

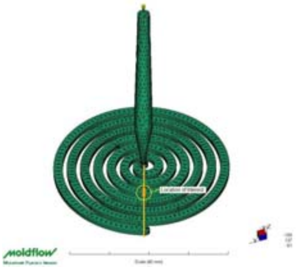

The effect of varying fiber concentration with slow-changing velocity field

Fiber Concentration →

13%

60%

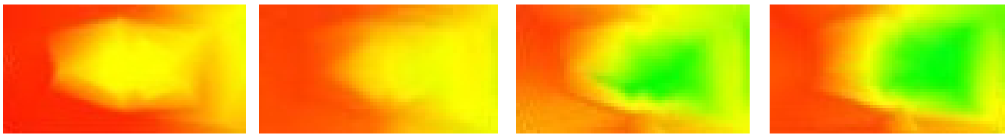

Zytel 70G13L NC010 | Zytel 70G30 HSLR BK039 | Zytel 70G43L NC010 | Zytel 70G60

Note: Variations in % filled could be a result of additives used to decrease the viscosity for highly filled polymers

Results: Influence of Process Parameters on Fiber Orientation and Mold Filling

		Fiber Alignment	Mold Filling
Fiber Concentration	↑	↓	⇩
Injection Pressure	↑	=	↑
Injection Flow Rate	↑	=	↑

Note: Open arrow represents a weak correlation

As the fiber concentration increases the material viscosity generally increases causing mold filling to decrease but manufacturers often use additives with highly-filled polymers to decrease viscosity so the correlation is weak

Summary

- The moldability analysis meta model is successfully integrated with a heat transfer model for a system-level optimization model
- Moldability considerations significantly influence the final solution
- The optimum heat exchanger is highly dependent on the values of material price and energy costs

A prototype fabricated in the Advanced Manufacturing Lab

Future Plans

- Refine mold filling meta model to account for different failure modes
- Experimentally validate fiber orientation prediction results
- Develop fiber orientation meta models
- Develop manufacturability rules for typical features found in HX
- Develop new material formulations
- Explore use of extrusion process

Task #3: Study seawater effects on structural properties of polymer composite HX

Background

- Seawater reduces the usable life of exotic metal heat exchangers
- Fiber reinforcement improves mechanical and thermal properties of polymers
- Polymer composite heat exchangers must be carefully designed to reflect the possible effects on thermo-mechanical properties associated with hygrothermal aging

Task Objectives

- Characterize the influence of the seawater on the mechanical properties of polymer composites
- Characterize the influence of the water temperature on the mechanical properties of polymer composites
- Determine how hygrothermally-aged mechanical properties influence the structural design of HX

Approach

- Design and mold test samples
- Immerse test samples in saltwater tanks at different temperatures and concentrations for pre-determined periods
- Measure mechanical properties before and after immersion
- Analyze and correlate the effects of temperature and salt concentration

Experimental Setup

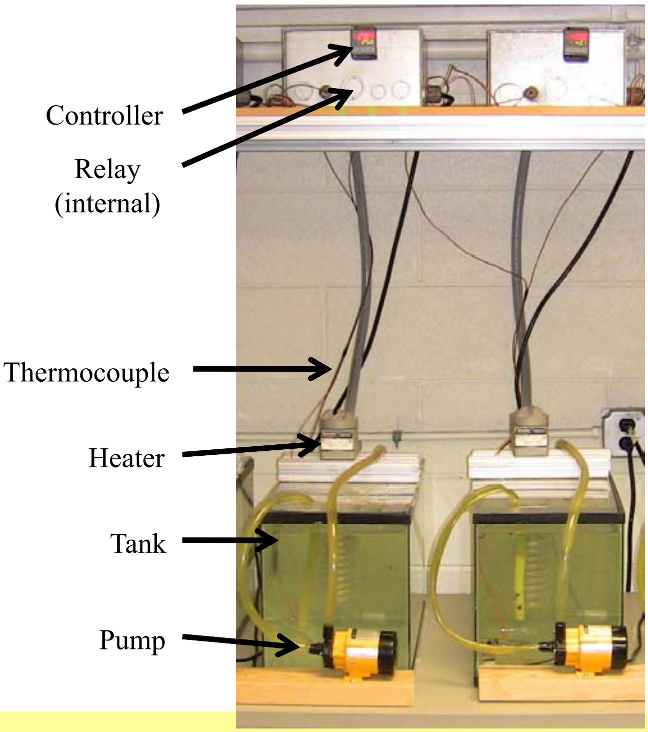

- Test Temperatures
  - 40 ◦C
  - 50 ◦C
  - 60 ◦C
- Test Salinities
  - Freshwater
  - 45 g/kg (representative of salinity in Arabian Gulf water)
- Temperatures monitored using LabVIEW
- Pumps prevent temperature and salinity stratification

Experimental Parameters

- ASTM standard tensile specimens
- 12 unreinforced PA12 and 12 reinforced PA12 specimens were immersed in each bath
- Six specimens of each material were left unaged for baseline comparison
- Immersion time based on diffusion times from previous study; confirmed by repeating weight measurements until additional immersion time no longer increased moisture content

Results: Effect of Aging Temperature on Unreinforced PA12

Temperature (°C)	Elastic Modulus (GPa)	Yield Strength (MPa)	Elongation at Yield (%)	Ultimate Strength (MPa)
40	0.73	19.9	3.0	43.6
Percent Retention	50.7%	50.0%	100%	105%
50	0.69	18.7	2.9	42.3
Percent Retention	49.3%	46.9%	99.3%	101%
60	0.69	17.9	2.8	38.3
Percent Retention	49.3%	45.0%	96.6%	91.7%

Results: Effect of Aging Temperature on Reinforced PA12

Temperature (°C)	Elastic Modulus (GPa)	Yield Strength (MPa)	Elongation at Yield (%)	Ultimate Strength (MPa)	Elongation at Failure (%)
40	14.0	55.6	0.62	84.5	2.8
Percent Retention	66.4%	69.0%	105%	82.0%	192%
50	16.0	53.2	0.56	84.9	3.0
Percent Retention	75.8%	66.0%	94.9%	82.3%	205%
60	11.6	54.4	0.70	84.8	3.1
Percent Retention	54.9%	67.5%	119%	82.3%	212%

Results: Comparison of Unreinforced and Reinforced PA12

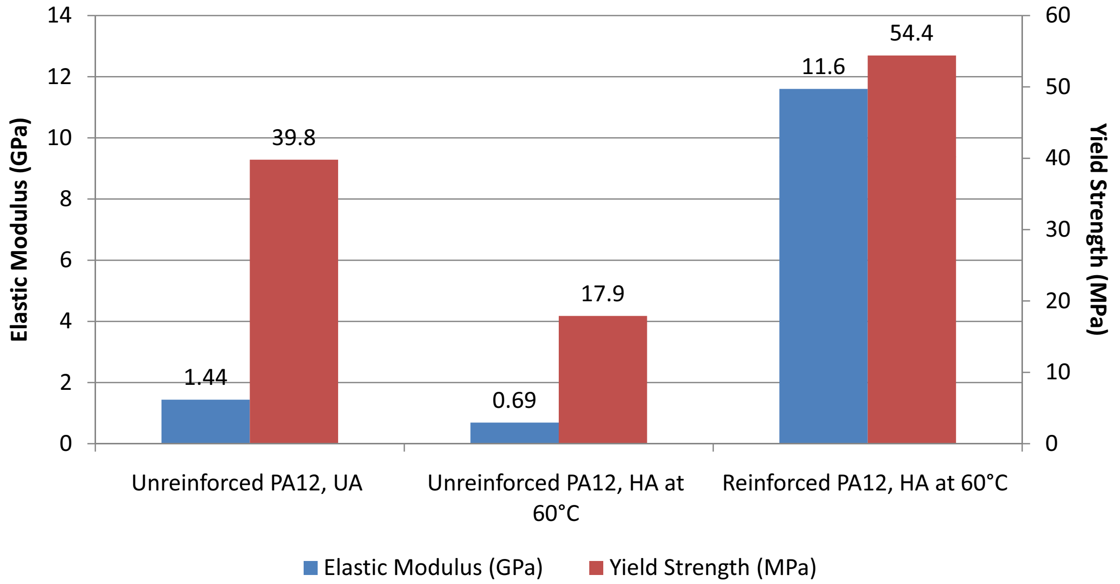

Summary

- Hygrothermally-aged reinforced PA12 retains 55%-82% of unaged properties while increasing in ductility
- Reinforced PA12 HA properties still significantly better than unaged unreinforced PA12 properties
- Increasing salinity to 45 g/kg does not significantly affect equilibrium moisture content or tensile properties of unreinforced or reinforced PA12
- Increasing water temperature from 40 to 60°C has no effect on equilibrium moisture content but does tend to reduce yield strength, ultimate strength, and elastic modulus and increase ductility at yield and failure

Future Plans

- Hygrothermally-age specimens at 25°C to determine whether absorbed moisture or temperature is responsible for deterioration of mechanical properties
- Investigate deterioration of polymer fiber interface
- Develop structural analysis model using hygrothermally-aged mechanical properties

---

Task #4: Create and experimentally characterize a large polymer composite HX module

Polymer Composite HX Module Prototype

PI Injection molding machine (ENGEL Victory 70)

Inlet Conditions:
U_{air} = 10 m/s at 90 °C
U_{water} = 0.5 m/s at 35 °C

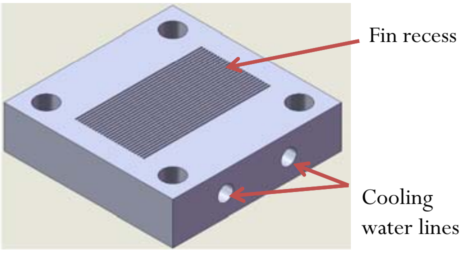

Moving injection mold part (air side module)

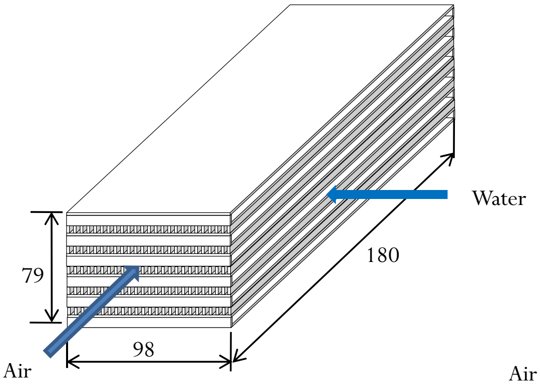

Single fin module

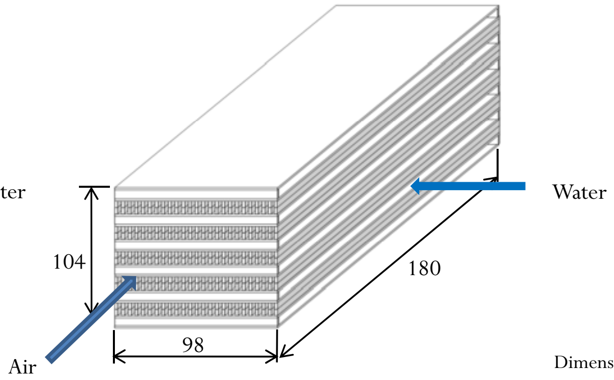

Double fin module

Dimensions in mm

Polymer HX Test Facility Concept Design

- Air Side:

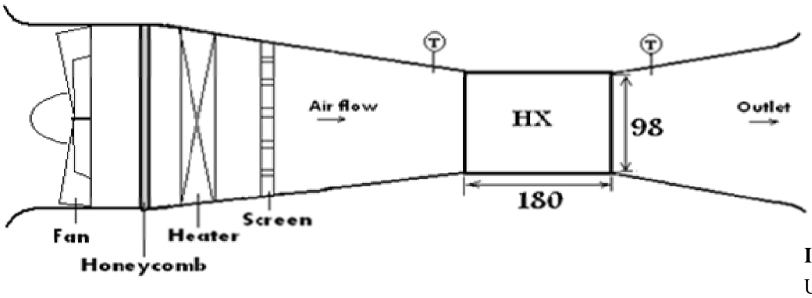

- Water Side:

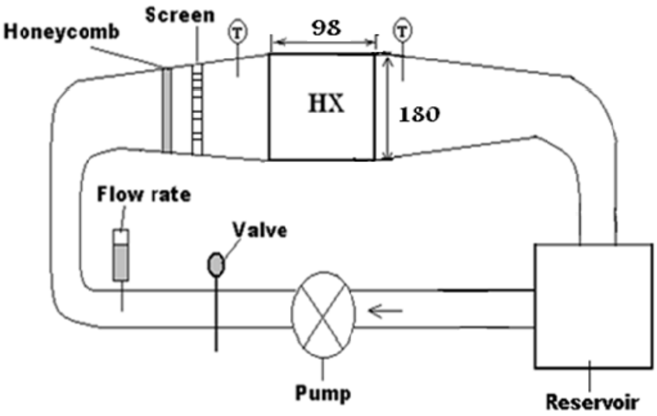

Inlet Conditions:
U_{air} = 10 m/s at 90 °C
U_{water} = 0.5 m/s at 35 °C

Single fin module:
Q_{total} = 443 W
ΔP_{air} = 211 Pa
ΔP_{water} = 148 Pa

Double fin module:
Q_{total} = 725 W
ΔP_{air} = 168 Pa
ΔP_{water} = 148 Pa

Future Plans

- Manufacture of prototype HX injection molds using PI CNC facilities.
- Polymer HX injection molding process to be developed using polyethylene and thermally enhanced polymer composite (Poly One: EM1000631360).
- Construction and commissioning of HX thermal characterization test facility.
- Thermal performance of prototype polymer HX modules to be characterized and assessed against numerical and empirical predictions.

Conclusions

Current Project Status

- Seven publications
- A test stand for an air-water crossflow HX was built and has been successfully used for experiments
- An experimental setup has been constructed for measuring mold filling
- Molds have been machined to successfully manufacture small polymer composite HX
- Six water baths with temperature regulation and stirring mechanisms have been constructed to conduct hygrothermal aging studies
- An analytical model of the thermo-fluid performance of several heat exchanger geometries has been constructed
- A mold filling meta model has been developed and integrated with thermal performance assessment module

Summary

- Project is on track to meet planned deliverables
- Preliminary findings indicate that polymer composites are a promising material for heat exchanger applications
- New materials and geometries will further expand the design space
- Technologies developed as a part of this project will also be useful in many other seawater applications

Electrostatic Gas-Liquid Separation from High Speed Streams—Application to Advanced On-Line/On-Demand Separation Techniques

UMD or UMN Team: Dr. S. Dessiatoun, Dr. A. Shooshtari
PI Team: Dr. M. Ohadi, Dr. M. Alshehhi, Dr. A. Goharzadeh

1st Annual PI Partner Schools Research Workshop
The Petroleum Institute, Abu Dhabi, U.A.E.
January 6-7, 2010

PI Partners

PI Sponsors

Presentation Outline

- Background
- Objectives
- Experimental Setup
- Results and Discussions
- Project Status
- Conclusions and Summary

Background

- Conventional Separation Technologies
  - Low efficiency
  - High pressure drop
  - Unable to separate very small particles

Inertial Separator

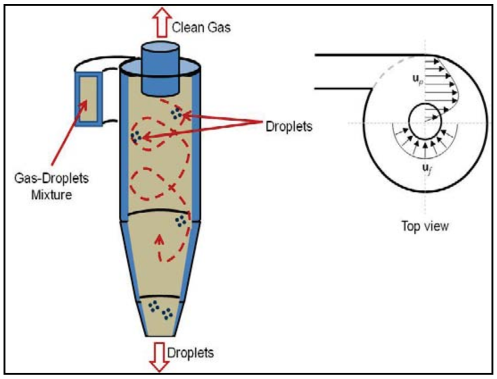

Coalescence Separator

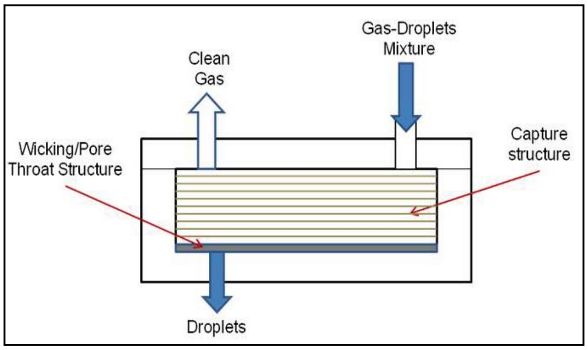

Background

- Feed gas separator
  - Small liquid droplets carrying with the gas flow are effecting downstream process equipment

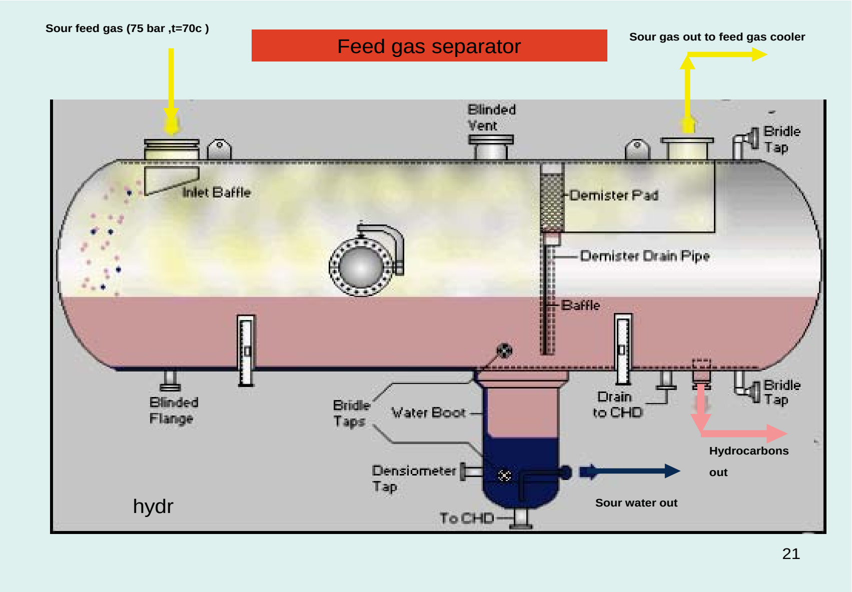

Background

- Electro-static separation
  - High efficiency
  - Low pressure drop
  - Only technique enable separation of submicron particle

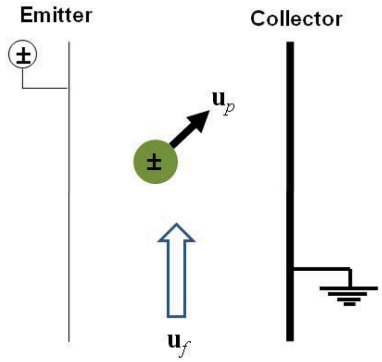

$$\frac{d\mathbf{u}_p}{dt} = C_{F_D}\frac{18\mu_f}{\rho_p d_p{}^2}\left(\mathbf{u}_f - \mathbf{u}_p\right) + \frac{\mathbf{g}(\rho_p - \rho_f)}{\rho_p} + \frac{\mathbf{E}}{{}^1/_6\,\pi d_p{}^3\rho_p}$$

$$\left[\underbrace{\frac{d_p kT_f}{2K_E e}\ln\left(1+\frac{\pi K_E d_p \bar{C}_i e\rho_i t}{2kT_f}\right)}_{\textbf{Diffusion Charging}} + \underbrace{\left(\frac{3\varepsilon_p}{\varepsilon_p + 2}\right)\left(\frac{\mathbf{E}d_p{}^2}{4K_E}\right)\left(\frac{\pi K_E Z_i\rho_i t}{1+\pi K_E Z_i\rho_i t}\right)}_{\textbf{Field Charging}}\right]$$

Background

Diffusion Charging (particles of submicron size)

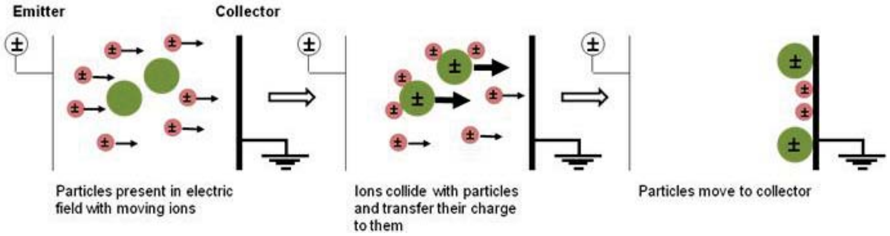

Field Charging (particles of micron size)

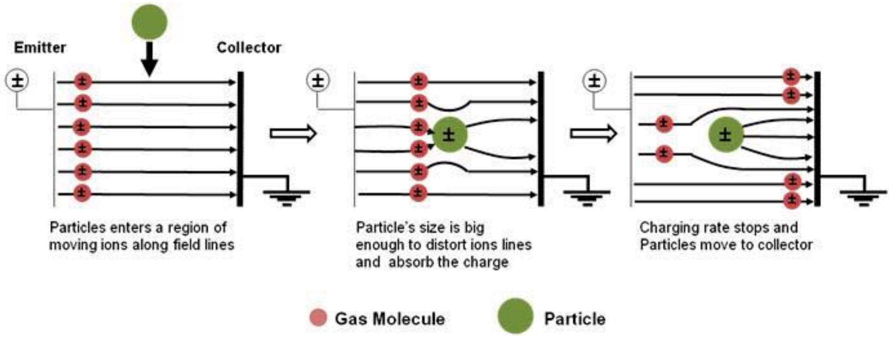

Background

- Effective Separation requires
  - Ionization of gas molecules based on corona discharge (ionic wind)
  - Charging of liquid droplets suspended in gas flow
  - Collecting of charged droplets
  - Removal of collected droplets (drainage)

Project Objectives

- Study the feasibility of using electrostatic force to separate fine suspended liquid droplets from a gas stream
- Study the separation performance on two different aerosols droplets with low and high relative permittivities
- Conduct a parametric study on the effect of electric field and flow conditions on the separation performance
- Develop a numerical modeling technique to predict the separation performance
- Design a laboratory-scale novel gas-oil and gas-water electrostatic separator to demonstrate the concept

Experimental Setup

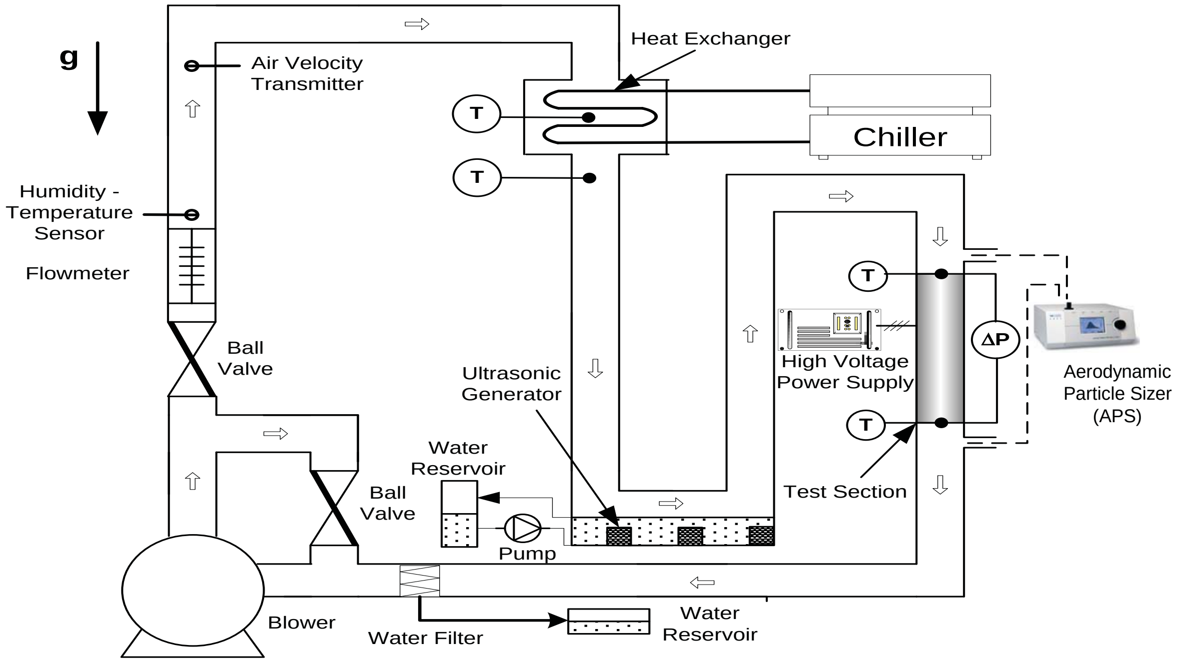

Experimental Setup

APS

1. Blower
2. Ball Valves
3. DAS Unit
4. Humidity Sensor Reader
5. AVT Reader
6. Flowmeter
7. Humidity Sensor Probe
8. APS Unit
9. HV Power Supply (-)
10. HV Power Supply (+)
11. Computer
12. AVT Probe
13. HX Vessel
14. Water Pool
15. Electrostatic Separator

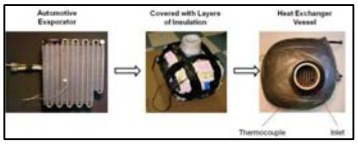

Heat Exchanger

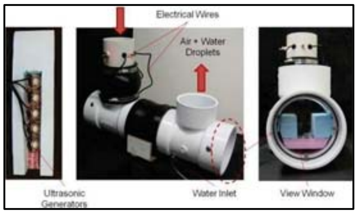

Ultrasonic Generation Unit

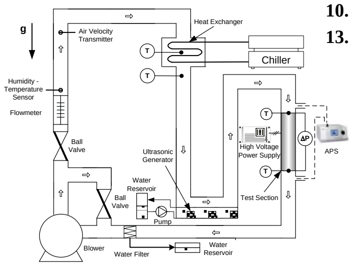

Results and Discussions

- Effect of Electrostatic Separation

Inlet

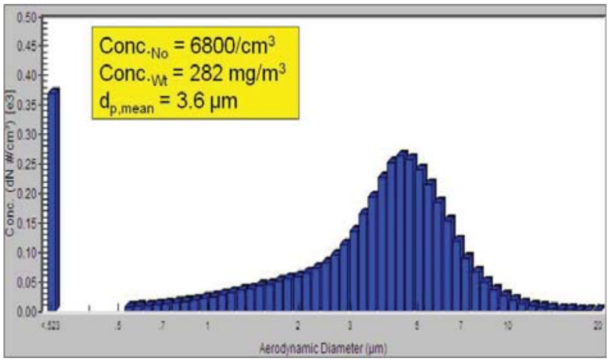

Outlet (7.0 kV)

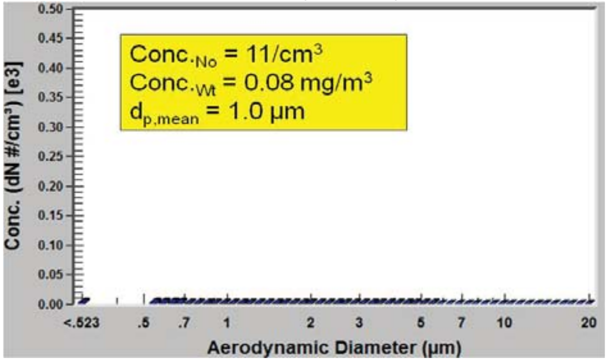

$$\eta = 1 - \frac{\textbf{Wt. of Escaped Particles}}{\textbf{Wt. of Injected Particles}}$$

Results and Discussions

- Water droplets separation

Negative Polarity

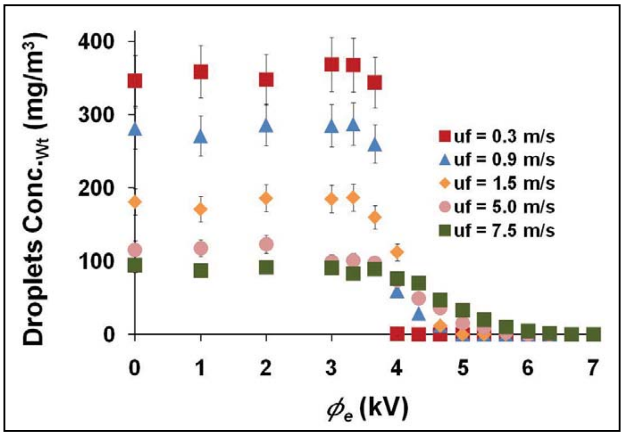

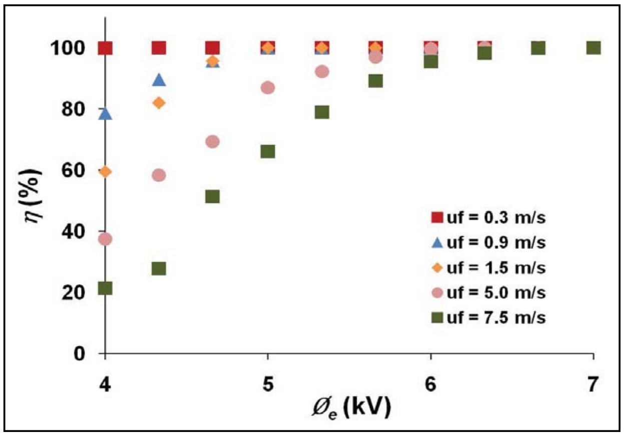

- ➢ Efficiency decreases as velocity increases
- ➢ η_{max} = 99.999 % for 0.3 m/s & 99.912 % for 7.5 m/s @ $\varnothing_e$ = 7 kV

Results and Discussions

Negative Polarity, $\mathbf{u}_f$ = 5.0 m/s

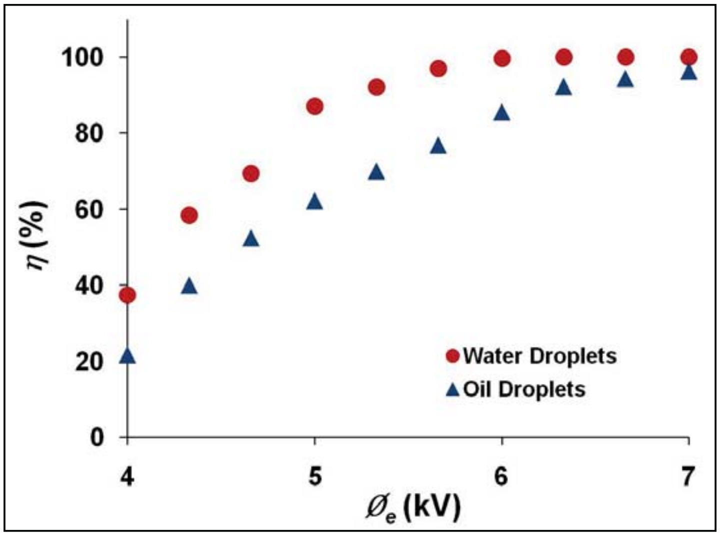

- Separation efficiency is better with higher relative permittivity
- η_{max} = 99.999 % for water & 96.267 % for oil @ $Ø_e$ = 7 kV;(99,9% @ 7.5 kV)

Results and Discussions

- Numerical Modeling - Computational Domain

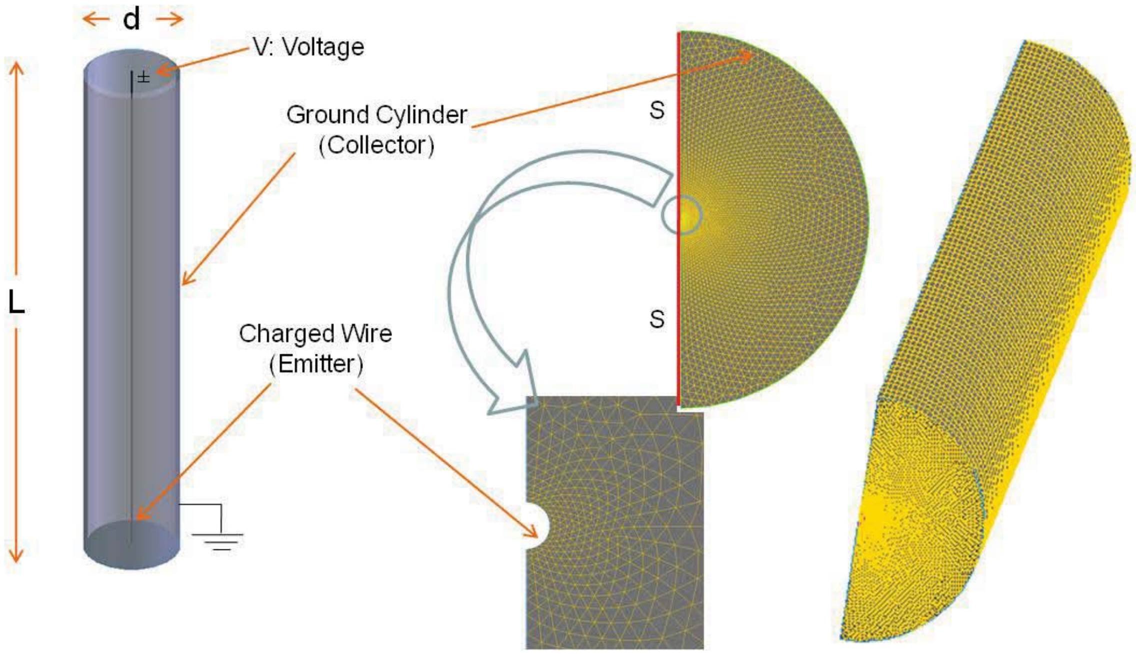

Results and Discussions

- Particles Tracking

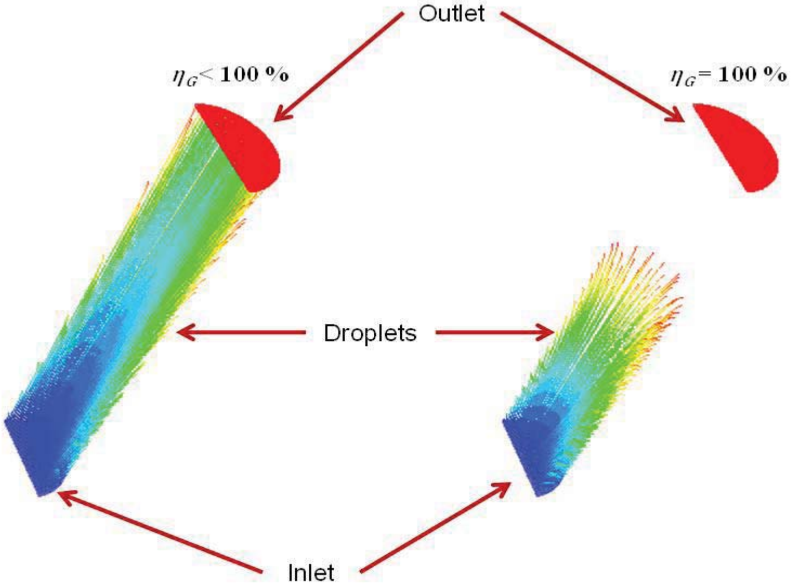

- Uniform surface injection
- 500 droplets injected at each study

Results and Discussions

- Effect of Voltage

$\mathbf{u}_f$ = 0.9 m/s, T_f = 300 K, L = 0.15 m

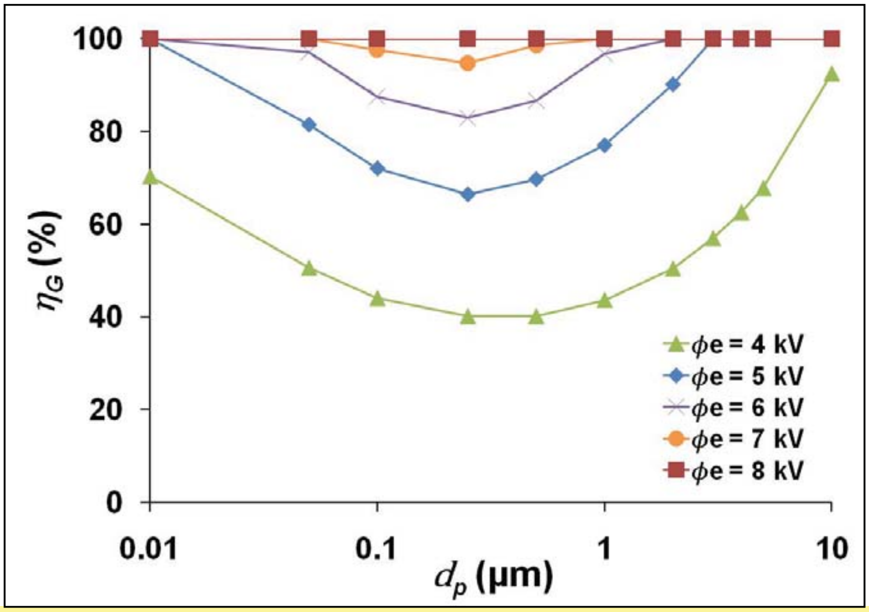

Project Status

- High efficiency of separation has been demonstrated for water and oil droplets at moderate voltages
- Numerical model has been developed and verified
- Technology demonstration unit development in progress

Conclusions and Summary

- Electrostatic separation of fine water or oil droplets from high velocity gas stream with high separation efficiency (near 100 %) was demonstrated
- Although relative permittivity of oil is much less than water (40 times), electrostatic separation has shown high effect equally well performance for oil.
- The numerical modeling is in good agreement with experimental data in predicting the grade efficiency and can be used for separator optimization
- Technology demonstration unit development is in progress

Experimental characterization of oil particle separation using EHD

Part of EERC Research project (An EHD-Enhanced Gas-Liquid Separator)

PI Investigator(s): Dr. Afshin Goharzadeh , Dr. Mohamed Alshehhi, Dr. Michael Ohadi,
UMD Investigators: Dr. Serguei Dessiatoun, Dr. Amir Shooshtari

Presentation Outline

I. Objectives

- Develop an experimental set-up at The Petroleum Institute.
- Based on flow visualization techniques using state-of-the-art facilities at the Mechanical Engineering Laboratories (PIV, LDV, High Speed Camera,…).
- Experimental results will be used to validate corresponding CFD analysis at UMD.

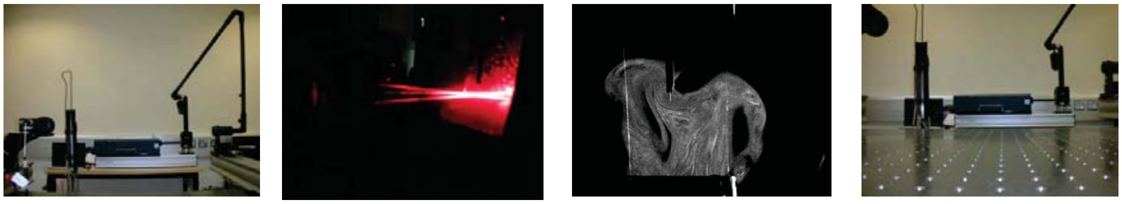

II. Experimental Setup

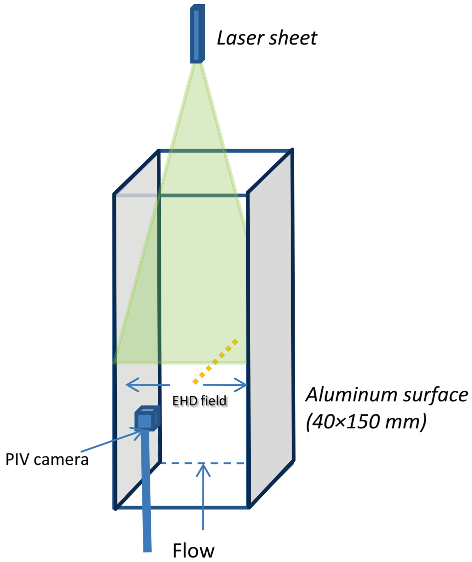

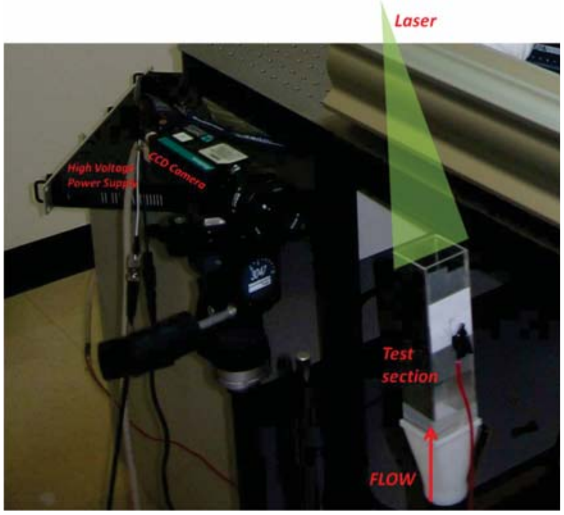

Fluid	**Air + Oil particles**
Flow rate:	42 lpm
Test section:	40 mm x 40 mm

CCD Camera	**1024 x1024 pix**
Laser	532 nm, YAG laser
High Voltage Power Supply	Max 60 kV

III. Results (PIV images)

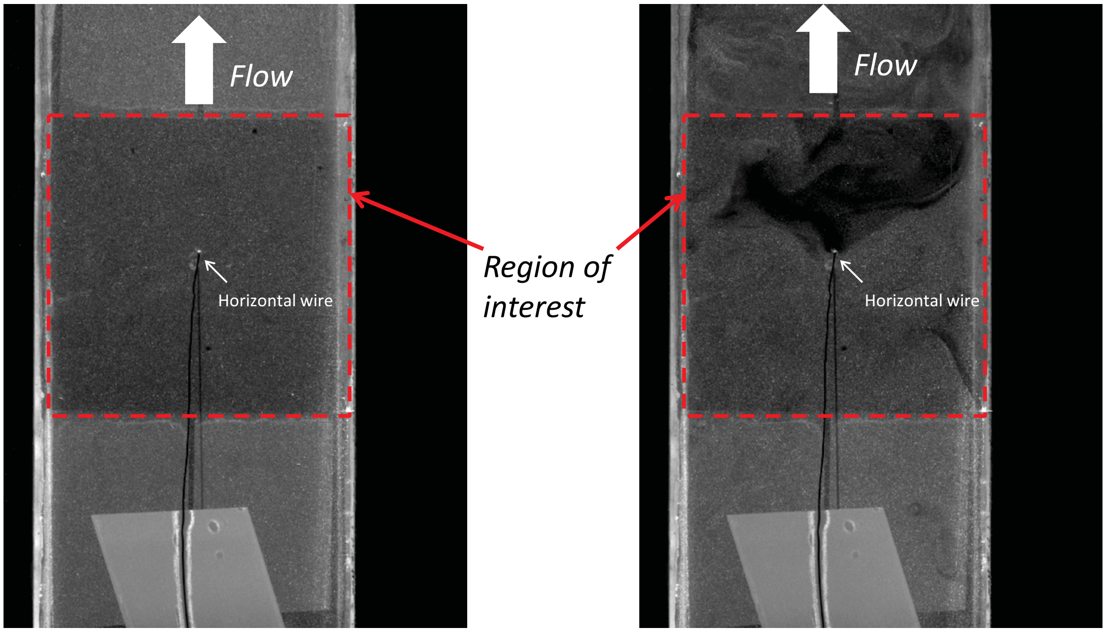

Experiment 1: U=0 V, I=0 A

Experiment 2: U=10 kV, I=0.07 mA

III. Results (2D velocity distribution)

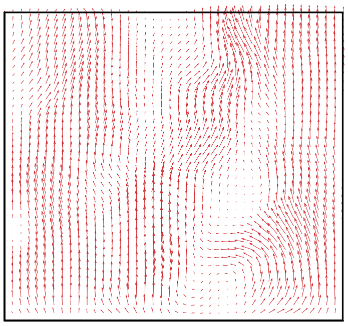

U = 0 kV, I = 0mA

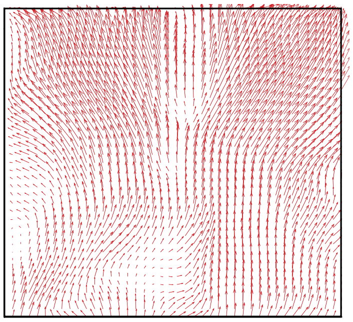

U = 10 kV, I = 0.04 mA

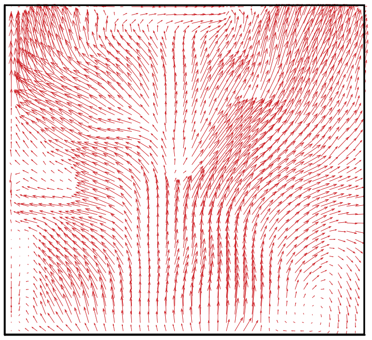

U = 12 kV, I = 0.05 mA

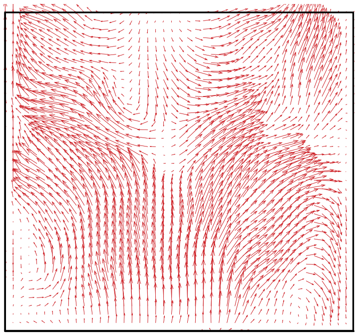

U = 14 kV, I = 0.11 mA

III. Results (2D velocity magnitude)

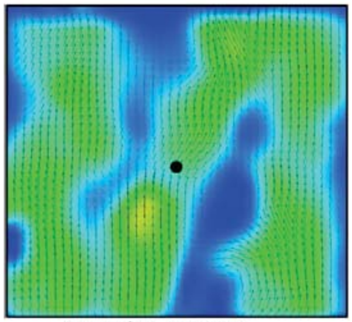

U = 0 kV, I = 0mA

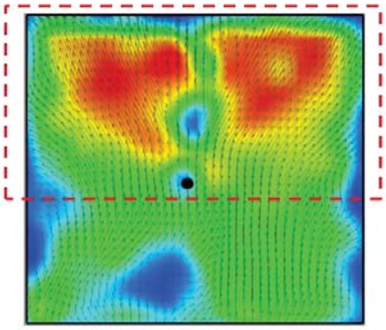

U = 10 kV, I = 0.04 mA

Flow field influenced by the electrical field U.

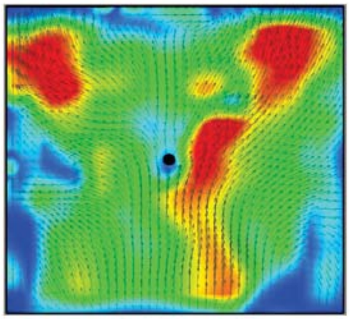

U = 12 kV, I = 0.05 mA

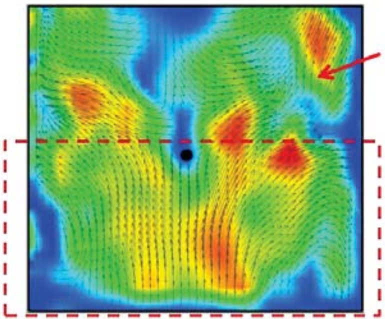

U = 14 kV, I = 0.11 mA

Number of oil particles decrease.

Flow field influenced by the electrical field U.

III. Results (velocity profiles)

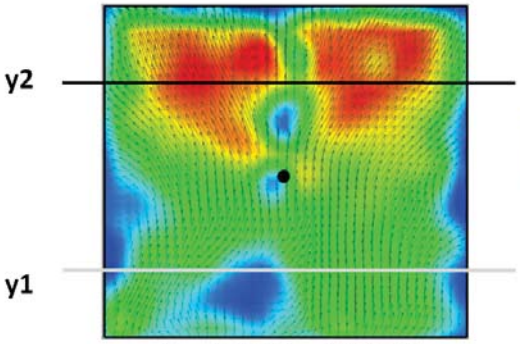

U = 10 kV, I = 0.04 mA

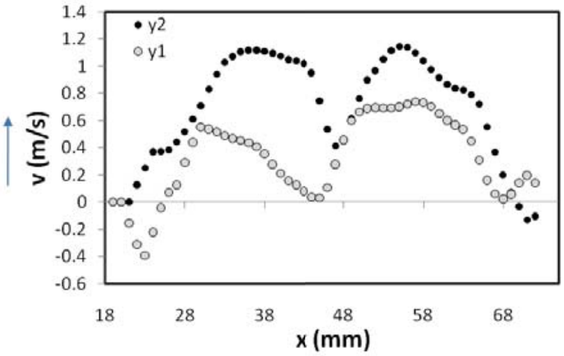

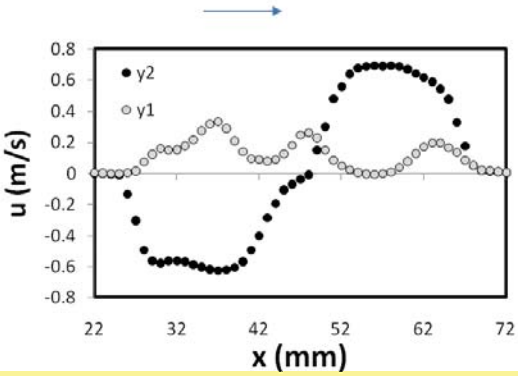

-The velocity magnitude increases downstream of horizontal wire:

+ 40% in x-direction
+ 50% in y-direction

IV. Conclusions

Application of High Voltage potential disturbs the flow field:

- Particle trajectories are deviated
- Velocity magnitude increase
- Particle density decrease

Future experiments:

- Influence of the flowrate Q.
- Detail analysis of the velocity distribution.
- Comparison with CFD predictions from UMD partners.

Microreactors for Oil and Gas Processes Using Microchannel Technologies

UMD Team: Dr. S. Dessiatoun & Dr. A. Shooshtari

PI Team: P. Singh (GRD), Dr. E. Al-Hajri,
Dr. A. Goharzadeh, Dr. M. Ohadi

1st Annual PI Partner Schools Research Workshop
The Petroleum Institute, Abu Dhabi, U.A.E.
January 6-7, 2010

PI Partners

PI Sponsors

Presentation Outline

- Background
- Objectives
- Summary of Accomplishments
- Literature Review
- Redesign Experiments
- Project Status
- Future Work

Summary of Accomplishments

- Literature survey
- Identification of potential chemical reactions that are of an interest to ADNOC
- Design and fabrication of a single microchannel test setup

Background

- Micro-reactor Characteristics
  - Continuous process
  - Reduced process hold up
  - Residence time control
  - Efficient mixing
  - High surface to volume ratio
  - Improved process control
  - Linear scale up by number up

Background

- Safety Benefits
  - Enhanced safety; new reactions possible
  - No scale up risks associated
  - No unstable intermediates accumulation
  - Elimination of batch critical process

- Chemistry Benefits
  - Improved yield and selectivity
  - Increased reaction rate
  - Expanded temperature range

Background

- Economic Benefits
  - Less capital risk
  - Lower manufacturing and operating cost
  - Less raw material, solvent, waste and energy
  - Less work up
  - Improved production management

Project Objectives

- Evaluate microreactor fabrication technologies and identify the most effective technology for oil and gas processing.

- Demonstrate the advantages of the selected technology on the laboratory scale microreactor which can be scaled up.

Chemical Reaction Identification

- Steam Methane Reforming (SMR)
  - Hydrogen economy creates demand for hydrogen.
  - SMR, a cost effective method of hydrogen production.
  - Scaling down of SMR with traditional technologies is highly cost ineffective.
  - SMR has least carbon footprints in comparison to other hydrogen production methods.

- H_2S Decomposition
  - H_2S Naturally occurs in many gas wells.
  - H_2S is produced from desulfurization of petroleum stocks.
  - H_2S is a liability in petroleum industry.
  - It can be turned into an asset by producing hydrogen.

Literature Review

- SMR Reactions

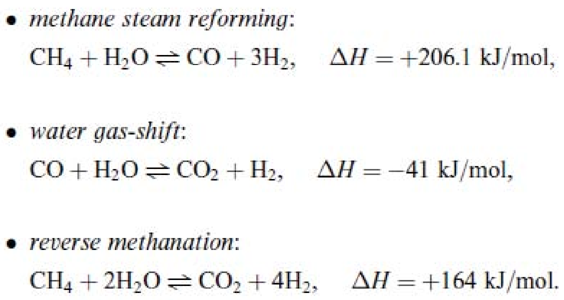

- *methane steam reforming*:
  $CH_4 + H_2O \rightleftharpoons CO + 3H_2, \quad \Delta H = +206.1$ kJ/mol,
- *water gas-shift*:
  $CO + H_2O \rightleftharpoons CO_2 + H_2, \quad \Delta H = -41$ kJ/mol,
- *reverse methanation*:
  $CH_4 + 2H_2O \rightleftharpoons CO_2 + 4H_2, \quad \Delta H = +164$ kJ/mol.

- Reaction Rates (*Zanfir et al*)

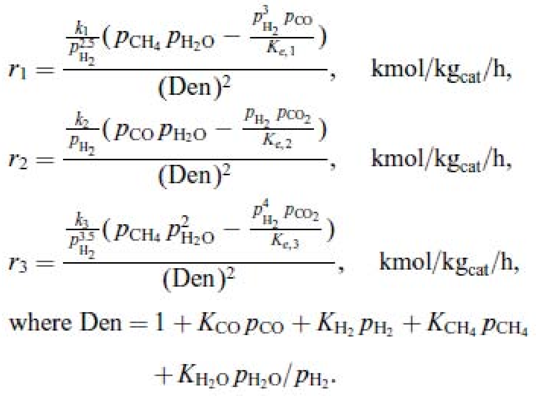

$$r_1 = \frac{\frac{k_1}{p_{H_2}^{2.5}}\left(p_{CH_4} p_{H_2O} - \frac{p_{H_2}^3 p_{CO}}{K_{e,1}}\right)}{(\mathrm{Den})^2}, \quad \mathrm{kmol/kg_{cat}/h},$$

$$r_2 = \frac{\frac{k_2}{p_{H_2}}\left(p_{CO} p_{H_2O} - \frac{p_{H_2} p_{CO_2}}{K_{e,2}}\right)}{(\mathrm{Den})^2}, \quad \mathrm{kmol/kg_{cat}/h},$$

$$r_3 = \frac{\frac{k_3}{p_{H_2}^{3.5}}\left(p_{CH_4} p_{H_2O}^2 - \frac{p_{H_2}^4 p_{CO_2}}{K_{e,3}}\right)}{(\mathrm{Den})^2}, \quad \mathrm{kmol/kg_{cat}/h},$$

$$\text{where Den} = 1 + K_{CO} p_{CO} + K_{H_2} p_{H_2} + K_{CH_4} p_{CH_4} + K_{H_2O} p_{H_2O}/p_{H_2}.$$

Literature Review

- Reaction kinetics by *Zanfir et al*

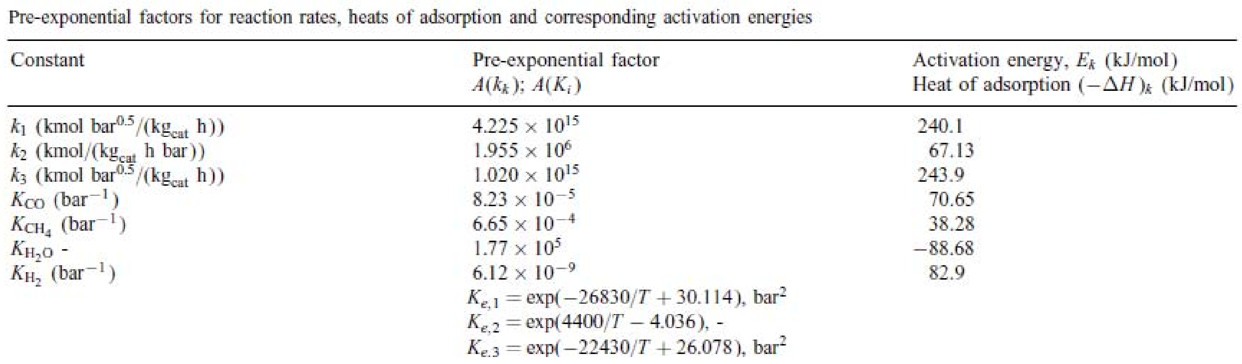

Pre-exponential factors for reaction rates, heats of adsorption and corresponding activation energies

Constant	Pre-exponential factor $A(k_k)$; $A(K_i)$	Activation energy, E_k (kJ/mol) Heat of adsorption $(-\Delta H)_k$ (kJ/mol)
k_1 (kmol $bar^{0.5}/(kg_{cat}$ h))	4.225×10^{15}	240.1
k_2 (kmol/(kg_{cat} h bar))	1.955×10^6	67.13
k_3 (kmol $bar^{0.5}/(kg_{cat}$ h))	1.020×10^{15}	243.9
K_{CO} (bar^{-1})	8.23×10^{-5}	70.65
K_{CH_4} (bar^{-1})	6.65×10^{-4}	38.28
K_{H_2O} -	1.77×10^5	−88.68
K_{H_2} (bar^{-1})	6.12×10^{-9}	82.9
	$K_{e,1} = \exp(-26830/T + 30.114)$, bar^2	
	$K_{e,2} = \exp(4400/T - 4.036)$, -	
	$K_{e,3} = \exp(-22430/T + 26.078)$, bar^2	

Literature Review

- Microreactor Design by *A.Y.Tonkovich et al.*
  - Parallel SMR & Methane combustion reactions
  - Heat recuperation system integrated
  - Fabrication: combination of conventional machining, wire electro-discharge machining, and laser cutting.
  - Catalyst loading: Reforming catalyst deposited on FeCrAlY substrate. Combustion catalyst washcoated

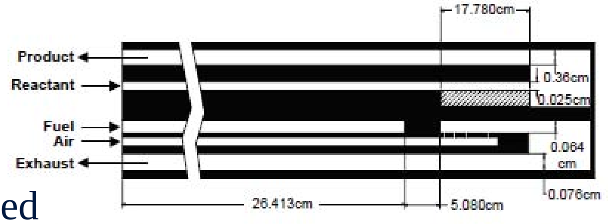

Microchannel steam reforming reactor with integrated methane partial oxidation and subsequent combustion.

  - Methane conversion ~ 91.7%
  - Volumetric heat transfer flux was 65 W/cm^3
  - Contact time of 6 ms
  - For commercial scale up reactor thermal losses <5%

Literature Review

- H2S decomposition ($2H_2S \leftrightarrow 2H_2 + S_2$)
  - Catalytic or noncatalytic thermal decomposition
  - Thermochemical decomposition
  - Electrochemical decomposition
  - Photochemical decomposition
  - Plasma method of decomposition

- H_2S decomposition not yet tried in microreactors

Technology Comparison

Shell and Tube 500 W heat exchanger

UMD 600 W evaporator

Experimental Work

- LiBr/Water absorption system
  - Enhance two-phase mixing in microchannels
  - Heat/Mass transfer investigation
  - Flow visualization

Experimental Work

- Components of Adsorber

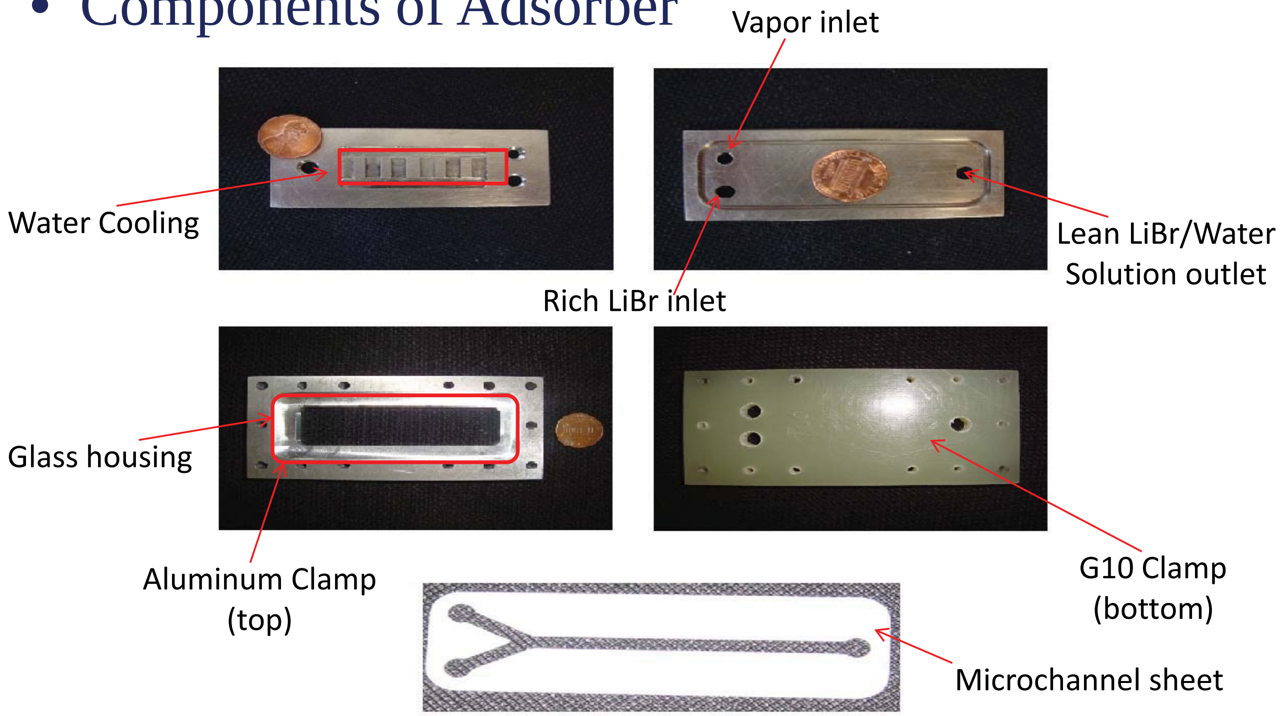

Experimental Work

- Components of Desorber

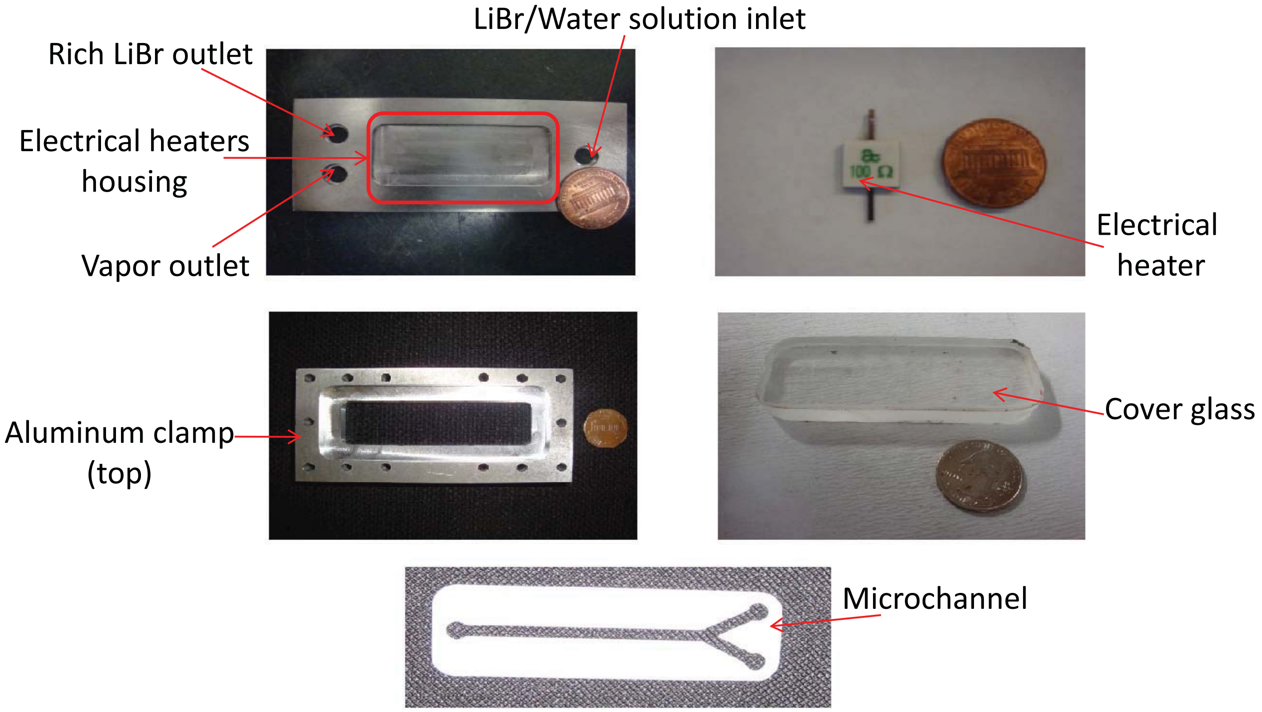

Experimental Work

- Recently fabricated microchannel using Rapid Prototyping machine.
  - Channel dimensions: thickness ~ 400 μm and width 2.8 mm (aspect ratio ~ 7)

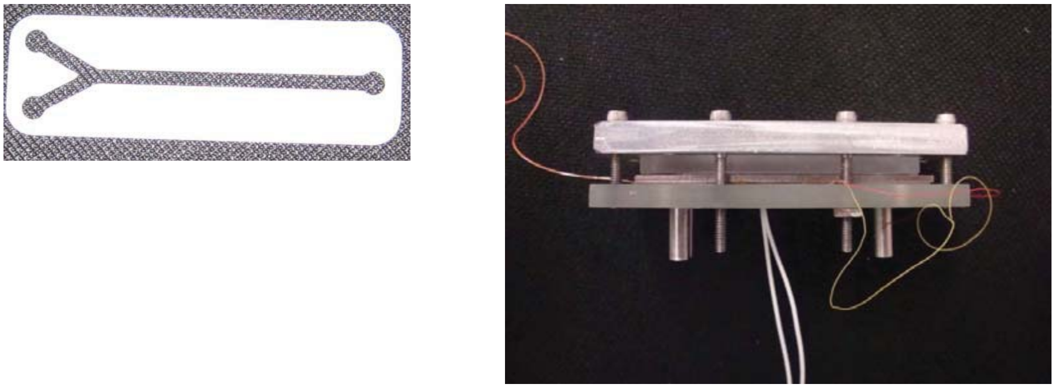

Experimental Setup

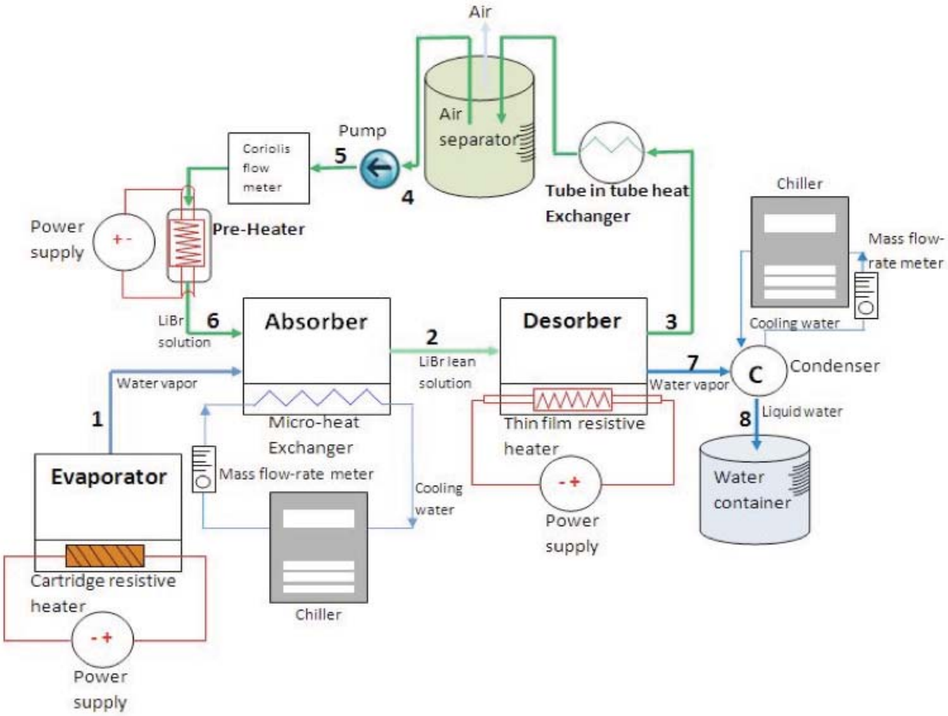

Project Status

- Literature review continues
  - – Reaction kinetics of H_2S decomposition.
  - – Catalyst selection study for both reactions.

- CFD simulation using COMSOL for both the SMR and H_2S decomposition processes.
  - – Simulations with different catalytic conditions
  - – Simulations with different reaction kinetics

Future Scope

- Find design parameters for microreactor
  - – Simulation
  - – Mathematical calculations
- Fabrication of microreactor.
- Test setup design and construction.
- Experimental study and analysis of results.
- Aid of simulation in remodeling and redesigning experimental setup.

Mathematical Modeling and Optimization in Oil and Gas Industry

ASSESSMENT OF THE INTEGRITY OF PIPELINES SUBJECT TO CORROSION-FATIGUE, PITTING CORROSION, CREEP AND STRESS CORROSSION CARCKING

UMD Team: M. Modarres, M. Nuhi
PI Team: A. Seibi

1st Annual PI Partner Schools Research Workshop
The Petroleum Institute, Abu Dhabi, U.A.E.
January 6-7, 2010

PI Partners

PI Sponsors

Presentation Outline

- Background
- Objectives
- Failure Mechanism Modeling and Applications
  - Corrosion-Fatigue
  - Pitting Corrosion
  - Creep
  - Stress Corrosion Cracking
- Conclusions

Objectives

- Develop Physics-based computationally simple probabilistic models for routine reliability assessments and health monitoring in the oil industry
  - PoF (Physics of Failure) models capture material degradation and failure mechanism and can be extrapolated to different levels.
  - Probabilistic models can adequately represent all of the factors that contribute to variability (e.g. material properties , Inspection devices accuracy, human errors, etc.)
  - Use of the probabilistic models to estimate reliability of components (our interest is pipeline reliability)

Problem Statement

Pitting and Fatigue leading to Pipe Failure - Ductile Iron

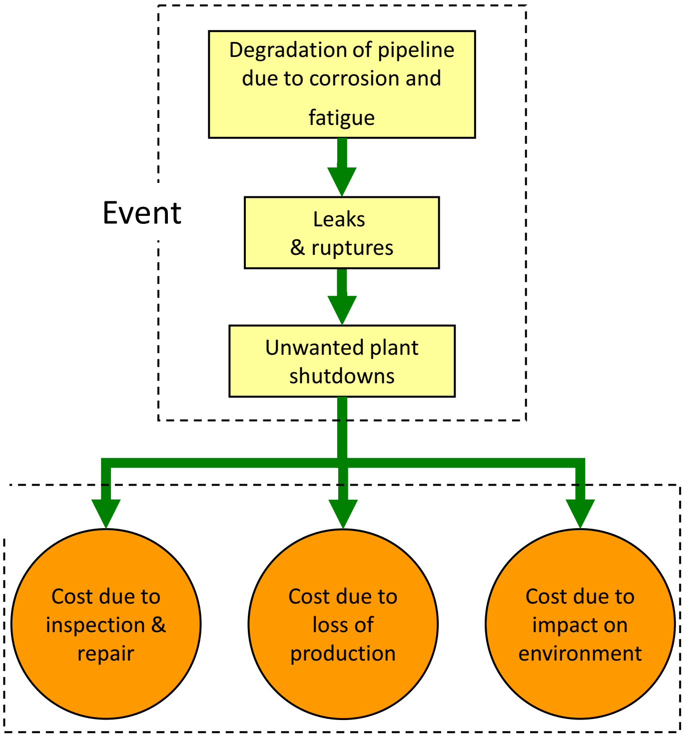

Event

Degradation of pipeline due to corrosion and fatigue

Leaks & ruptures

Unwanted plant shutdowns

Cost due to inspection & repair

Cost due to loss of production

Cost due to impact on environment

Corrosion Inside the Pipe

Consequences

Problem:
Cost of corrective maintenance

Solution:
Predictive maintenance

Pictures from: (http://your-tech-assistant.eltex-pipe.com)

Corrosion-Fatigue in Pipes

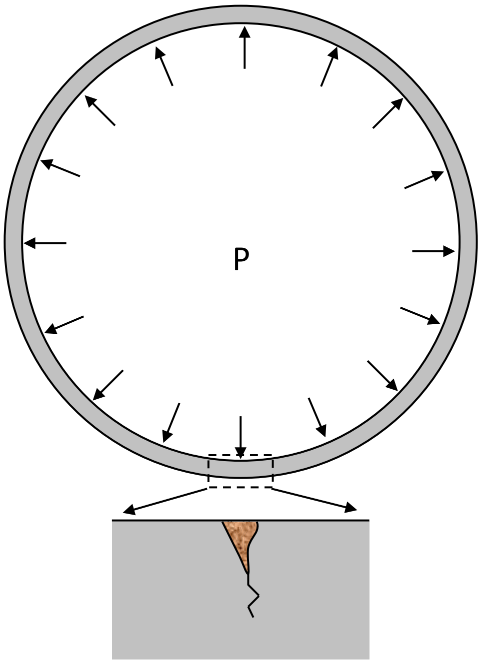

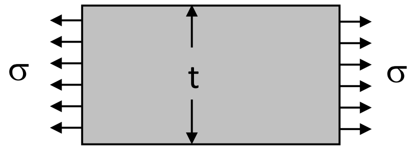

$$\sigma = \frac{PD}{2t}; \frac{t}{D} << 1; D = diameter; t = tickness$$

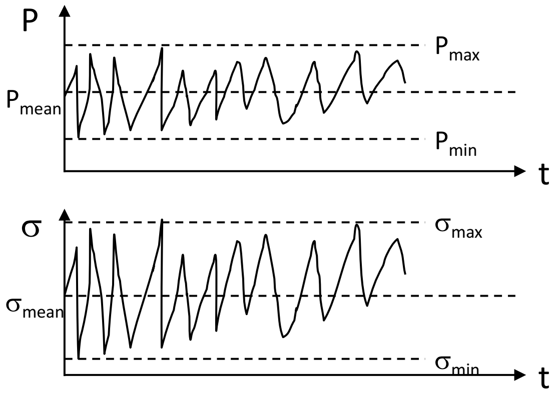

Corrosion-Fatigue Modeling Approach

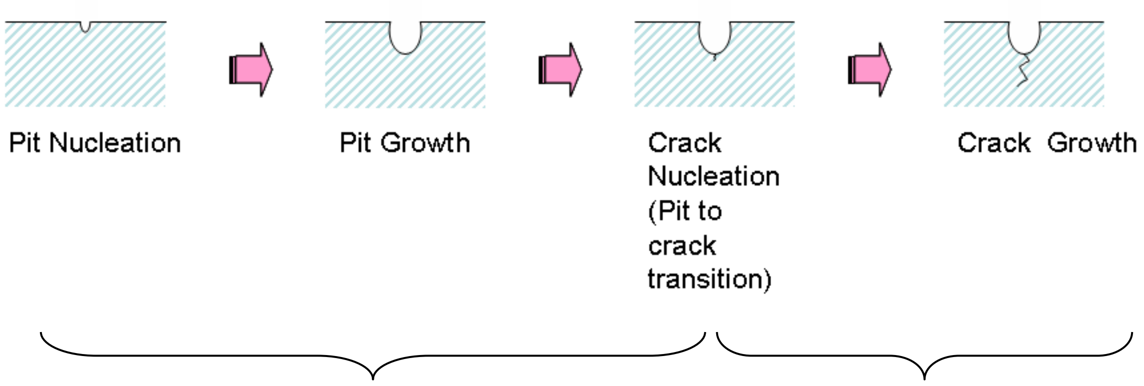

Pit Nucleation

Pit Growth

Crack Nucleation (Pit to crack transition)

Crack Growth

Corrosion is Dominant

Fatigue is Dominant

The criterion for transition :

$$\left(\frac{da}{dt}\right)_{crack} \geq \left(\frac{da}{dt}\right)_{pit}$$

Damage-Endurance Reliability Models

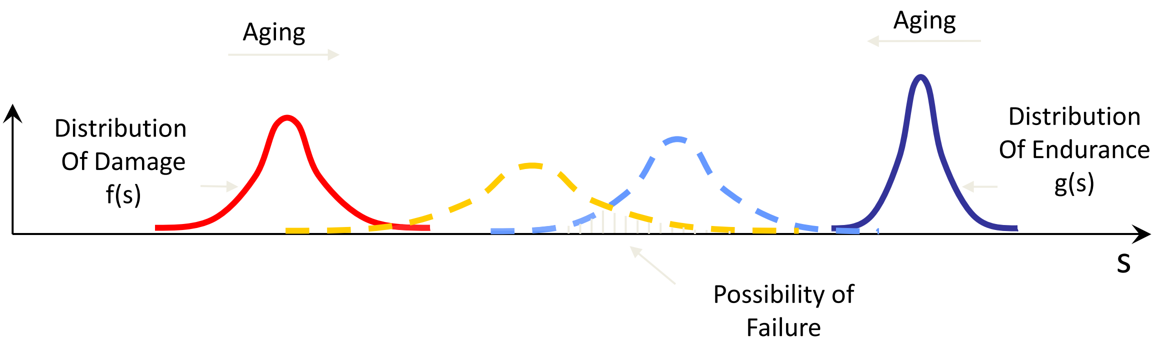

$$P(Damage > Endurance) = \int_{0}^{\infty} \left\{ \int_{0}^{s} g(x)\,dx \right\} f(s)\,ds$$

Probabilistic Fracture Mechanics Approach to Fatigue Reliability

Damage-Endurance Model

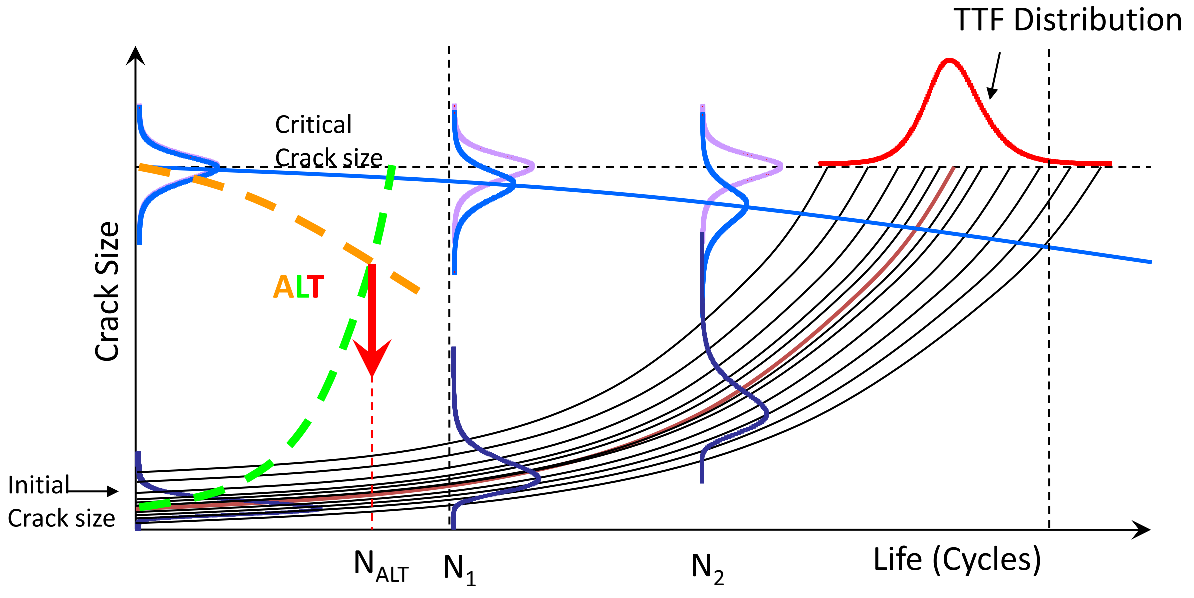

Damage-Endurance Modeling Corrosion-Fatigue

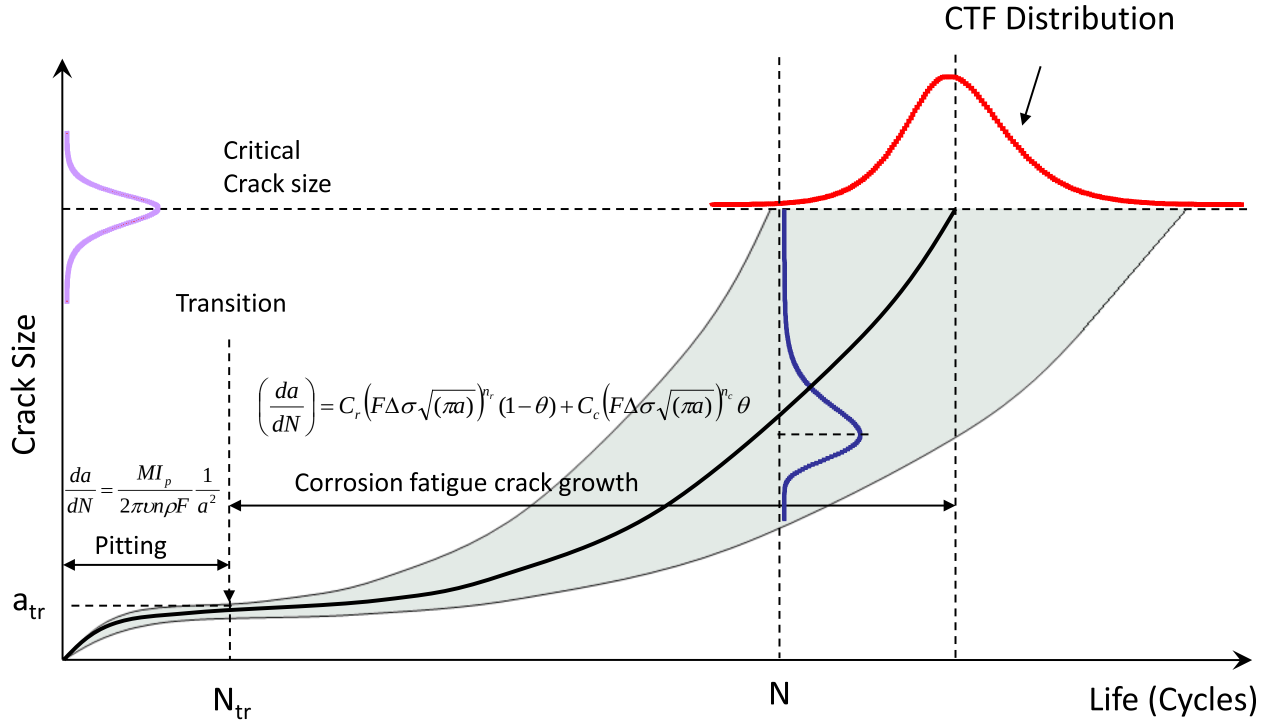

$$\left(\frac{da}{dN}\right) = C_r\left(F\Delta\sigma\sqrt{(\pi a)}\right)^{n_r}(1-\theta) + C_c\left(F\Delta\sigma\sqrt{(\pi a)}\right)^{n_c}\theta$$

$$\frac{da}{dN} = \frac{MI_p}{2\pi\upsilon n\rho F}\frac{1}{a^2}$$

Physics-Based Simulation Results

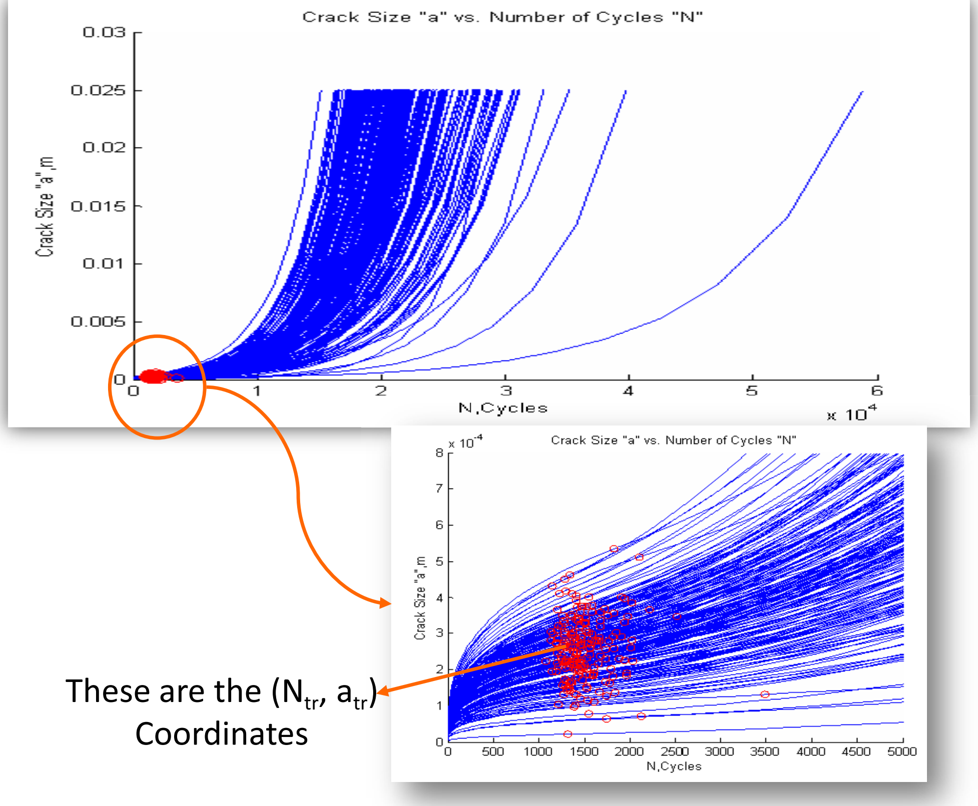

These are the (N_{tr}, a_{tr})
Coordinates

Semi-Empirical Simplified Model Development

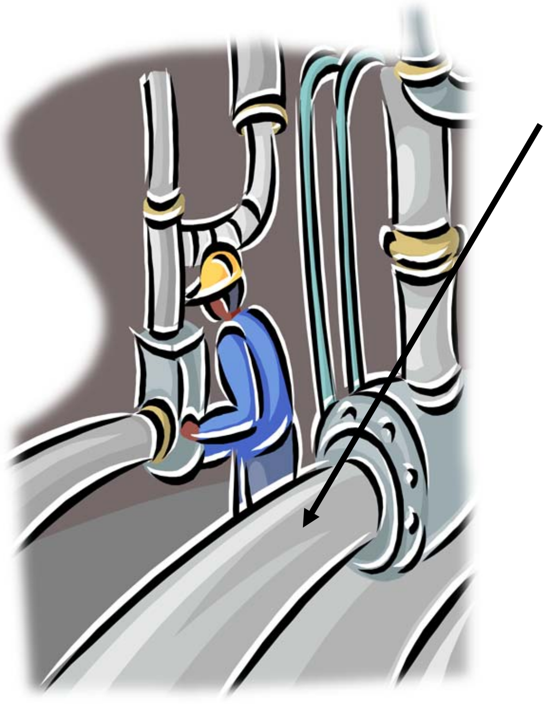

Find the correlation of A & B with the physical parameters of the pipeline:

- **Loading Stress "σ"**
- **Loading Frequency "ν"**
- **Temperature "T"**
- **Flow Characteristic "C" (e.g., Ip, [Cl⁻], pH, …)**

$$Damage, D = f(v_i, t_i | \Theta)$$
$$D \approx \text{e.g. crack size, a}$$
$$v_i \approx \text{variables (e.g. T}, \sigma, \nu, [\text{Cl}^-], \ldots)$$
$$t_i \approx \text{index of time (e.g. N,...)}$$
$$\Theta \approx \text{vector of model constants (e.g. } \varepsilon_i, A, B, \ldots)$$

Proposed Simple PoF-Based Corrosion-Fatigue Semi-Empirical Model

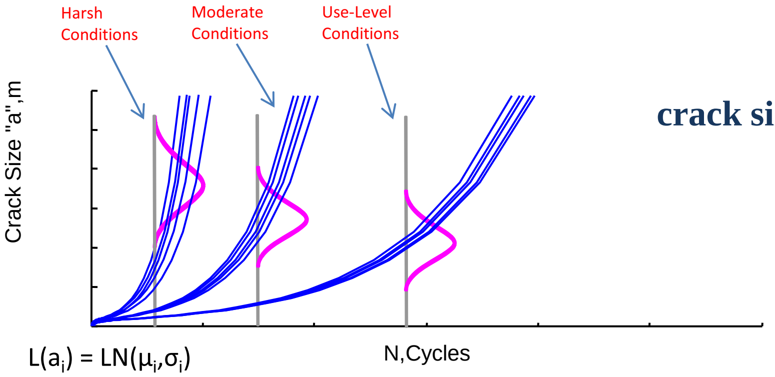

crack size vs. stress, cycle, etc.

$L(a_i) = LN(\mu_i, \sigma_i)$
$\mu_i = \ln[f(s_i, T_i, \nu_i, Ip_i, N_i)]$

$$a_i = \left[A \cdot s_i^{0.182} \cdot v_i^{-0.288} \cdot Ip_i^{0.248} \cdot N_i^{1/3} + B \cdot s_i^{3.24} \cdot v_i^{-0.377} \cdot Ip_i^{0.421} \cdot N_i^2 \cdot e^{(4\times10^{-10} \cdot s_i^{2.062} \cdot v_i^{0.024} \cdot N_i)}\right]$$

$$where\ a = crack\ size,\ v = load\ frequency,\ s = stress\ amplitude\ , I_p = Current\ \text{int}\,ensity,\ N = cycle\ No.$$

$$L(a) = f(a) = \frac{1}{\sigma \cdot a\sqrt{2\pi}} \exp\left[-\frac{1}{2\sigma^2}(\ln a - \ln(A \cdot s^{0.182} \cdot v^{-0.288} \cdot Ip^{0.248} \cdot N^{1/3} + B \cdot s^{3.24} \cdot v^{-0.377} \cdot Ip^{0.421} \cdot N^2 \cdot e^{(4\times10^{-10} \cdot s^{2.062} \cdot v^{0.024} \cdot N)}))^2\right]$$

Data Collection: Experimental Validation

Corrosion-Fatigue Testing

Set-Up (Cortest Test Facility)

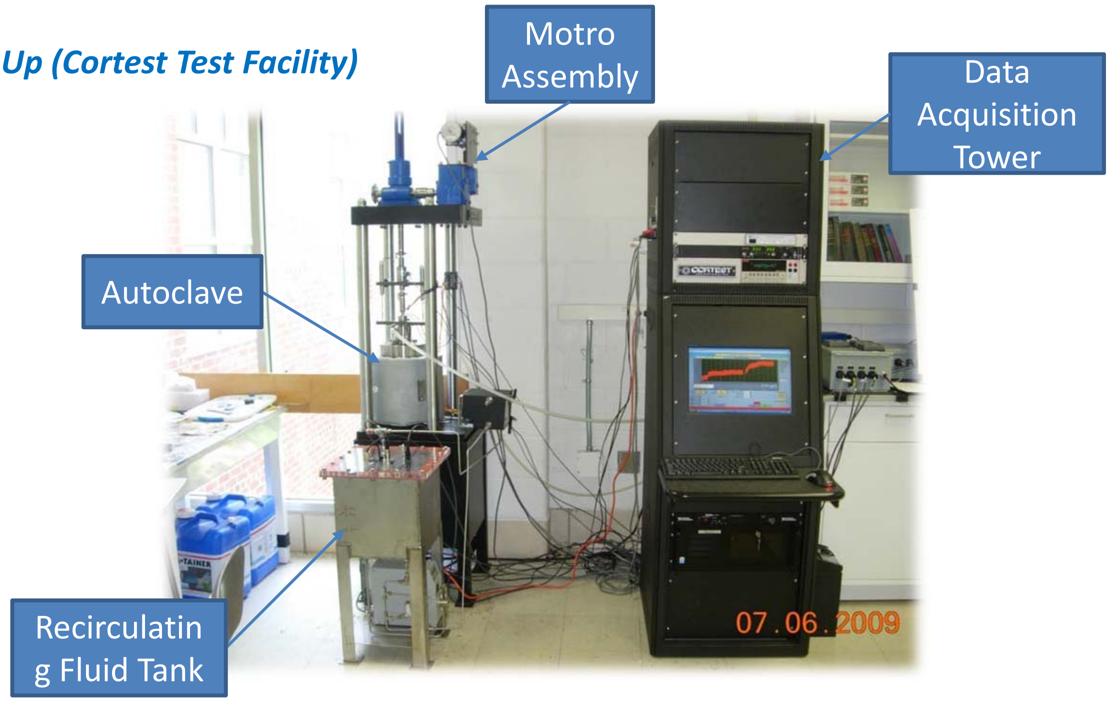

Cortest Corrosion-Fatigue Testing Results

- Crack length vs. number of cycle from Cortest corrosion-fatigue testing:
  - in sea water of 250 ppm $Na_2S_2O_3$-$5H_2O$ at 383 K, and 100 and150-MPa,
  - at different frequencies of 0.004 Hz and 0.00165 Hz.
  - Pictures from broken specimen with connected screws(for applied current and voltage) are shown at the bottom.

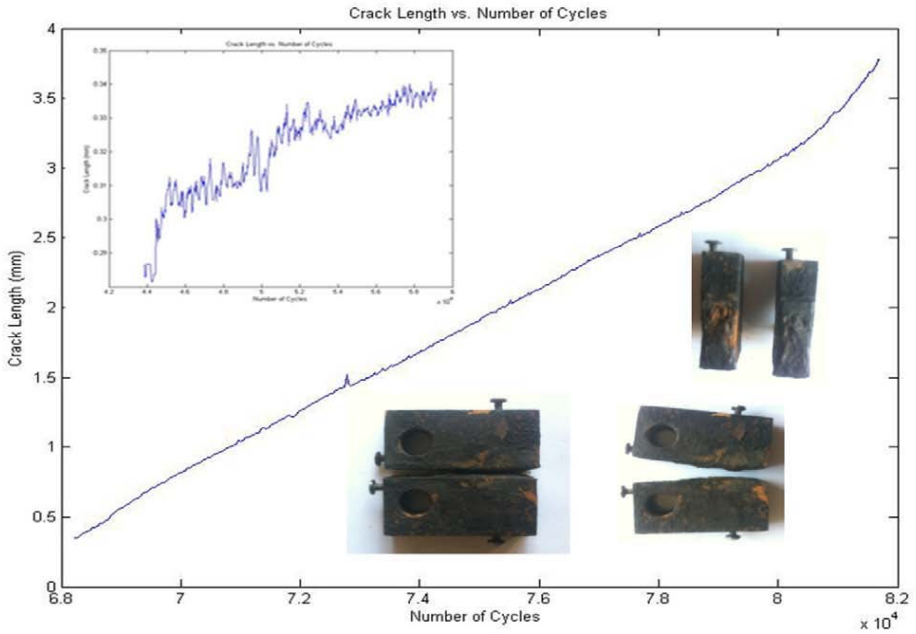

Broken specimen from Cortest corrosion-fatigue testing

- Broken specimen (two side views plus broken surface parts)

voltage - current - connections

Model Parameter Estimation

Bayesian Inference Framework using Markov Chain Monte Carlo Simulation Approach

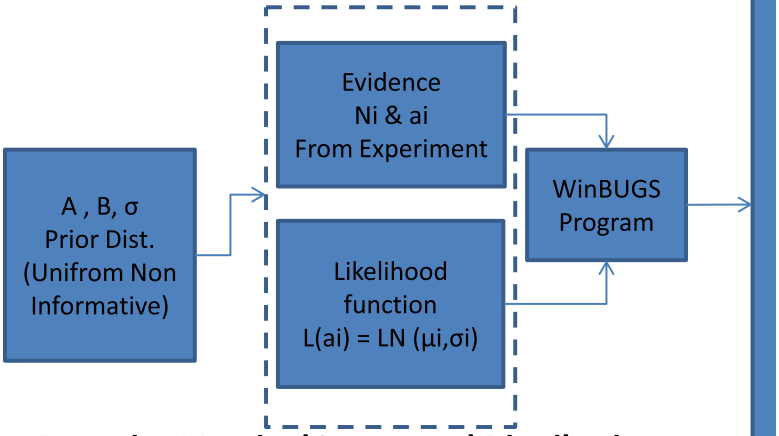

A , B, σ
Prior Dist.
(Unifrom Non Informative)

Evidence
Ni & ai
From Experiment

Likelihood function
L(ai) = LN (μi,σi)

WinBUGS Program

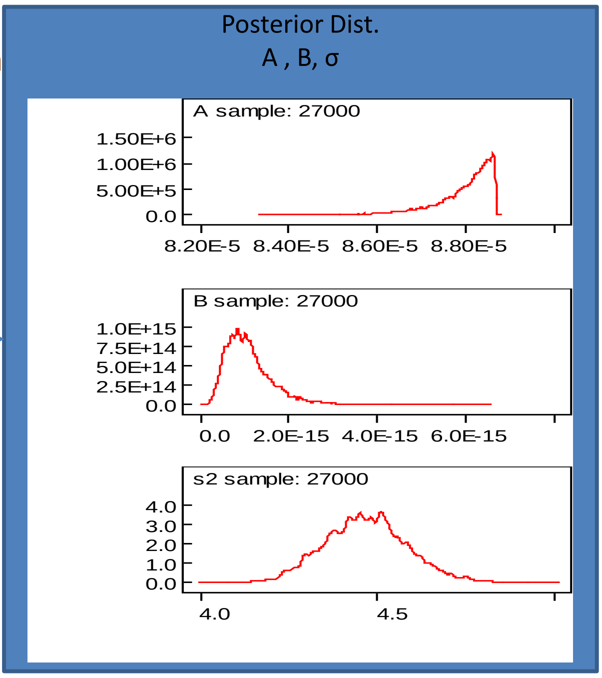

Posterior Dist.
A , B, σ

Posterior Marginal Lognormal Distributions and s, A & B

$$A \begin{cases} \mu_A = -9.34 \\ \sigma_A = 7.41x\ 10^{-3} \end{cases} \quad B \begin{cases} \mu_B = -34.524 \\ \sigma_B = 0.4686 \end{cases} \quad s2 \begin{cases} \mu_{s2} = 4.468 \\ \sigma_{s2} = 1188 \end{cases}$$

Reliability and Health Monitoring Application

A harsh pipeline environment:

- Higher Loading Stress

Frequency of Exceedance for Each Observed Number of Pits in the Refinery Pipeline.

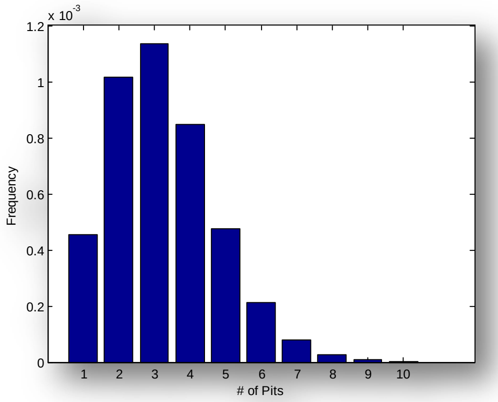

The new frequency of exceedance for the bulk pipeline is estimated to be 548 pits/25 yrs life of pipeline!!!! → Drastically Increased

Reliability and Health Monitoring Application (Cont.)

Run simulation

Using proposed Empirical Model

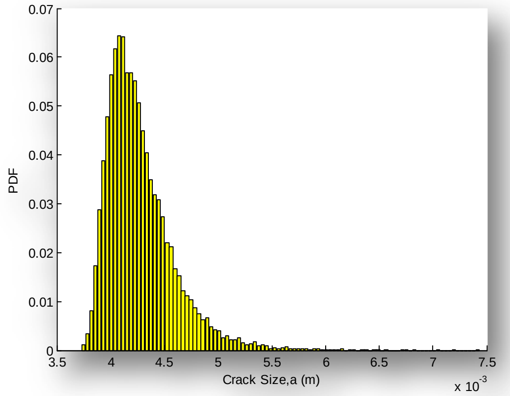

- "a_i" Lognormal distribution: μ= -5.47 ; σ=0.06

Pitting Corrosion (Phase II)

- With Collaboration from PI Summer Interns Abdullah M. Al Tamimi & Mohammed Mousa Mohamed Abu Daqa

Background

Pitting Corrosion (X70Carbon Steel)

- Pitting Corrosion: An electrochemical oxidation reduction process, which occurs within localized holes on the surface of metals coated with a passive film.
- It might be accelerated by chloride, sulphate or bromide ions in the electrolyte solution.
- Pitting corrosion has a great impact on the oil and gas industry.
- There are three main stages for the pitting corrosion to occur:

1-Pit Initiation

2- Pit Propagation

3-Fracture:

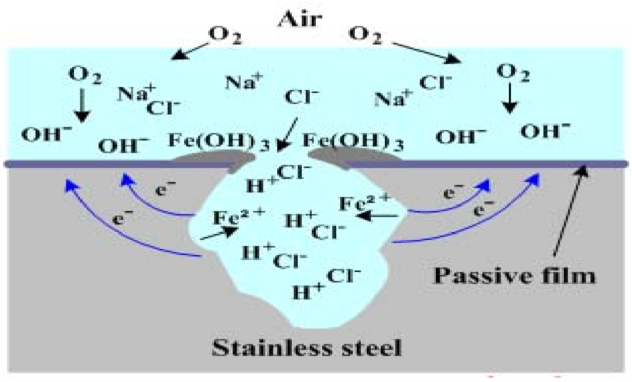

Objectives of Pitting Corrosion

- **Objectives**
  1. Measuring pits depth,
  2. Measuring pits density, and
  3. Measuring the mass loss.
- **Two Corroding Environments (X70 Carbon Steel at 323 K)** :

  - H_2S = $Na_2S_2O_3$-$5H_2O$ with 100 100ppm, 150ppm, 200ppm, 300ppm and 400ppm concentration, in 5,10, 24 hours time period;

  - Chloride(Sea Water) with 100 100ppm, 150ppm, 200ppm, 300ppm and 400ppm concentration, in 5, 10, 24 hours time period.

Experimental Setup/1

- The scheme of the experimental setup:

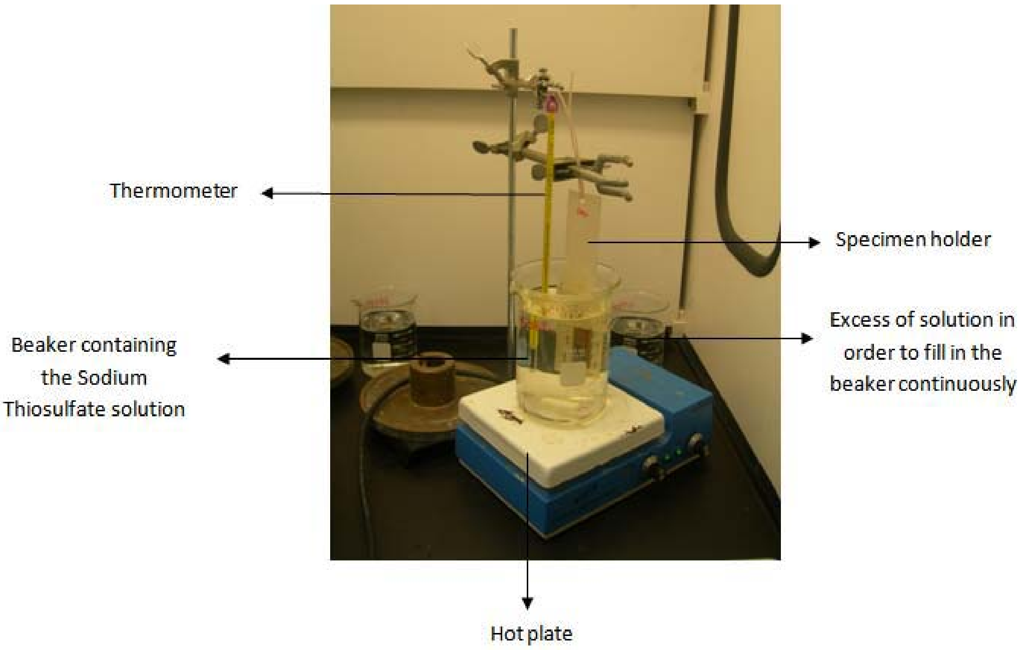

Experimental Setup/2

- The scheme of the experimental setup:

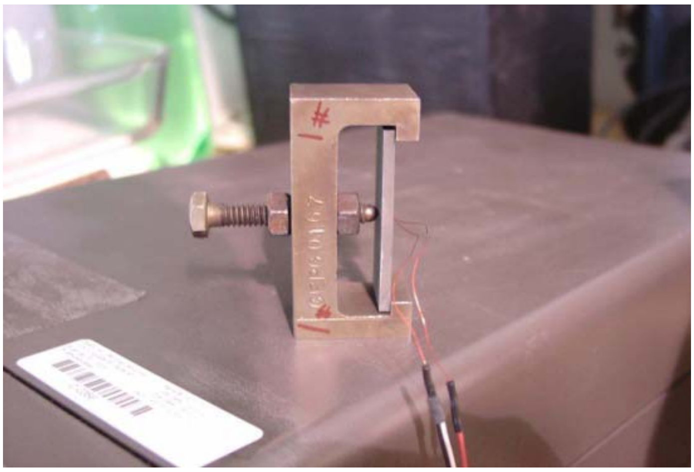

Static stress corrosion specimen with a strain gage on it to measure the applied stress.

Examples of Pitting Corrosion H_2S and Chloride-Results

- Morphology of the samples are studied by:
  - 1- Optical Microscope, Nikon Optiphot 66
  - 2- Sensitive Weighing Machine, METTLER TOLEDO AB104
  - 3- Scanning Electron Microscope, HITACHI SU-70 SEM
- Morphology of Pits on X70 Carbon Steel surface in corrosive environments

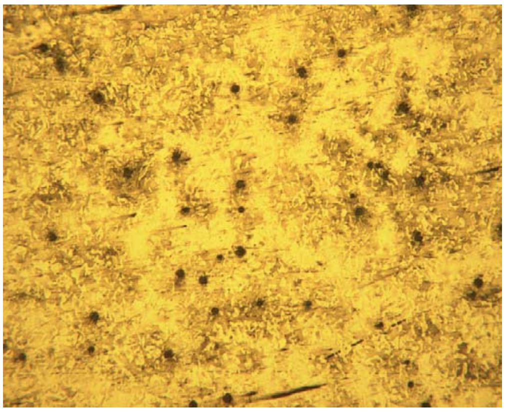

in H_2S (Mx200)

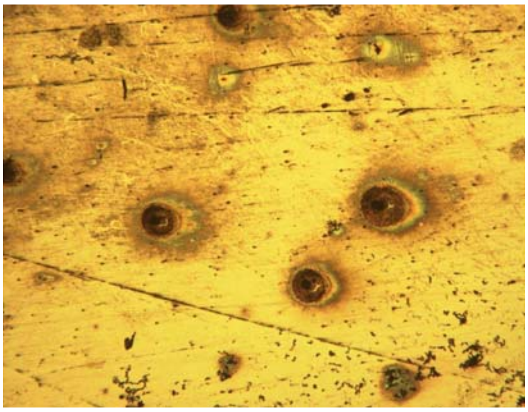

in Chloride (Mx200)

Pitting Depth of X70 Carbon Steel (H_2S and Chloride-Results)

- Pit depths for unstressed samples (left for H2S, right for Chloride) followed Weibull distributions.

$D_{H_2S} \sim Weib(\beta = 6.55 \;\;,\;\; \alpha = 11.99\mu m)$ $D_{[Cl^-]} \sim Weib(\beta = 1.32 \;\;,\;\; \alpha = 57.68\mu m)$

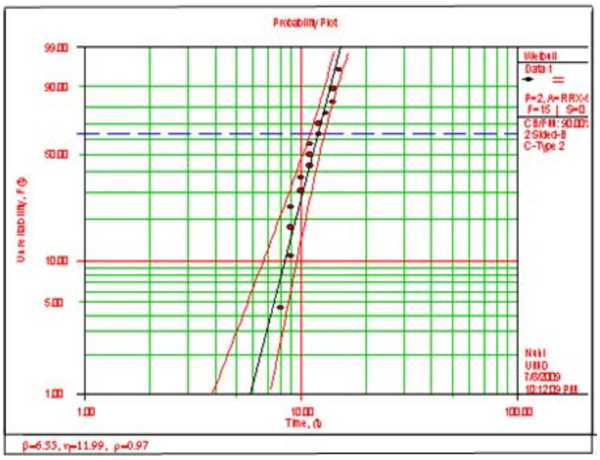

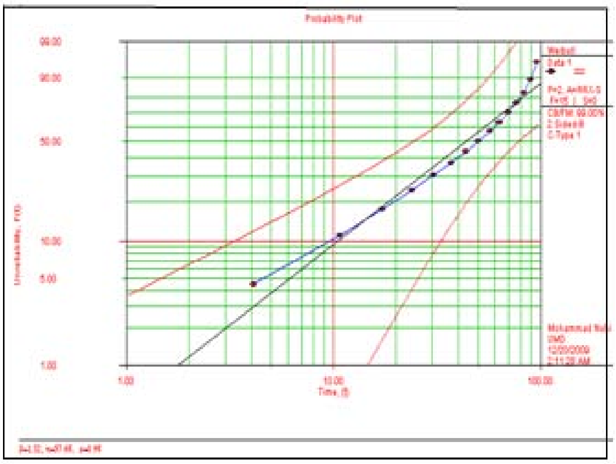

Pit Depth Distribution 400 ppm

Pitting Density of X70 Carbon Steel (H_2S and Chloride-Results)

- Pit densities followed the lognormal distributions.

$PD_{[h_2S]} \sim LN(\mu = 3.06 \;\;,\;\; \sigma = 0.39)$ $PD_{[Cl^-]} \sim LN(\mu = 2.18 \;\;,\;\; \sigma = 0.30)$

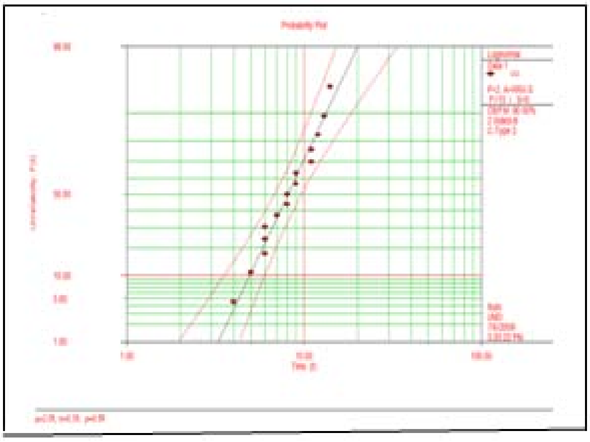

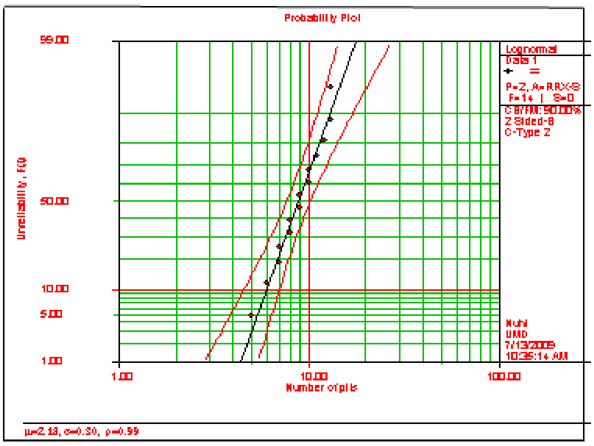

- Pit Density distribution 400ppm, 5hours are given in [pits/cm^2]

  The actual mean: [8 pits/cm^2] (left), [9 pits/cm^2] right

Estimation of Pitting Corrosion Characteristics (stressed and unstressed)

- 250 ppm H_2S (Sodium-thio-sulfate) at 80°C (353K).
- Mean Intensity: 14 in 250x250 µm^2 (0.0625 mm^2).
- The lognormal plotting diagrams of the unstressed and stressed

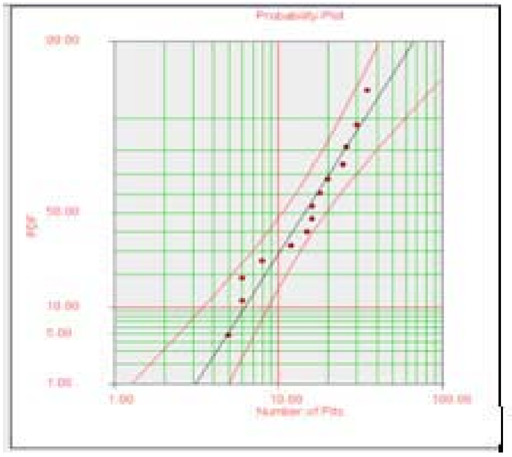

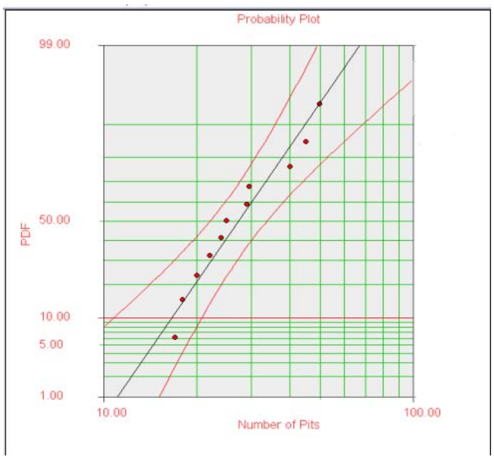

Unstressed : ρ = $\mathcal{LN}$(μ=2.67, σ=0.66)

Stressed : ρ = $\mathcal{LN}$(μ=3.31, σ=0.39).

Pit Growth Rate Model

- Pit depths (d) increases with the concentrations according to a power law and time according to the t$^{1/3}$-law (justified by the literature): $d = A\ t^m$

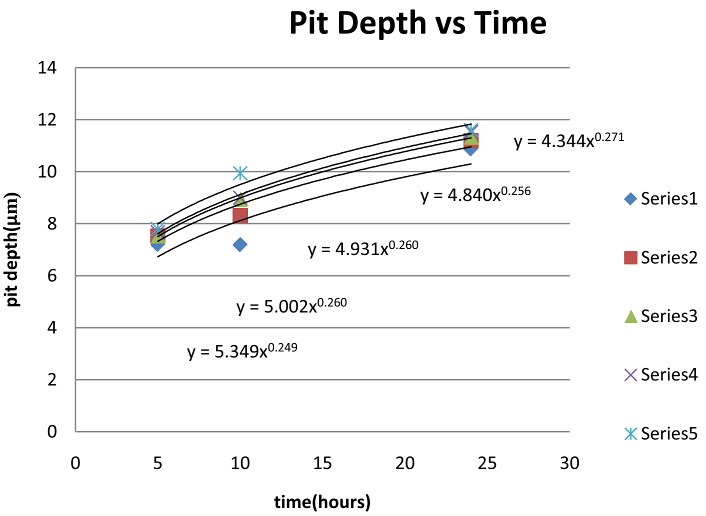

Creep Modeling Background

- Creep is the time-dependent, thermally assisted deformation of materials under constant static load (stress).
- Mathematical description of the process is difficult and is in the form.

$$\dot{\varepsilon} = f(\sigma, \quad T, \quad t)$$

- Creep at low temperatures (primary stage) are described by:

$$\varepsilon = \varepsilon_0 + \alpha \quad \log(1 + \gamma \quad t)$$

$$\varepsilon = \varepsilon_0 \beta \quad t^{1/3}$$

  - where α, β and γ are material constants;
- There is no general agreement on the form of the equations at high temperatures.

Creep Modeling Background (Cont.)

- A typical creep curve shows three distinct stages with different creep rates, determined by several competing mechanisms from:

- strain hardening,
- softening processes such as recovery and crystallization,
- damage processes such as cavitation, necking and cracking.

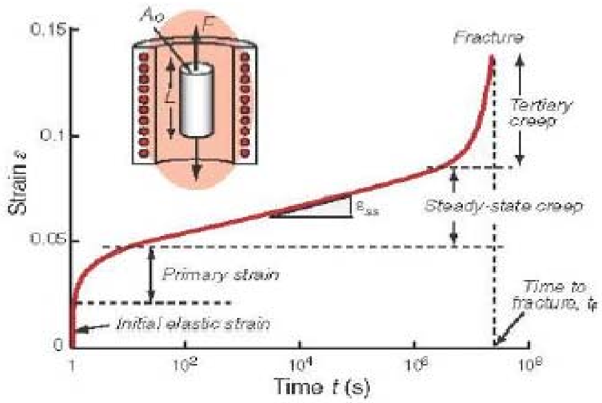

- Creep testing and the creep curve, showing how strain ε increases with time t up to the fracture time. [http://faculty.mercer.edu/bubacz_m/Links/CH13.pdf]

Creep Approach Modeling

- Only literature search completed with some preliminary experimental preparations. The approach includes
  1. Using simulation of detailed models propose an empirical model.
  2. Perform accelerated creep tests.
  3. Use experimental results to assess parameters and uncertainties of the proposed empirical model accelerated life testing.

Creep Accelerated Test Set up

- The creep test is carried out by applying a constant load to a tensile specimen maintained at a constant temperature, (according to ASTM E139-70).

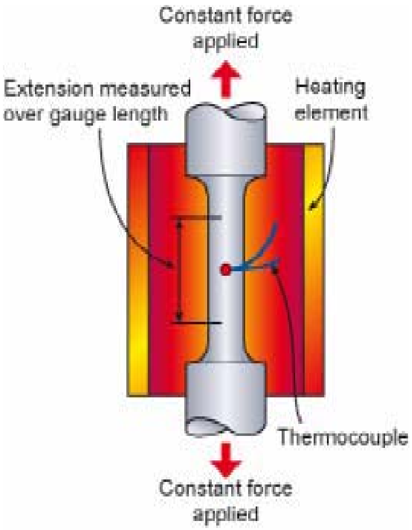

[http://www.sut.ac.th/engineering/Metal/pdf/MechMet]

Creep and SCC Experimental Setup

- Two chambers designed for creep and SCC tests under different environmental conditions and applied stress:
- Left: chamber for Dog-bone
- Right: chamber for CT-specimen (The prototypes specimens at work, installed on MTS-machine).

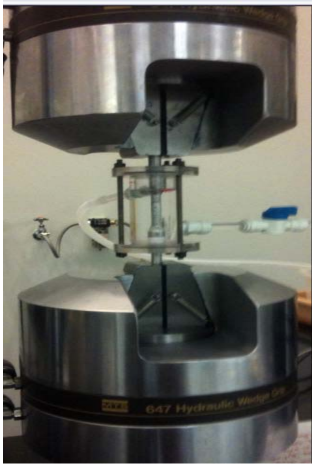

Dog-bone –specimen

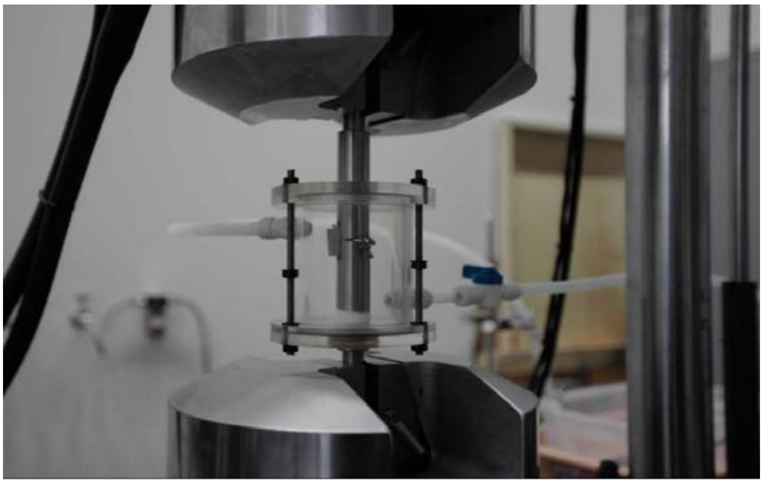

CT-specimen

Stress Corrosion Cracking (SCC)

- SCC is a combination of static tensile stress below yield and corrosive environment.
- Tensile stresses may be external forces, thermal stresses, or residual stresses.
- The kinetics of SCC depends on three necessary conditions:

1. **The chemical and metallurgical state** of the material (chemical composition , thermal conditions, grain size, presence of secondary phases and precipitate, etc.)
2. **The environmental conditions** (environmental composition, temperature, pressure, pH, electrochemical potential, solution viscosity etc.)
3. **Stress state** (uniaxial, triaxial, etc.) and on crack geometry of the material.

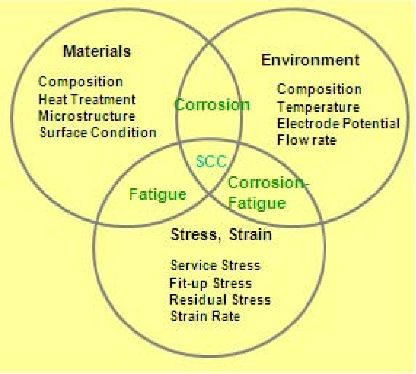

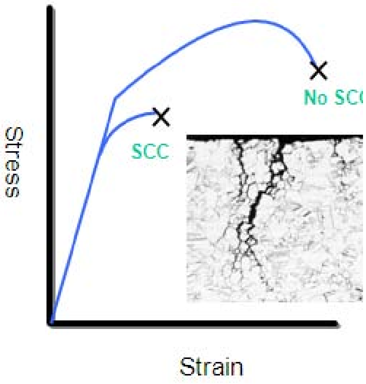

Stress Corrosion cracking(Factor Affecting)

- General relationship for the penetration of SCC following commonly accepted dependencies (after Staehle).
- There are many submodes of SCC and, because of the large number of variables in Staehle’s equation, there is a great range of possibilities in the study of SCC. This contributes to the complexity of the subject

$$X = A.[H^+]^n.[x]^p.\sigma^m.e^{(E-E_0/b)}.e^{Q/RT}.t^q$$

- Where X is the depth of SCC penetration;
- A depends on alloy composition and structure;
- $[H^+]$ is PH; x is the environmental species;
- σ is stress;
- E is electrochemical potential;
- Q is the activation energy;
- R is gas constant; T is temperature;
- t is time;
- n, p, m, b, q are empirical constant

[Kenneth R. Trethewey; Materials & Design; Volume 29, Issue 2, 2008, Pages 501-507]

SCC Planned Tests

- Tests on statically loaded (stressed) smooth specimens

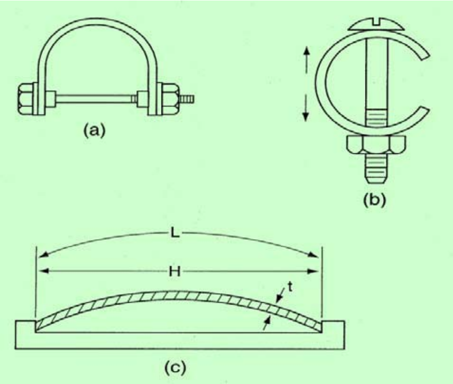

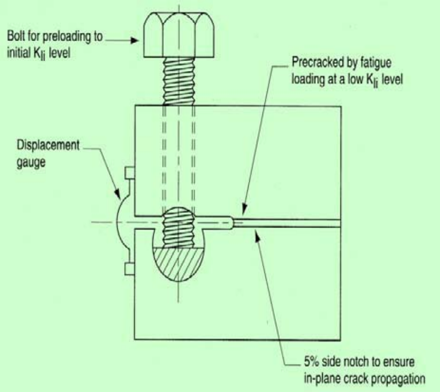

Planned Tests on statically loaded pre-cracked samples

- Fracture mechanics testing for SCC conducted with either :
  - a constant load or
  - with a fixed crack opening displacement,
- the *da/dt* is measured.
- The crack depth is determined as a function of time and the stress intensity.
- K_{1SCC} is the min. stress intensity below which SCC does not occur.

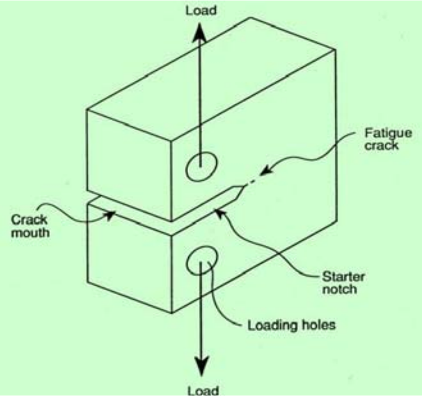

CT- specimen for fracture- mechanic-type testing where crack velocity vs. stress intensity is obtained

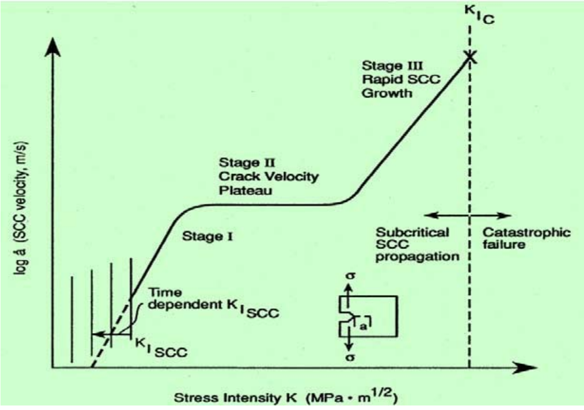

Schematic plot of data from fracture- fracture-type Testing. K_{ISCC} is shown to

Conclusions

- Reliability models for Corrosion-Fatigue has been developed, verified and demonstrated
- Pitting corrosion is nearly completed with models developed for pitting depth and density
- Literature search for creep models is completed, model developed and validation to follow
- SCC modeling will start in the future-- Preliminary test planning is performed

Robust Optimization of Engineering-Business Decisions for Petrochemical Systems

PI Team: A. Almansoori, S. Al Hashimi and N. Al Qasas
UMD Team: W. Hu, S. Azarm and P.K. Kannan

Acknowledgement: P. Kamaha, M. Li

1st Annual PI Partner Schools Research Workshop
The Petroleum Institute, Abu Dhabi, U.A.E.
January 6-7, 2010

PI Partners

PI Sponsors

Presentation Outline

- Objective and Tasks
- Integrating Engineering and Business Decisions
  - – Roadmap
  - – Dashboard
- Multi-Objective Robust Optimization (MORO)
  - – Developed approaches
  - – Timeline of improvements
- Case study and other test results
- Conclusions

Project Objective

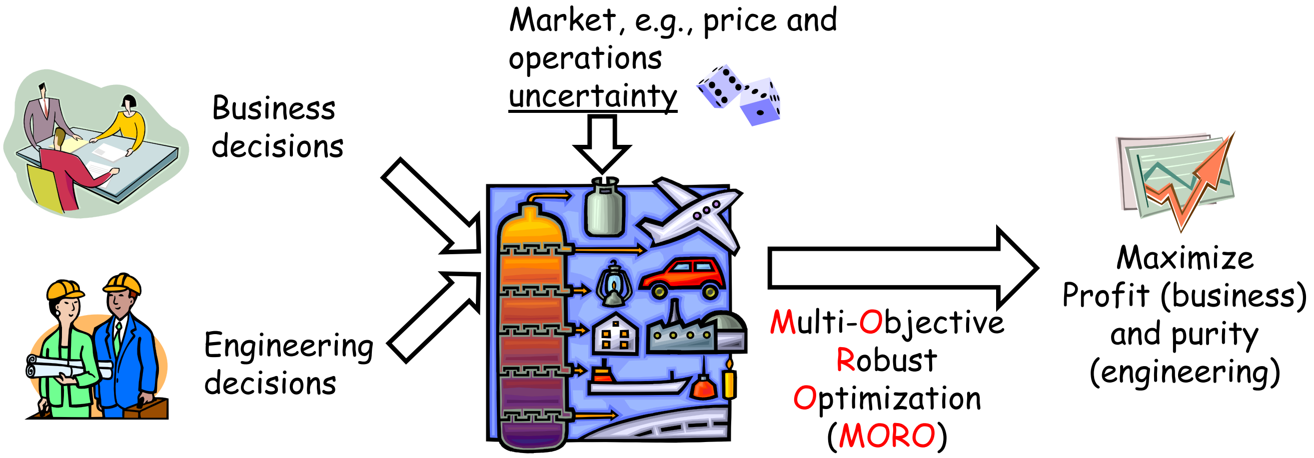

Market, e.g., price and operations uncertainty

Business decisions

Engineering decisions

Multi-Objective Robust Optimization (MORO)

Maximize Profit (business) and purity (engineering)

Objective: To provide a roadmap for integration of engineering and business decisions and an approach for obtaining multi-objective optimum and robust solutions under uncertainty for petrochemical systems

Tasks:

1. Integrate engineering and business decisions
2. Obtain multi-objectively optimum and robust solutions -- solutions that are “insensitive” to uncertainty

---

Task 1:

Integrate engineering and business decisions

Integration Roadmap

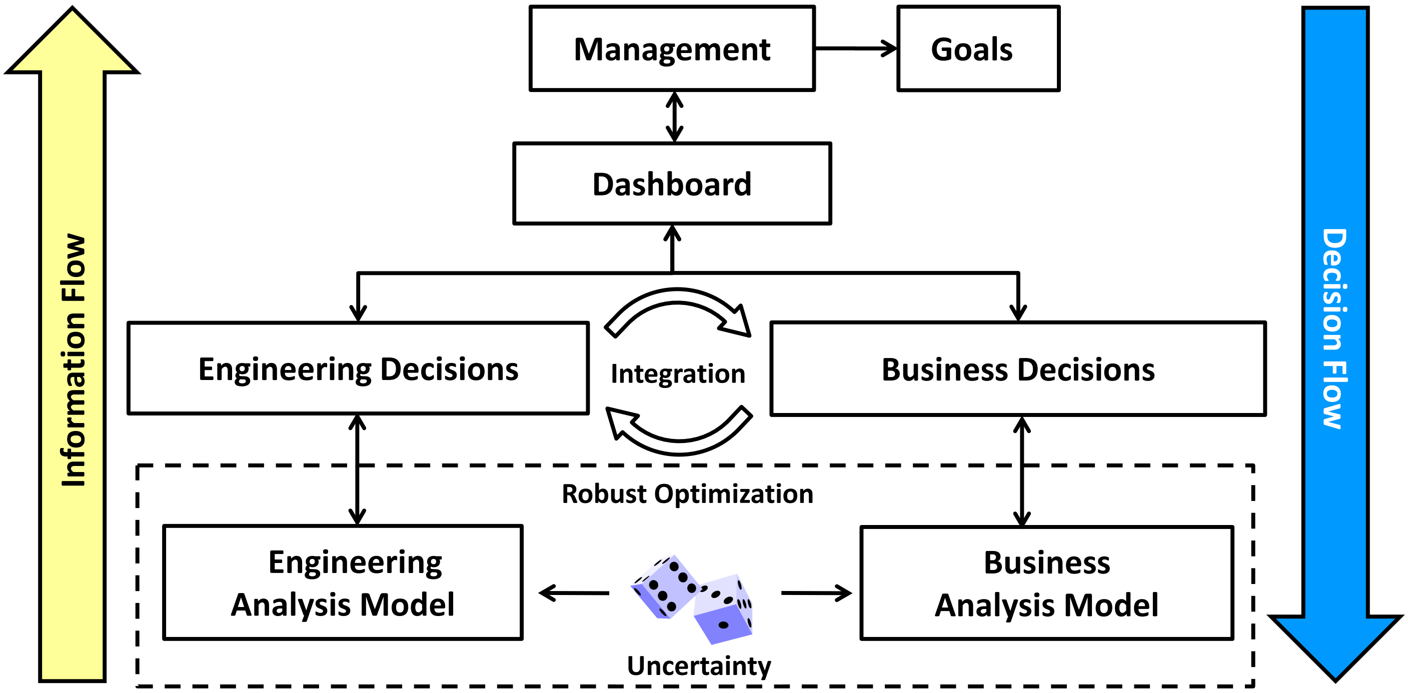
Information Flow

Management

Goals

Dashboard

Engineering Decisions

Integration

Business Decisions

Robust Optimization

Engineering Analysis Model

Business Analysis Model

Uncertainty

Decision Flow

Engineering and Business Analysis Models

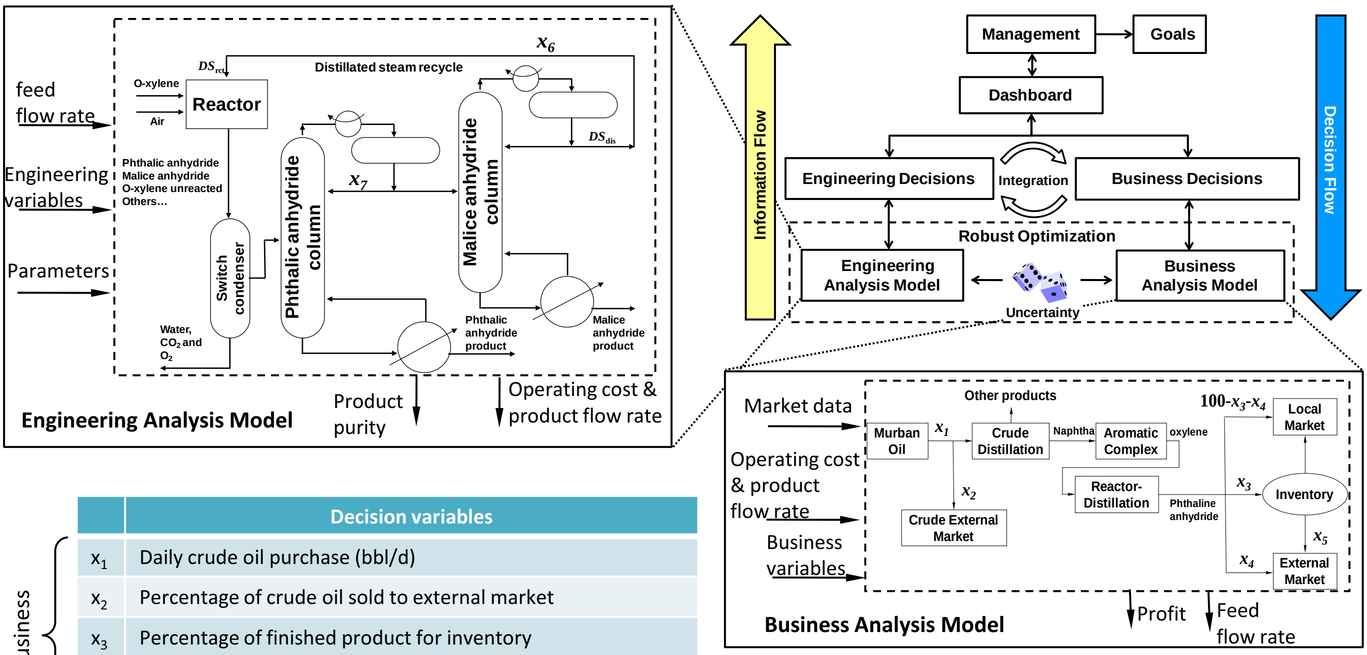

		Decision variables
Business	x_1	Daily crude oil purchase (bbl/d)
	x_2	Percentage of crude oil sold to external market
	x_3	Percentage of finished product for inventory
	x_4	Percentage of finished product sent to external market
	x_5	Percentage of inventory released to external market
Eng.	x_6	Flow rate of recycled stream
	x_7	Phthalic anhydride column minimum reflux ratio

Assumptions
Case study is based on only one product
Yield of naphtha is 4%
Cost associated with inventories and stock out

Robust Optimization of Engineering-Business Model

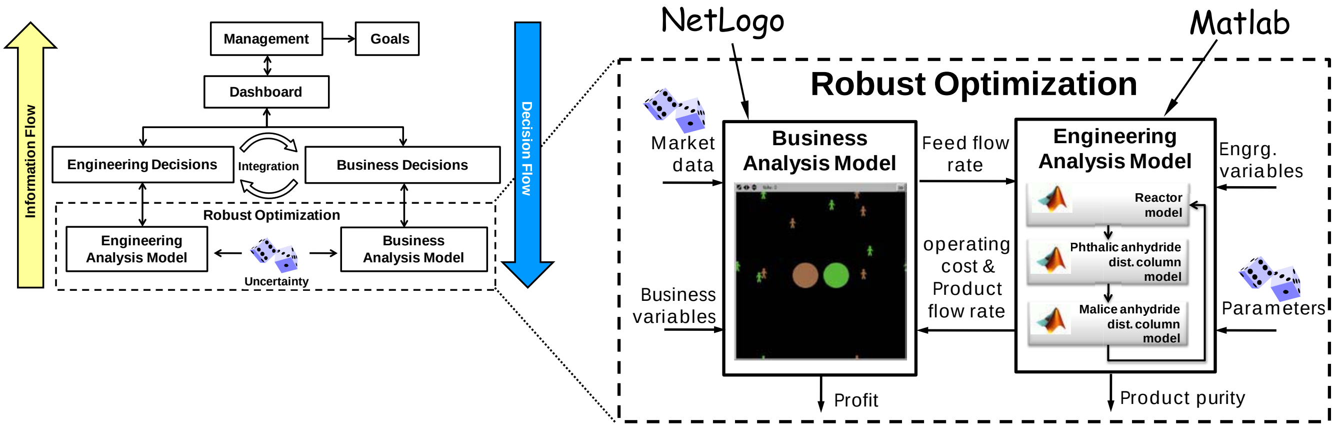
Information Flow

Management

Goals

Dashboard

Engineering Decisions

Integration

Business Decisions

Robust Optimization

Engineering Analysis Model

Uncertainty

Business Analysis Model

Decision Flow

NetLogo

Matlab

Robust Optimization

Market data

Business variables

Business Analysis Model

Feed flow rate

operating cost & Product flow rate

Engineering Analysis Model

Reactor model

Phthalic anhydride dist. column model

Malice anhydride dist. column model

Engrg. variables

Parameters

Profit

Product purity

Robust Optimization Problem

objectives: maximize profit
maximize product purity

by changing: engineering and business variables

subject to: constraints on inventory, production capacity, with price and parameter uncertainty

---

Decision Support Role of Dashboard

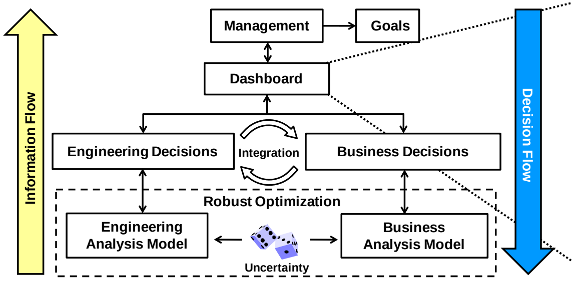
Information Flow

Management

Goals

Dashboard

Engineering Decisions

Integration

Business Decisions

Robust Optimization

Engineering Analysis Model

Uncertainty

Business Analysis Model

Decision Flow

Dashboard

Dashboard is an interface between management and engineering-business decision model

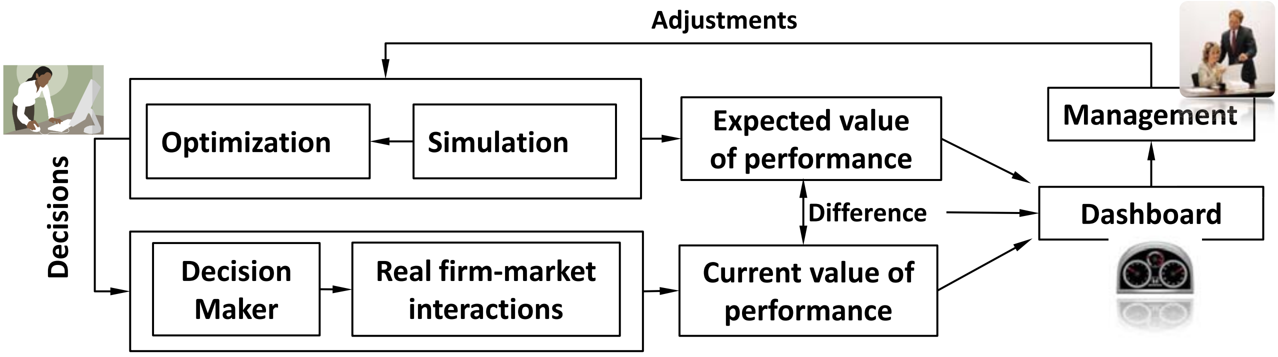
Adjustments

Decisions

Optimization

Simulation

Expected value of performance

Difference

Management

Dashboard

Decision Maker

Real firm-market interactions

Current value of performance

Dashboard’s Main Functions

Enhanced Dashboard interface (new version)

“Firm Performance”: shows real-time (actual) data/figures

“Simulation Result”: shows estimates based on analysis models

“Recommended Decisions”: shows optimal decisions obtained from analysis models

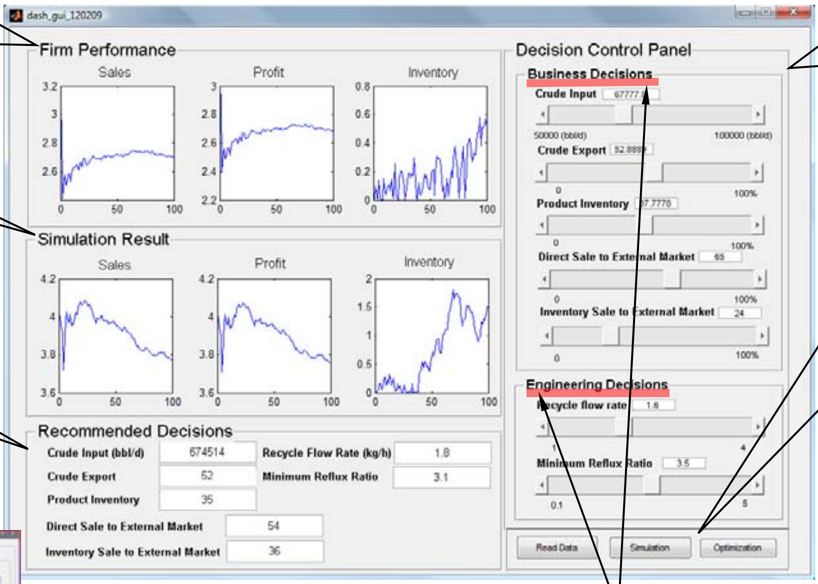

Recommended Decisions

Crude Input (bbl/d)	674514	Recycle Flow Rate (kg/h)	1.8
Crude Export	52	Minimum Reflux Ratio	3.1
Product Inventory	35		
Direct Sale to External Market	54		
Inventory Sale to External Market	36		

Decision Control Panel

Business Decisions

Crude Input 67777.

Crude Export 52.888

Product Inventory 7.7770

Direct Sale to External Market 65

Inventory Sale to External Market 24

Engineering Decisions

Recycle flow rate 1.6

Minimum Reflux Ratio 3.5

Management uses “Decision Control Panel” to implement actual decisions

“Real Data”: updates firm performance

“Simulation”: run business and engineering analysis models

“Optimization”: obtain optimal decisions

Preliminary integration of business and engineering decision-making modules in the “Decision Control Panel”

Previous Dashboard interface (old version, August 2009)

Task 2:

Obtain multi-objectively optimum and robust solutions

Multi-Objective Robust Optimization (MORO): Problem Definition

$$\begin{aligned} &\underset{\mathbf{x}}{\text{minimize}} && f_m(\mathbf{x},\mathbf{p}) && m=1,\dots,M \\ &\text{subject to} && g_j(\mathbf{x},\mathbf{p})\le 0 && j=1,\dots,J \end{aligned}$$

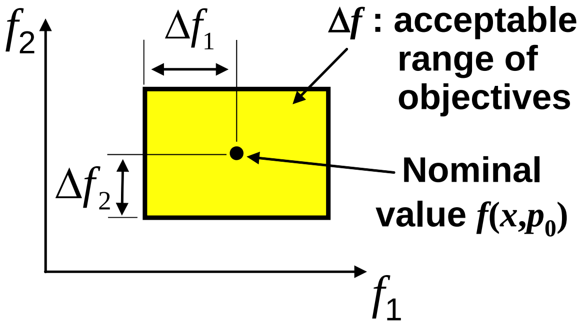

Δf : acceptable range of objectives

Nominal value $f(x,p_0)$

Objective Function Space

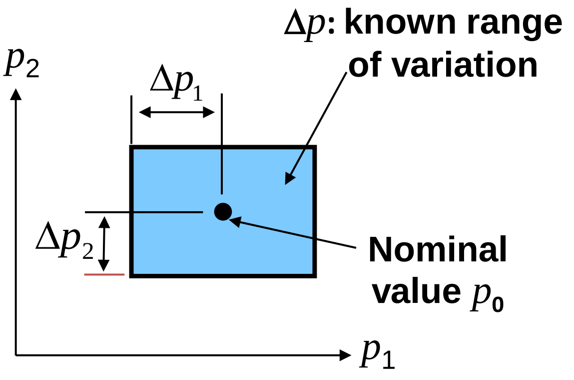

Δp: known range of variation

Nominal value p_0

Parameter Space

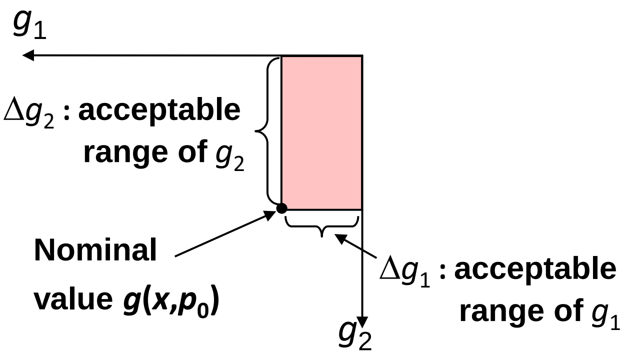

Δg_2 : acceptable range of g_2

Nominal value $g(x,p_0)$

Δg_1 : acceptable range of g_1

Constraint Function Space

Robustness Determination: Basic Idea

Multi-Objective Robustness

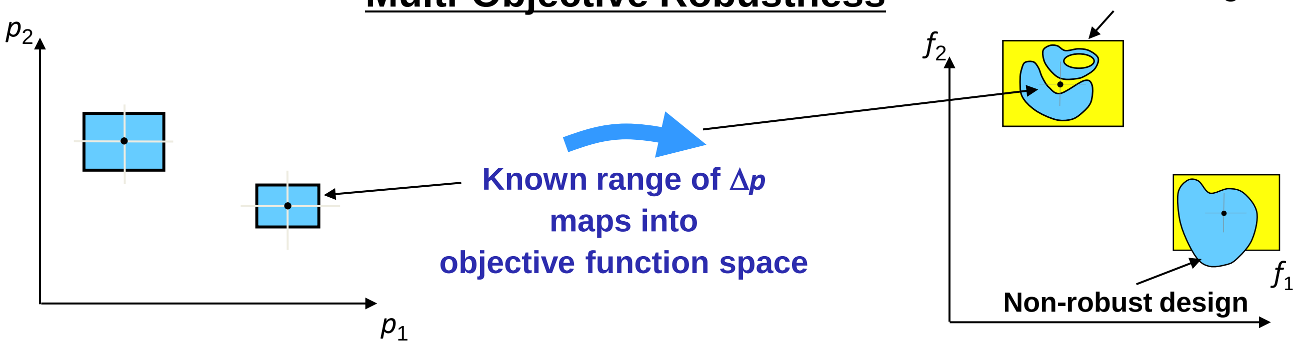

Robust design

Known range of Δp maps into objective function space

Non-robust design

Feasibility Robustness

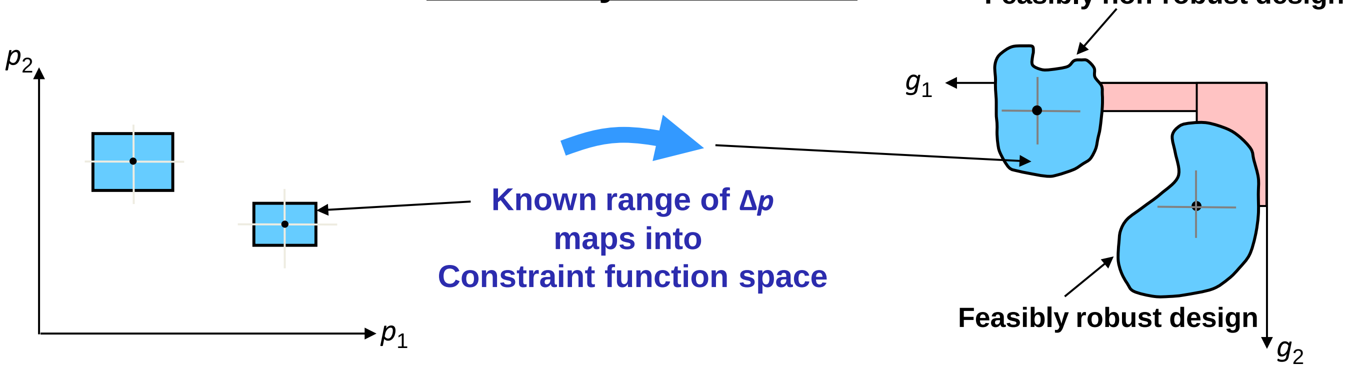

Feasibly non-robust design

Known range of Δp maps into Constraint function space

Feasibly robust design

Multi-Objective Robust Optimization (MORO): Approaches

- Three approaches have been developed/implemented with improvements since Jan 2008:
  - *Previous MORO approach* (developed before the start of this project – implemented for PI project in Jan 2008)
  - *Improved MORO approach* (developed and implemented during mid 2008 until August 2009)
  - *Approximation assisted improved MORO approach* (developed and implemented since Aug 2009)

Previous MORO Approach*

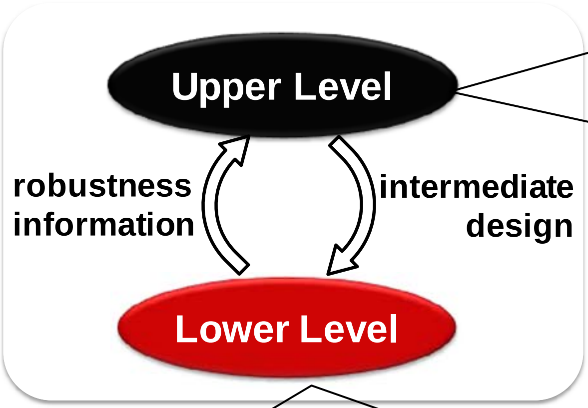

$$\min\ f_m(\mathbf{x},\mathbf{p}), m=1,\ldots,M$$
$$\text{s.t. } \mathrm{WCV}(\mathbf{x},\mathbf{p}) \le 0,\ j=1,\ldots,J$$

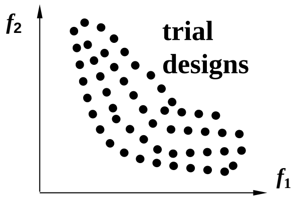

upper level subproblem searches for trial designs

lower level subproblem requires a large # of function calls

$$\mathrm{WCV}(\mathbf{x},\mathbf{p}) = \max_{\Delta\mathbf{p}} \left\| r_i(\mathbf{x},\mathbf{p}+\Delta\mathbf{p}) \right\|_\infty i=1,\ldots,J+M$$
$$\text{s.t.}\quad \Delta\mathbf{p}^L \le \Delta\mathbf{p} \le \Delta\mathbf{p}^L$$
$$r_i = \begin{cases} g_i(\mathbf{x},\mathbf{p}+\Delta\mathbf{p}); i=1,\ldots,J \\ \left| f_{i-J}(\mathbf{x},\mathbf{p}+\Delta\mathbf{p}) - f_{i-J}(\mathbf{x},\mathbf{p}) \right| - \Delta f_{i-J}; \\ i=J+1,\ldots,J+M \end{cases}$$

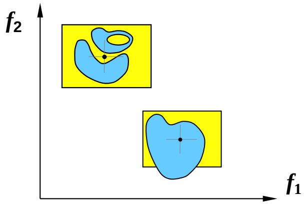

lower level evaluates robustness for each trial design from upper level

* Li, M., Azarm, S., and Boyars, A., 2006, “A New Deterministic Approach Using Sensitivity Region Measures for Multi-Objective Robust and Feasibility Robust Design Optimization,” *Journal of Mechanical Design*, 128(4), 874-883

Improved MORO Approach

collects Robust Pareto Points (RPPs)

lower level subproblem requires fewer # of function calls compared to "Previous MORO Approach"

$$\min\ f_m(\mathbf{x},\mathbf{p}), m=1,\ldots,M$$

$$\text{s.t. } g_j(\mathbf{x},\mathbf{p}+\Delta\mathbf{p}) \le 0,\ j=1,\ldots,J$$

$$\left|f_m(\mathbf{x},\mathbf{p}+\Delta\mathbf{p}) - f_m(\mathbf{x},\mathbf{p})\right| - \Delta f_m \le 0, m=1,\ldots,M$$

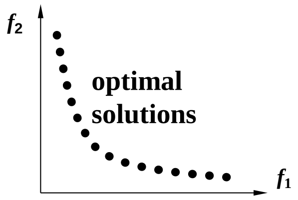

upper level obtains Pareto optimal solutions

$$\text{WCV} = \max_{\Delta\mathbf{p}} \left\| r_i(\mathbf{x},\mathbf{p}+\Delta\mathbf{p}) \right\|_\infty i=1,\ldots,J+M$$

$$\text{s.t.}\quad \Delta\mathbf{p}^L \le \Delta\mathbf{p} \le \Delta\mathbf{p}^L$$

lower level evaluates robustness for optimal solutions

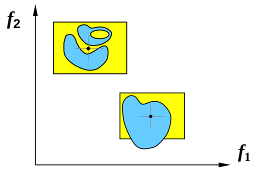

Approximation Assisted Improved MORO Approach

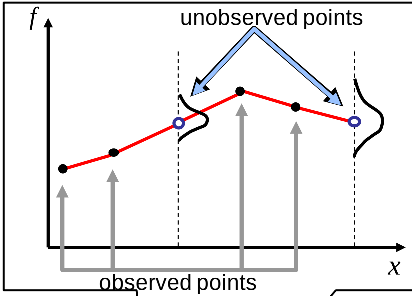

Kriging meta-model predicts f for an "unobserved" point, given actual value for "observed" points

RPPs collection is used as "observed points" to improve accuracy of metamodel

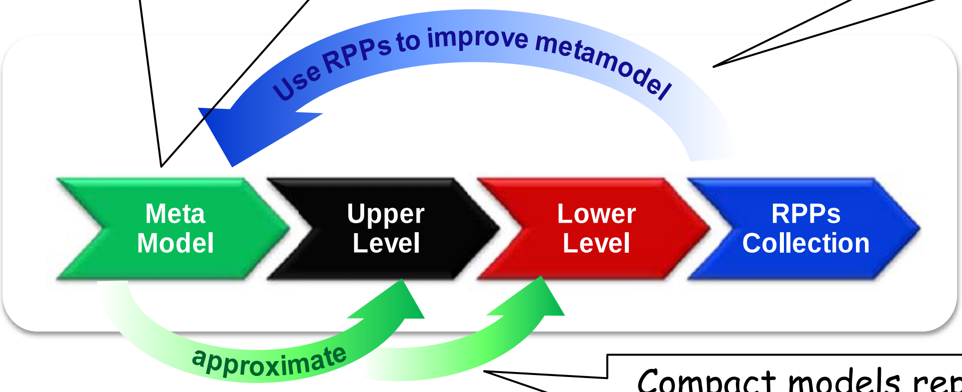

upper and lower level subproblems require much less # of function calls because they are approximated!

Compact models replace (expensive) functions in the upper and lower level subproblems

MORO Approaches: Timeline of Improvements

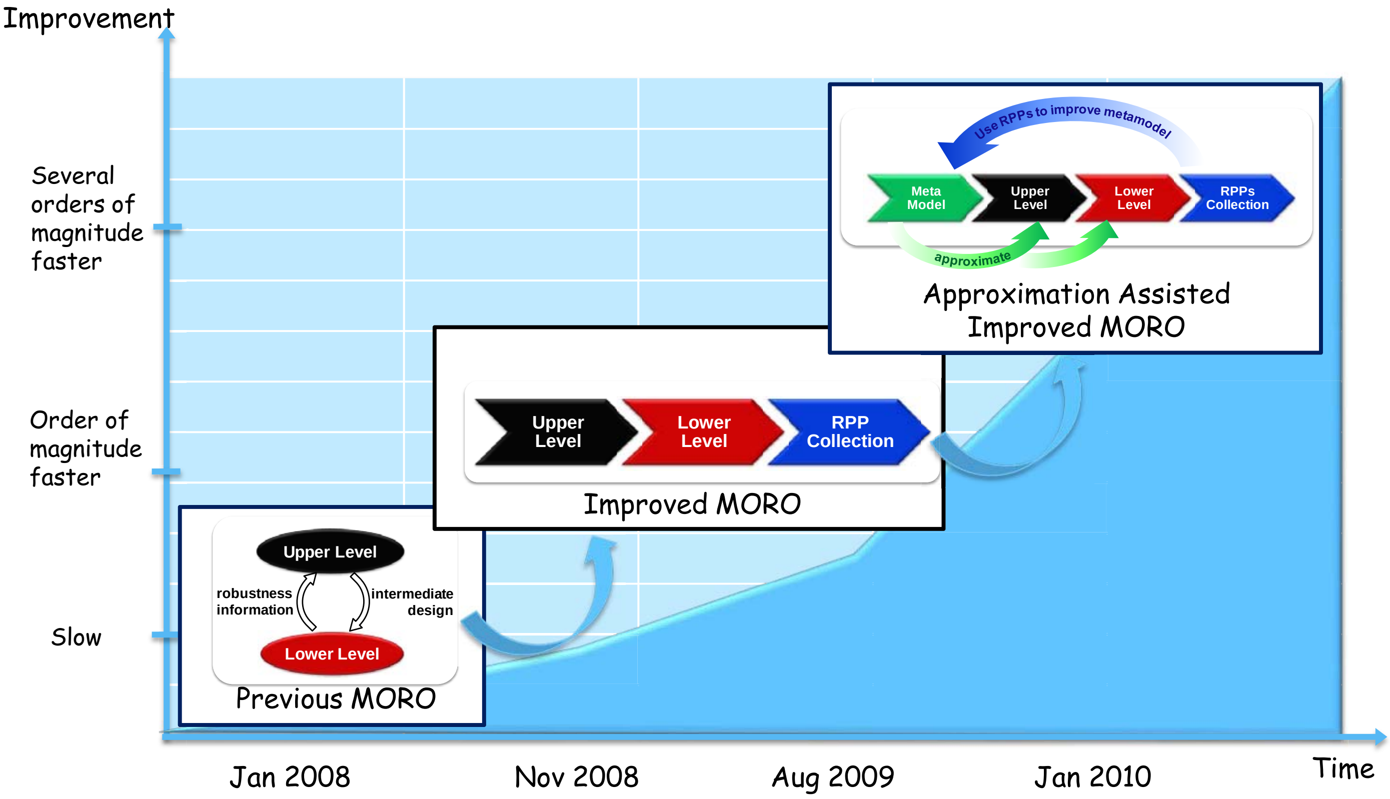

Case Study

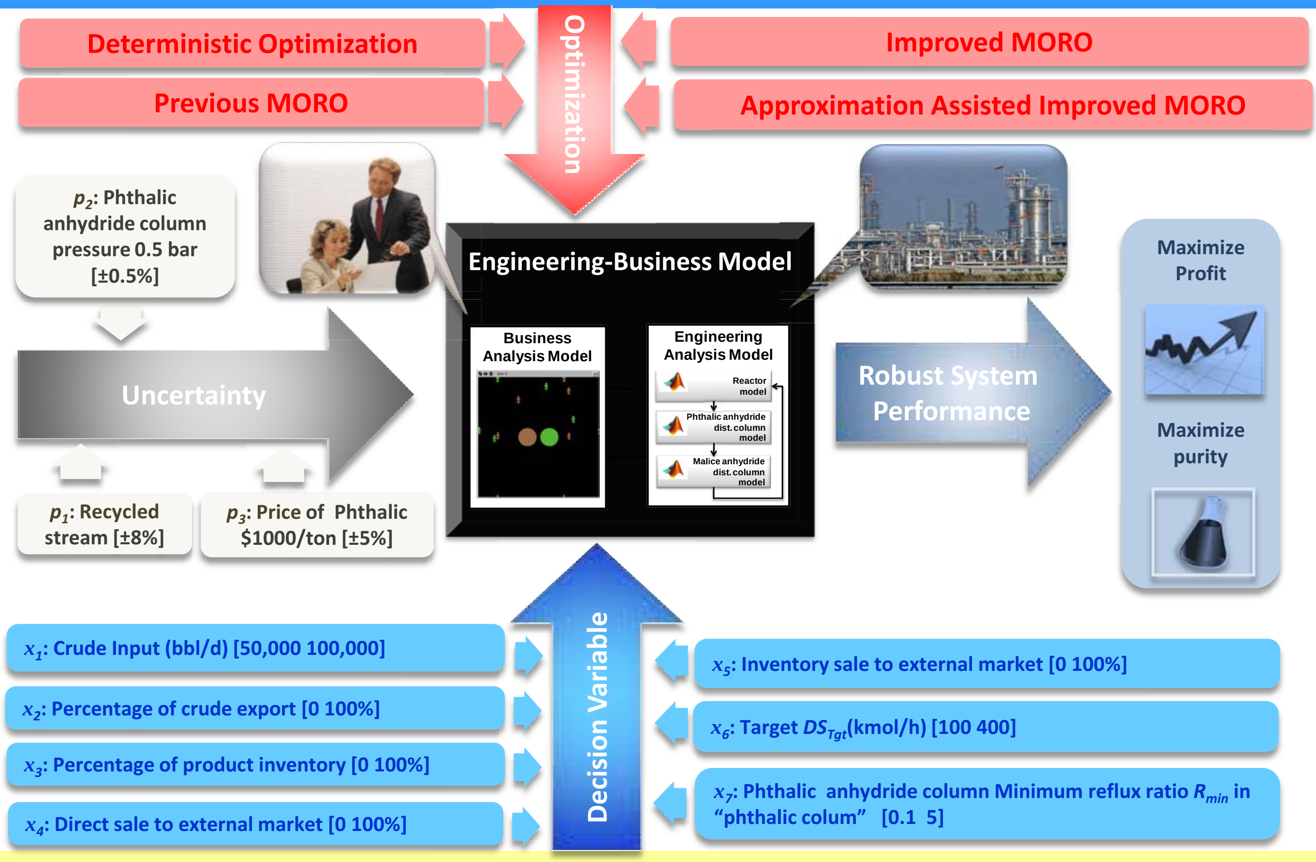

p_2: Phthalic anhydride column pressure 0.5 bar [±0.5%]

p_1: Recycled stream [±8%]

p_3: Price of Phthalic $1000/ton [±5%]

x_1: Crude Input (bbl/d) [50,000 100,000]

x_2: Percentage of crude export [0 100%]

x_3: Percentage of product inventory [0 100%]

x_4: Direct sale to external market [0 100%]

x_5: Inventory sale to external market [0 100%]

x_6: Target DS_{Tgt}(kmol/h) [100 400]

x_7: Phthalic anhydride column Minimum reflux ratio R_{min} in “phthalic colum” [0.1 5]

Case Study: Results

- Robust Pareto solutions obtained by different approaches compares well
- Computational cost by the approximation assisted approach is orders of magnitude less than the previous and improved approaches

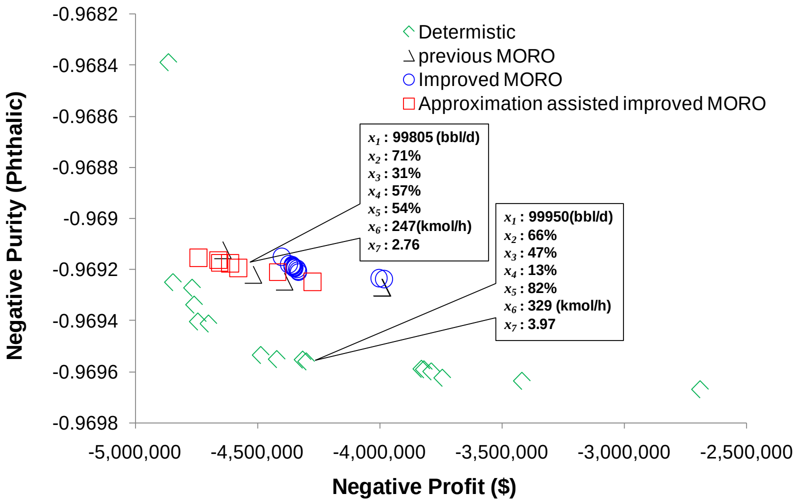

Computational cost (# of function calls) for the reactor-distillation example:

	Previous Approach	Improved Approach	Approximation Assisted Improved Approach
Reactor-distillation example	897,104	57,368	178

Other Test Examples: Results

$$\min_{\mathbf{x}} \quad f_1(x) = px_1$$
$$\min_{\mathbf{x}} \quad f_2(x) = (p + x_2)/x_1$$
$$\text{s.t.} \quad g_1(x) = 6 - 9x_1 - (p + \Delta p)x_2 \le 0$$
$$g_2(x) = 1 - 9x_1 + (p + \Delta p)x_2 \le 0$$
$$x_1 \in [0.1,1],\ \ x_2 \in [0,5], p \in [-0.3,0.3]$$
$$AOVR = (0.3,0.6)$$

$$\min f_1(x) = x_1$$
$$\min f_2(x) = g(x)(1 - \sqrt{f_1(x)/g(x)}$$
$$s.t.: g(x) = 1 + (p + \Delta p) + 9\sum_{i=2}^{5}(x_i - x_1)^2/4$$
$$x_i \in [0,1], \Delta p \in [-0.2,0.2]$$
$$AOVR = (0.1,0.15)$$

$$\min f_1(x) = x_1$$
$$\min f_2(x) = g(x)(1 - f_1(x)/g(x)^2)$$
$$s.t.: g(x) = 1 + p + 9(\sum_{i=2}^{5}(x_i - x_1)^2)/4$$
$$x_i \in [0,1], p \in [-0.2,0.2]$$
$$AOVR = (0.1,0.3)$$

$$\min f_1(x) = \sqrt{x_1 + (p + \Delta p)}$$
$$\min f_2(x) = g(x)[(1 - (f_1(x)/g(x))^2]$$
$$s.t.: g(x) = 1 + 9(\sum_{i=2}^{5}(x_i^2 - x_1)^2)/4$$
$$x_i \in [0,1], \Delta p \in [-0.2,0.2]$$
$$AOVR = (0.3,0.15)$$

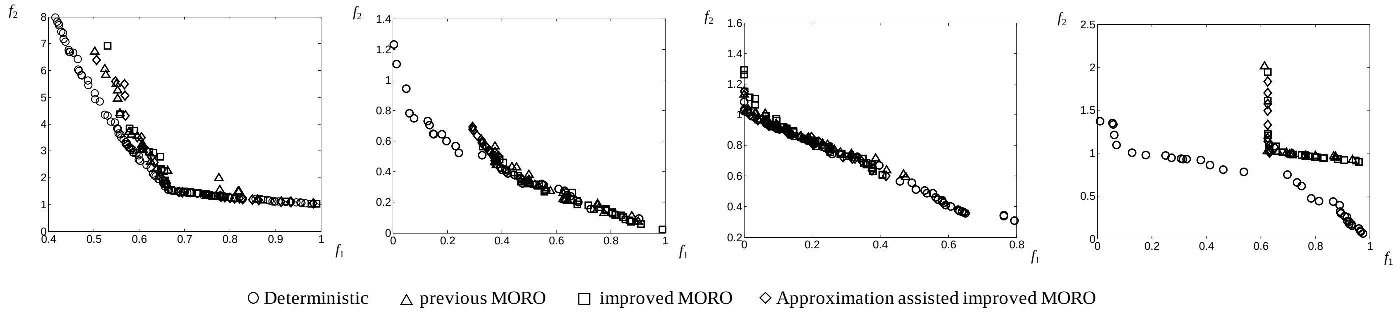

#	Previous MORO approach			Improved MORO approach			Approximation assisted improved MORO approach		
	max	min	mean	max	min	mean	max	min	mean
1	1,779,343	2,343,413	2,021,219	223,437	287,661	257,209	251	560	457
2	3,051,525	3,752,498	3,355,853	198,524	236,391	220,588	375	502	466
3	3,233,346	3,843,556	3,499,124	137,727	268,945	186,358	458	864	657
4	3,893,237	4,445,568	4,279,752	175,441	257,744	193,740	474	741	614

Project Status

- Met with our PI partners on a monthly (or more) basis by MSN
- Almansoori (PI) visited University of Maryland (UMD) during July 2009:
  - Worked and interacted with UMD students/faculty on the research project
  - Explored possibility of a joint graduate level course in engineering-business decision making
- Azarm and Kannan visited PI in August 2009 and met and presented an update of PI-UMD work to ADONC OP CO: ADGAS, ADCO, ZADCO, Takreer, and Borouge
  - Several companies indicated interests. Work is ongoing with Takreer for problem definition and exchange of data in "Optimizing of Carbon emission in a refinery"

Project Status (cont'd)

- Work Accomplished
  - Developed an integrated engineering-business decision support framework with dashboard that can help enhance the effectiveness and quality of decisions for petrochemical system problems
  - Significantly improved the computational effort in multi-objective simulation-based optimization under uncertainty
- Work Remaining
  - Extend Approximation Assisted Robust optimization (AARO) to handle petrochemical system problems with multiple subsystems, each having multiple objectives
  - Apply AARO to problems in carbon emissions (w/ Takreer)

Summary

- Interim Conclusions
  - Engineering-business optimization is crucial in efficient and cost-effective energy system management
  - Approximation assisted robust optimization technique enables handling a broad class of energy system problems with significantly less computational efforts
- Expected Benefit to ADNOC/PI
  - Optimization models and methods that can be used for optimizing specific systems that are in use at ADNOC facilities
  - Business and engineering decisions can be ranked not only based on cost but also robustness (or "insensitivity" to uncertainty) as ADNOC plants are very integrated, will grow in the future and subject to uncertainty

---

2009 Publications that Acknowledged PI-UMD Collaboration

The following statement included in our publications listed below:

"The work presented in this paper was supported in part by The Petroleum Institute (PI), Abu Dhabi, United Arab Emirates, as part of the Education and Energy Research Collaboration (EERC) agreement between the PI and University of Maryland, College Park."

1. Li, G., M. Li, S. Azarm, S. Al Hashimi, T. Al Ameri and N. Al Qasas, 2009, "Improving Multi-Objective Genetic Algorithms with Adaptive Design of Experiments and Online Metamodeling," *Structural and Multidisciplinary Optimization* , 37(5), 447-461.
2. W. Hu, M. L., S. Azarm, S. Al Hashimi, A. Almansoori, and N. Al-Qasas, 2009, "Improving Multi-Objective Robust Optimization under Interval Uncertainty Using Worst Possible Point Constraint Cuts," *Proceedings of the ASME International Design Engineering Technical Conferences*, San Diego, CA, paper No. DETC2009-87312.
3. Li, M., S. Azarm, N. Williams, S. Al Hashimi, A. Almansoori, and N. Al Qasas, 2009, "Integrated Multi-Objective Robust Optimization and Sensitivity Analysis with Irreducible and Reducible Interval Uncertainty," *Engineering Optimization*, 41(10), 889–908
4. Hu, W, M. Li, S. Azarm, A. Almansoori, , S. Al Hashimi and N. Al-Qasas, 2009, "Improving Multi-Objective Robust Optimization under Interval Uncertainty Using Approximation and Constraint Cuts", *Journal of Mechanical Design* (submitted/under revision).
5. Kamaha, P., W. Hu, A. Almansoori, S. Al Hashimi, P. K. Kannan, and S. Azarm, 2009, "Corporate Dashboards for Integrated Business and Engineering Decisions in Oil Refineries: An Agent-Based Approach," *Decision Support Systems* (under preparation).

Simulation, Optimization, and Control of Solid Oxide Fuel Cell System

UMN Team: Sujit S. Jogwar, Dimitris Georgis, Prodromos Daoutidis, Jeffrey J. Derby
PI Team: Ali S. Almansoori

1^{st} Annual PI Partner Schools Research Workshop
The Petroleum Institute, Abu Dhabi, U.A.E.
January 6-7, 2010

PI Partners

PI Sponsors

Fuel cells are a promising means of efficiently producing electricity

- Fuel cells (FCs): William Grove (1839)
  "A fuel cell is an electrochemical 'device' that continuously converts chemical energy into electric energy (and some heat) for as long as fuel and oxidant are supplied"
- Various types of fuel cells

AFC	Low T	Military and space applications
PEMFC	Low T	Automotive applications
PAFC	Intermediate T	Combined energy & power generation
MCFC	High T	Stand alone power system
SOFC	High T	Stationary power production

Typical fuel for FC is H_2

Challenges with H_2 storage and transportation
$\Rightarrow$ *in situ* H_2 production

Solid Oxide Fuel Cells (SOFCs)

Anode:

$$H_2 + O^{2-} \rightarrow H_2O + 2e^-$$

Cathode:

$$\frac{1}{2}O_2 + 2e^- \rightarrow O^{2-}$$

(Net) $H_2 + \frac{1}{2}O_2 \rightarrow H_2O$

$$\Delta H^o_{298} = -241.83 \; KJ/mol$$

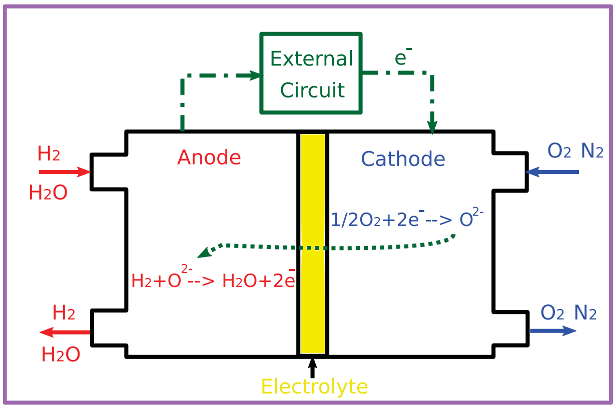

- Common geometries: planar, tubular
- High temperature operation ⇓
  - Tolerance to impurities
  - Potential for energy integration

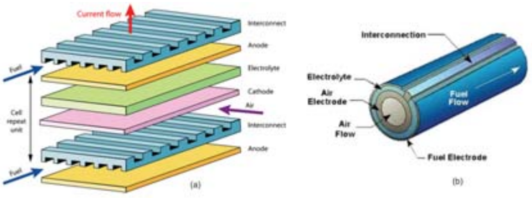

SOFC performance may be improved by systems and energy integration

- SOFC: High T effluent ⇒ Potential energy source
- Fuel processor: Hydrocarbon fuel → H_2
  Methane Steam Reforming - Endothermic ⇒ Energy sink
- Air preheater: $T_{Air,Ambient} \rightarrow T_{Air,in-SOFC}$
  ⇒ Energy sink

Potential for coupling energy sources and sinks

Objective: Recover and recycle most of the energy available with SOFC effluent

Energy integrated SOFC system

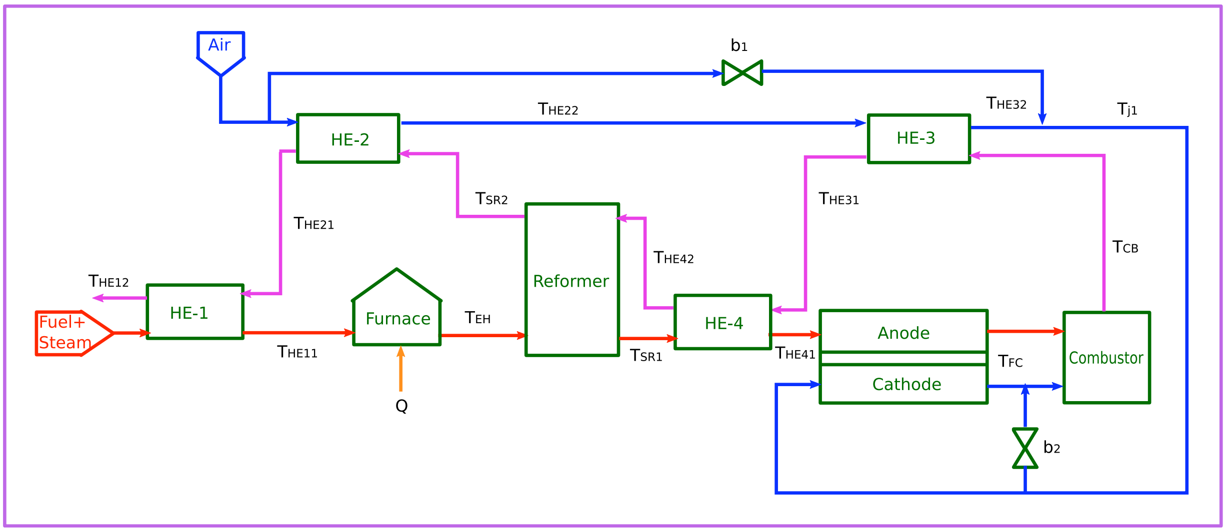

- SOFC
- Steam Reformer
- Catalytic Burner
- Furnace
- Heat Exchangers (4)

Assembling a lumped-parameter model of the SOFC system, I

Electrochemical Equations

$$V_1 = E_o + \frac{RT_{FC}}{2F} \, ln \left(\frac{p_{H_2} p_{O_2}^{0.5}}{p_{H_2O}} \right)$$

$$V_2 = \frac{RT_{FC}}{F} \, sinh^{-1} \left(\frac{I_L}{2I_o} \right)$$

. . . Activation polarization

$$V_3 = \frac{RT_{FC}}{2F} \, ln \left\{ \left(\frac{p_{H_2} p_{O_2}^{0.5}}{p_{H_2O}} \right) / \left(\frac{p_{H_2}^{TPB} (p_{O_2}^{TPB})^{0.5}}{p_{H_2O}^{TPB}} \right) \right\}$$

. . . Concentration polarization

$$V_4 = I_L \times R_i$$

. . . Ohmic polarization

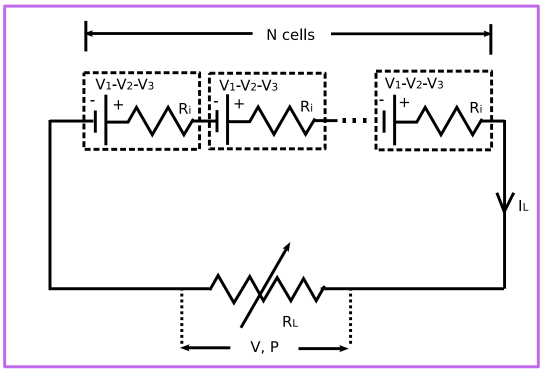

SOFC stack with N cells in series

$$\begin{aligned} V &= N(V_1 - V_2 - V_3 - V_4) \\ P &= V \times I_L \end{aligned}$$

Assembling a lumped-parameter model of the SOFC system, II

Material and energy balance equations

$$\begin{aligned}
\frac{dp_{H_2}}{dt} &= \frac{\dot{n}_{fuel}RT_{FC}}{V_{an}P_{FC}}(p_{H_2,in}-p_{H_2}) - \frac{NRT_{FC}}{V_{an}}\frac{I_L}{2F} \\
\frac{dp_{O_2}}{dt} &= \frac{\dot{n}_{air}RT_{FC}}{V_{ca}P_{FC}}p_{O_2,in} - \frac{\dot{n}_{air,out}RT_{FC}}{V_{ca}P_{FC}}p_{O_2} - \frac{NRT_{FC}}{V_{an}}\frac{I_L}{4F} \\
\frac{dp_{H_2O}}{dt} &= \frac{\dot{n}_{fuel}RT_{FC}}{V_{an}P_{FC}}(p_{H_2O,in}-p_{H_2O}) + \frac{NRT_{FC}}{V_{an}}\frac{I_L}{2F}
\end{aligned}$$

$$\frac{dT_{FC}}{dt} = \frac{1}{\rho_c C_{p,c} V_c}\left[Q_{fuel,in} + Q_{air,in} - Q_{fuel,out} - Q_{air,out} - \Delta H(T_{FC})\frac{I_L}{2F} - VI_L\right]$$

Enthalpy flow: $Q(T) = \sum_i \dot{n}_i \int_{T_{ref}}^{T} C_{p,i}(\tilde{T})d\tilde{T}$

Cathode side exit flow: $\dot{n}_{air,out} = \dot{n}_{air} - I_L/4F$

Lumped-parameter model of the steam reformer

$$\begin{aligned}
CH_4 + H_2O &\rightleftharpoons CO + 3H_2 \quad \Delta H^o_{298} = +246KJ/mol \\
CO + H_2O &\rightleftharpoons CO_2 + H_2 \quad \Delta H^o_{298} = -41KJ/mol
\end{aligned}$$

$$\begin{aligned}
\frac{dp^{SR}_{CH_4}}{dt} &= \frac{\dot{n}_{in}RT_{SR1}}{V_{SR}P_{SR}}p^{SR}_{CH_4,in} - \frac{\dot{n}_{out}RT_{SR1}}{V_{SR}P_{SR}}p^{SR}_{CH_4} - \frac{m_{cat}RT_{SR1}}{V_{SR}}r_1{}^{a} \\
\frac{dp^{SR}_{H_2O}}{dt} &= \frac{\dot{n}_{in}RT_{SR1}}{V_{SR}P_{SR}}p^{SR}_{H_2O,in} - \frac{\dot{n}_{out}RT_{SR1}}{V_{SR}P_{SR}}p^{SR}_{H_2O} - \frac{m_{cat}RT_{SR1}}{V_{SR}}(r_1+r_2) \\
\frac{dp^{SR}_{CO_2}}{dt} &= \frac{\dot{n}_{in}RT_{SR1}}{V_{SR}P_{SR}}p^{SR}_{CO_2,in} - \frac{\dot{n}_{out}RT_{SR1}}{V_{SR}P_{SR}}p^{SR}_{CO_2} + \frac{m_{cat}RT_{SR1}}{V_{SR}}r_2 \\
\frac{dp^{SR}_{CO}}{dt} &= \frac{\dot{n}_{in}RT_{SR1}}{V_{SR}P_{SR}}p^{SR}_{CO,in} - \frac{\dot{n}_{out}RT_{SR1}}{V_{SR}P_{SR}}p^{SR}_{CO} + \frac{m_{cat}RT_{SR1}}{V_{SR}}(r_1-r_2) \\
\frac{dp^{SR}_{H_2}}{dt} &= \frac{\dot{n}_{in}RT_{SR1}}{V_{SR}P_{SR}}p^{SR}_{H_2,in} - \frac{\dot{n}_{out}RT_{SR1}}{V_{SR}P_{SR}}p^{SR}_{H_2} + \frac{m_{cat}RT_{SR1}}{V_{SR}}(3r_1+r_2)
\end{aligned}$$

$$\begin{aligned}
\frac{dT_{SR1}}{dt} &= \frac{Q_{fuel,in} - Q_{fuel,out} + UA_{SR}\Delta T_{LM} - m_{cat}\left(r_1\Delta H_1(T_{SR1}) + r_2\Delta H_2(T_{SR1})\right)}{\varepsilon\rho_g(T_{SR1})C_{p,g}(T_{SR1}) + (1-\varepsilon)\rho_{cat}C_{p,cat}} \\
\frac{dT_{SR2}}{dt} &= \frac{1}{V_{SR2}CPM(T_{SR2})}\left(Q_{hot,in} - Q_{hot,out} - UA_{SR}\Delta T_{LM}\right)
\end{aligned}$$

---

[a] r_1, r_2 taken from Xu & Froment AIChE J 1989

Lumped-parameter model of the heat exchangers

- Heat exchangers HE1, HE2, HE3 and HE4

$$\begin{aligned}\frac{dT_{HEi1}}{dt} &= \frac{1}{V_{HEi1}CPM(T_{HEi1})}(Q_{HEi1,in} - Q_{HEi1,out} - UA_{HEi}\Delta T_{LM})\\ \frac{dT_{HEi2}}{dt} &= \frac{1}{V_{HEi2}CPM(T_{HEi2})}(Q_{HEi2,in} - Q_{HEi2,out} + UA_{HEi}\Delta T_{LM})\end{aligned}$$

- Furnace

$$\frac{dT_{EH}}{dt} = \frac{1}{V_{EH}CPM(T_{EH})}(Q_{EH,in} - Q_{EH,out} + Q_{EH})$$

- Burner

$$\frac{dT_{CB}}{dt} = \frac{1}{V_{CB}CPM(T_{CB})}\left(Q_{in} - Q_{out} - \sum_{i=3}^{5} r_i \Delta H_i\right)$$

Steady operating curves

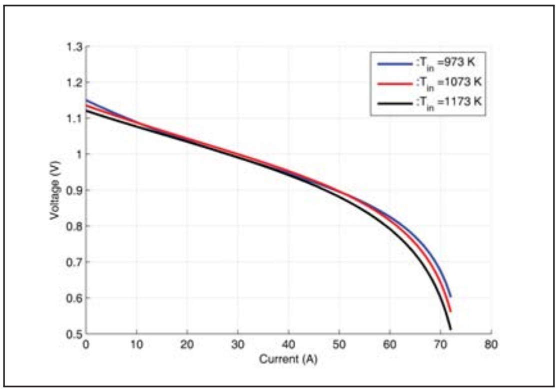

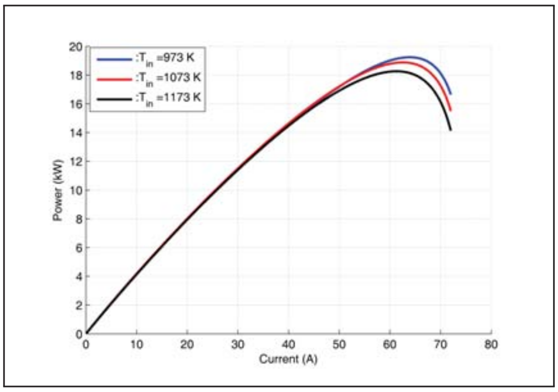

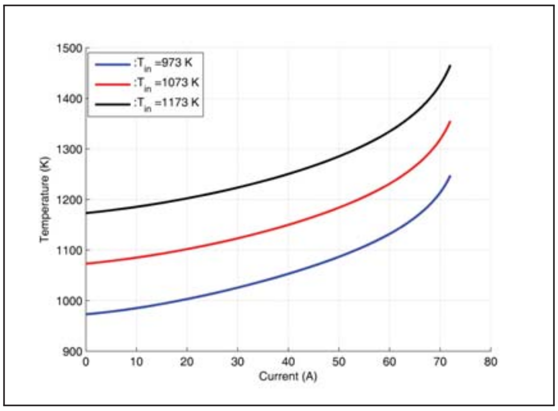

Open-loop dynamics

- 20% increase in steam flow

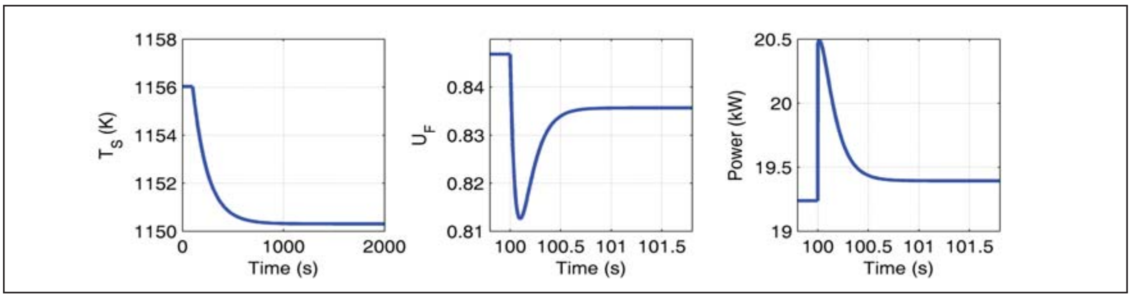

- 10 K increase in reformer inlet temperature

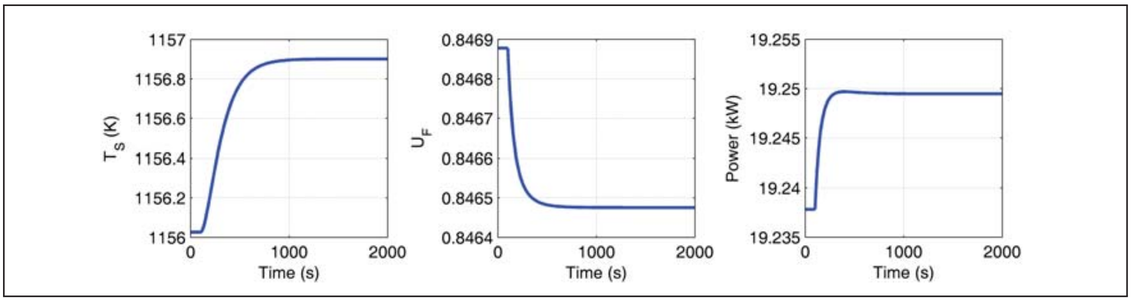

Multi-time scale dynamics?

Control objectives

- Fuel cell power control:
  Deliver power as per requirements from the external load
- Fuel cell temperature control:
  Maintain ionic conductivity of the electrolyte and avoid thermal stresses
- Fuel utilization control:
  Efficient operation and avoid fuel starvation
- Fuel cell air inlet temperature control:
  Maintain the operating point of the fuel cell
- Reformer inlet temperature control:
  Maintain steady production of H_2

Fuel cell power control

- Electrical side vs Chemical side
  Faster response through electrical side
- Natural choice for manipulated input: R_L
- PI controller

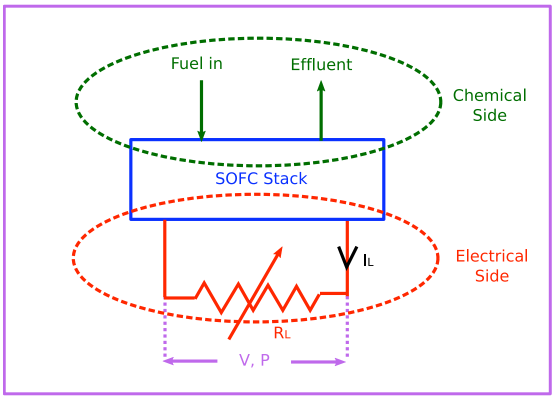

$$\boxed{R_L = R_{L,nom} - K_P\left((P_{set} - P) + \frac{1}{\tau_{I,P}}\int_0^t (P_{set} - P)d\hat{\tau}\right)}$$

$$K_P = 1 \times 10^{-4} W\Omega^{-1}$$

$$\tau_{I,P} = 0.5s$$

Fuel cell temperature control

- Potential manipulated input: Cathode-side air flow rate
- Control relevant model:

$$\boxed{\frac{dT_{FC}}{dt} = \frac{1}{\rho_c C_{p,c} V_c}\left[\dot{n}_{fuel} c_{p,f}(T_{HE41} - T_{FC}) + \dot{n}_{air} c_{p,a}(T_{j1} - T_{FC}) - \Delta H(T_{FC})\frac{I_L}{2F} - VI_L\right]}$$

- Inversion based nonlinear controller

$$\boxed{\beta_{FC}\frac{dT_{FC}}{dt} + T_{FC} = v} \qquad \beta_{FC} = 10min$$

- External integral action for offset-free response

$$\boxed{v = T_{FC,set} + K_{FC}\left((T_{FC,set} - T_{FC}) + \frac{1}{\tau_{I,FC}}\int_0^t (T_{FC,set} - T_{FC})d\tilde{t}\right)}$$

$$K_{FC} = 1.67 \times 10^{-3},\ \tau_{I,FC} = 10min$$

Fuel utilization control

- Fuel utilization (FU)

$$\boxed{FU = 1 - \frac{\dot{n}_{H_2,FC,out}}{\dot{n}_{H_2,FC,in}}}$$

- Power control through electrical side ⇒ sub-efficient fuel utilization
- Potential manipulated input: Fuel flow into the system
- PI controller

$$\boxed{\dot{n}_{in} = \dot{n}_{in,nom} + K_{FU}\left((FU_{set} - FU) + \frac{1}{\tau_{I,FU}}\int_0^t (FU_{set} - FU)d\tilde{t}\right)}$$

$K_{FU} = 0.4 mols^{-1}$, $\tau_{I,FU} = 1min$

Fuel cell air inlet temperature control

- Potential manipulated input: bypass valve b_1
- PI controller

$$\boxed{b_1 = b_{1,nom} - K_{Air}\left((T_{j1,set} - T_{j1}) + \frac{1}{\tau_{I,Air}}\int_0^t (T_{j1,set} - T_{j1})d\tilde{t}\right)}$$

$K_{Air} = 5 \times 10^{-4} K^{-1}$, $\tau_{I,Air} = 10s$

Reformer air inlet control

- Potential manipulated input: Furnace duty
- Control relevant model:

$$\boxed{\frac{dT_{EH}}{dt} = \frac{1}{V_{EH} c_{p,f}} [\dot{n}_{fuel} c_{p,f} (T_{HE11} - T_{EH}) + Q_{EH}]}$$

- Inversion based nonlinear controller

$$\boxed{\beta_{EH} \frac{dT_{EH}}{dt} + T_{EH} = v} \qquad \beta_{EH} = 30s$$

- External integral action for offset-free response

$$\boxed{v = T_{EH,set} + K_{EH} \left((T_{EH,set} - T_{EH}) + \frac{1}{\tau_{I,EH}} \int_0^t (T_{EH,set} - T_{EH}) d\tilde{t} \right)}$$

$K_{EH} = 0.033 \times 10^{-3}$, $\tau_{I,EH} = 30s$

Controller performance: Power demand change

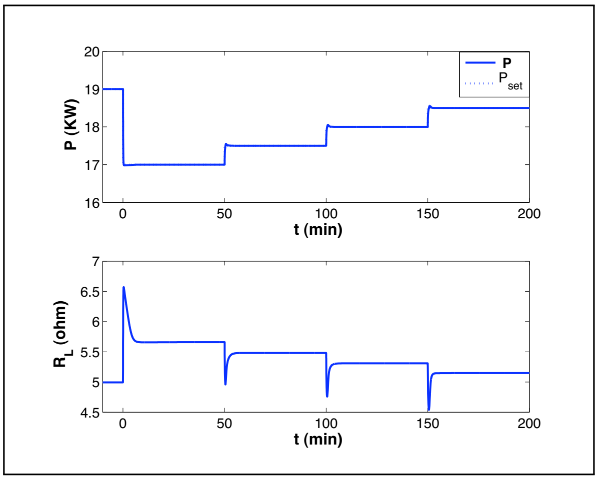

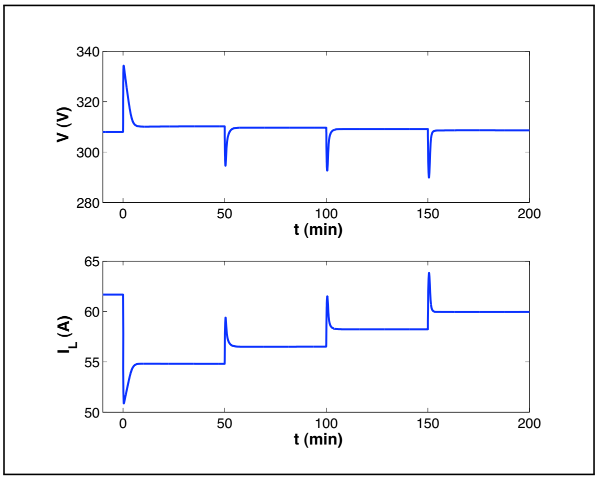

- Series of set point changes
  19KW → 17KW → 17.5KW → 18KW → 18.5KW
- Rapid load following

Controller performance: Power demand change

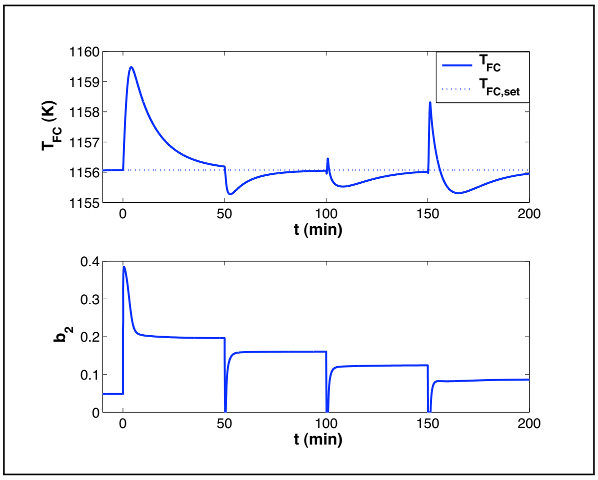

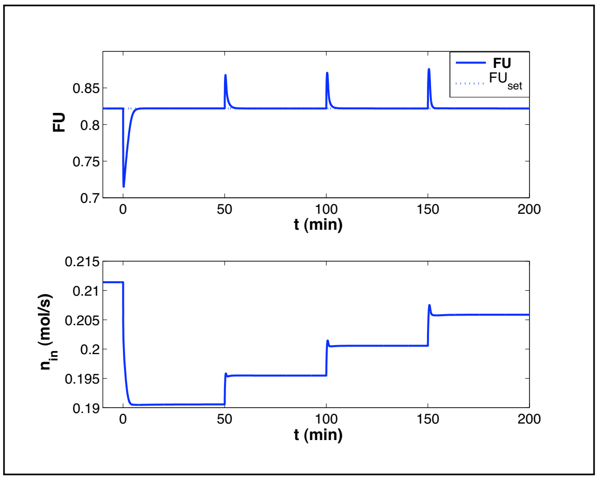

- Excellent performance of model based controller for T_{FC}
- FU controller maintaining fuel efficiency

Controller performance: Power demand change

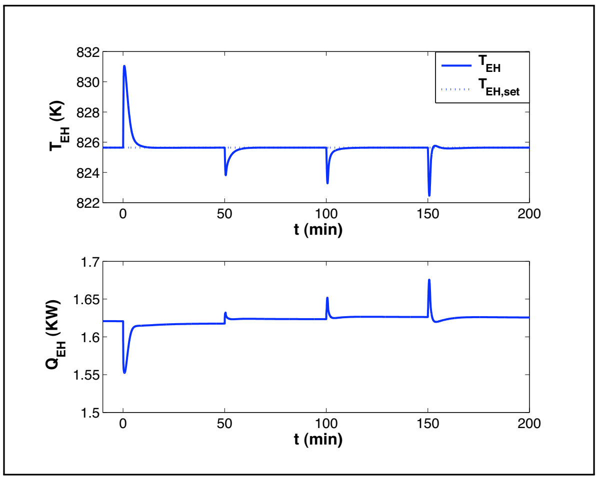

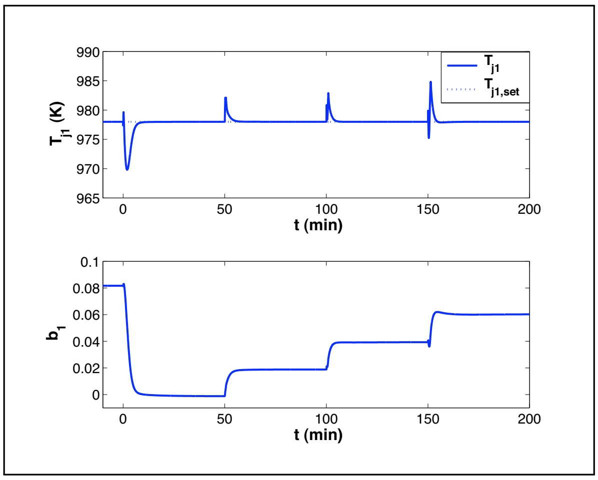

- Interactions leading to disturbances in other loops

Concluding remarks

- Fuel Cell + Reformer ⇒ Promising approach for stationary power production
- High T SOFC ⇒ Potential for energy integration
- Energy integrated SOFC system
  - Dynamic modeling
  - Open-loop studies
  - Controller design
- Simulation case demonstrating feasibility and flexibility of operation

---

Future research directions

- Short term:
  - Flowsheet optimization
  - Energy flow and time scale analysis
- Long term:
  - Distributed modeling
  - Internal reforming

Short-term goals

Flowsheet Optimization

- Finding optimal operating point
- Analysis of alternate configurations
- Pinch analysis for optimal coupling of energy sources/sinks

Time Scale Analysis

- Presence of small and large energy flows: order of magnitude analysis
- Large energy recycle ⇒ Multi-time scale dynamics[a]
- Hierarchical control

---

[a] Jogwar et al. IECR 2009

Long-term goals

Distributed Modeling

- Modeling transport processes
- Identification and control of hot spots
- Use of detailed model for simulations

Internal Reforming

- Reforming and electrochemical reactions in the same unit
- Capability to process wide varieties of fuels[a]
- Analysis and comparison with external reforming

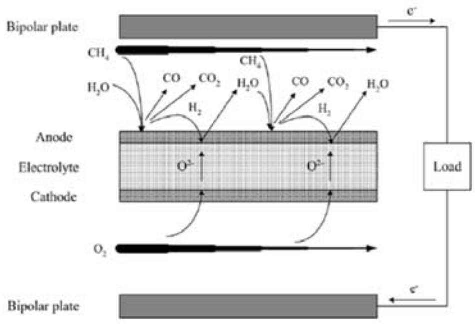

---

[a] Li et al. J. Power Sources 2007

Acknowledgments

Abu Dhabi - Minnesota Institute for Research Excellence

Thank You

Management and Control of Energy Systems

DYNAMICS AND CONTROL OF DRILL STINGS

UMD Team:Bala Balachandran and Chien-Min Liao
PI Team: Hamad Karki and Youssef Abdel-Magid

1st Annual PI Partner Schools Research Workshop
The Petroleum Institute, Abu Dhabi, U.A.E.
January 6-7, 2010

PI Partners

PI Sponsors

Presentation Outline

- Introduction and Motivation
- Project Objectives and Background
- Modeling, Simulations, & Results
- Experimental Arrangement & Results
- Comparisons
- Control Scheme
- Summary and Future Work

Source: www.spe.org

Introduction: DRILL RIG AND DRILL STRING

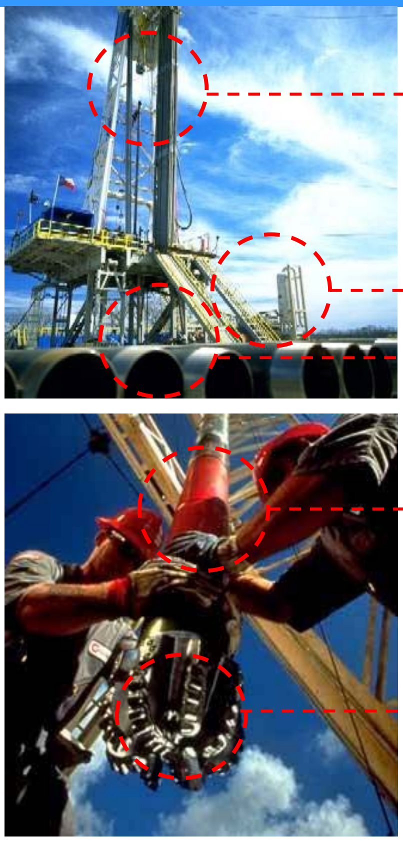

Hoisting Sys.

Power Unit

Drill Pipes

Drill Collar

Drill Bit

Drill-String Failures

Cost in Millions of Dollars

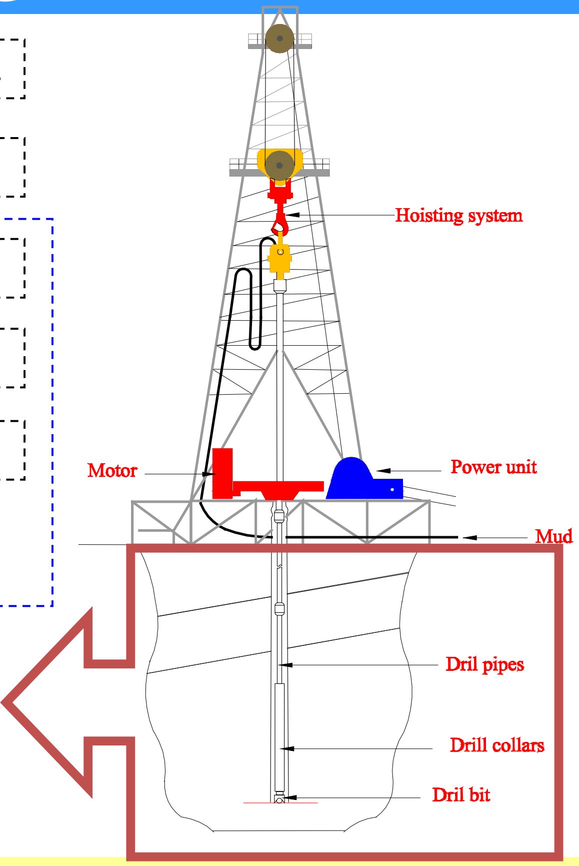

Motivation: Drill-String Failures

- Drill pipe washouts, occur twice per week
- Drill stem separation occurs 1 in 7 wells
  - 45% of deep well drilling failures are related to drill string failures

Failure Types of Drill String

- (a) Bending Failure (b) Torsion Failure

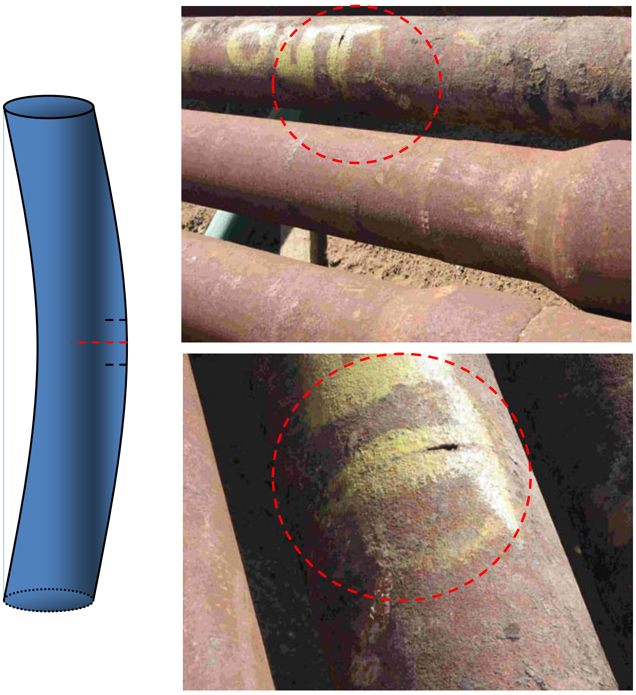

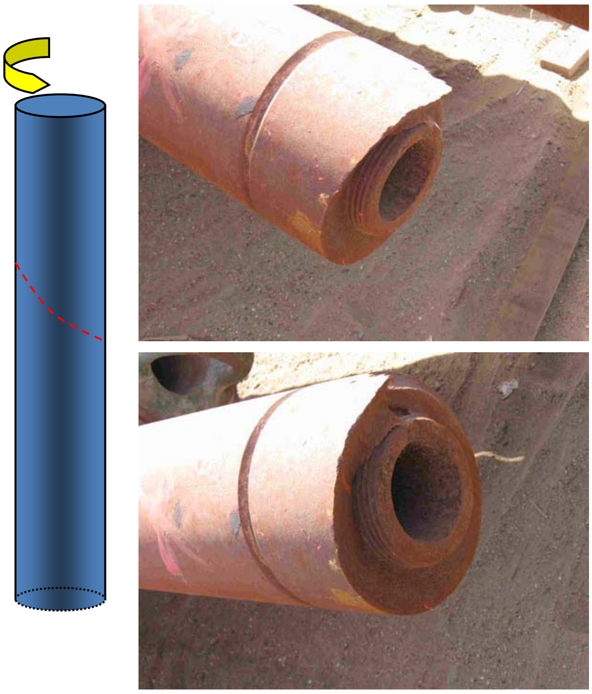

Causes of Drill-String Failure

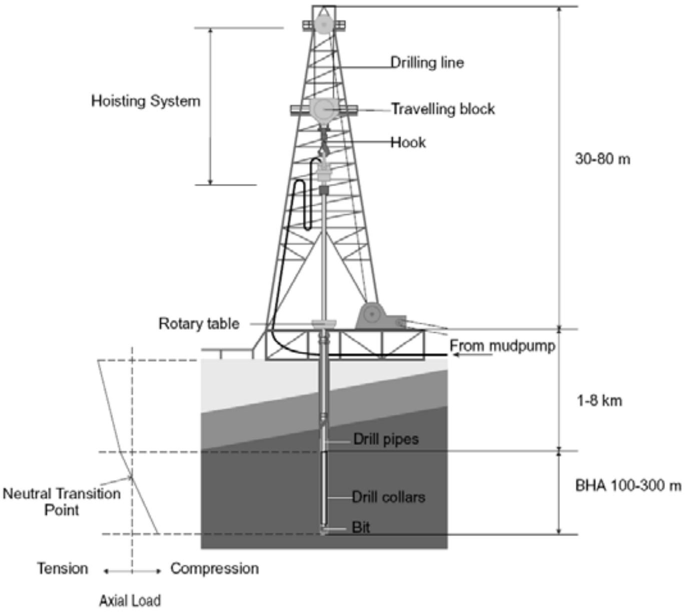

- Manufacturing flaws
- Vibrations (torsion-bending-axial)
- Whirling
- Friction – Stick-slip interactions
- Corrosion
- Fatigue
- Doglegs
- …

Current research is focused on dynamics and control

Diagram sources: Leine et al., (2005) "*Stick-Slip Whirl Interaction in Drillstring Dynamics*", *IUTAM Symposium on Chaotic Dynamics and Control of Systems and Processes in Mechanics*, 287–296.

Project Objectives

- Understand the current state-of-the-art and identify gaps that need to be filled
- Develop and analytically and numerically study control-oriented models for drill strings
- Investigate control of an under-actuated nonlinear system (drill string) with complex interactions with the environment
- Build complimentary drill-string testbeds at PI and UMD to validate models and refine them

Background: Drill-String Vibrations

Type of Vibrations	Description
Axial (Longitudinal)	Due to interaction between drill bit and the rock. Also called as “bit bounce” to describe the contact / non-contact aspects
Bending (Lateral)	Caused by pipe eccentricity, leading to centripetal force during rotation
Torsion (rotational)	Caused by interactions between the bit and the rock or the drill string with the borehole; stick-slip vibration
Hydraulic	In circulation system, stemming from pump pulsations

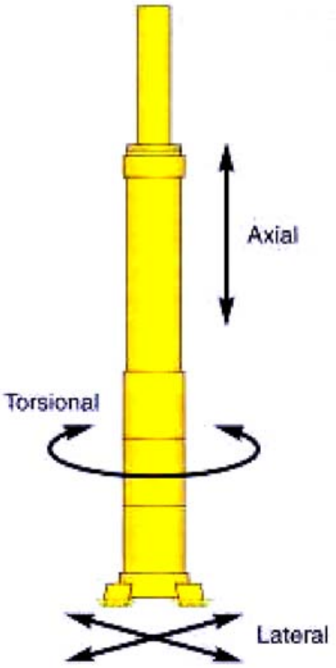

Sources: Tucker, R,.“Engineering Technology", April 2000; Leine et al. (2002).

State-of-the-Art: Drill-String Models

	Spanos *et al.* (2003)	**Leine *et al.* (2002)**	**Melakhessou *et al.*(2003)**	**Navarro-Lopez *et al.* (2009)**
Dimensions	Lateral 1D	Lateral 2D	Lateral 2D	Axial 1D
Vibrations	Lateral	Torsion	Bending & Torsion	Torsion & Axial
Stick-slip	N	Y (String-Shell)	Incomplete	Y (Bit-Rock)
Model features	Simple spring model for soil	Drill mud modeled as fluid force	Unbalanced mass on the rotor	A series of mass-spring-damper systems
Comparisons with experiments	N	Comparisons with qualitative aspects of field data	Limited comparisons with experiments	N

Gaps that Need to be Filled

•Nonlinear dynamics of this system is not well understood given that the drill string can undergo axial, torsion, and lateral vibrations and operational difficulties include sticking, buckling, and fatiguing of strings

•Most of the current models cannot provide spatial information about drill-string failures

•Need drill-string testbeds that can capture at least one or more aspects of the operating conditions in a realistic manner

•Control strategies based on change of rotary speed have been studied to a limited extent, but strategies based on change on weight on bit, drill mud, application of axial force, torque modulation schemes, and nonlinear dynamics (limit cycles and bifurcations) remain largely unexplored

Goals of Current Research

- Understand the axial, torsional, and lateral vibrations of drill-string system
- Examine coupling amongst different modes of vibration in drill-string system such as axial and torsion coupling and torsion and bending coupling
- Model and characterize stick-slip interactions between drill string and outer shell as well as between drill string and well bottom
- Validate reduced-order models through experiments

Current Research: Reduced-Order Models

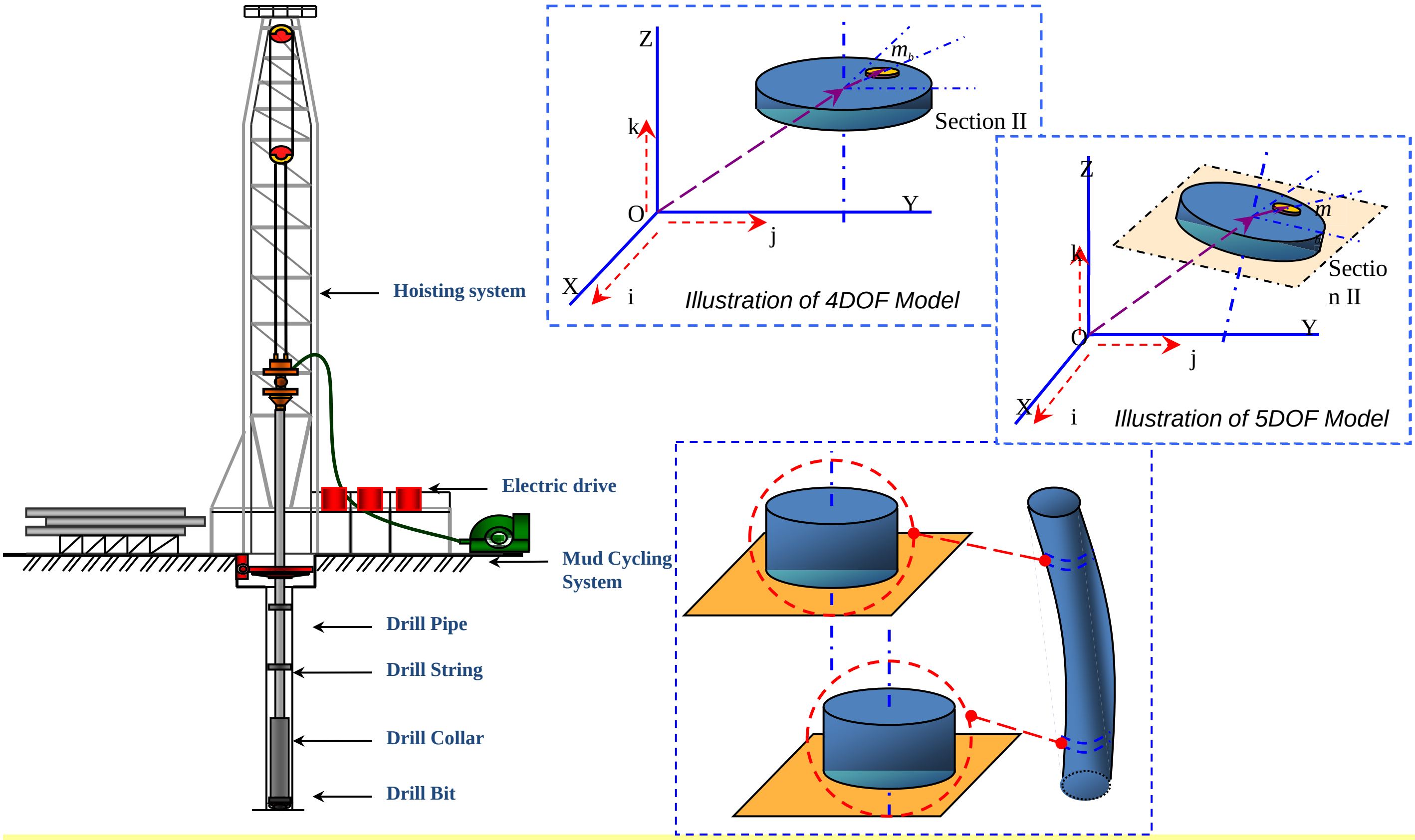

Current Research: Model Features

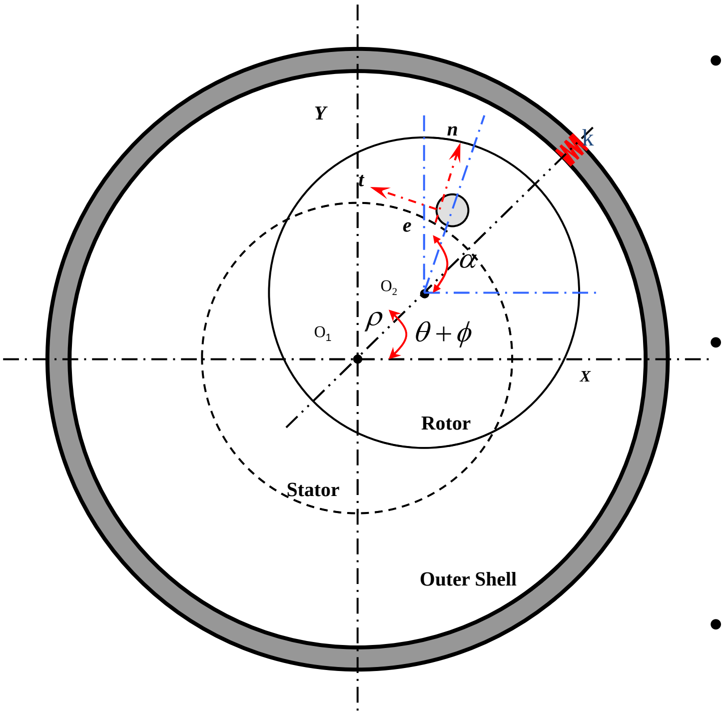

- Drill string modeled as a rotating, flexible shaft with a mass imbalance and stick-slip interactions with an outer shell
- Dynamics of developed four degree-of-freedom and five degree-of-freedom models have been and are being studied
- Experimental arrangements have been designed and constructed at PI and UMD

Current Research: One Reduced-Order Model

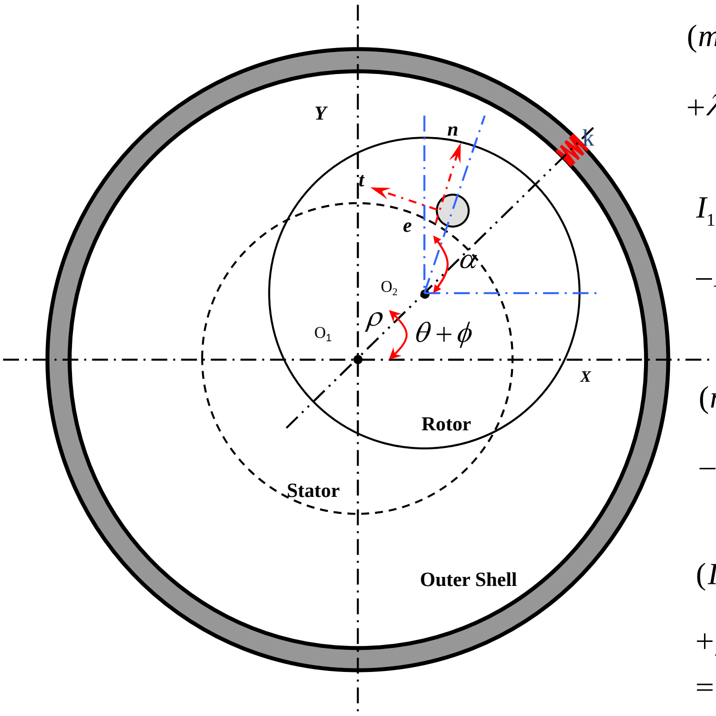

$$(m+m_b)\ddot{\rho}-(m+m_b)\rho(\dot{\theta}+\dot{\varphi})^2+K_r(\rho-\rho_0)$$

$$+\lambda K_p(\rho-\delta)+K_t\rho\varphi^2-em_b(\ddot{\alpha}\sin(\beta)+\dot{\alpha}^2\cos(\beta))=0$$

$$I_1\ddot{\theta}+(m+m_b)\rho^2(\ddot{\theta}+\ddot{\varphi})+2\ m+(m_b)\rho\dot{\rho}(\dot{\theta}+\dot{\varphi})$$

$$-K_{tor}(\alpha-\theta)-em_b\rho(\dot{\alpha}^2\sin(\beta)-\ddot{\alpha}\cos(\beta))=-\lambda F_t\rho$$

$$(m+m_b)\rho\ (\ddot{\theta}+\ddot{\varphi})+2\ m+(m_b)\dot{\rho}(\dot{\theta}+\dot{\varphi})+K_t\rho\ \varphi$$

$$-em_b(\dot{\alpha}^2\sin(\beta)-\ddot{\alpha}\cos(\beta))=-\lambda F_t$$

$$(I_2+m_be^2)\ddot{\alpha}+K_{tor}(\alpha-\theta)+em_b[-\ddot{\rho}\sin(\beta)$$

$$+\rho(\ddot{\theta}+\ddot{\varphi})\cos(\beta)+\rho(\dot{\theta}+\dot{\varphi})^2\sin(\beta)+2\dot{\rho}(\dot{\theta}+\dot{\varphi})\cos(\beta)]$$

$$=M_{ext}-\lambda F_tR$$

C.-M. Liao et al., 2008,"Drill String Dynamics", Twelfth Conference on Nonlinear Vibrations, Dynamics and Multibody Systems, Blacksburg, VA, USA, June 1-5, 2008

C.-M. Liao et al., 2009, "Drill-String Dynamics: Reduced Order Models", 2009 ASME International Mechanical Engineering Congress and Exposition, Lake Buena Vista, FL, USA, Nov. 13-19, 2009, IMECE2009-10339.

Current Research: Stick-Slip Interactions

$$\delta = 0.5*(D_{shell} - d_{string})$$

$$\lambda = \begin{cases} 0; \rho \le \delta \\ 1; \rho > \delta \end{cases}$$

$$F_{normal} = \begin{cases} 0 & \rho \le \delta \\ K_{contact}*(\rho - \delta) & \rho > \delta \end{cases}$$

$$F_t = \begin{cases} Ft_{equ} & ;V_{relative} = 0 \quad and \quad |Ft_{max}| \ge |Ft_{equ}| \\ Ft_{max} & ; \qquad else \end{cases}$$

Model allows for drill string to have no contact with the outer shell, bounce motions from it, sliding along it without rolling, or rolling contact

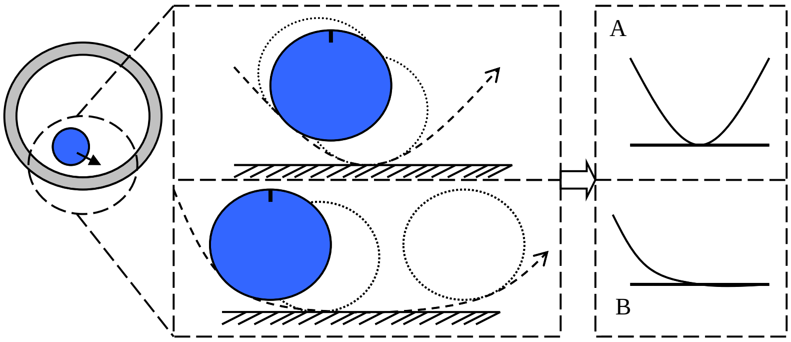

$$Ft_{\max} = -Sign(V_{relative})*\mu*F_{normal}$$

$$Ft_{equ} = -\frac{M_{ext}}{\frac{I_2}{0.5*m*d_{string}} + 0.5*d_{string}}$$

Current Research: Qualitative Comparisons with Prior Literature

Current Results; μ=0.1

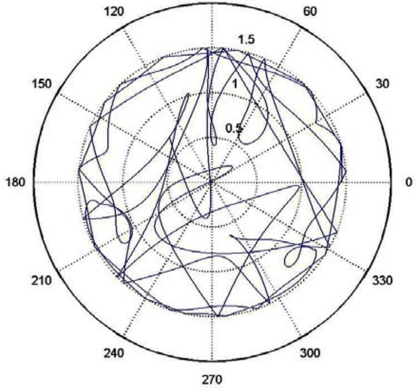

Current Results; μ=0.3

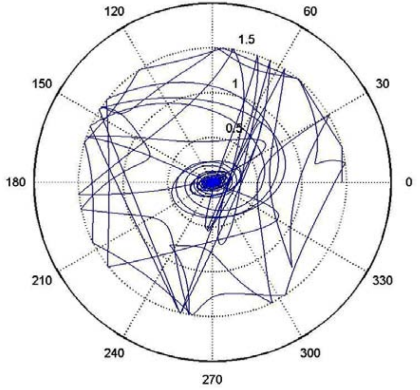

Current Results; μ=0.9

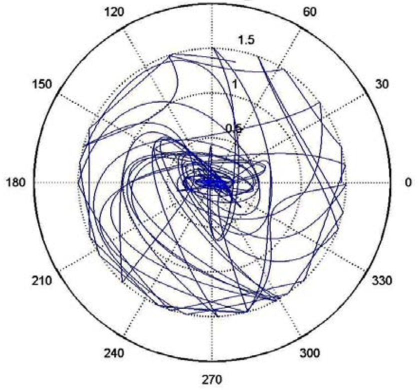

Prior Work; μ=0.1

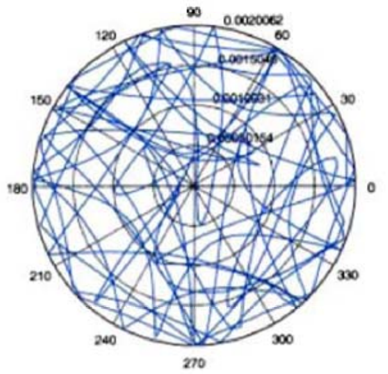

Prior Work; μ=0.3

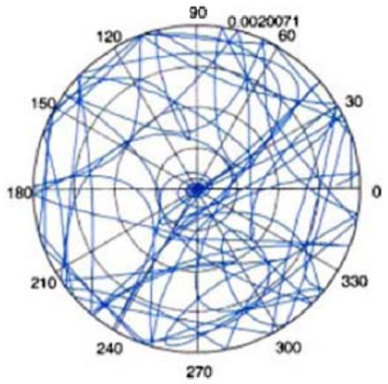

Prior Work; μ=0.9

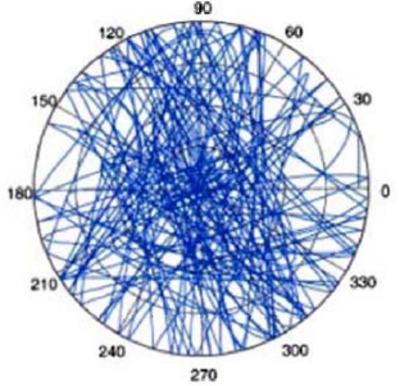

Current Research: Simulation Results

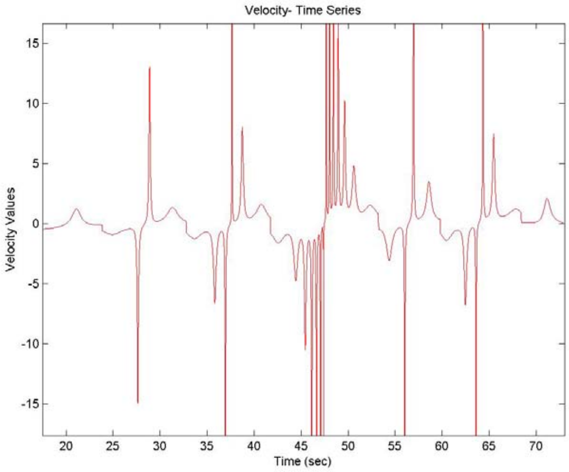

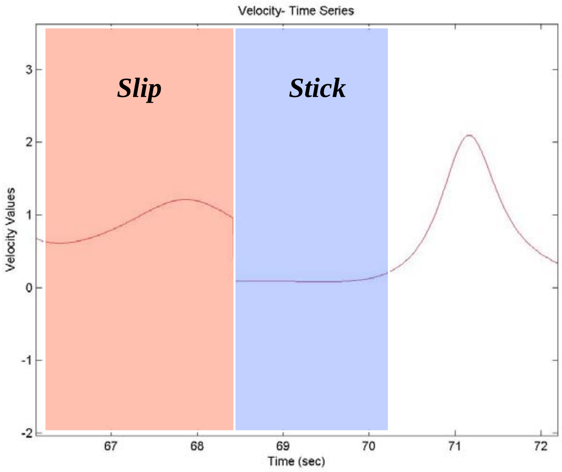

- Stick-Slip interactions can be captured within the model

Experimental Arrangement at PI

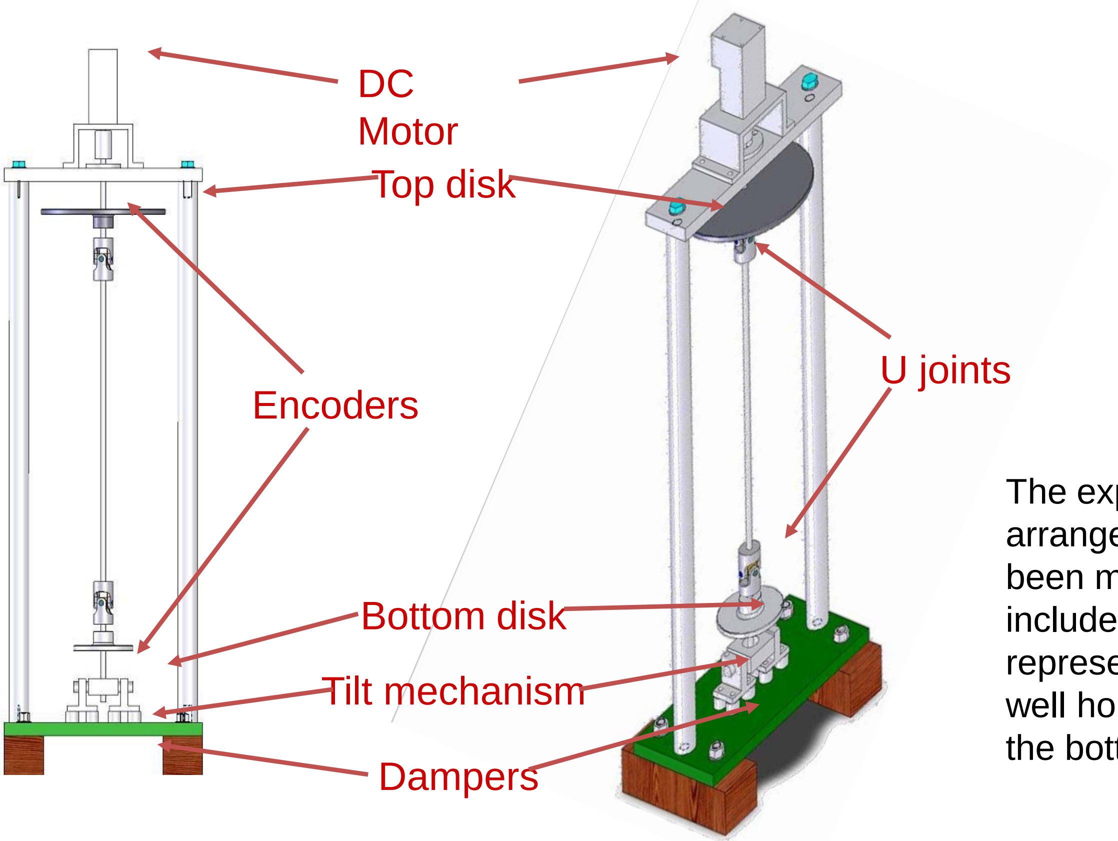

The experimental arrangement has been modified to include a representative well housing at the bottom.

Experimental Arrangement at UMD

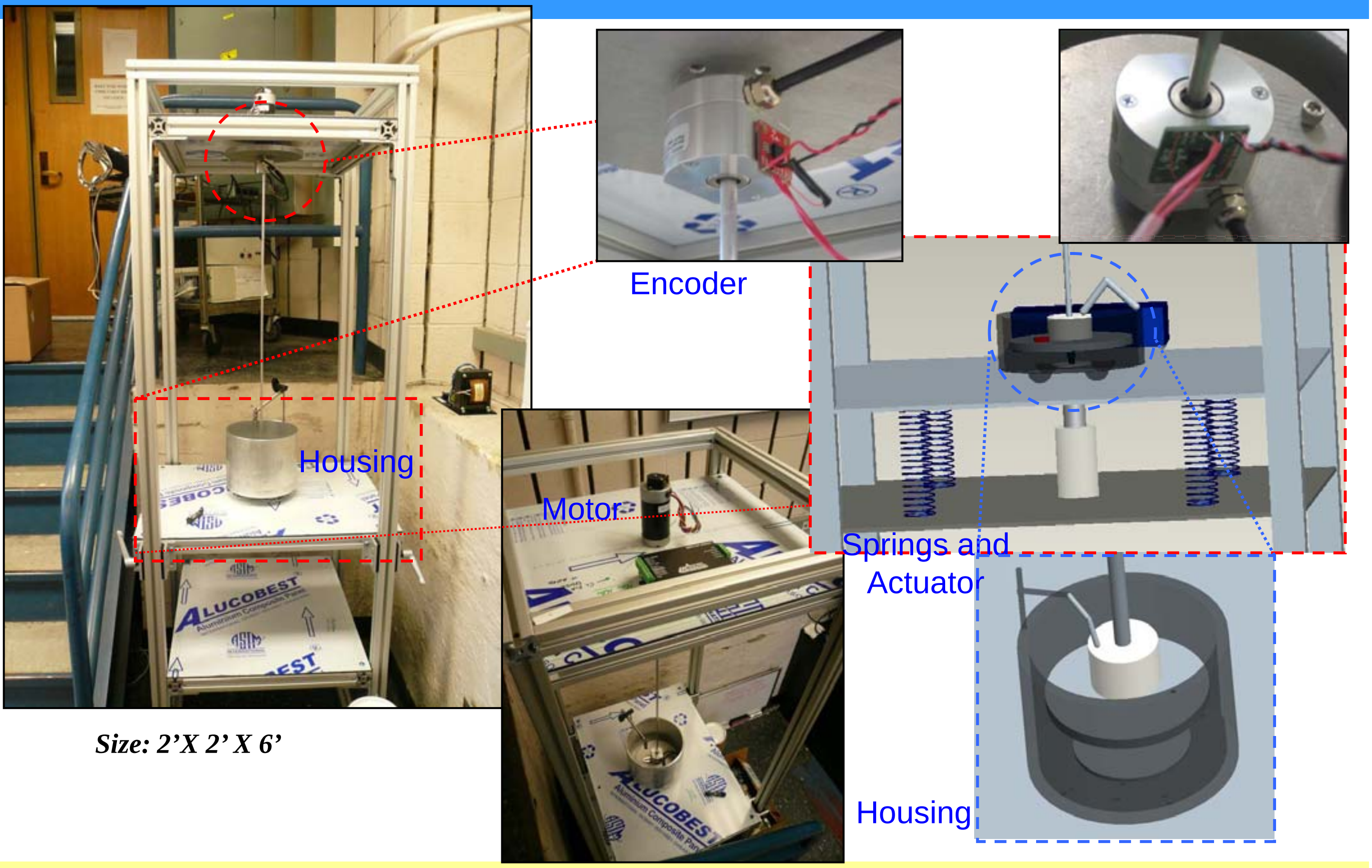

Size: 2'X 2' X 6'

Experimental Arrangement and Qualitative Results

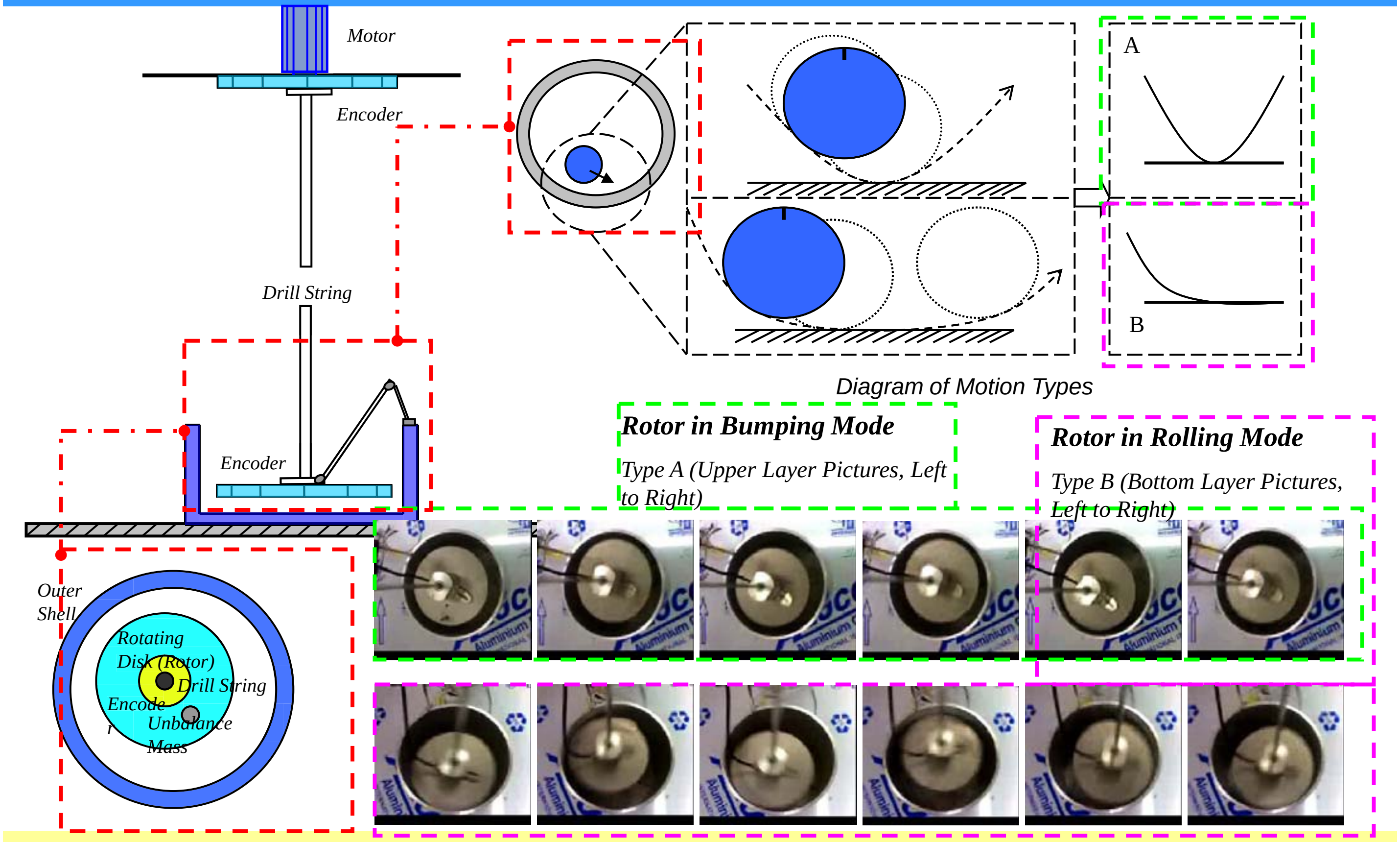

Diagram of Motion Types

Rotor in Bumping Mode

Type A (Upper Layer Pictures, Left to Right)

Rotor in Rolling Mode

Type B (Bottom Layer Pictures, Left to Right)

Qualitative Comparisons with Experiments

Predicted Rotor Trajectory

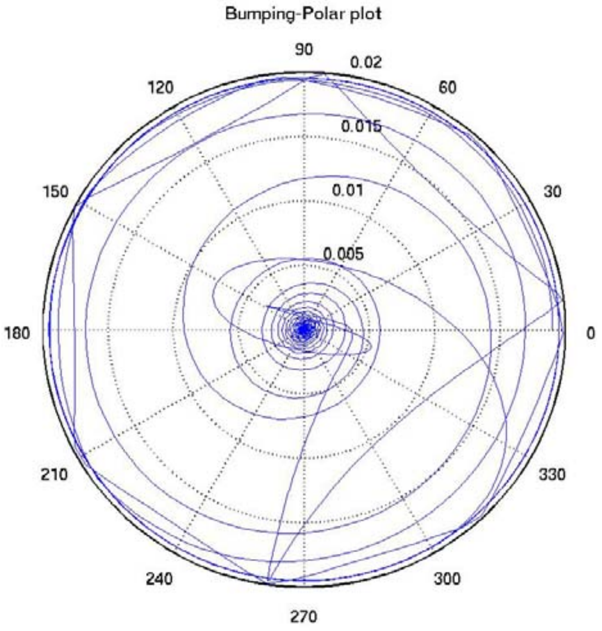

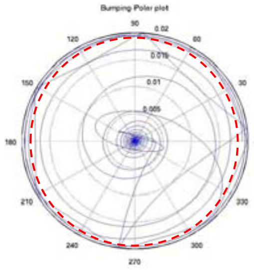

Rolling Motion

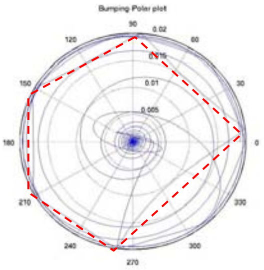

Bumping Motion

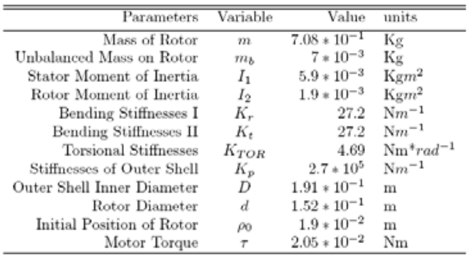

Parameters	Variable	Value	units
Mass of Rotor	m	$7.08 * 10^{-1}$	Kg
Unbalanced Mass on Rotor	m_b	$7 * 10^{-3}$	Kg
Stator Moment of Inertia	I_1	$5.9 * 10^{-3}$	Kgm^2
Rotor Moment of Inertia	I_2	$1.9 * 10^{-3}$	Kgm^2
Bending Stiffnesses I	K_r	27.2	Nm^{-1}
Bending Stiffnesses II	K_t	27.2	Nm^{-1}
Torsional Stiffnesses	K_{TOR}	4.69	$Nm^{*}rad^{-1}$
Stiffnesses of Outer Shell	K_p	$2.7 * 10^5$	Nm^{-1}
Outer Shell Inner Diameter	D	$1.91 * 10^{-1}$	m
Rotor Diameter	d	$1.52 * 10^{-1}$	m
Initial Position of Rotor	ρ_0	$1.9 * 10^{-2}$	m
Motor Torque	τ	$2.05 * 10^{-2}$	Nm

Table of Parameter Values

Current Research: Control Scheme

- Have examined suppression of torsion oscillations by using Genetic Algorithms

Karkoub, M., Abdel-Magid, Y., and Balachandran, B.,(2008) "Drill String Torsional Vibration Suppression Using GA Optimized Controllers," Canadian Journal of Petroleum Technology, accepted for publication

Project Status and Summary: Progress, Accomplishments, and Inferences

- Drill string has been modeled as a flexible rotating shaft with mass imbalance and stick-slip interactions with outer shell – Four degree-of-freedom and five degree-of-freedom models have been developed; five degree-of-freedom model helps capture tilt angle effects not previously studied.

- Numerical investigations indicate that the string bounces off the outer shell for low values of friction coefficient and sticks and slips along the outer shell as the friction coefficient is increased; present model provides a reasonable description of the interactions with the outer shell compared to previous models.

- Experimental arrangements have been tailored to better understand coupling amongst different modes of vibration, stick-slip interactions, and explore control of them.

- Reduced-order models validated and extended through comparisons with experiments

---

Related Research at UMD: Horizontal Drilling

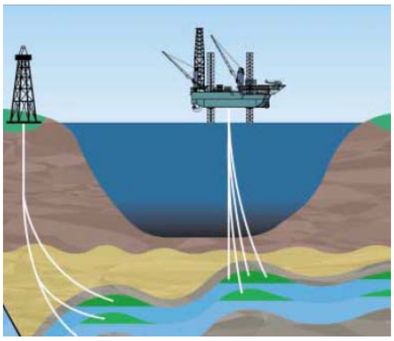

Onshore and Offshore Drilling

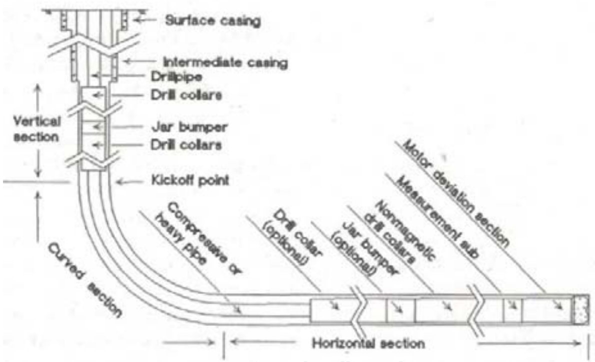

Source: Horizontal Drilling, Short, J.A.

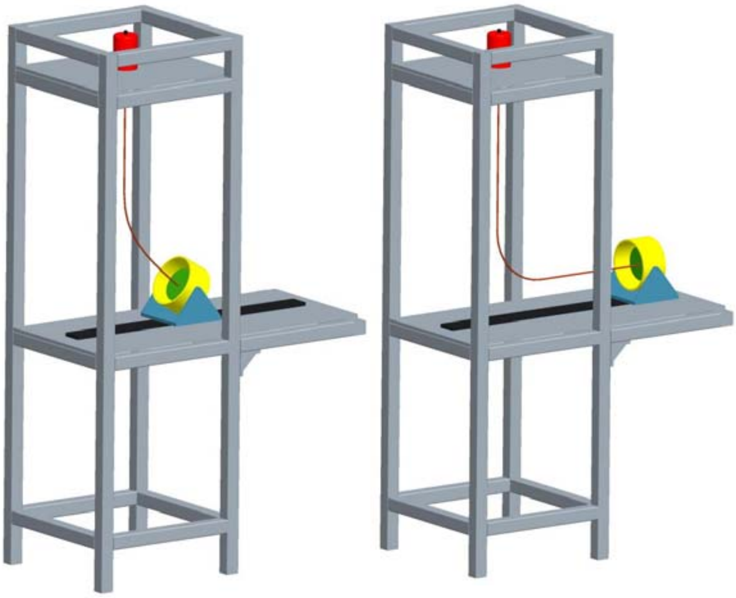

Experimental arrangement for horizontal drilling studies
(N. Vlajic and B. Balachandran, 2009)

Related Research at UMD: Rub-Roll Interactions

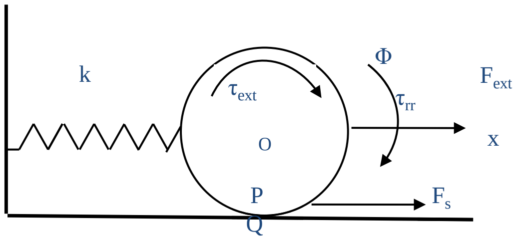

Simultaneous Rub and Roll of Flexibly Connected Disk
(S. P. Singh and B. Balachandran, 2009)

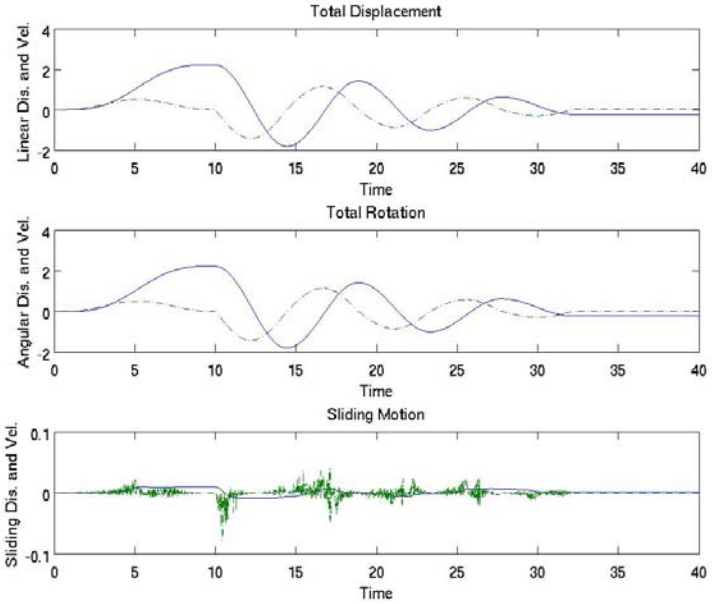

Response of the Disk Subjected to Ramp Excitation: (a) total travel distance of the disc, (b) rotation of the disc, and (c) sliding of the disc. Solid lines are used to depict the displacement responses and dashed lines are used to represent the velocity responses

Project Status: Interactions and Impact

•**Impact on Industry**: PI and UMD investigators have been interacting with the National Drilling Company since 2007 (with a recent visit in October 2009) and one example of the impact the collaborative research can have on the industry is the following: Guide the choice of optimal mud parameters for keeping the motions of the drill string close to the center of the oil well.

•**Impact on Research and Education**: Experimental testbeds have been established at PI and UMD, and these testbeds are being used to carry out research as well as educate students: Two undergraduate students from PI visited UMD in Summer 2009 to work on drill string dynamics and control along with the doctoral student at UMD. A doctoral researcher from England is visiting PI to carry out experiments on the PI testbed.

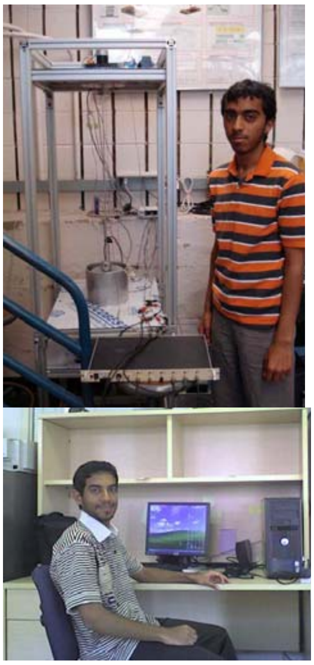

PI undergraduate students Alawi Abdulla and Waled Saeed visiting UMD in Summer 2009

Studies on Mobile Sensor Platforms

UMD Team: Bala Balachandran and Nikhil Chopra
PI Team: Hamad Karki and Sai Cheong Fok

1st Annual PI Partner Schools Research Workshop
The Petroleum Institute, Abu Dhabi, U.A.E.
January 6-7, 2010

PI Partners

PI Sponsors

Presentation Outline

- Introduction and Motivation
- Project Objectives
- Research Approach and Considerations
- Numerical Studies, Results, and Discussion
- Summary and Future Work

Introduction and Motivation

- Mobile sensor platforms can be employed in a variety of operations including environmental and structural health monitoring operations in harsh and remote environments:
  - Need for continuous, autonomous monitoring capabilities
  - Potential Applications: i) external and/or internal inspection of oil storage tanks, ii) inspection inside oil pipes, where corrosion problems have been reported with increasing water content, and iii) monitoring outside offshore platforms

Introduction and Motivation

- Illustrative example of the use of cooperating sensor platforms in oil storage tanks for external or internal inspection. In an internal inspection, these platforms can be used for periodical inspection for corrosion, cracks, and leaks. These platforms can be envisioned for estimating geometrical profile parameters, such as, for example, the tank bottom thickness.

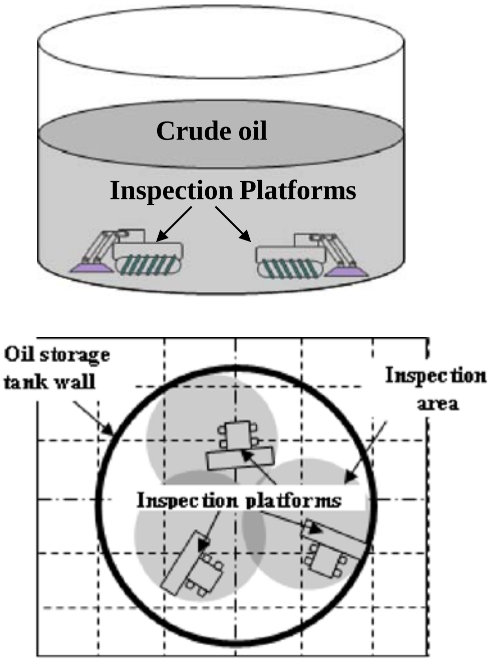

Representative example for use of mobile sensor platforms: Inspection inside an oil storage tank.

Introduction and Motivation

- Basic Building Blocks of Mobile Sensor Platforms
    - Sensors
    - Actuators and Mechanisms
    - Power
    - Motion Planning Algorithms

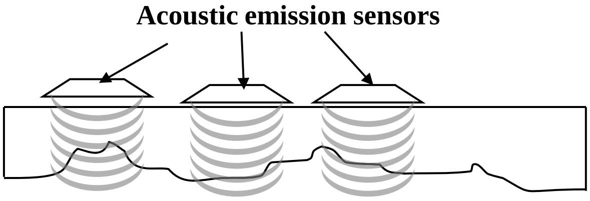

Representative example of sensors that can be used in mobile sensor platforms for structural inspection.

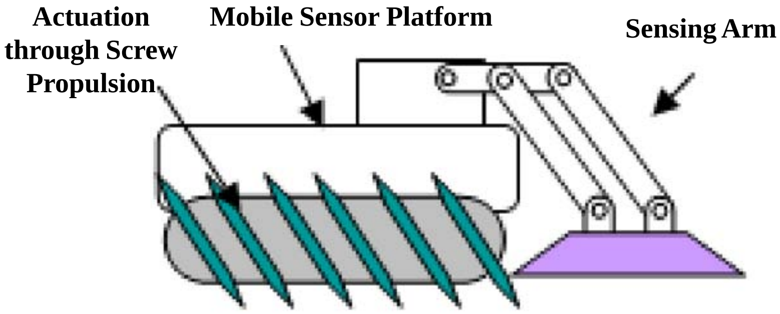

Representative mobile sensor platform.

Project Objectives

•Understand the current state-of-the-art and identify gaps that need to be filled with the overall goal of carrying out a combined analytical, numerical, and experimental effort to develop mobile sensor platforms and appropriate simultaneous localization and mapping (SLAM) algorithms for cooperative sensor platforms to operate in a harsh environment

•Develop SLAM algorithms based platforms taking into account system constraints such as constrained communication, the type of sensors considered, allowable dynamics, and factors such as sensor failures and reliability of the considered sensors

•Build complimentary experimental test platforms at the University of Maryland and the Petroleum Institute to validate models and refine them as well as to examine sensors, actuators, and power schemes – some of the experimental work is to be carried out as a part of senior design courses in Mechanical Engineering at the Petroleum Institute

Research Approach and Considerations

- Simultaneous localization and mapping (SLAM) algorithms (also known in the literature as concurrent mapping and localization (CML) algorithms) for cooperating sensor platforms operating in harsh environments are being investigated

- Although, one can use a single sensor system to carry out a geometrical profile measurement inside a storage tank or a pipe, or carry out external monitoring outside an offshore platform, cooperating platforms can provide redundancy to sensor failures as well as superior localization and mapping capabilities.

Research Approach and Considerations

- Although the SLAM problem has been studied in open terrestrial and aerial environments (e.g., Thrun, 2002; Durrant-Whyte and Bailey, 2006), the same is not true for environments such as those encountered in an oil tank or pipe (e. g., Sogi *et al*., 2000). These submerged environments pose a significant challenge due to complex dynamics of the sensor platforms, as well as related issues of motion control, cooperative path planning, and information fusion.

Research Approach and Considerations

•**Problem Features**: In the SLAM problem, one fundamentally seeks a solution where a sensor platform can incrementally develop a map of the unknown environment while simultaneously localizing itself within the map. In the research context here, while the topology of the oil tank floor or an oil pipe may be well known, the structural aspects of the tank (say, the map of tank thickness along the tank floor) or the oil pipe are features of an unknown map to be estimated by the sensor platform.

•**Communication Challenges**: The challenges are primarily due to the fluid environment which constrains the motion of the sensor platform, while preventing use of common localizing devices such as the global positioning system. The acoustic medium constrains the inter-sensor platform communication and complicates the information fusion process. These challenges will be addressed as part of the proposed approach, which is expected to evolve, as a better definition of the problem is made.

Research Approach and Considerations

•**Sensors, Actuators, and Power**: Sensors that make use of wave physics (for example, acoustic emission sensors) will be studied along with other sensors for possible use in these mobile platforms. In addition, appropriate actuation mechanisms to realize the desired mobility of these platforms will also be investigated. The experimental test platforms to be developed as a part of the work will be used to examine and develop different mobile platform architectures as well as their power needs for mobility as well as continuous monitoring.

Research Approach and Considerations

•**SLAM Problem:** Obtain a simultaneous estimate of both mobile sensor platform (so called vehicle) and key marker locations (could be structural features) in a oil pipe or storage tank (so called landmark locations)

At any time instant k, the following quantities are defined:

- x_k: State vector describing the location and orientation of the vehicle inside the oil pipe or relative to the storage tank
- u_k: Control applied at time *k-1* to drive the mobile sensor platform to a state x_k at time *k*
- m_i: Vector describing the location of the *ith* time invariant landmark or marker location
- z_{ik}: Observation of the *ith* landmark at time *k*

Define the sets:

- $U_{0:k}$: The history of control inputs
- $Z_{0:k}$: The set of all landmark observations
- m: The set of all landmarks

In the SLAM problem, one is essentially estimating the probability distribution

$$P(x_k, m | Z_{0:k}, U_{0:k}, x_0)$$

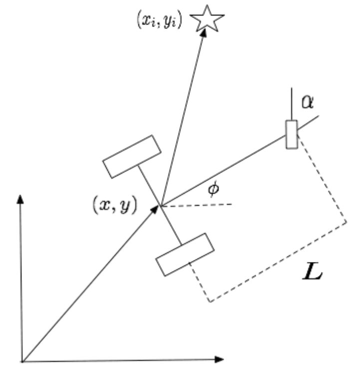

Representative mobile sensor platform

Research Approach and Considerations

Extended Kalman Filter (EKF) SLAM

- The motion model is $x_k = f(x_{k-1}, u_k) + w_k$, where *f(.)* denotes the mobile sensor platform (so called vehicle) kinematics and w_k are the additive Gaussian motion disturbances.
- The observation model is given by $z_k = h(x_k, m) + v_k$ where *h(.)* is the observation model and v_k are the additive Gaussian noise components.
- By using the observations and the control inputs, the standard Extended Kalman Filter (EKF) time and observation update are employed to estimate the joint posterior density of the landmark locations and the vehicle state.
- The solution has the benefits and the pitfalls as the standard EKF solution. The computational effort grows quadratically with the number of landmarks.
- The algorithm, by definition requires linear models for the motion update and also for the observations. Linearization can help accomplish the above goals. However, it can potentially lead to drastic inconsistencies in the solutions.

Research Approach and Considerations

FASTSLAM

- This algorithm has its origins in recursive Monte Carlo sampling or particle filtering. This approach can handle nonlinear motion and observation models.

- Rao-Blackwellization filter is used in the sample space where the joint state is partitioned as $P(x_1,x_2)= P(x_2|x_1)P(x_1)$. If the conditional $P(x_2|x_1)$ can be calculated analytically, sampling is only required for $P(x_1)$.

- In context of the SLAM problem, the SLAM state can be factored as

$$\mathbf{P(X_{0:k}, m| Z_{0:k}, U_{0:k}, x_0)= P(m| X_{0:k}, Z_{0:k})\, P(X_{0:k}| Z_{0:k}, U_{0:k}, x_0)}$$

where the probability distribution is on the trajectory $X_{0:k}$ rather than a particular position x_k. This is due to the fact that the when conditioned on the trajectory, the landmarks become independent.

- Recursive estimation is performed by particle filtering for the position states and the EKF is used for the map states.

Numerical Studies, Results, and Discussion

- **Extended Kalman Filter SLAM Study**

System Kinematics

$$\begin{Bmatrix} \dot{x} \\ \dot{y} \\ \dot{\phi} \end{Bmatrix} = \begin{Bmatrix} v\cos\phi \\ v\sin\phi \\ {}^{v}\!/\!{}_{L}\tan\alpha \end{Bmatrix}$$

Observation or Sensor Model

$$\begin{bmatrix} z_r \\ z_\beta \end{bmatrix} = \begin{bmatrix} \sqrt{(x_i-x)^2+(y_i-y)^2} \\ \tan^{-1}\left(\dfrac{y_i-y}{x_i-x}\right)-\phi+\dfrac{\pi}{2} \end{bmatrix}$$

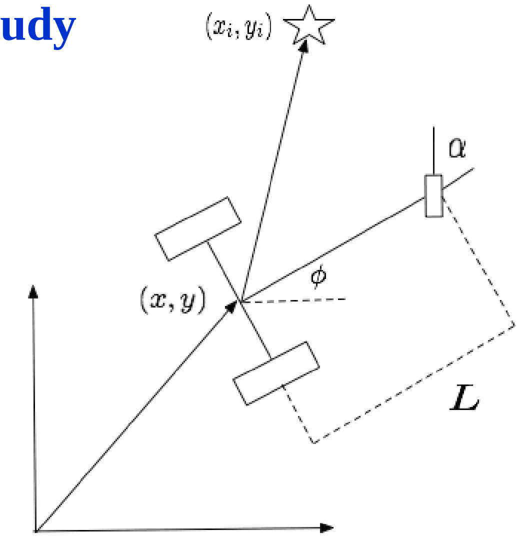

Conceptual illustration of mobile sensor platform moving with a speed *v* on the plane.

Numerical Studies, Results, and Discussion

- **Influence of low noise level in range sensor information**

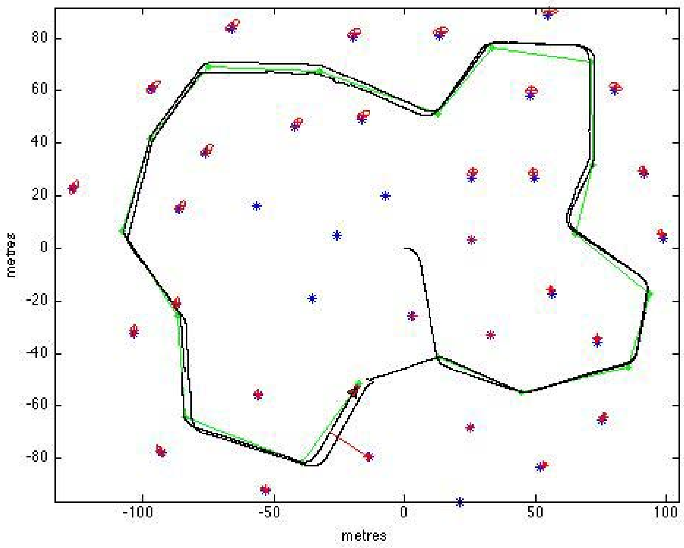

Results with low noise in range sensing. Good localization and mapping are realized even with noise in sensor information

Green – Actual Path

Black – Path Being Tracked

Blue – Locations of Actual Landmarks

Red – Apparent Locations of Landmarks

Numerical Studies, Results, and Discussion

- **Influence of high noise level in range sensor information**

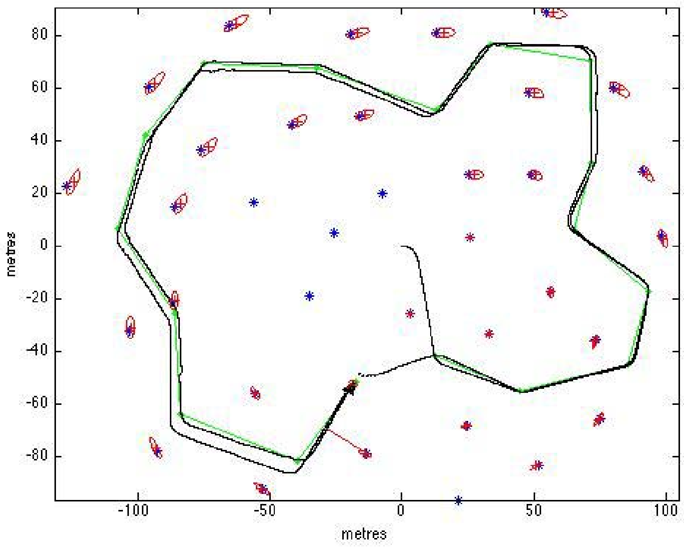

Results with high noise in range sensing illustrate the deleterious effect of noise.

Green – Actual Path

Black – Path Being Tracked

Blue – Locations of Actual Landmarks

Red – Apparent Locations of Landmarks

Numerical Studies, Results, and Discussion

•Influence of high noise level in kinematics and low noise level in sensor information

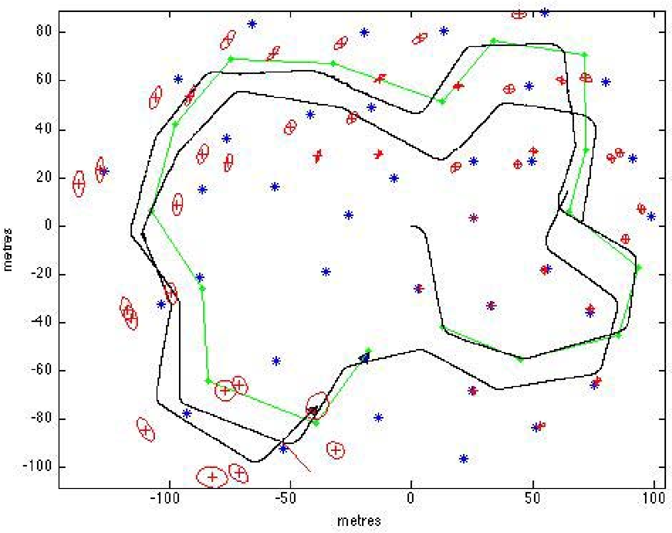

Illustration of deleterious effects of noise

Green – Actual Path

Black – Path Being Tracked

Blue – Locations of Actual Landmarks

Red – Apparent Locations of Landmarks

Numerical Studies, Results, and Discussion

- **FASTSLAM Study**
- **Allows efficient computation when compared to EKF SLAM**

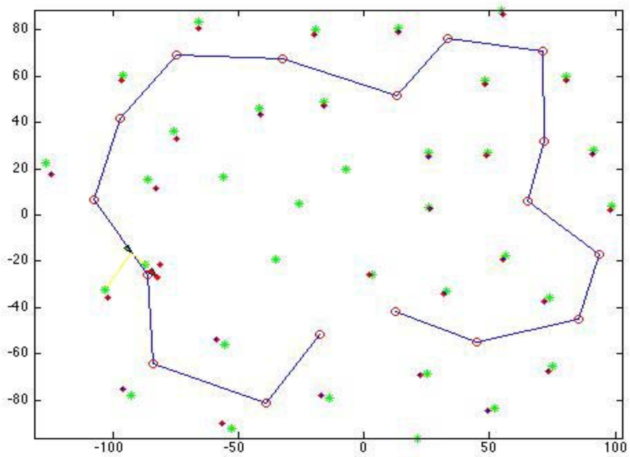

Results with high noise in range sensing. Relatively good localization and mapping are realized even with noise in sensor information

Blue – Path Being Tracked

Green – Locations of Actual Landmarks

Red – Apparent Locations of Landmarks

Numerical Studies, Results, and Discussion

- **Influence of high noise level in kinematics and low noise level in sensor information**
- **Noise in the kinematics appears to play a dominant role in influencing the estimation process**

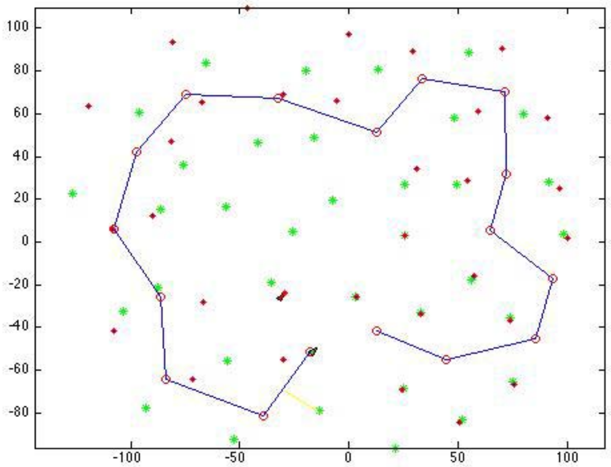

Blue – Path Being Tracked

Green – Locations of Actual Landmarks

Red – Apparent Locations of Landmarks

Project Status and Summary: Progress, Accomplishments, and Inferences

Schedule

•April 1, 2009 to December 31, 2009: Carry out analytical and numerical investigations into SLAM algorithm based mobile platforms as a representative exploration into mobile sensor platforms for application in oil storage tanks or oil pipes. Investigate experimental test platforms.

•January 1, 2010 to December 31, 2010: Continuation of analytical, experimental, and numerical efforts, with focus to be on development of basic building blocks for mobile sensor platforms (mapping algorithms, sensors, actuators and power).

•January 1, 2011 to December 31, 2011: Continuation of experimental and numerical studies and formulation of recommendations for appropriate sensor and mobile platform configurations for use in oil pipes and oil storage tanks and other applications recommended by ADNOC Industries.

Project Status and Summary: Progress, Accomplishments, and Inferences

•Numerical studies on SLAM algorithms have been initiated and they are to be continued in 2010; ADNOC Fellow Mr. Hesham Ishmail (started in Fall 2009) to be involved in these efforts and a new doctoral student (Ms. Jai Rubyca) to join in Spring 2010:

- Limitations in the presence of noise have been studied
- Strengths and weakness of various algorithms and suitability for use in fluid environments to be addressed
- Common localizing devices such as GPS based devices cannot be used
- Acoustic sensors could be used, but issues still be resolved
- Prior SLAM studies have focused on single platforms; extension to cooperating sensor platforms being carried out in this work
- Preliminary results to be reported in a conference manuscript, which has been accepted for a March 2010 SPIE Conference in San Diego, CA
- Senior design projects on cooperative mobile sensor platforms initiated at PI

•With guidance from industry (visited the Abu Dhabi Company for Onshore Oil Operations (ADCO) in Summer 2009 and October 2009), during 2010, scaled experimental test platforms are to be constructed at UMD and PI to evaluate sensors, actuators, and mapping schemes

Project Status: Interactions and Impact

Impact on Research and Education:

▪Experimental testbeds are being planned at PI and UMD, and these testbeds can be used to carry out research as well as educate students. One ADNOC Fellow, who started at PI, is currently working at UMD under the guidance of Professors Balachandran and Chopra. Senior project design teams at PI have worked on internal inspection of oil storage tank structures under the guidance of Professors Karki and Fok.   It is anticipated that future summer interns from PI will benefit from the experimental testbed to be constructed at UMD.

▪In a broader context, the drill-string dynamics and control work and the current work on mobile sensor platforms are expected to be critical components of Professor Karki's research program at PI in the area of dynamics and control.

Impact on Industry: PI and UMD investigators have been interacting with the Abu Dhabi Company for Onshore Oil Operations (with a recent visit in October 2009) and one example of the impact the collaborative research can have on the industry is the following: Guide the choice of mobile sensor platforms to carry out continuous and autonomous monitoring operations in harsh environments (e.g., oil pipes).

Use of Horizontal Wells to Improve Pattern Waterflood in Fractured Carbonate Reservoirs

CSM Team:
Waleed Al-Ameri (PI), MS Student
Dr. E. Ozkan, Dr. M. Kazemi & Dr. R. Graves

PI Team: Ghedan

1st Annual PI Partner Schools Research Workshop
The Petroleum Institute, Abu Dhabi, U.A.E.
January 6-7, 2010

PI Partners

PI Sponsors

Dr. Rick Sarg (GE)

Dr. Hossein Kazemi (PE)

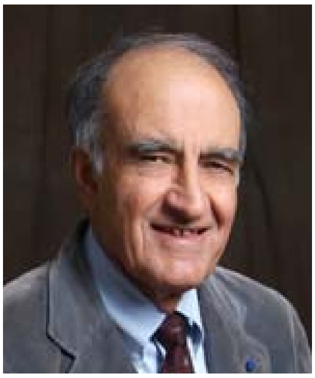

CSM GEOSCIENCE/ ENGINEERING TEAM

Dr. Manika Prasad (PE)

Dr. Mike Batzle (GP)

Dr. Ramona Graves (PE)

Dr. Erdal Ozkan (PE)

MISSION

- The research projects reported in the following slides were designed to produce the greatest amount of oil from Zakum field.
- In addition, these projects were designed as part of an educational process for the UAE graduate students studying at CSM, and a means for collaboration and technology transfer to the Petroleum Institute.

Background

- Thamama 1A Research Program consists of **FIVE** CSM/PI projects.
- The **research group** is an **integrated team** of petroleum engineers, geologists, petrophysicists, and geophysicists from CSM and PI.

Presentation Outline

- Background
- Objectives
- Results and Discussions
- Project Status
- Conclusions and Summary

Project Objectives

Use of Horizontal Wells to Improve Pattern Waterflood in Fractured Carbonate Reservoirs

(Ozkan, Kazemi, Graves and Ghedan)

Primary graduate student

Waleed Al-Ameri (PI), MS Student

Research topic - *"Evaluation and numerical/analytical modeling of efficacy of horizontal wells in the Thamama 1A in the Upper Zakum field"*

Results and Discussions

Case 1:

- * Single porosity
- * 2 vertical producers
- * Vertical injectors and producers are perforated all 15 layers
- * **RF= 23.5%**

Case 3:

- * Dual porosity
- * 2 horizontal injectors and 2 horizontal producers
- * Horizontal well length is 500 ft (in the x axis)
- * Horizontal injectors are completed in layer 18
- * Horizontal producers are completed in layer 27
- * **RF= 17.7%**

Case 2:

- * Single porosity
- * 2 horizontal injectors and 2 horizontal producers
- * Horizontal well length = 500 ft (In the x axis)
- * Horizontal injectors are completed in layer 3
- * Horizontal producers are completed in layer 12
- * **RF= 25.2%**

Case 4:

- * Dual porosity
- * 2 horizontal injectors and 2 horizontal producers
- * Horizontal injectors are completed in layer 18
- * Horizontal producers are completed in layer 27
- * **RF= 17.4%**

Results and Discussions

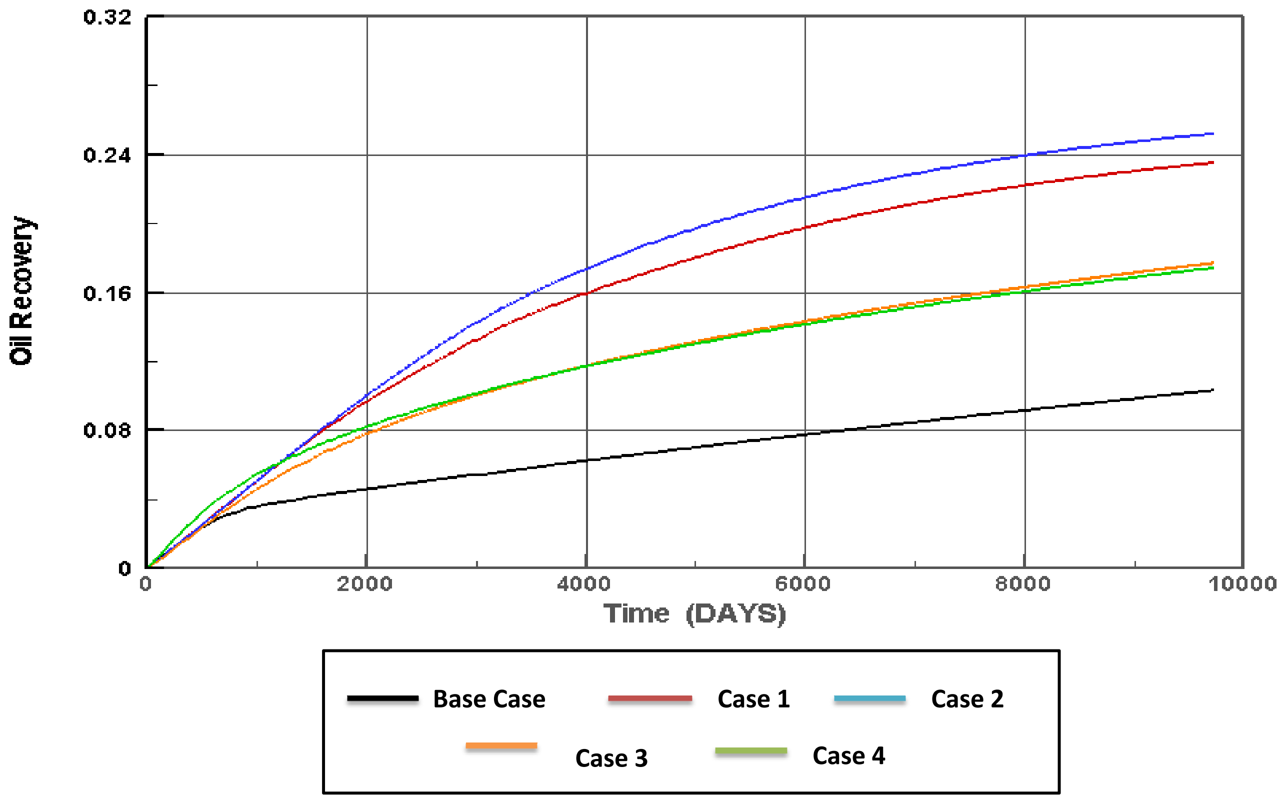

Project Status

- Over 50 Eclipse simulation runs
  - Single Porosity
  - Dual Porosity
  - No Injection (Base Case – depletion)
  - Only water Injection
  - Water Injection
  - Water Injection followed by Gas Injection

All cases run with varying well patterns/combination of horizontal and vertical wells

---

Project Status

- Remaining Eclipse simulation runs
  - Dual Porosity
  - Water Injection followed by Gas Injection

These will be selected cases chosen by the results of the dual porosity water injection with varying well patterns/combination of horizontal and vertical wells.

Conclusions and Summary

- Final Simulations Cases to be completed in January.
- Eclipse modeling, results, conclusions, and recommendations will be completed by June 2010. (Waleed Al-Ameri thesis written and defended).
- These cases will be the starting point for the simulation in Project 8.

Catalytic Processes

Development of 1. Zeolite Catalysts for Alkane Metathesis and 2. Adsorbents for H_2S Removal

UMN Team: Aditya Bhan, Matteo Cococcioni, Michael Tsapatsis, Alon McCormick, *Parveen Kumar*, *Ian Hill, Mark Mazar*

PI Team: Saleh Al Hashimi, Radu Vladea, Narasimaharao Katabathini

1st Annual PI Partner Schools Research Workshop
The Petroleum Institute, Abu Dhabi, U.A.E.
January 6-7, 2010

PI Partners

PI Sponsors

Presentation Outline of Metathesis Experiments

- Alkane metathesis overview
- Alkane activation
- Reactor setup and characterization tools
- $H^+ \rightarrow Ga^{3+} \rightarrow Ta^{5+}$ effects on alkane activation
- Project Status
- Conclusions and Summary
- Future Work

Alkane metathesis interconverts alkanes at low temperatures and pressures

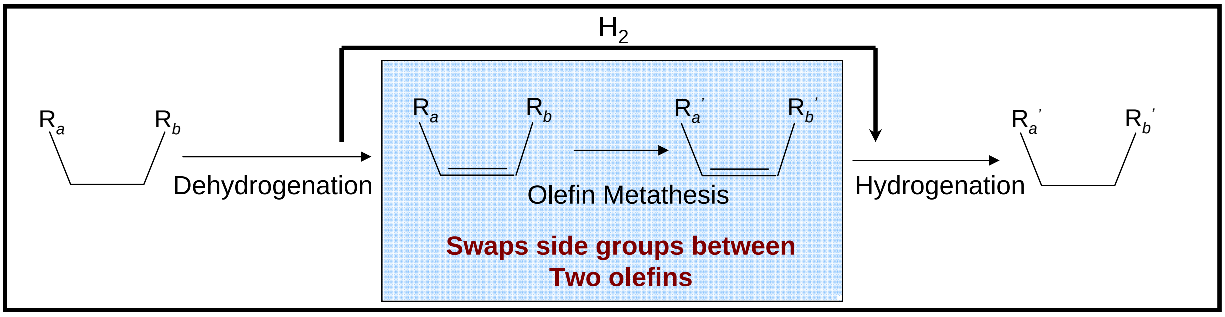

Swaps side groups between Two olefins

$2C_3H_8 \rightarrow C_2H_6 + C_4H_{10}$

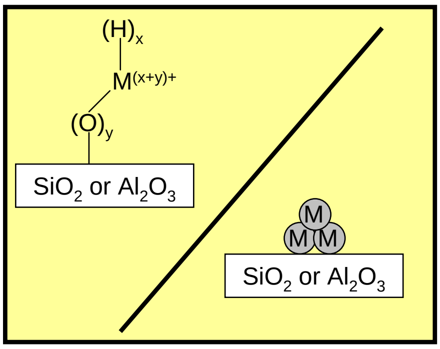

- **Non-oxidative alkane chain length redistribution at 523 K and 1 bar**
- **Reported catalysts consist of high-valent metal clusters or hydrides on amorphous silica or alumina surfaces**

Taoufik, M. et al. *Topics in Catalysis* **2006**, *40,* 65.
Nemana, S. et al. *Chem. Commun.* **2006**, *38*, 3996

Project Objectives

Exchange of high-valent cations into zeolites

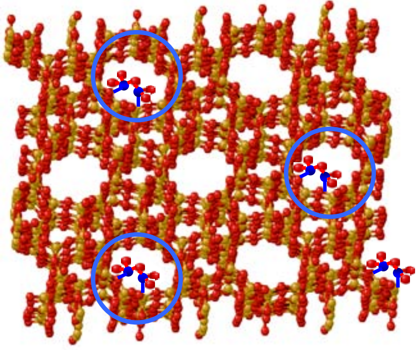

- **Site isolated cations in constrained (<1 nm) environments**
- **Follow the “elementary steps” of catalyst synthesis and reactions experimentally and theoretically**
- **Electrophillic metal cations with high reactivity for C-C and C-H bond cleavage**

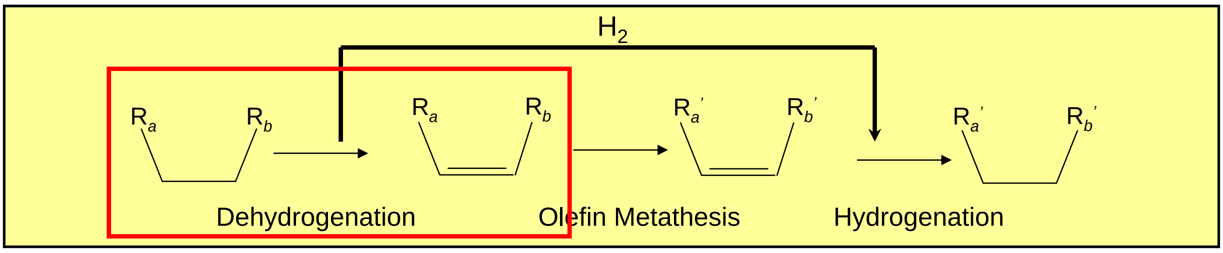

Initial objective: Study alkane activation as a function of cation valence

High-pressure batch or flow reactor allows catalytic operation at various conditions

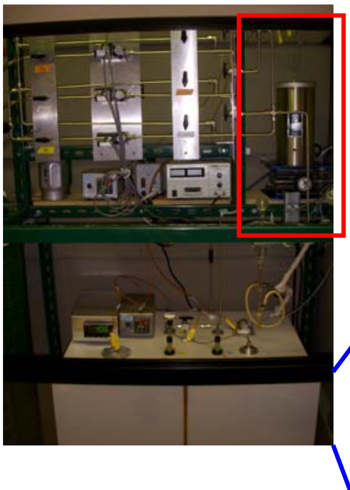

Flow reactor set-up

Gas chromatography (GC) use for online detection of effluent composition

High temperature, gradientless recirculation batch reactor used for isotopic studies

Quartz IR cell allows in-situ analysis of catalysts at high temperature

- **Quantification of zeolitic protons and ion exchange**

- **In-situ monitoring of pretreatment and reaction conditions**

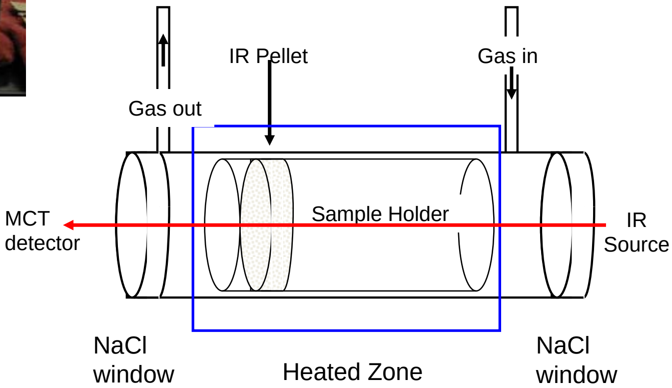

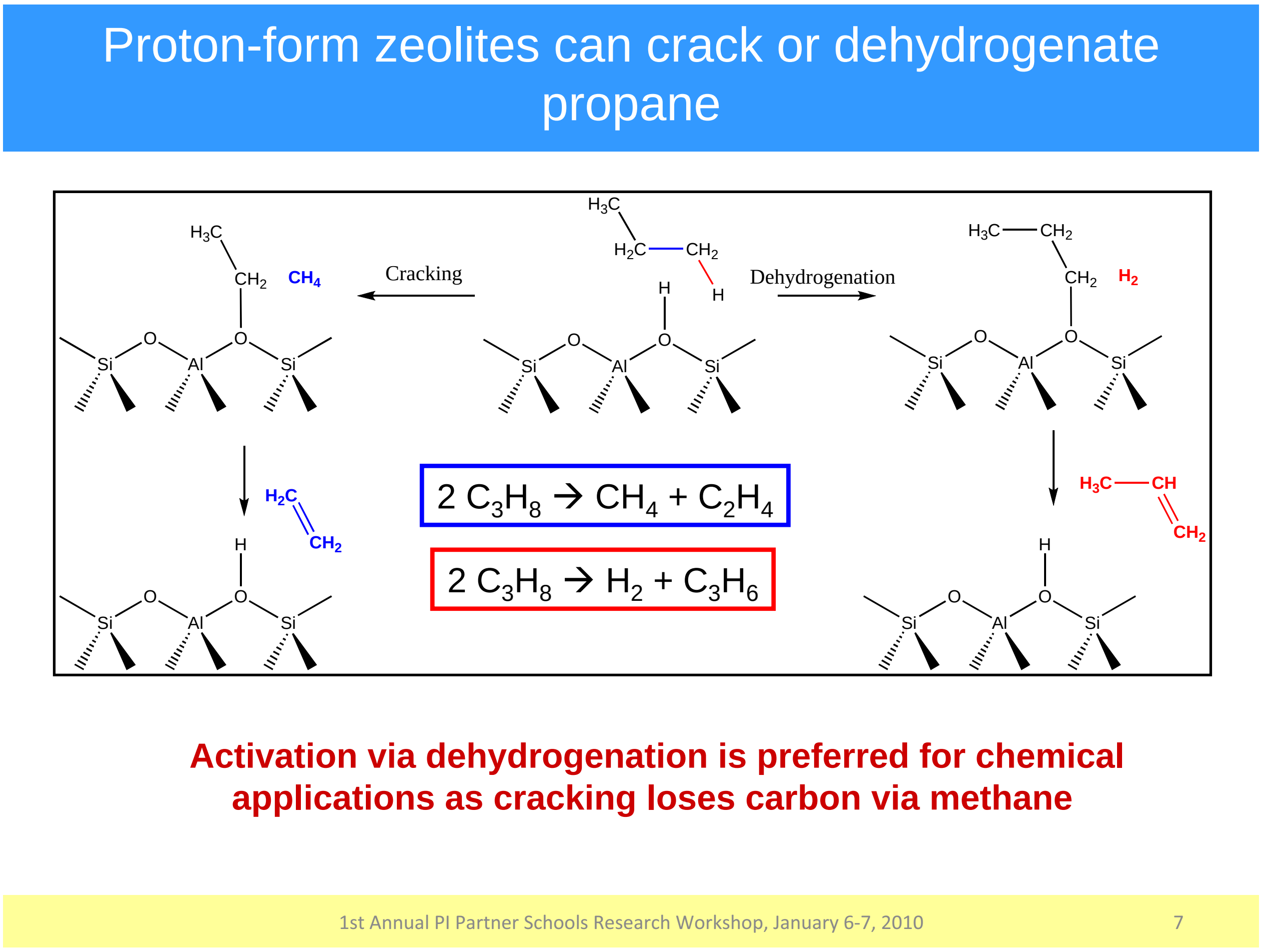

Proton-form zeolites can crack or dehydrogenate propane

$2\ C_3H_8 \rightarrow CH_4 + C_2H_4$

$2\ C_3H_8 \rightarrow H_2 + C_3H_6$

Activation via dehydrogenation is preferred for chemical applications as cracking loses carbon via methane

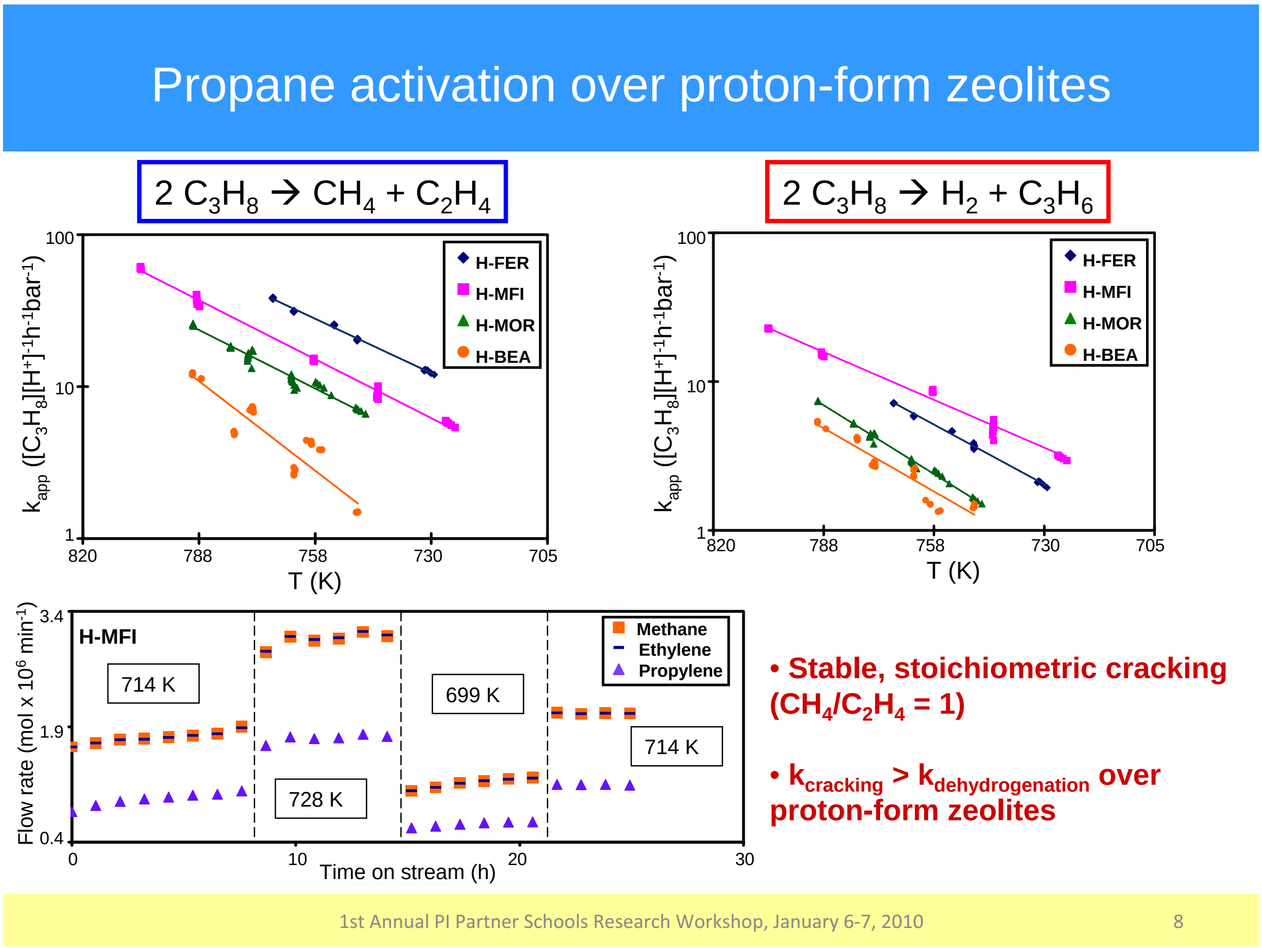

Propane activation over proton-form zeolites

$2\ C_3H_8 \rightarrow CH_4 + C_2H_4$

$2\ C_3H_8 \rightarrow H_2 + C_3H_6$

- **Stable, stoichiometric cracking (CH_4/C_2H_4 = 1)**
- **$k_{cracking} > k_{dehydrogenation}$ over proton-form zeolites**

Ga-form zeolites preferentially dehydrogenate propane

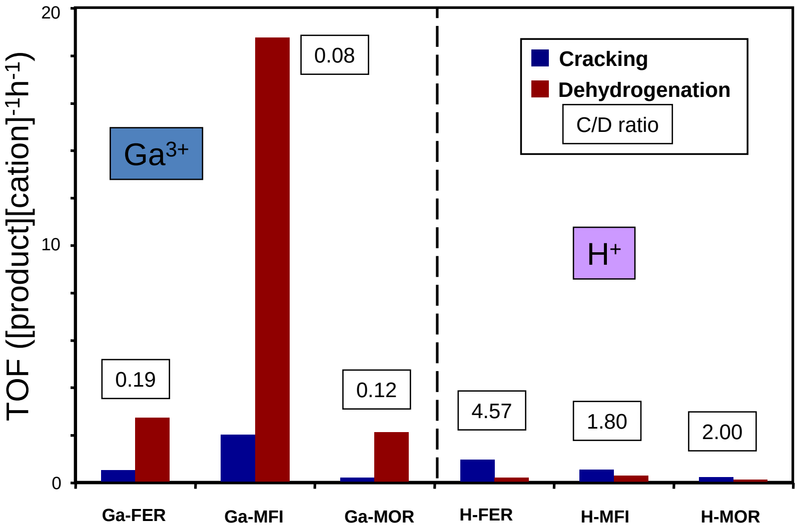

~0.0500 g H-form/~0.0030 g Ga-Form zeolite. 5.5 kPa C_3H_8 in 115 kPa He reactant feed at 1.67 mL h^{-1}. Rates calculated at 758 K and < 2% conversion.

Synthesis procedure

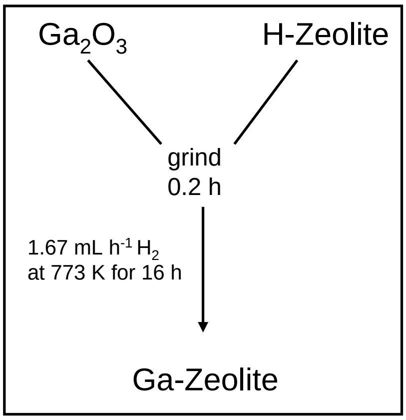

Ga_2O_3 H-Zeolite

grind
0.2 h

1.67 mL h^{-1} H_2
at 773 K for 16 h

Ga-Zeolite

El-Malki et al. *J. Phys. Chem. B.* **1999**, *103*, 4611

Factor of 20 decrease in C/D ratio by exchanging Ga cations for zeolitic protons

---

Synthesis of Ta on SiO_2/Al_2O_3

$$TaCl_5 + 5\ C_7H_7MgCl \xrightarrow[\text{1. DEE, 4 h} \quad \text{2. } C_7H_8]{} Ta(C_7H_7)_5 + 5\ MgCl_2$$

$\downarrow$

Filter over celite

$$Ta(C_7H_7)_5 + [SiO_2/Al_2O_3]\text{-}OH \xrightarrow[\text{1. } C_7H_8\text{, 16 h} \quad \text{2. Vacuum dry}]{} ([SiO_2/Al_2O_3]\text{-}O)_n\text{-}Ta(C_7H_7)_{5-n} + n\ C_7H_8$$

$$([SiO_2/Al_2O_3]\text{-}O)_n\text{-}Ta(C_7H_7)_{5-n} + H_2 \xrightarrow[\text{1.67 mL } h^{-1}\ H_2\text{, 16 h, 423 K}]{} Ta\text{-}[SiO_2/Al_2O_3] + 5\text{-}n\ C_7H_8$$

Synthesis performed in an oxygen and moisture free environment to prevent the formation of Ta_2O_5

Groysman et al. *Organometallics* **2003**, *22*, 3793.

Ta on SiO_2/Al_2O_3 converts propane into butane and ethane

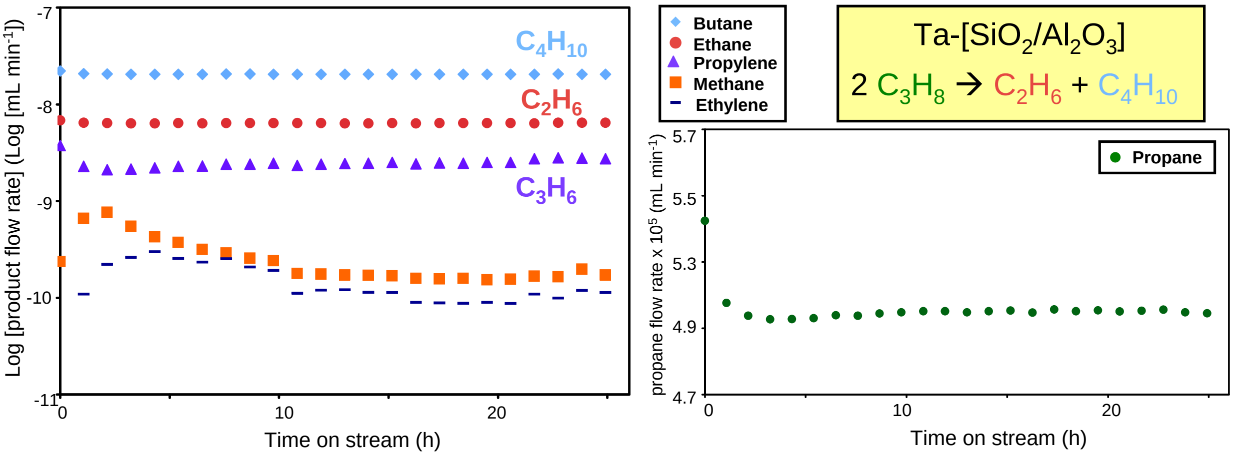

Ta-$[SiO_2/Al_2O_3]$

$2\ C_3H_8 \rightarrow C_2H_6 + C_4H_{10}$

T = 513-528 K; 0.27 g catalyst, 5 wt% Ta. 0.017 mL h^{-1} Propane. P_{total} = 1 bar.

- **Steady-state formation of propane metathesis products is observed for Ta-$[SiO_2/Al_2O_3]$ at a maximum conversion of 0.05 %.**

- **C_4H_{10}/C_2H_6 = 3.2, indicating the presence of side reactions that either consume C_2H_6 or generate C_4H_{10}**

Increasing cation valency increases dehydrogenation selectivity

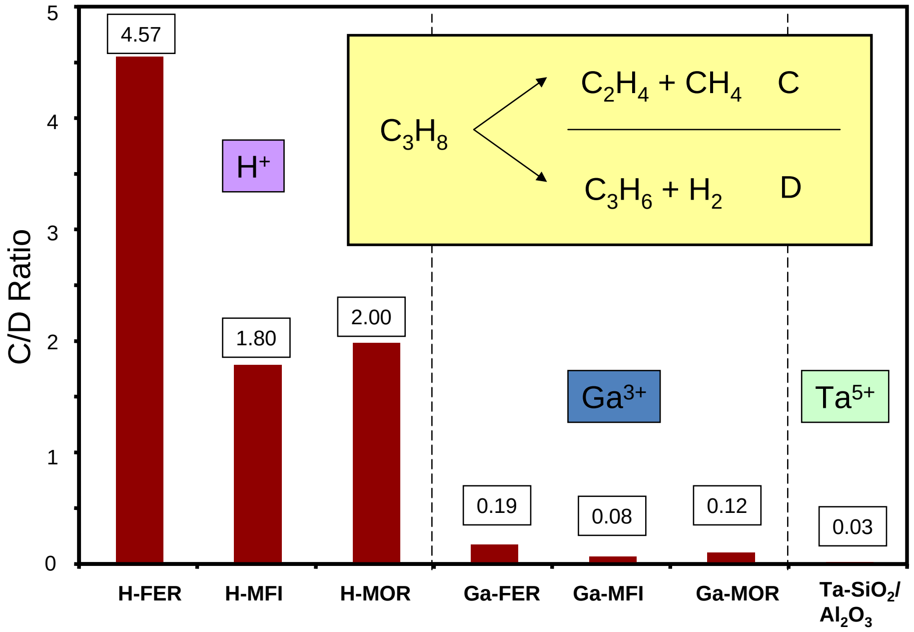

Dehydrogenation selectivity increases with increasing cation valency: H$^+$ < Ga^{3+}< Ta^{5+}

Project Status

- Assessed effect of zeolite topology on parallel alkane cracking and dehydrogenation reactions
- Developed protocols for synthesis and characterization of cations in zeolitic materials
- Investigated the effect of counter-ion valency to show that Ga^{3+} and Ta^{5+} cations selectively dehydrogenate alkane reactants

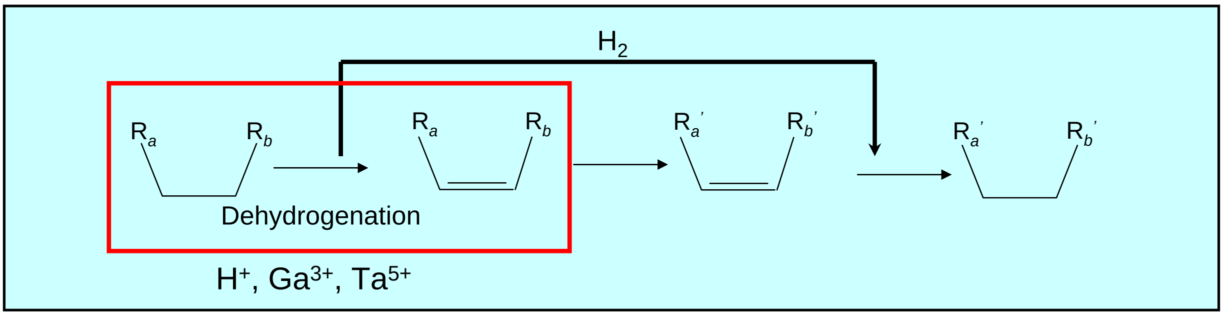

Conclusions and Summary

- **Low temperature, low pressure alkane metathesis is feasible on supported Ta catalysts with high selectivity towards metathesis products**
- **Increasing the valency of supported catalytic centers increases selectivity towards alkane dehydrogenation products**

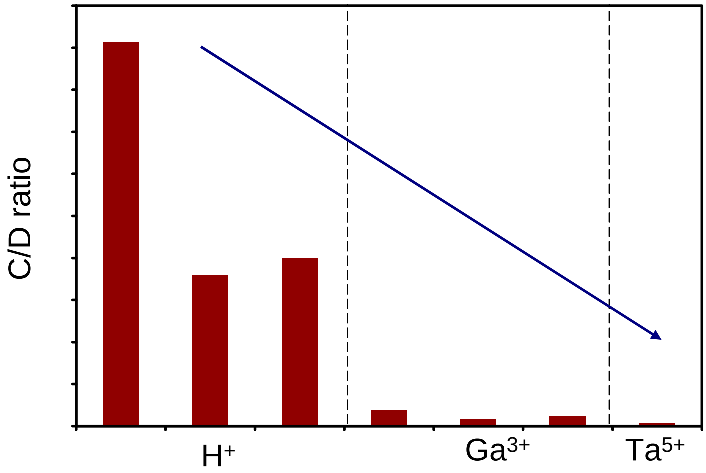

Future Work

- **Synthesis of W and Mo alkane metathesis catalysts**

- **Synthesize Ta catalysts on zeolite supports to study catalyst structure/reactivity relationships**

- **Elucidate the mechanistic cycle for alkane metathesis through rate parameterization**

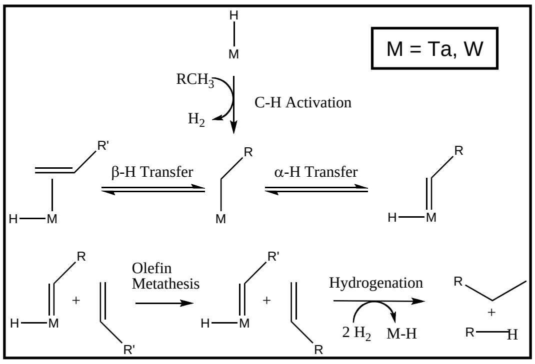

Basset, J.M. et al. *Angew. Chemie Int. ed.* **2006**. *45.* 6082-6085.

Presentation Outline for Metathesis Simulations

- Objectives
- Background
- Computational setup: active center models
- Preliminary results
- Summary and future work

Objectives

We want to to design a zeolite-supported catalyst that is able to perform the conversion of alkane molecules.

We need to:

- identify good candidate systems (support and active centers)
- assess and compare their reactivity in critical steps of the reaction

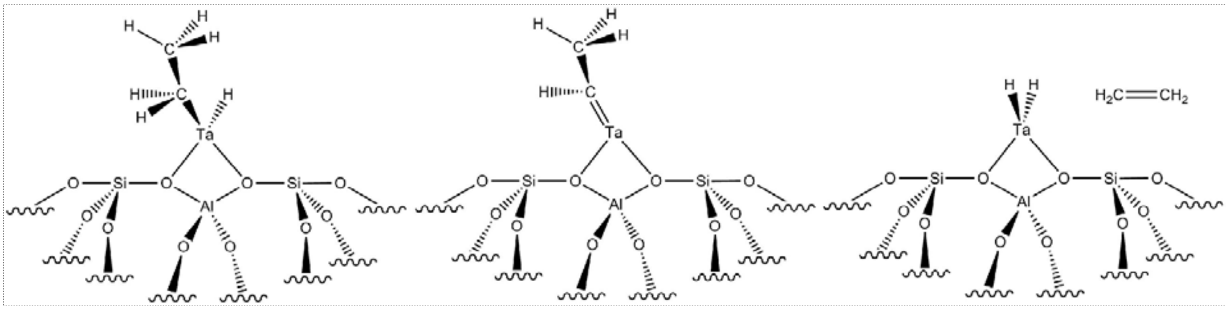

Background

Quantistic (DFT) calculations will be used to assess the kinetics of important reactions steps on various metal active centers

We need to:

- Construct a model for the active center
- Define a computational protocol to evaluate the reactivity of different species (e.g., calculate activation barriers)
- Study the chemical evolution of the system during critical steps of the catalytic process

Computational setup: definition of the active center

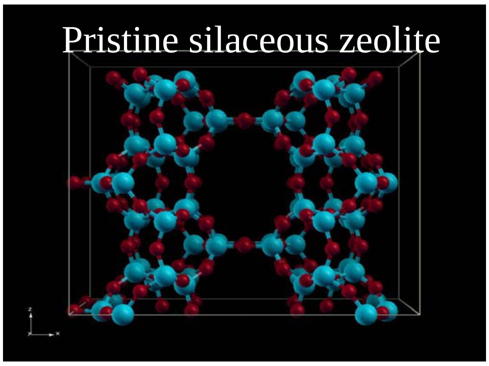
Pristine silaceous zeolite

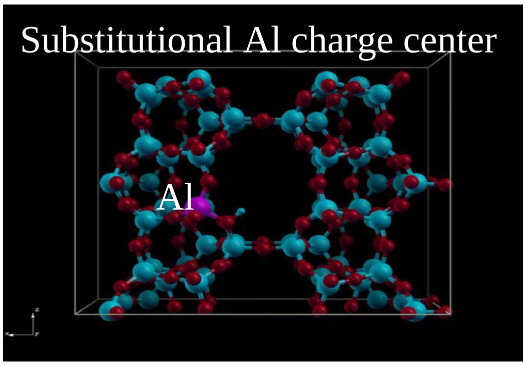
Substitutional Al charge center

TaH_2 active center

Substitutional Al defect creates a charge deficiency in the system

Charge deficiency induces a high oxidation state in Ta and makes the metal center able to activate strong C-H bonds

Cluster models around the active center will be used to speed up calculations

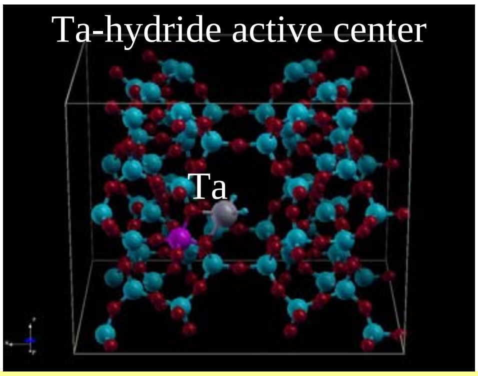
Ta-hydride active center

Modeling the chemistry

- Calculations of reactions in the periodic support (zeolite) are too expensive
- Idea: model the chemistry on small clusters of atoms around the active center and refine the kinetics (e.g., activation barrier) with single-point calculations in the periodic systems
- Ideal cluster size: 17T
  - Calculations on 17T clusters are quite expensive too
  - Initial screening performed on 5T clusters (NEB)
  - Refinement of energetics will be performed on bigger cluster and on zeolite

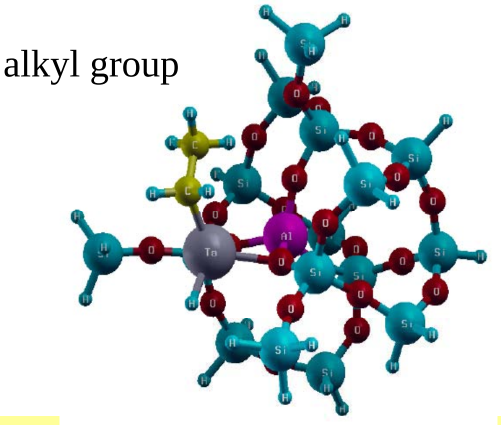

Preliminary results: dehydrogenation of the alkyl group

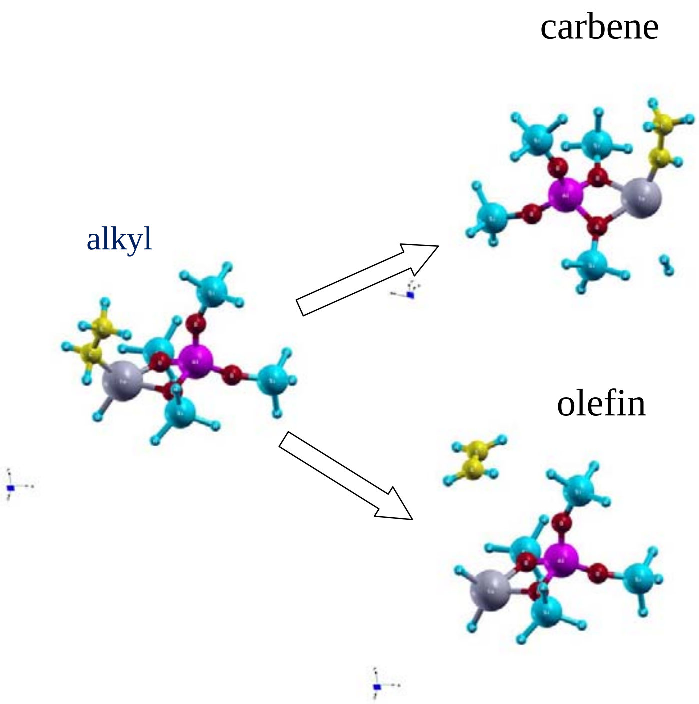

- •Calculations on 17T clusters are quite expensive
- •Initial screening performed on 5T clusters (NEB)
- •Refinement of energetics will be performed on bigger cluster and on zeolite

---

alpha-H elimination to ethene

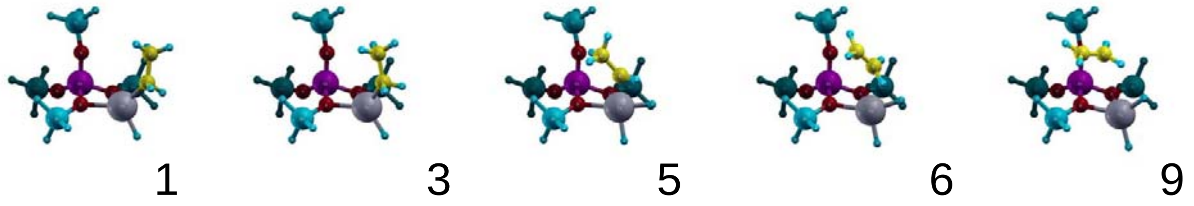

image 5 is the transition state

forward reaction energy barrier: 2.15 eV

backward reaction energy barrier: 0.6 eV

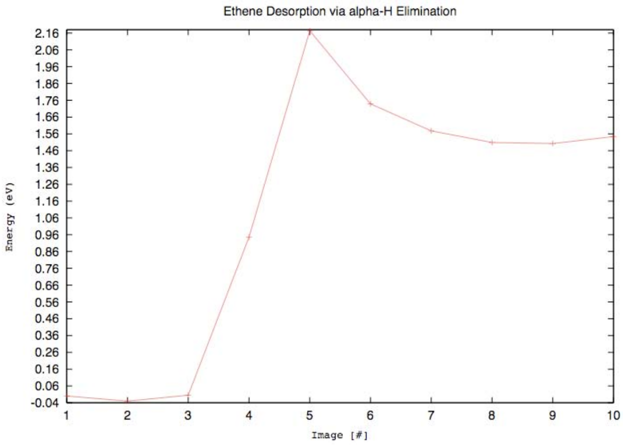

beta-H elimination to ethene

1

3

4

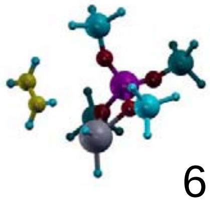

6

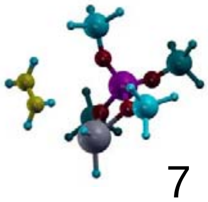

7

image 6 is the transition state

forward reaction energy barrier: 1.75 eV

backward reaction energy barrier: 0.15 eV

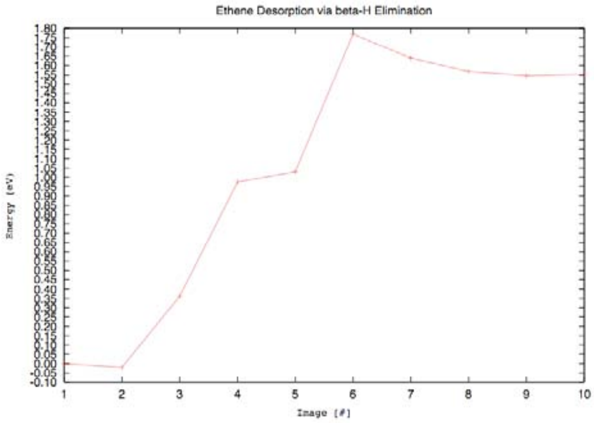

dehydrogenation to carbene

1

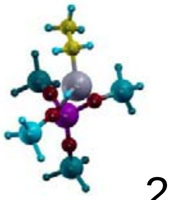

2

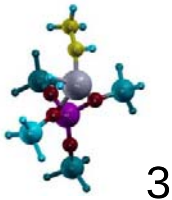

3

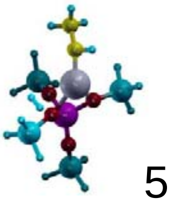

5

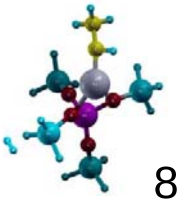

8

No activation barrier

carbene has an energy 1.35-1.4 eV higher than the alkyl

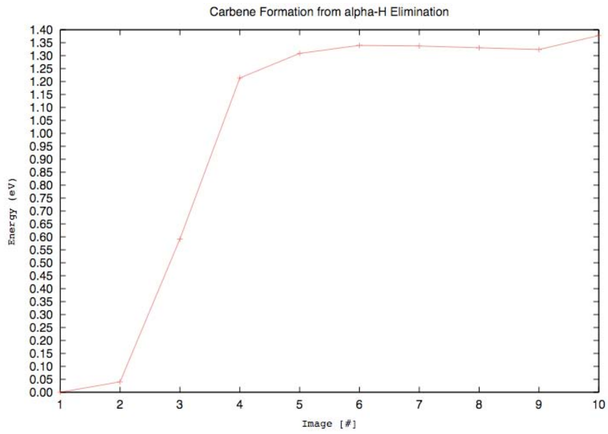

Conclusions and future work

- beta-H elimination to ethene has lower activation energy than alpha-H elimination

- Carbene is unstable towards hydrogenation to alkyl

Future developments:

- Screening of other TM centers (W, Mo)

- Study of other chemical steps (e.g. metathesis)

- Refinement of energetics in 17T clusters and zeolite

Part 2:
Adsorbents for H_2S Removal

- Problem Description: Demonstrate the feasibility of using molecular sieve adsorbents and membranes to concentrate streams that are dilute in H_2S.
- Benefits: New environmental separation method(s) to separate and concentrate dilute H_2S. Develop in-house technical expertise to address sulfur emission issues.

Packed Bed Flow System Schematic

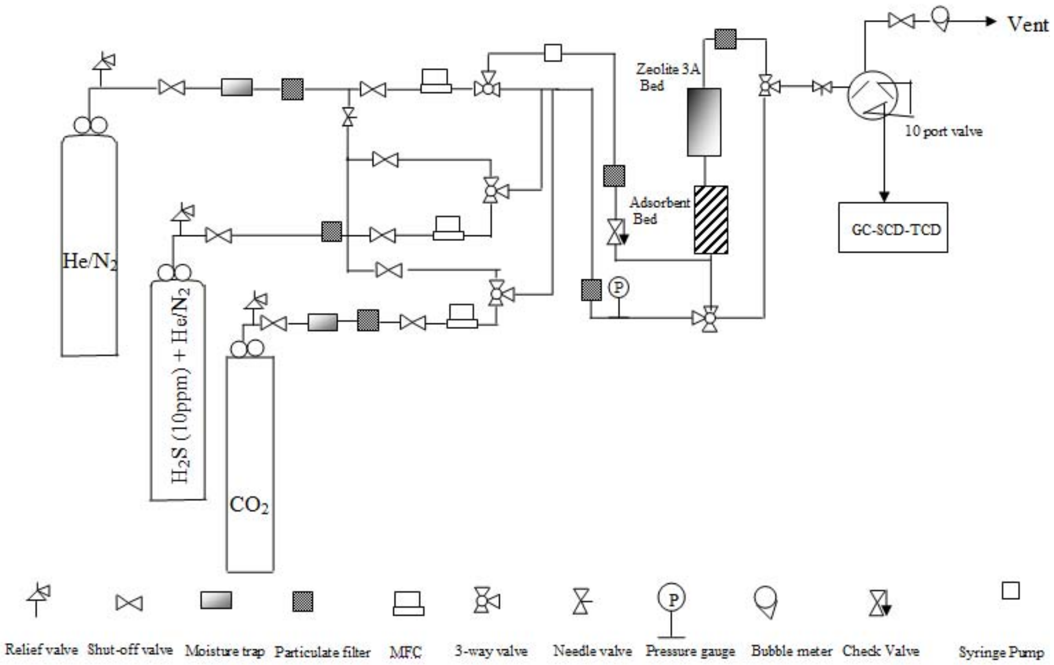

Packed Bed Flow System Picture

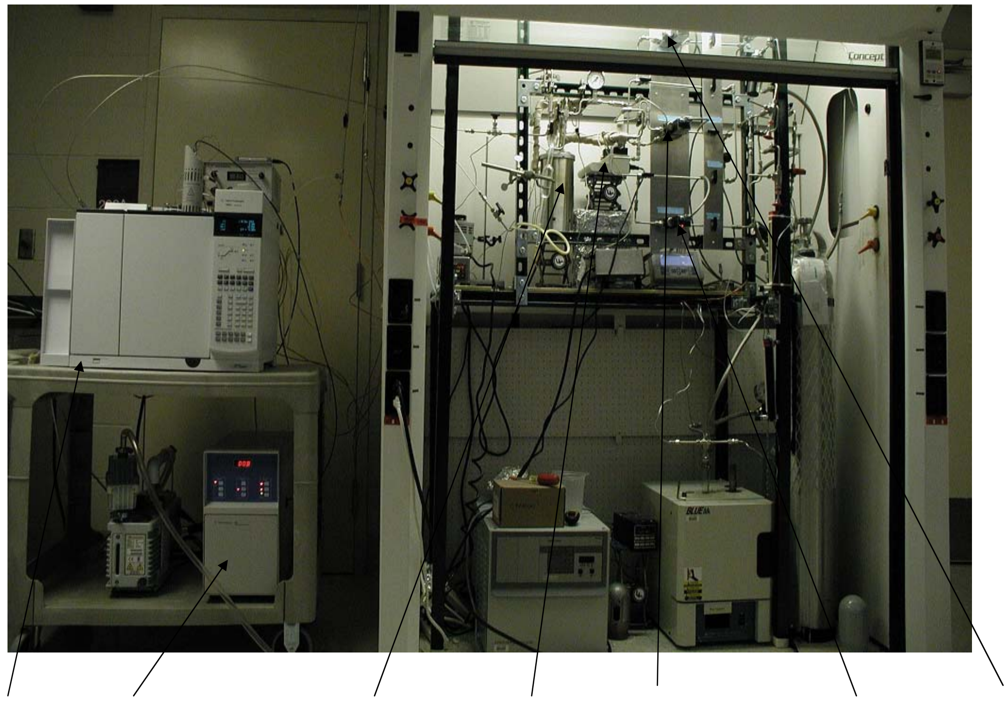

GC SCD Detector Adsorbent Bed in Furnace Syringe Pump N$_2$/He MFC H$_2$S in N$_2$/He $_2$MFC CO/CO$_2$ MFC

Adsorbents Tested

- Sodium forms of Zeolite X and Zeolite Y (NaX, NaY)
- Silver exchanged Zeolite X and Zeolite Y (AgX, AgY)
- Copper exchanged Zeolite X and Zeolite Y (CuX, CuY)
- Nickel exchanged Zeolite X and Zeolite Y (NiX, NiY)

Zeolite AgY breakthrough experiment

- 45 mg of Zeolite AgY was diluted with 135 mg Zeolite 3A and heated at 300 ^{0}C in Helium (100 ml/min) for 4h.
- H_2S in He (10 ppmw) at 100 ml/min was passed through the adsorbent bed (~1 in. length) in a tubular adsorbent bed at R.T

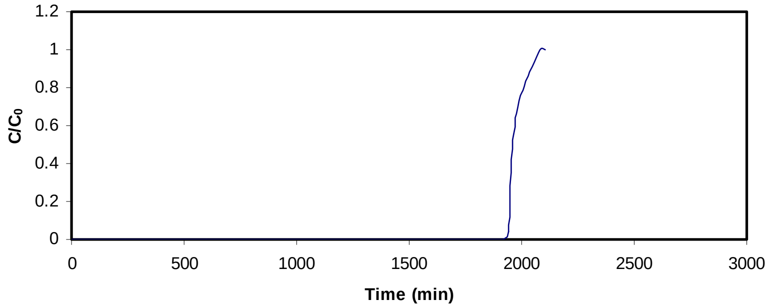

H_2S in Helium Flow rate (ml/min)	Breakthrough time (min)	Mean residence time (min)	Adsorption capacity (mmol/g)
75	1940	1976	1.37

H_2S (10 ppm) Breakthrough Experiments (R.T.)

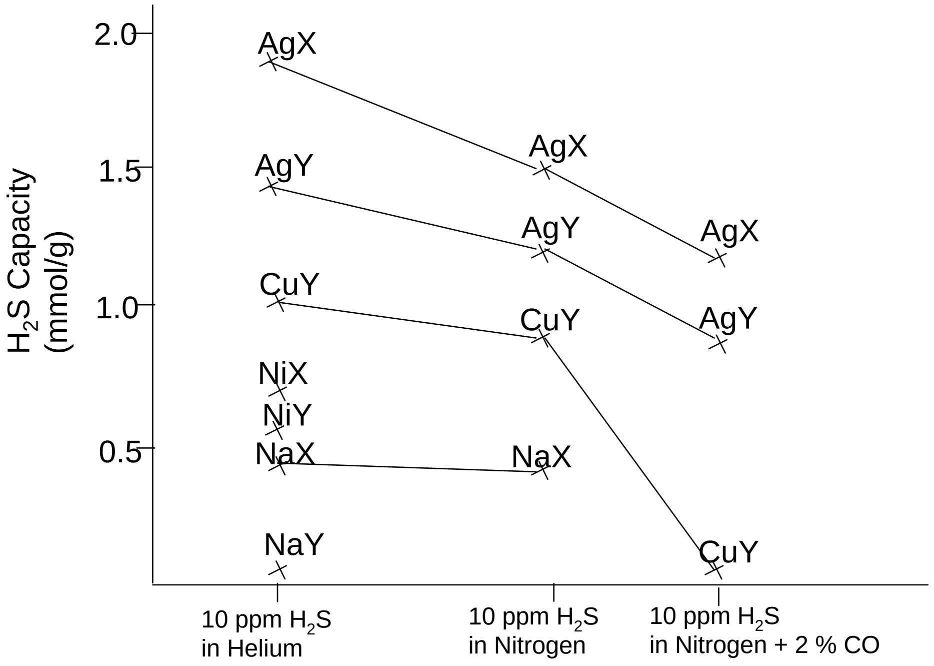

H_2S (10 ppm) Breakthrough Experiments at 150^0C

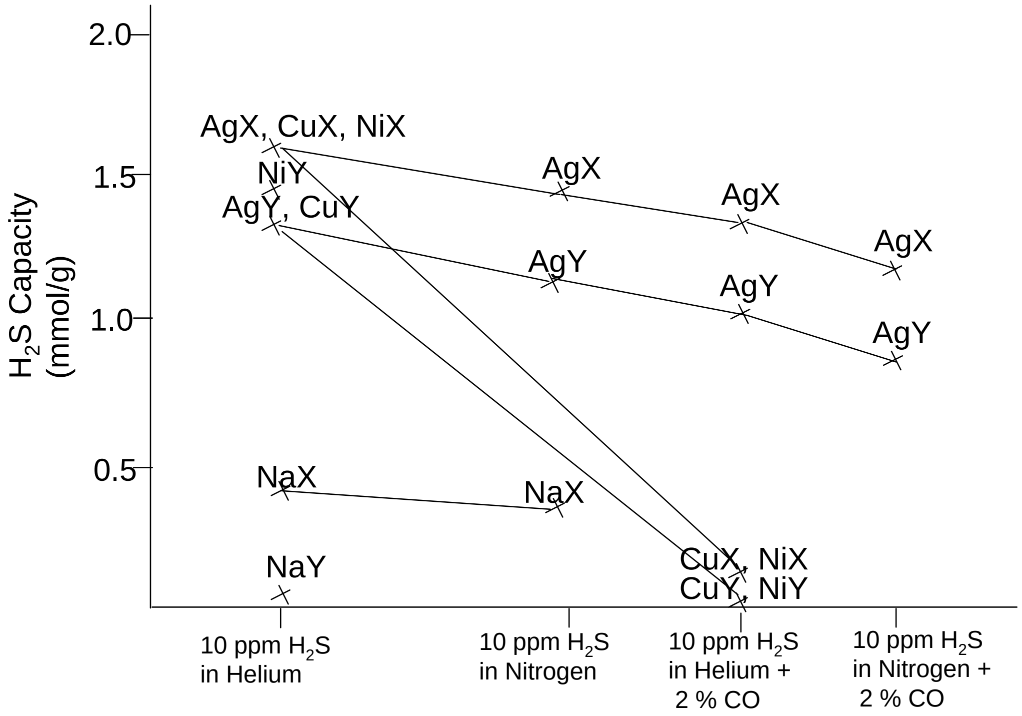

H_2S Breakthrough Experiments: Effect of H_2O and CO_2

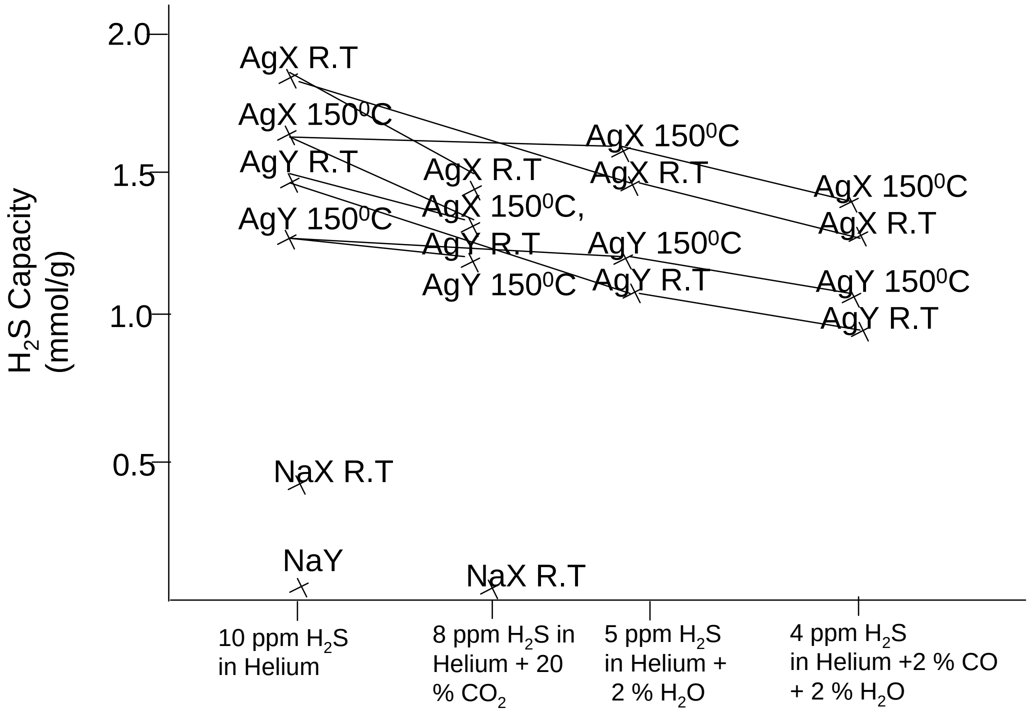

Conclusions from Experiments

- AgY, AgX, CuY, CuX, NiY, NiX adsorb H_2S stronger than NaX and NaY
- AgX adsorbents show higher H_2S adsorption capacity than AgY adsorbents
- H_2S adsorption capacities for zeolite adsorbents decrease in presence of N_2 compared to those in presence of Helium
- CuX, CuY, NiX, NiY samples show high H_2S adsorption capacities at 150 ^{0}C compared to R.T
- A small decrease in H_2S adsorption capacity is observed in presence of 20 % CO_2 in the feed mixture for Ag modified zeolites while NaX samples lose their H_2S adsorption capacity completely
- A small decrease in H_2S adsorption capacity is observed in presence of 2 % H_2O in the feed mixture for modified samples at room temperature while the H_2S adsorption capacities are unchanged at 150^{0}C
- AgX samples show high H_2S adsorption capacity in presence of CO_2 and water together, and also show high H_2S adsorption capacities in presence of CO
- H_2S adsorption capacities for NiX, NiY, CuY, and CuX samples are almost negligible at 150^{0}C in presence of CO

Cluster model of Y Zeolites

Unit cell of Y zeolite, 576 atoms

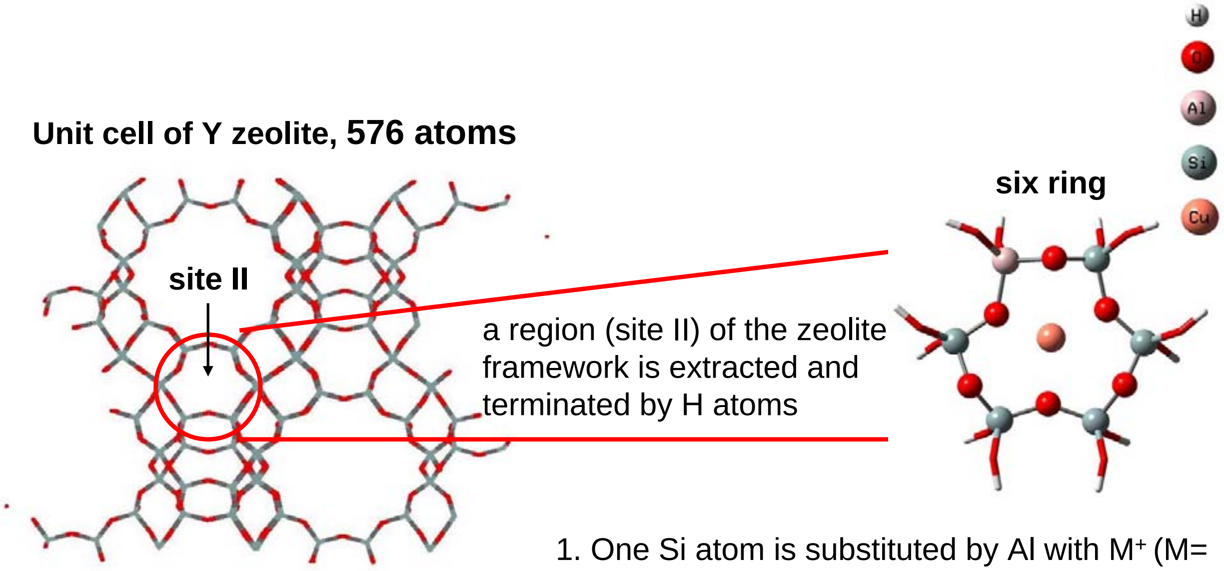

a region (site II) of the zeolite framework is extracted and terminated by H atoms

crystallographic data

1. One Si atom is substituted by Al with M^+ (M= Cu or Ag or Na) as the charge balancing cation
2. Terminating OH groups are fixed

Quantum Chemical Calculations

Schrödinger Equation: $\hat{H}\Psi = E\Psi$

Ψ : wavefunction

DFT (Density Functional Theory):

- The fundamental variable is the electron density $\rho(r)$ in place of the wavefunction
- The energy functional $E[\rho]$ is a minimum for the true electron density

Software: Gaussian 03

Level of Theory: B3LYP

Basis set: SDD for M^+, and 631+G(d) for all other atoms

Bare Zeolite Cluster Model

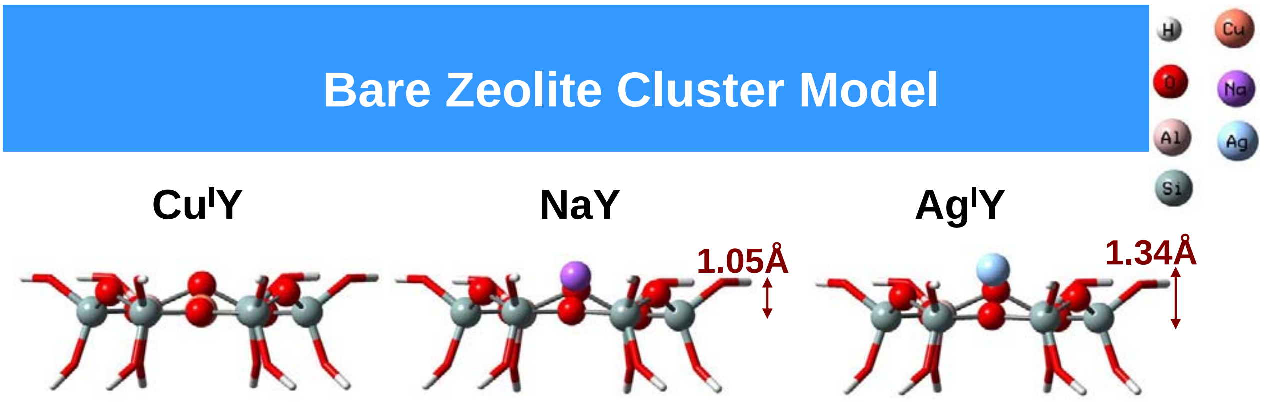

Ionic radii* : Cu^+ (77 pm) < Na^+ (102 pm) < Ag^+ (115 pm)
M^+ to the six-ring plane : Cu^+ (0.02 Å) < Na^+ (1.05 Å) < Ag^+ (1.34 Å)

Electronic properties of cation on zeolite cluster:

		Charge	Electron configuration	
Transition metal	Cu^+	0.76	$[Ar]4S^{0.19}3d^{9.90}4p^{0.13}$	given up 4s electron instead of 3d electrons
	Na^+	0.86	$[Ne]3S^{0.04}3p^{0.10}$	given up 3s electron
	Ag^+	0.83	$[Kr]5S^{0.08}4d^{9.98}5p^{0.10}$	given up 5s electron instead of 4d electrons

*Acta Cryst. A32 751-767 (1976)

Adsorption of Small Molecules

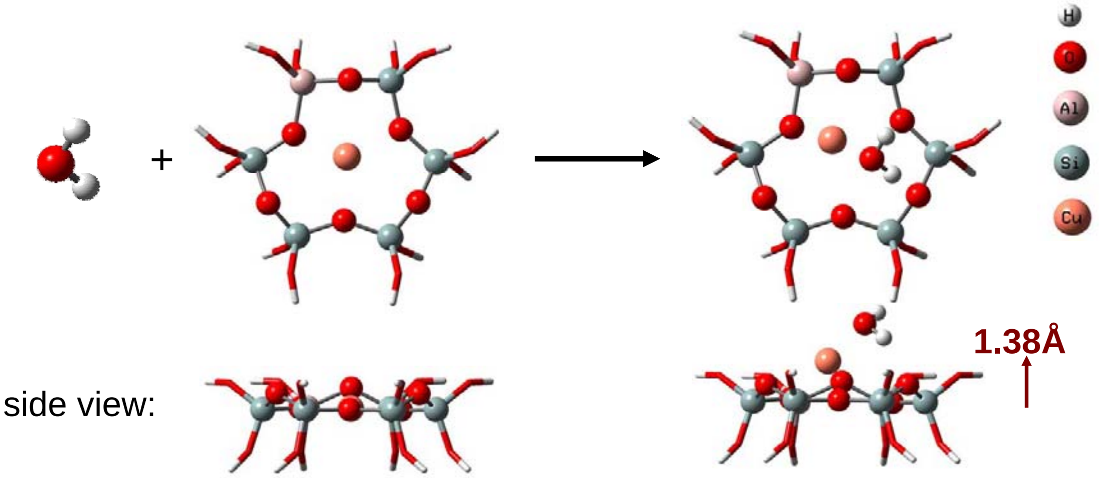

$$\Delta E = E(Z+X) - E(Z) - E(X)$$

Z: zeolite cluster
X: adsorbate

Adsorption of Small Molecules on Cu^IY Zeolites

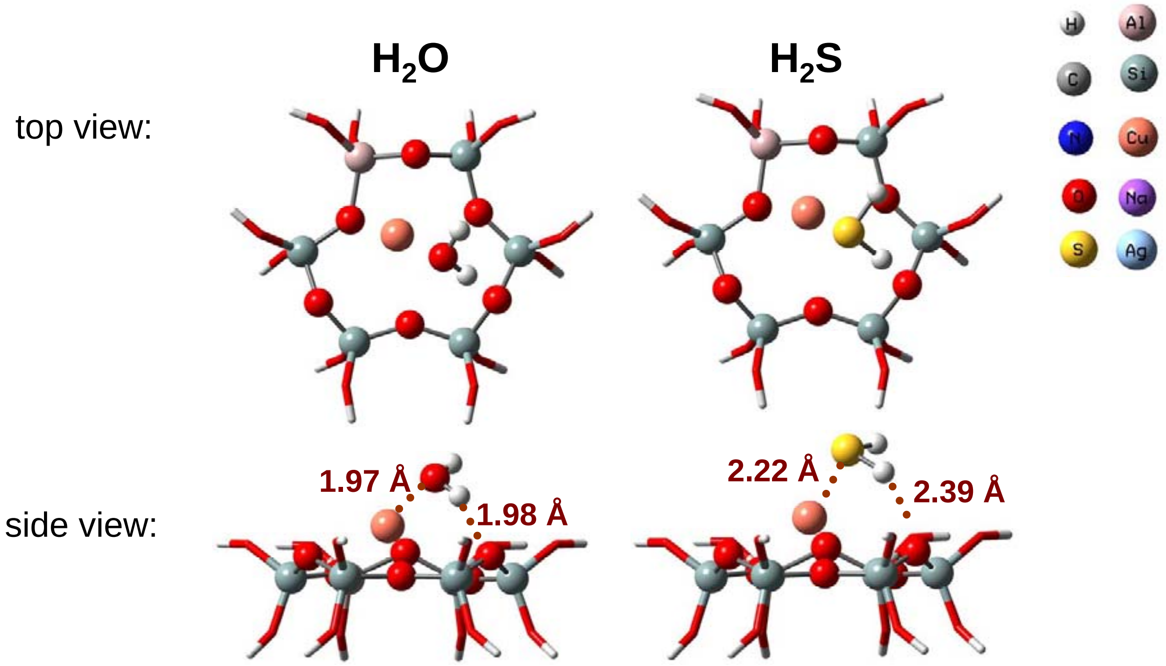

Adsorption of Small Molecules on Cu^IY zeolites

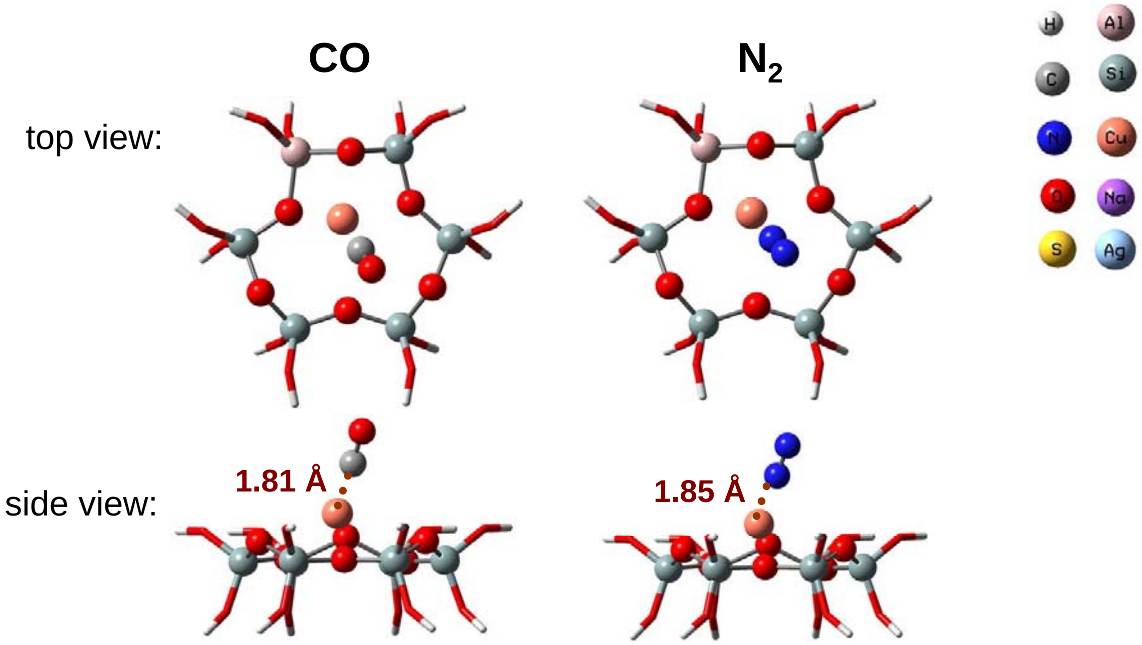

ΔQ of Cations upon Adsorption

	Change of number of electrons	CO	H_2O	H_2S	N_2	
Cu^+	Δ4s	+0.16	+0.10	+0.13	+0.06	→accepting e's
	Δ3d	-0.17	-0.05	-0.03	-0.13	→donating e's
Na^+	Δ3s	+0.06	+0.01	+0.03	+0.04	→invariant
	Δ3p	-0.1	-0.1	-0.1	-0.1	→invariant
Ag^+	Δ5s	+0.23	+0.07	+0.17	+0.09	→accepting e's
	Δ4d	-0.18	-0.03	-0.05	-0.07	→donating e's

Energetics of Small Molecules adsorbed on Cu^IY and Ag^IY

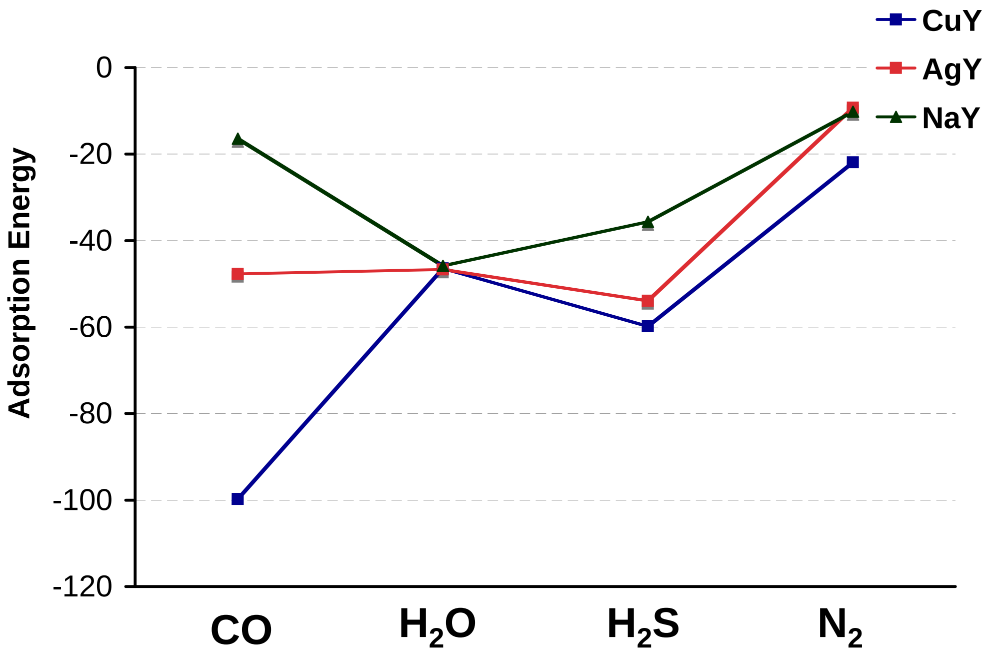

Remarks on the Computational Work

- On zeolite cluster, Cu^+, Na^+, and Ag^+ exhibit different properties (locations and electron configurations) due to their nature (ionic radii and transition metal characteristics).
- Upon adsorption, CO and N_2 undertake end-on configurations, whereas H_2O and H_2S coordinate to metals with O atom and S atom, respectively.
- The trend for electrons exchanged between Cu^+ and Ag^+ and adsorbate is different from that between Na^+ and adsorbate. This indicates that the adsorption mechanism is different for transition metal exchanged zeolites.
- Competitive adsorption need to be further studied by optimizing more than single adsorbate molecules on the zeolite cluster.

Coatings for Catalytic and Separation Processes

UMN Team: M. Tsapatsis, L. Francis, W. Suszynski,
H. Zhang, K. Varoon
PI Team: S. Al Hashami, R. Vladea, O. Murizawa

1st Annual PI Partner Schools Research Workshop
The Petroleum Institute, Abu Dhabi, U.A.E.
January 6-7, 2010

PI Partners

PI Sponsors

bp

TOTAL

ADNOC

JODCO

Presentation Outline

- Background and Objectives
- Dip Coating Process
- Coatings for Catalytic Processes
  - Gamma Alumina
  - Carbon
- Zeolite Coatings for Separation Processes
- Project Status
- Conclusions and Summary

Background

- Coatings for Catalytic Processes
  - Coated foams have applications as catalyst supports for hydrotreating/hydrocracking of crude oils
  - Catalytic coatings are comprised of a mesoporous support (or catalytic) layer and catalytic particles
  - Rotating catalytic bed reactors are the basis for more efficient reactor designs incorporating the foams
- Coatings for Separation Processes
  - Zeolites have high selectivity for gas separations
  - Zeolite coatings for separation processes must have a controlled, defect-free structure

Project Objectives

- Prepare catalytic coatings with controlled porosity and distribution of catalytic particles
- Explore support coating chemistries and structures as well as coating processes
- Characterize coatings before and after hydrotreating / hydrocracking reactions
- Prepare and characterize zeolite coatings for gas separation processes

Dip Coating on Flat Surfaces

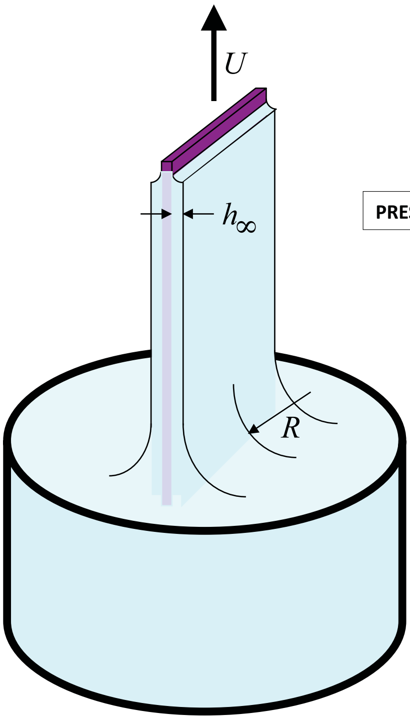

$$Uh_\infty = q = \frac{h^3}{3\mu}\left(-\frac{dp}{dx}\right) + Uh + \frac{h^3}{3\mu}(-\rho g)$$

PRESSURE GRADIENT FLOW

VISCOUS DRAG FLOW

GRAVITATIONAL CONTRIBUTION

$$h_\infty \propto \frac{(\mu U)^{2/3}}{\sigma^{1/6}(\rho g)^{1/2}}$$

Liquid coating thickness controlled by adjusting viscosity and withdrawal rate

For cylinders, added term – radius of cylinder

Foam Supports

- Foams have advantages*
  - Low pressure drop
  - Varied shapes and sizes
  - Enhanced radial convection
- Open cell structure
- Al, C and SiC foams available with a variety of pore dimensions (*ERG Materials and Aerospace Corporation*)
- For this research:
  - Carbon foam with 10 ppi
  - Amorphous

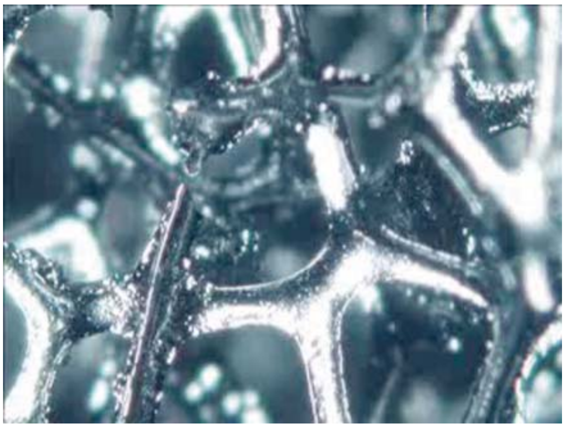

Video from Hirox 3D Microscope

0.5 mm

*Twigg & Richardson, *Chem. Eng. Res. Des.* 2002.

Dip Coating of Foams

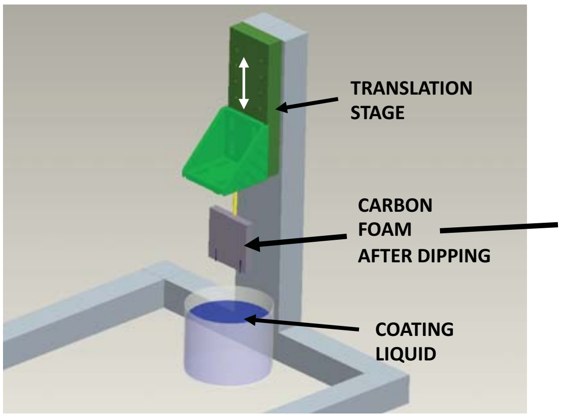

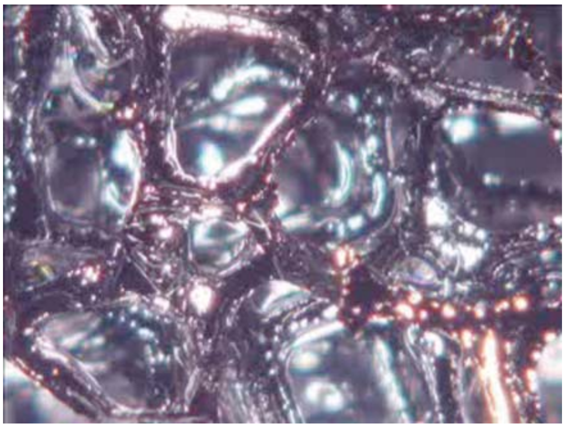
Video from Hirox 3D Microscope

- Complex foam structure affects coating, drainage
- Surface tension traps liquid in cell openings
- Requires removal by air knife or centrifuge

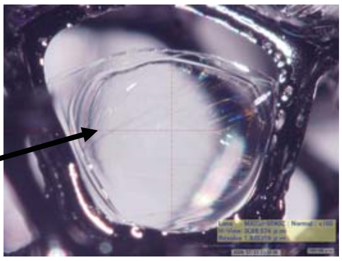
Solid film present in some carbon foam cells after drying

γ-Alumina Coatings

- Mesoporous catalyst and catalyst support layer
- Applied to a variety of supports, including ceramic monoliths (structured supports), metals
- Route:

AlOOH
(Boehmite)
Aqueous Sol

$\longrightarrow$

Deposit
Dry
Heat/Calcine

γ-Al_2O_3
mesoporous
coating

Polymer binder or γ-Al_2O_3 particles may be added to the sol

Experimental Methods: γ-Alumina Coatings

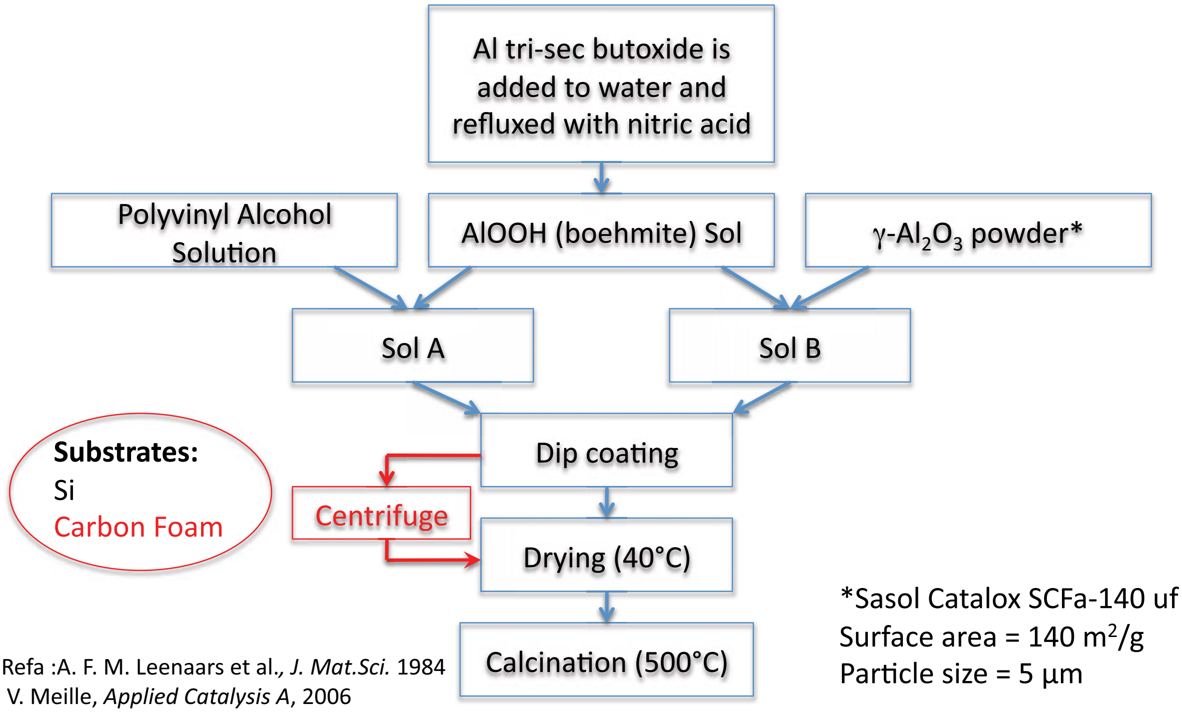

Al tri-sec butoxide is added to water and refluxed with nitric acid

Polyvinyl Alcohol Solution

AlOOH (boehmite) Sol

γ-Al_2O_3 powder*

Sol A

Sol B

Substrates:
Si
Carbon Foam

Dip coating

Centrifuge

Drying (40°C)

Calcination (500°C)

Refa :A. F. M. Leenaars et al., *J. Mat.Sci.* 1984
V. Meille, *Applied Catalysis A*, 2006

*Sasol Catalox SCFa-140 uf
Surface area = 140 m^2/g
Particle size = 5 µm

γ-Alumina Coatings on Si

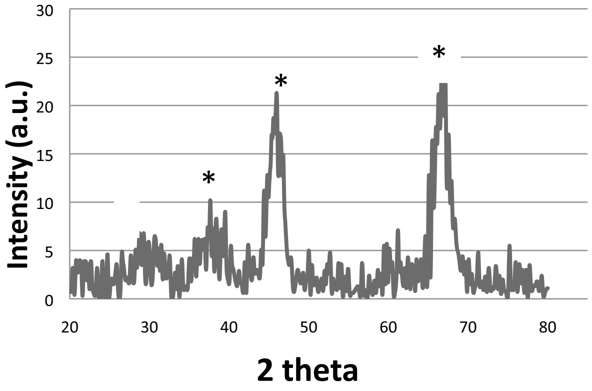

X-Ray diffraction shows γ-Al_2O_3(*) after drying Sol A and heating it to 500°C

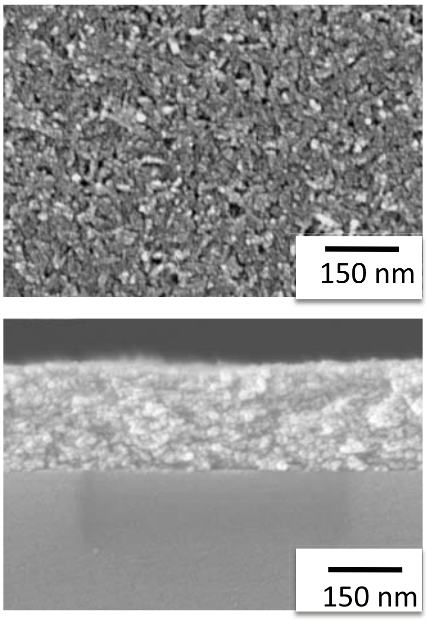

SEM of coating made from Sol A after heating

Coating Sol A Deposited on Foam

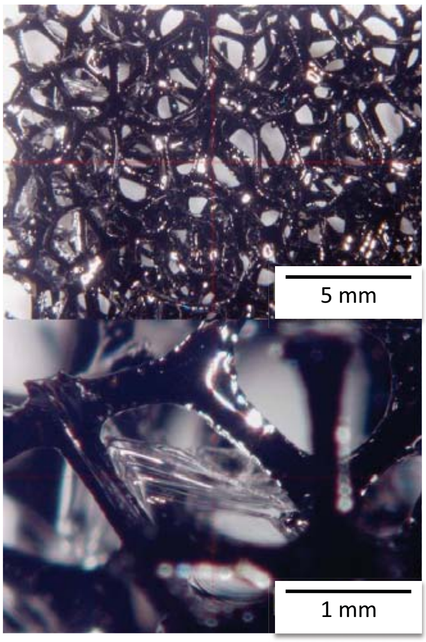

Without Centrifuge Treatment

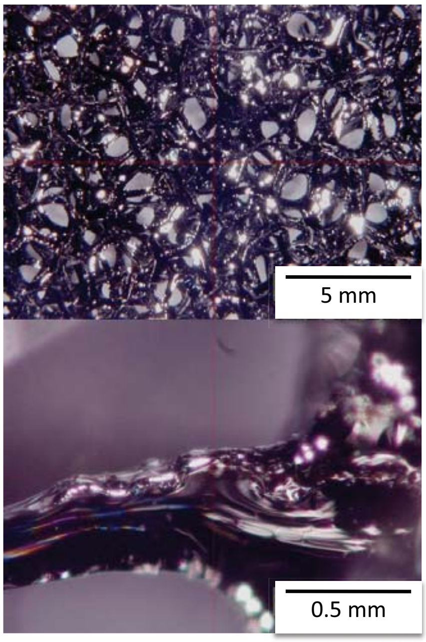

With Centrifuge Treatment

γ-Alumina Coatings on Foam

- Coatings from Sol A (AlOOH + PVA) are about 100-200 nm per deposition after heating
- Many depositions would be needed to build coating thickness

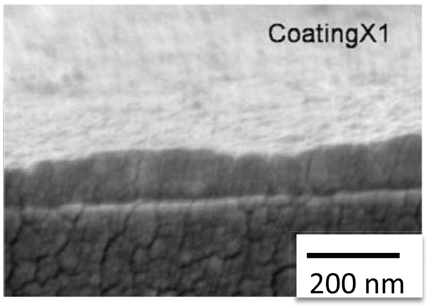

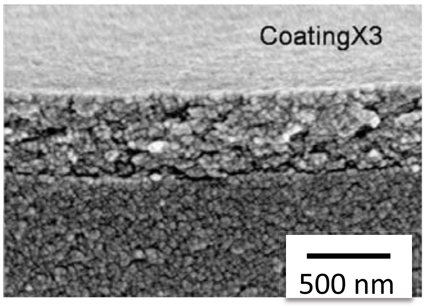

γ-Alumina Coatings on Foam (Sol B)

- Coatings from Sol B (AlOOH + γ-Al_2O_3 powder) are about 10 - 20 µm per deposition after heating
- Some cracking observed
- Optimization of composition and deposition conditions needed to achieve adequate thickness without cracks
- Experiments underway

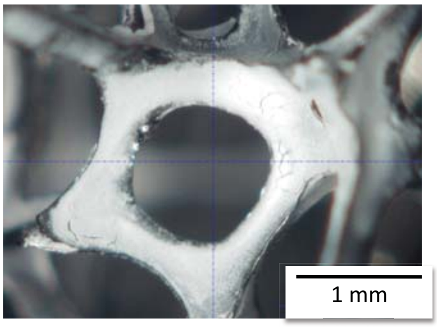

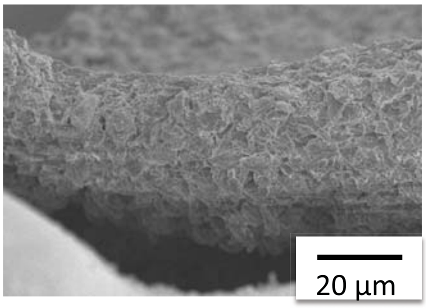

Carbon Coatings

- Mesoporous catalyst and catalyst support layer
- Advantages – stability in alkaline and acidic media, ability to tailor surface functionality/activity
- Route:

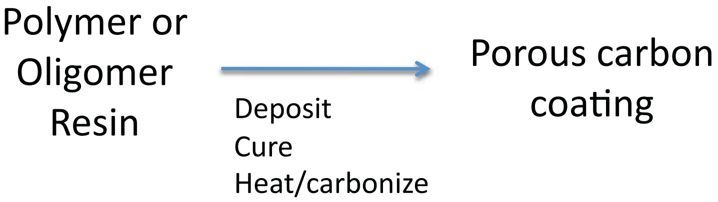

Polymer or Oligomer Resin

Deposit
Cure
Heat/carbonize

Porous carbon coating

Mesoporous carbon particles may be added to the resin

Experimental Methods: Carbon Coatings

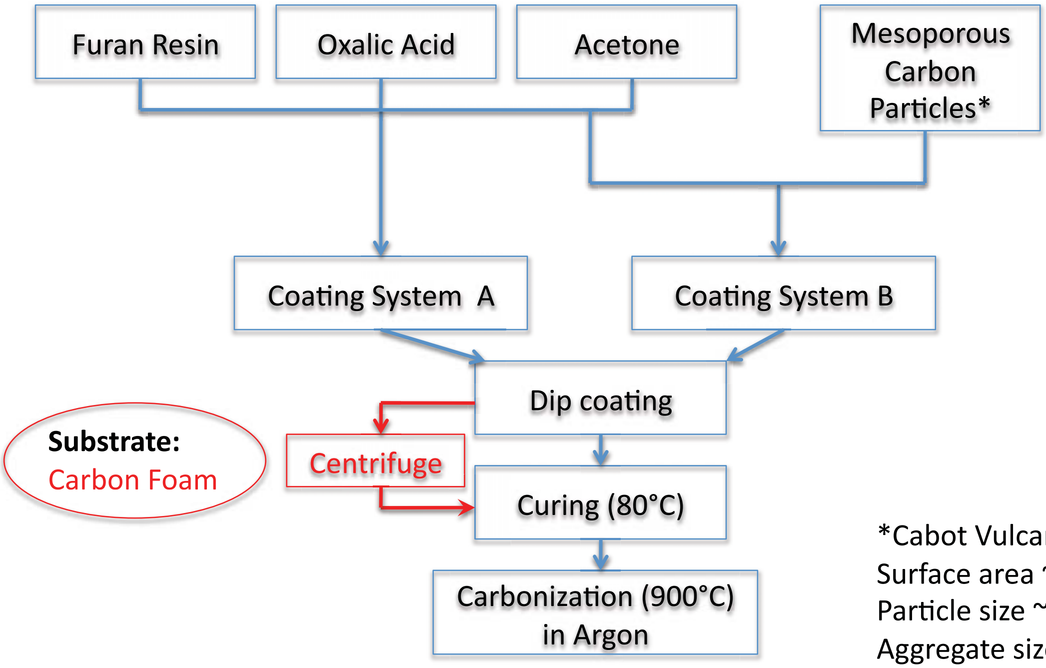

Furan Resin

Oxalic Acid

Acetone

Mesoporous Carbon Particles*

Coating System A

Coating System B

Dip coating

Substrate: Carbon Foam

Centrifuge

Curing (80°C)

Carbonization (900°C) in Argon

*Cabot VulcanX72R
Surface area ~ 220 m^2/g
Particle size ~ 10 nm
Aggregate size ~ 300nm

Ref: E. Garcia-Bordeje, et al., *Carbon*, 2002

Carbon Coatings on Foam – Coating A

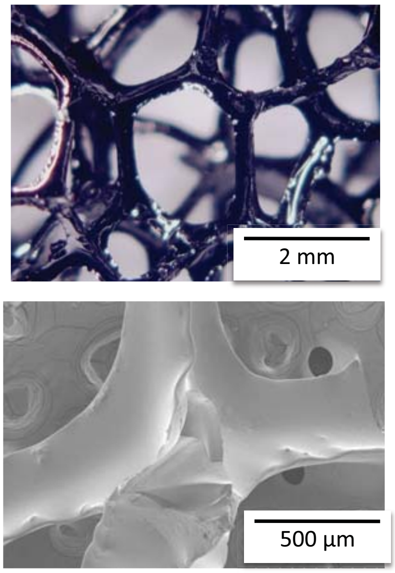

After Curing

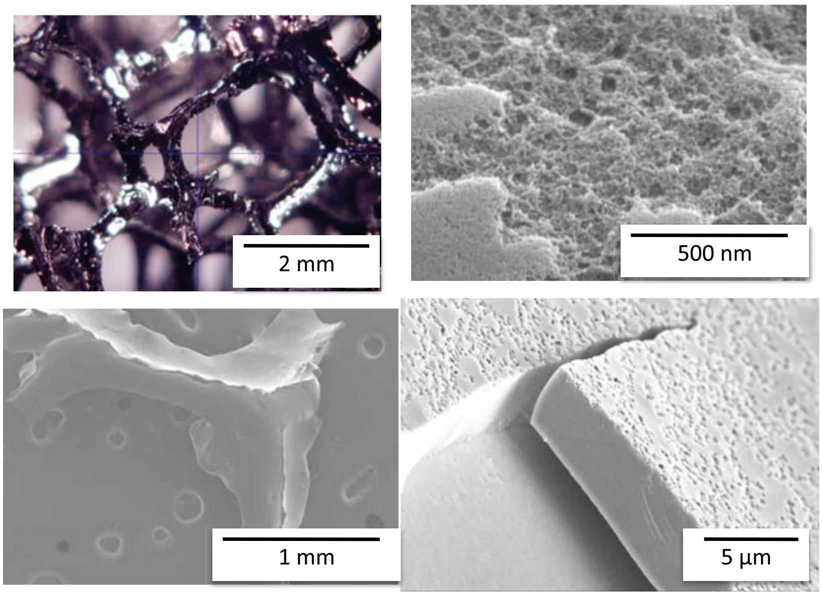

After Carbonization

Carbon Coatings on Foam – Coating B

- Thicker coatings containing mesoporous carbon prepared
- Cracking observed
- Relative amounts of resin and carbon particles will be adjusted

- More characterization underway

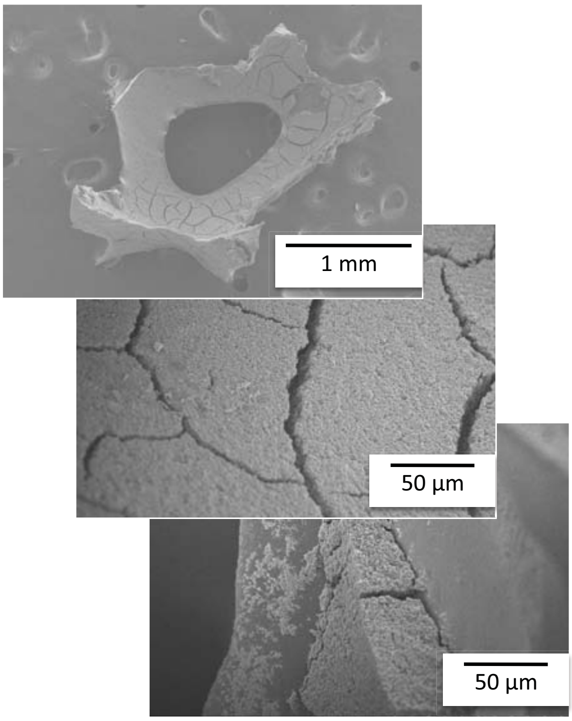

Zeolite Coatings for Gas Separations

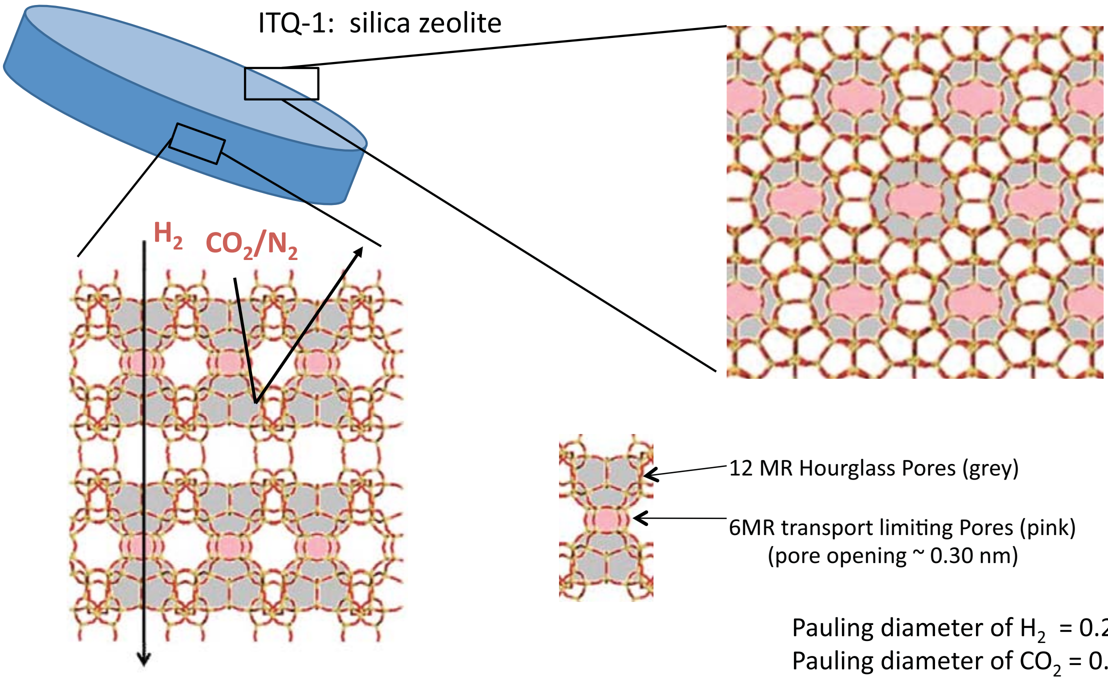

ITQ-1: silica zeolite

12 MR Hourglass Pores (grey)

6MR transport limiting Pores (pink)
(pore opening ~ 0.30 nm)

Pauling diameter of H_2 = 0.24 nm
Pauling diameter of CO_2 = 0.37 nm

Hydrothermally Synthesized Zeolite Particles

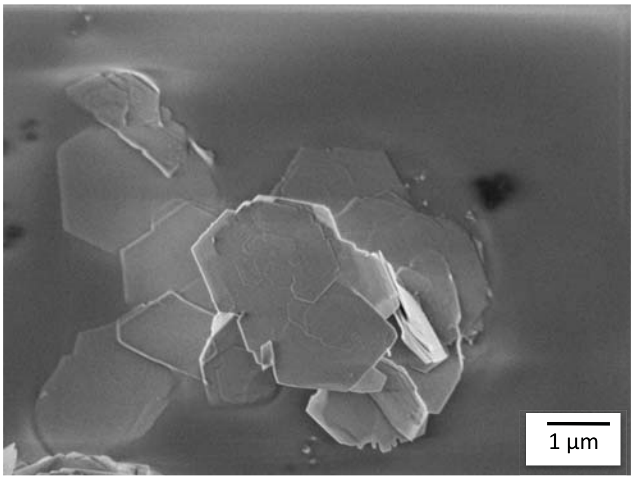

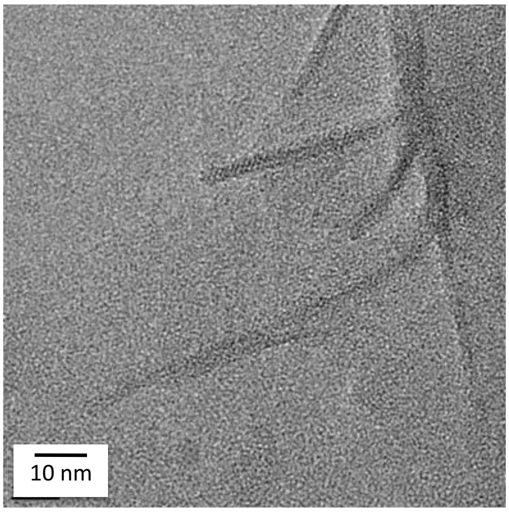

- Thin circular disc with diameter 1-2 μm and thickness 30-40 nm
- Each disc consists of 2.5 nm thin sheets stacked on top of each other

Experimental Methods – Zeolite Coatings

Zeolite suspension in water

↓

Dip coating

↓

Drying (80°C)

↓

Calcination (540°C)

Substrate:
Stainless Steel Tubes
(Pall Corp)

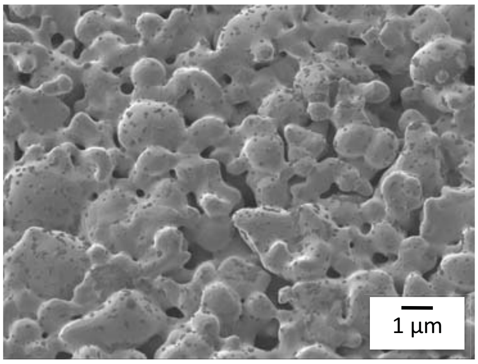

Zeolite Coatings

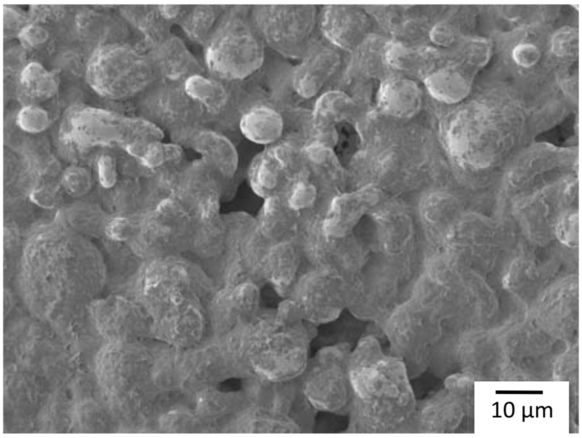

Zeolite coating directly on stainless steel tube → holes

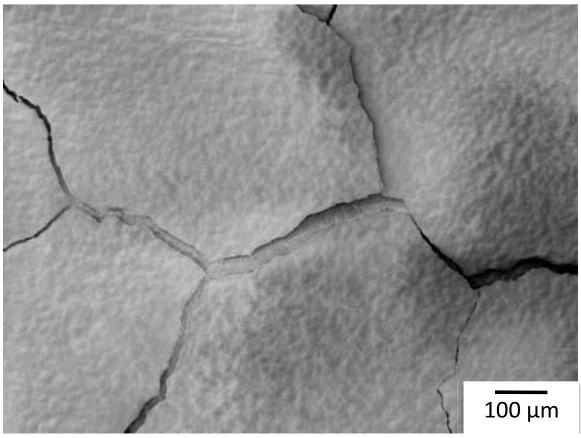

Zeolite coating stainless steel tube that was precoated with thick PVA/zeolite layer to planarize → cracks

Zeolite Coatings (con't)

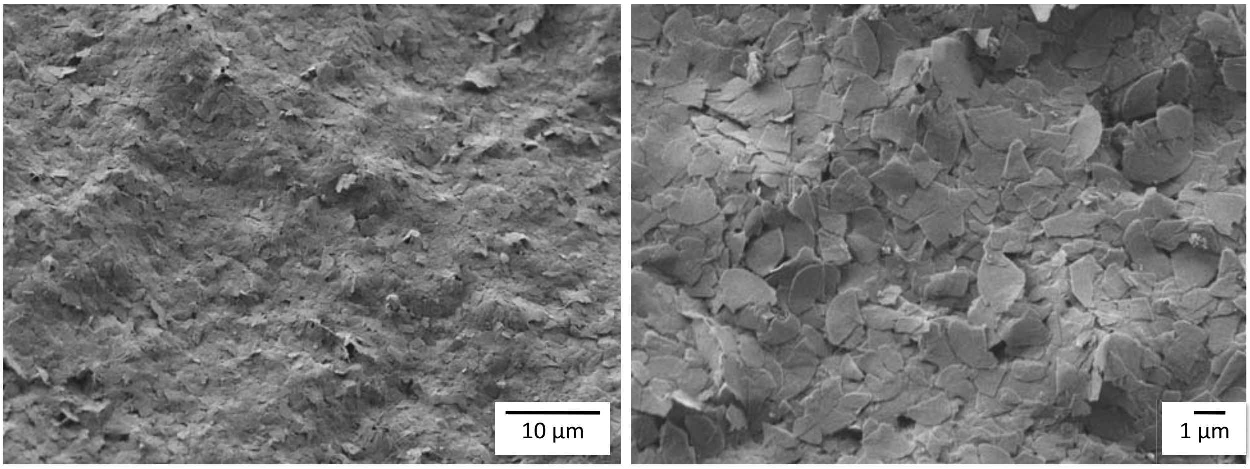

Zeolite coating stainless steel tube that was precoated with thin PVA/zeolite layer → crack-free coating without holes

Zeolite Coatings – Separations Results

	Permeance (mol/m^2.Pa.s)				Selectivity			
T (˚C)	He	H_2	CO_2	N_2	H_2/He	H_2/CO_2	H_2/N_2	CO_2/N_2
22 C	9.09E-06	1.37E-05	3.58E-06	4.42E-06	1.50	3.81	3.09	0.81
400 C	2.76E-06	3.71E-06	9.69E-07	1.26E-06	1.34	3.83	2.95	0.77
640 C	1.89E-06	2.68E-06	6.77E-07	8.58E-07	1.42	3.96	3.12	0.79

- Knudson diffusion due to loose assembly of zeolite nanoparticles
- Experiments with CVD to fix these gaps/defects underway
- Zeolite coatings suitable for catalytic applications

Project Status and Next Steps

- Methods for producing γ-alumina, carbon and zeolite coatings established
- More characterization and refinement needed
- Fundamental processing issues identified:
  - Control of liquid quantity and distribution (foams)
  - Prevention of cracks, removal of defects (zeolites)
- Next steps:
  - Processing studies, implementation of “dip and spin”
  - Surface functionalization of carbon coatings
  - Catalytic performance studies
  - Improving microstructure of zeolite layer

Dip Coating of Foams

- Methods to remove excess liquid
  - Gravity
  - Air knife
  - Centrifuge
- New method for better control
  - Spin coater with custom made sample holder

LARGER SAMPLE
UP TO 55 x 55 x 20 mm

SPEED WELL CONTROLLED
UP TO 10,000 rpm

- Planned experiment

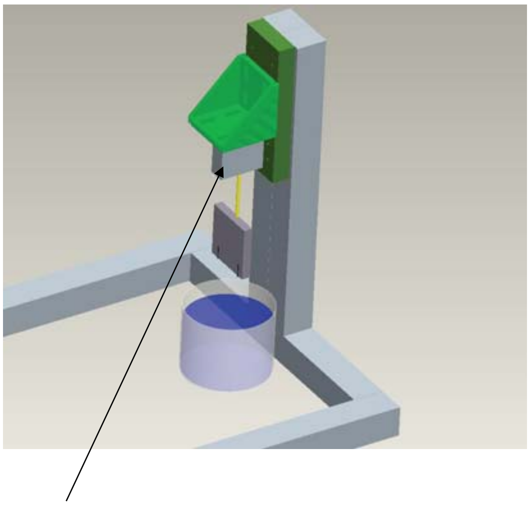

Load cell added for weight measurement during and after coating

---

"Dip and Spin"

Video

Conclusions and Summary

- Coatings for catalysis and separations prepared using dip coating and thermal treatments
- "Dip and spin" has promise for controlling deposition on complex 3D foams
- Research directions include process improvements and characterization of performance

Atomic-Resolution Quantitative Electron Microscopy

UMN Team: K. Andre Mkhoyan, Jeffrey J. Derby, William W. Gerberich, Christopher Macosco, Kirby Liao, Anudha Mittal and Andrew Wagner

1st Annual PI Partner Schools Research Workshop
The Petroleum Institute, Abu Dhabi, U.A.E.
January 6-7, 2010

PI Partners

PI Sponsors

Scanning Transmission Electron Microscope (STEM)

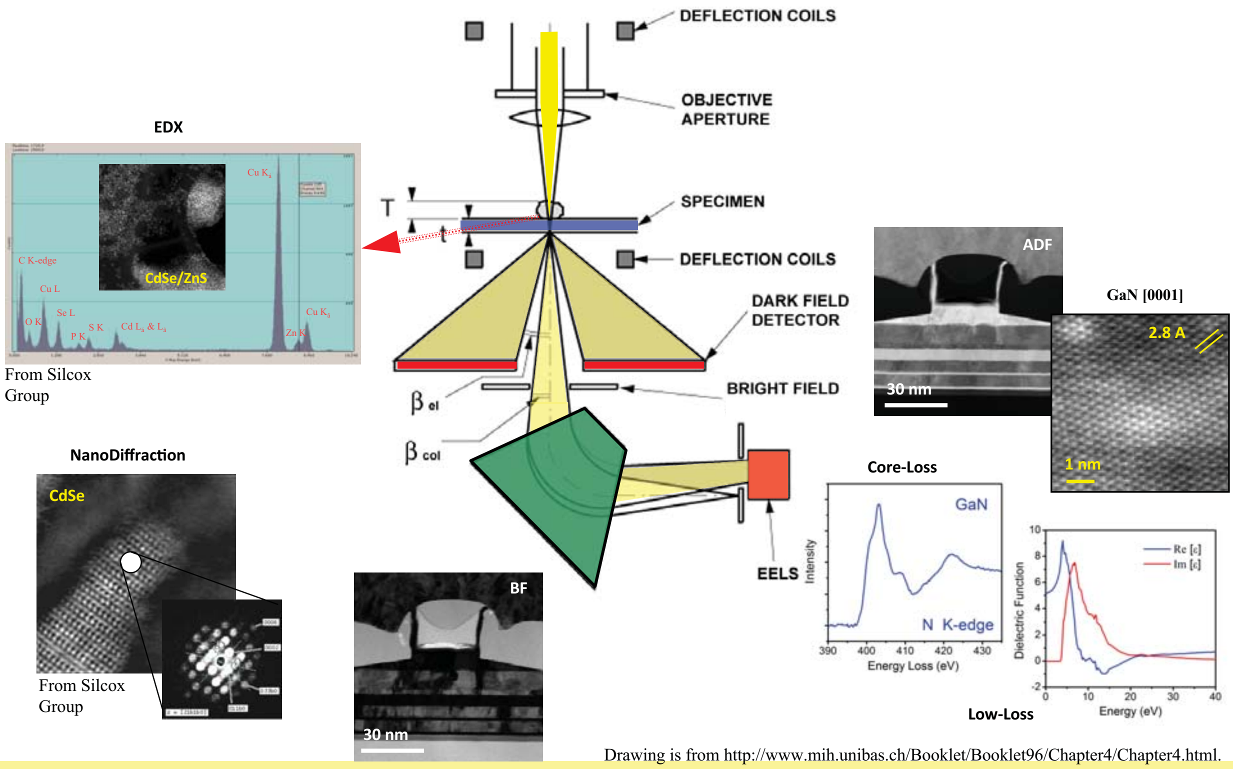

From Silcox Group

From Silcox Group

Drawing is from http://www.mih.unibas.ch/Booklet/Booklet96/Chapter4/Chapter4.html.

Electron Energy Loss Spectroscopy (EELS)

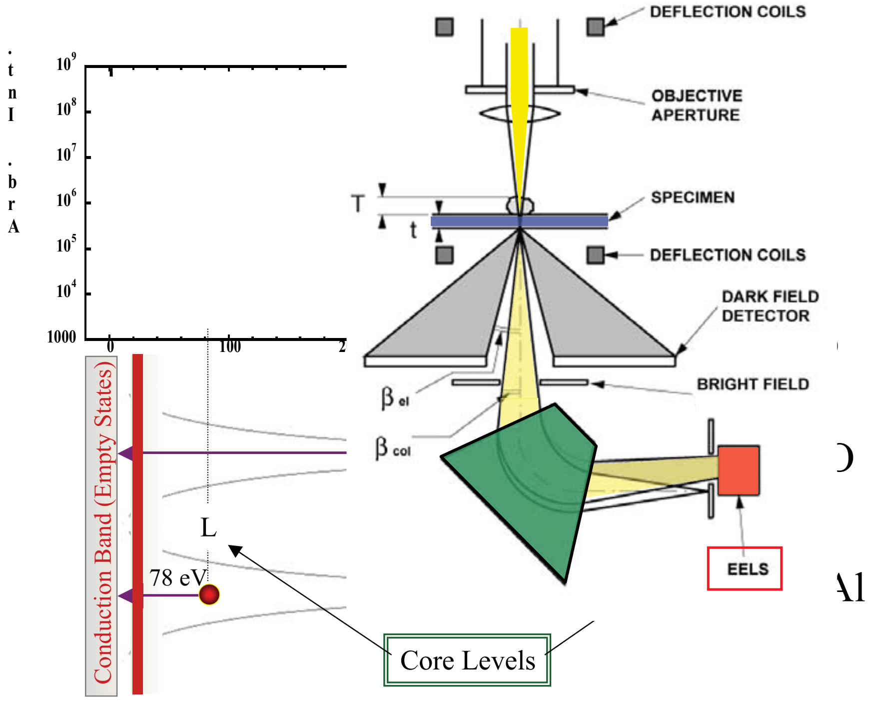

Core-Loss EELS

$$\frac{d^2\sigma(E,q)}{dEdq} = \frac{8\pi e^4}{\hbar^2 \upsilon^2}\frac{1}{q}\sum_{i,f}\left|\hat{\varepsilon}_q \cdot \langle f|\vec{r}|i\rangle\right|^2 \delta\left(E - E_f + E_i\right)$$

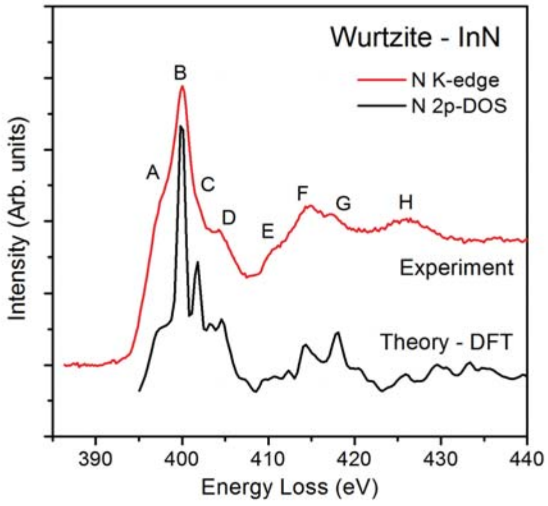

Graphene-Oxide (GO) Films

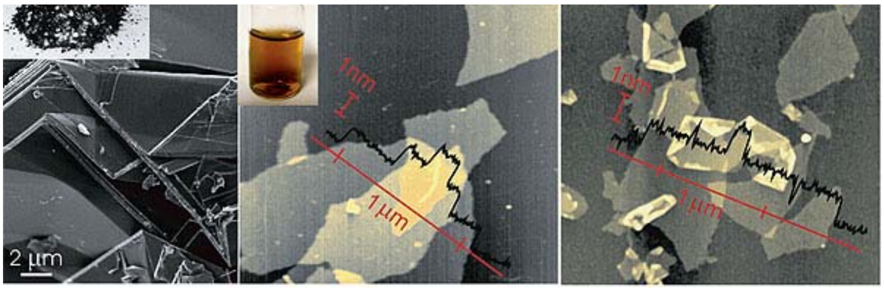

S. Stankovich et al., *Nature* 442, 282 (2006).
Ruoff Group at Northwestern University

on filtration membrane

on glass

on plastic

G. Eda et al., *Nature Nanotechnology* 3, 270 (2008).

AFM Imaging of GO Films and Thickness Measurements

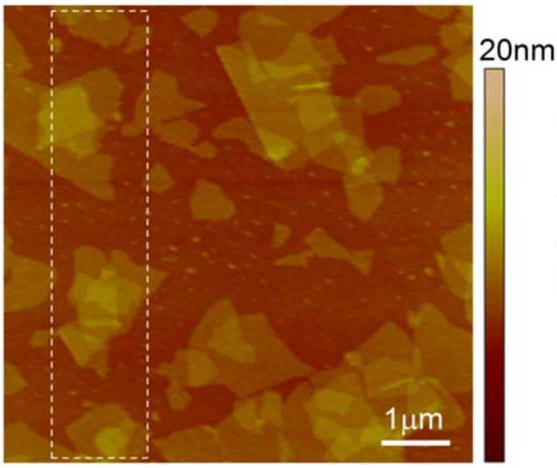

Histogram

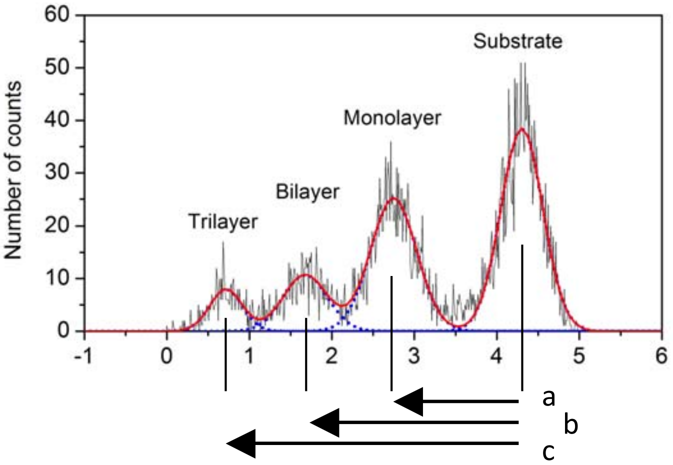

a = 1.6 nm

b = 2.6 nm

c = 3.6 nm

a : b : c ≠ 1 : 2 : 3

a : b : c = 1 : 1.6 : 2.2

Quantitative ADF-STEM Imaging of GO Films with Single Electron Counting

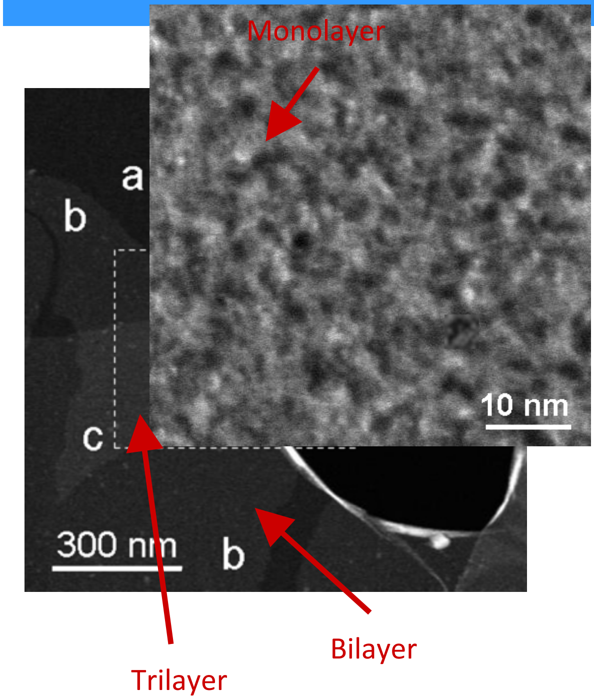

- Strong contrast variation

Quantitative ADF-STEM Imaging of GO Films with Single Electron Counting

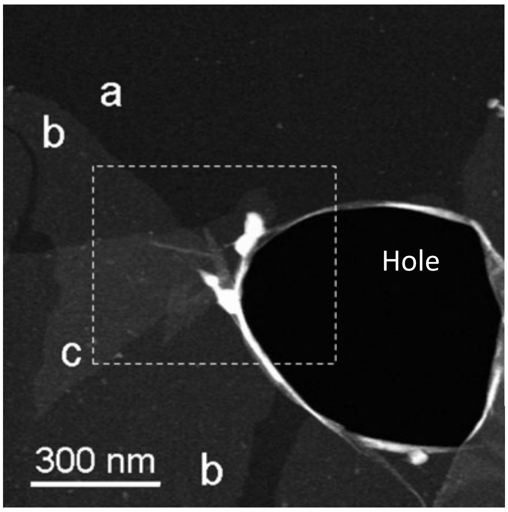

Histogram

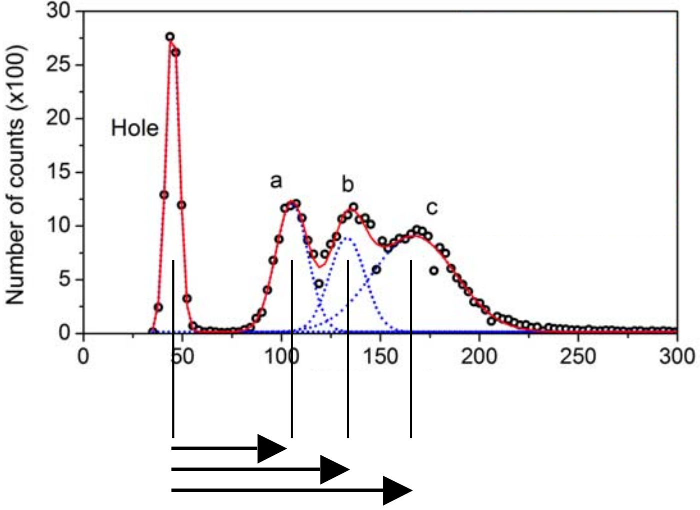

$a : b : c \neq 1 : 2 : 3$

$a : b : c = 1 : 1.5 : 2.0$

Packing of the GO Films and Surface Roughness

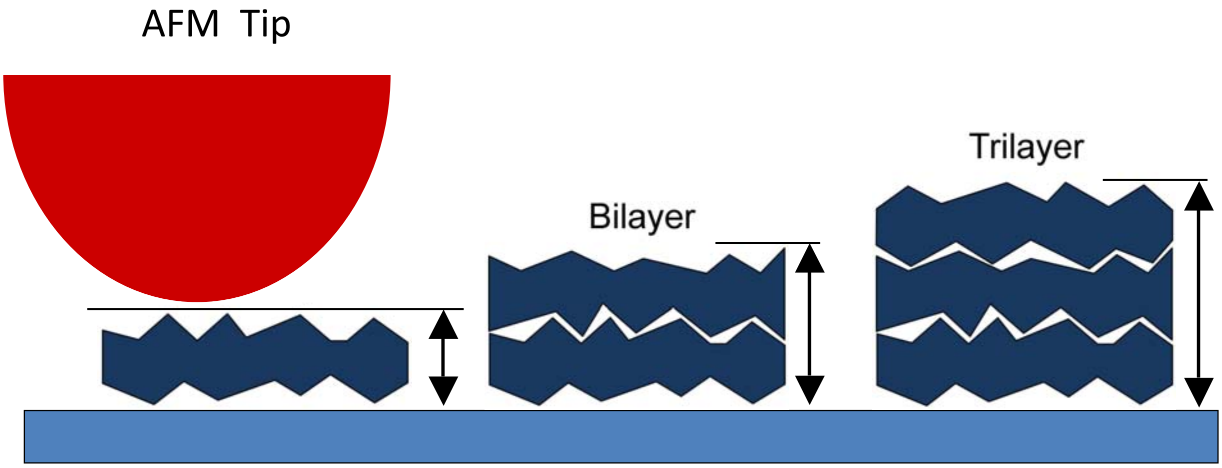

a = 1.6 nm

b = 2.6 nm

c = 3.6 nm

Thickness of single sheet = 1.6 nm

Roughness = 0.6 nm

Measuring Core-edge EELS: O K-edge

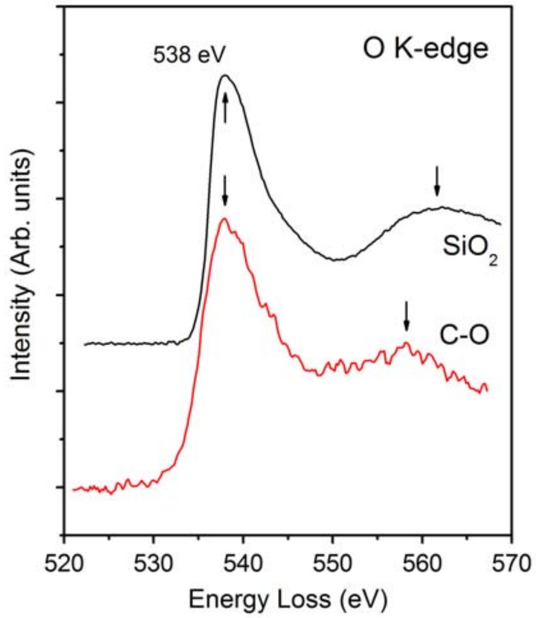

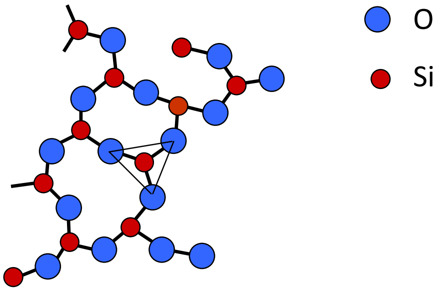

We should not expect to have:

- Peroxy Radicals
- Peroxy Link

Measuring Core-edge EELS: C K-edge

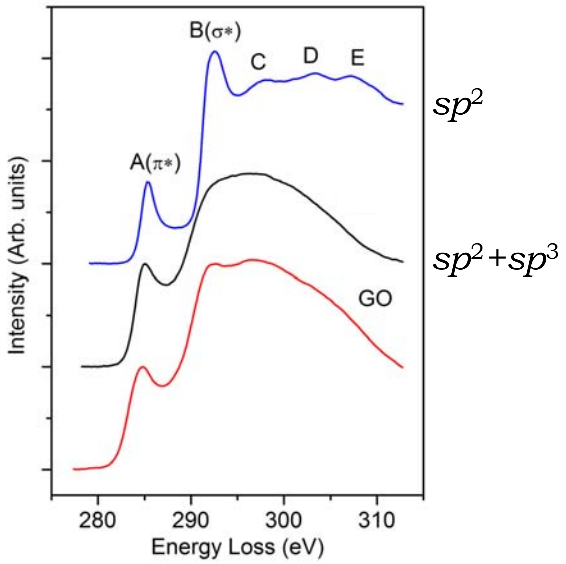

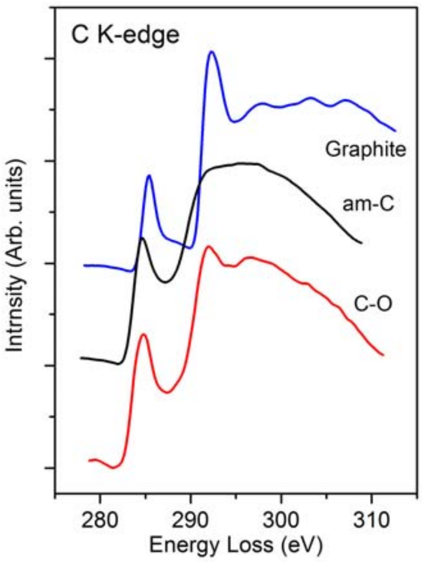

	A(π^*)	B(σ^*)	C	D	E
Graphite	285.4	292.5	298.2	303.4	307.2
a-C	284.7		~296		
GO	284.8	292.6	296.7	302.9	

Determination of sp^2 and sp^3 Fractions in GO

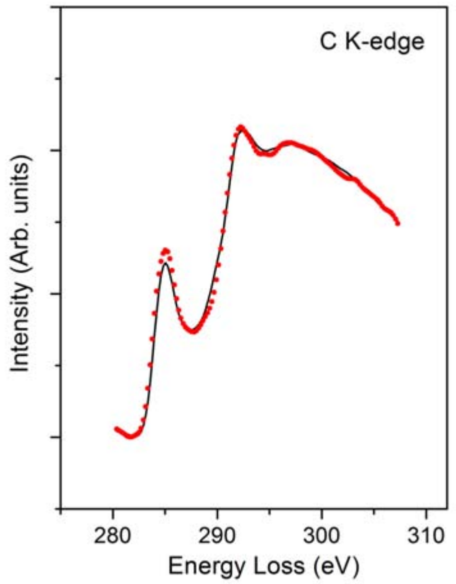

Linear least-square curve fitting

$$I(E) = \alpha_1 I^g(E) + \alpha_2 I^{am}(E)$$

$I^g(E)$ - Spectrum from Graphite

$I^{am}(E)$ - Spectrum from a-C

The best fit occurs at:

$\alpha_1 = 0.15$ & $\alpha_2 = 0.85$

⇩

Fraction of sp^3 is ~ 40%

Ab Initio Calculated Atomic Structure of Graphene with Single O Atom

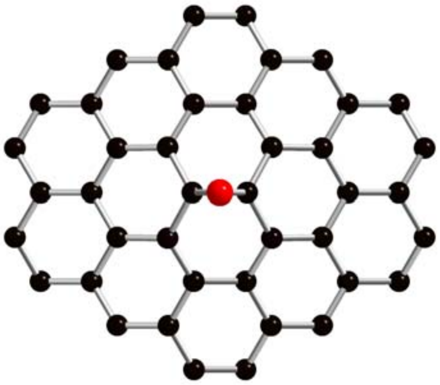

DFT calculations using a *plane wave pseudopotential* approach

1st case – pristine graphene

2nd case - graphene supercell with a single oxygen atom.

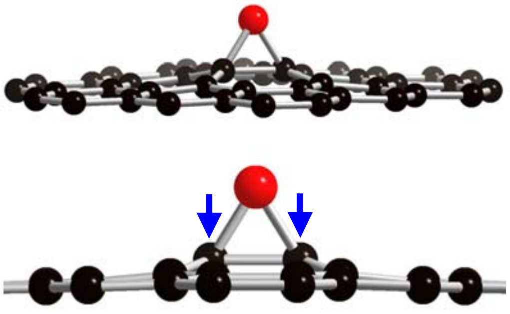

- Two carbon atoms bonded to the oxygen atom are pulled above the graphene plane
- The bond length between these two carbon atoms expands from 1.407 Å in graphene to 1.514 Å, (Diamond - 1.54 Å)

Ab Initio Calculated Density-of-States of Graphene with Single O Atom

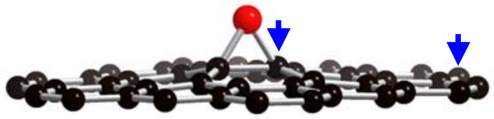

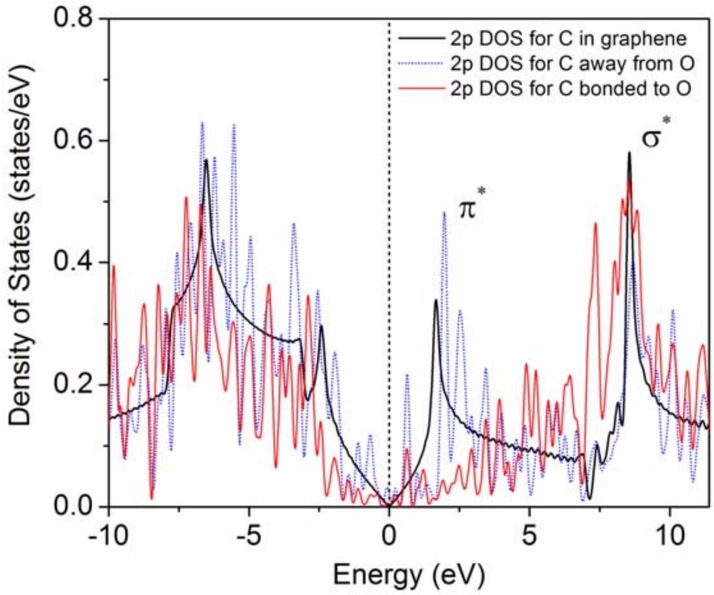

Aqueous Only Route to Graphene from Graphite Oxide

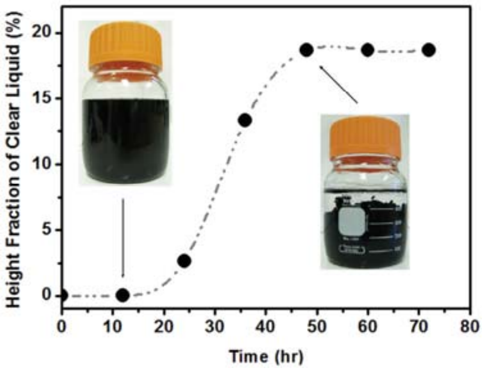

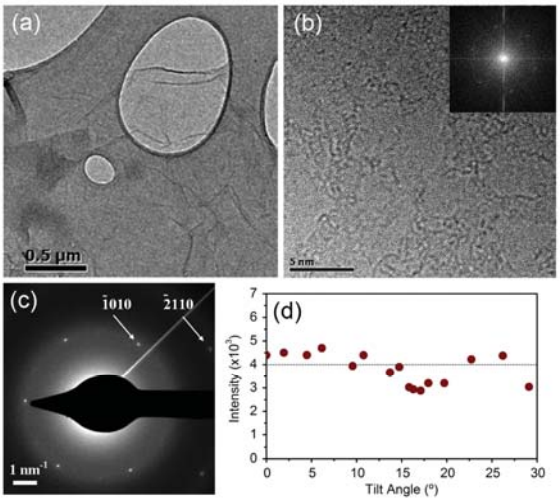

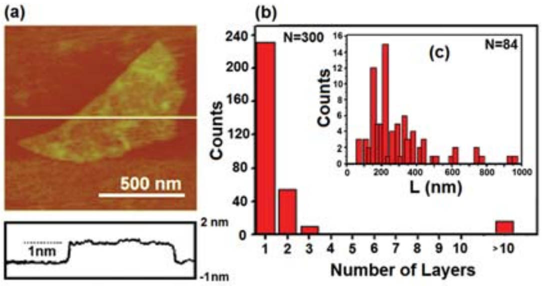

Si Nanoparticles and Mechanical Properties

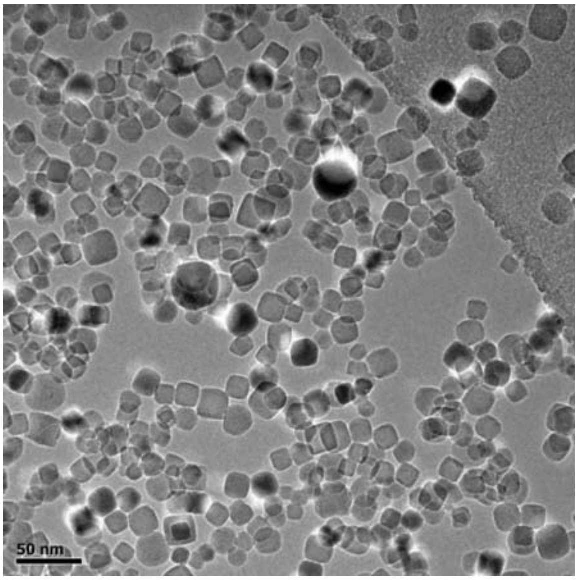

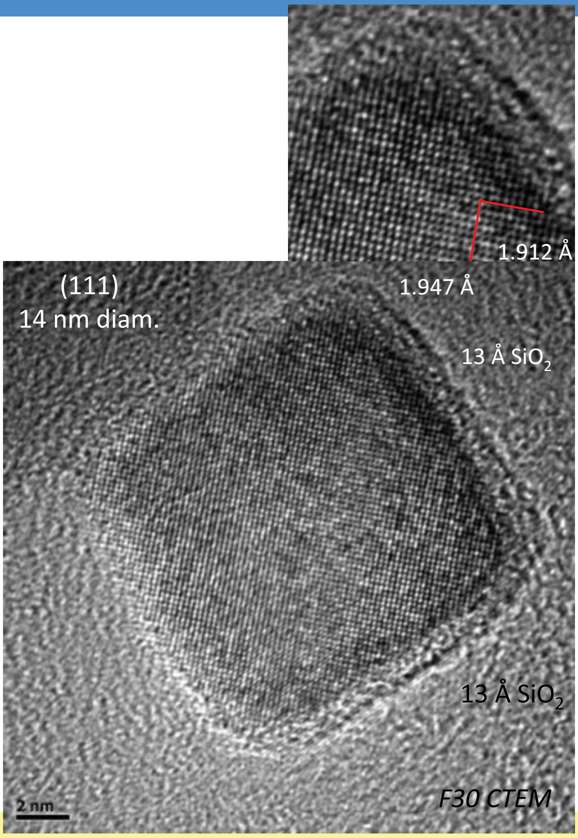

Acknowledgements

Chhowalla Group Members (Rutgers)

Prof. Manish Chhowalla

Dr. Cecilia Mattevi

Goki Eda

Dr. Steve Miller

Theory Group (Cornell)

Dr. Derek Stewart

Silcox Group Members (Cornell)

Prof. John Silcox

Alex Contryman

Mick Thomas

Materials Development and Characterization for Upstream Processes

Development of HIGH INTERSTITIAL STAINLESS TEELS for Use in DOWNHOLE DRILLING APPLICATIONS

CSM: **David Olson & Brajendra Mishra**

1st Annual PI Partner Schools Research Workshop
The Petroleum Institute, Abu Dhabi, U.A.E.
January 6-7, 2010

PI Partners

PI Sponsors

Presentation Outline

- Background
- Objectives
- Experimental Setup
- Results and Discussions
- Project Status
- Conclusions and Summary

Background

High Nitrogen Steels (HNS)

- C+N ≥ 0.5 wt. pct.
  - Advantages
    - Improved mechanical properties
      - strength AND toughness
      - Longer time to fatigue failure
    - Enhanced Corrosion Resistance
      - Decrease in pitting potential
      - Increase in passivity
  - Drawbacks
    - Low N retention at atmospheric pressure d
    - High pressure casting adds expense to process
    - Difficulties in Machining

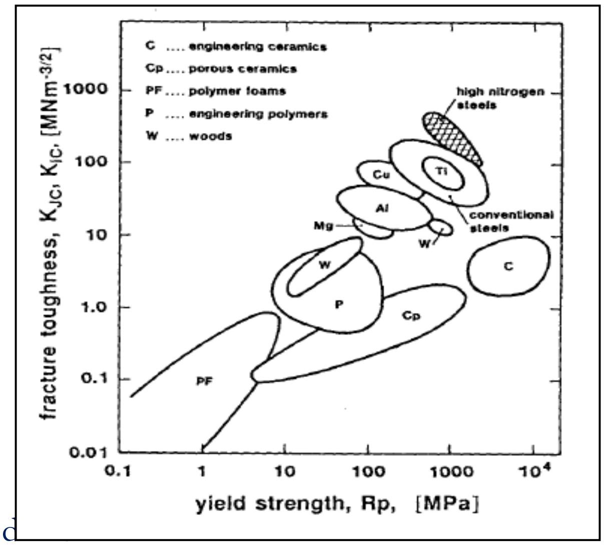

PRE(N+C)

PRE = %Cr+3.3%Mo+37(%N+%C)+4.5(%Mo)(%N+%C)-.6%Mn

Speidel and Uggowitzer, 1993

Project Objectives

High Nitrogen Steels (HNS)

- C+N ≥ 0.5 wt. pct.
  - Advantages
    - Improved mechanical properties
      - strength AND toughness
      - Longer time to fatigue failure
    - Enhanced Corrosion Resistance
      - Decrease in pitting potential
      - Increase in passivity
  - Drawbacks
    - Low N retention at atmospheric pressure difficult
    - High pressure casting adds expense to process
    - Difficulties in Machining

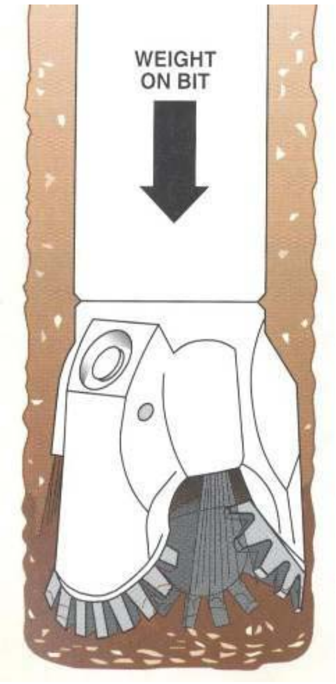

Baker, 2000

Experimental Setup

Over 20 Heats Conducted (2007-2009)

- **ALLOYING**
  - Argon blanket
  - Furnace additions
  - Ladle additions
  - In-mold additions
- **SPARGING**
  - N_2 (gas) injection into ladle
- **CASTING**
  - Sand mold
  - Ceramic filter
- **RIMMING**
  - N (liquid) cover
  - Immediately after casting
  - Creates high pressure N environment

Pitting corrosion test

PRE (N+C)

PRE= Cr + 3.3%Mo +37(%N+%C) +4.5(%Mo)(%N+%C)-0.6%Mn

Results and Discussions

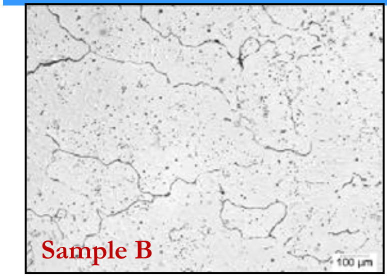

26.6

HRC

131 ksi

(UTS)

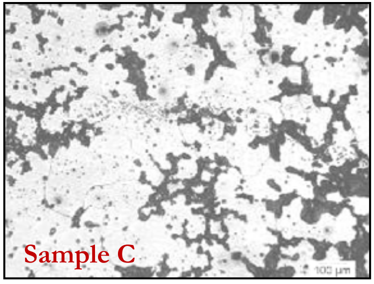

48.6

HRC

231 ksi

(UTS)

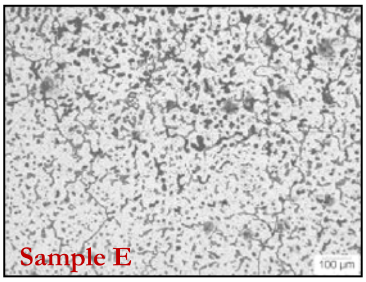

27.8

HRC

134 ksi

(UTS)

Immersion Test Results (3.2 wt. pct NaCl solution)	Initial Weight (g)	End Weight (g)	Weight Loss (mg)	Weight Loss (%)	Corrosion Rate (mg/mm^2/day)	Penetration Rate (µm per year)	Penetration Rate (mils per year)	**Final Rank**
Sample A	8.5169	8.51	2.4	0.03	0.000985	47.317	1.86	**6**
Sample B	4.0419	4.04	0.5	0.01	0.000208	9.972	0.39	**3**
Sample C	7.6096	7.61	0.3	0.00	0.000204	9.801	0.39	**2**
Sample D	4.4637	4.46	0.8	0.02	0.000612	29.383	1.16	**5**
Sample E	3.5785	3.58	0.2	0.01	0.000139	6.661	0.26	**1**
High N Martensite	14.065	14.05	13.8	0.10	0.007525	356.683	14.04	**13**
High P γ w/ N	12.314	12.30	10.8	0.09	0.000456	21.638	0.85	**4**
NPD-Namo 2005 Questec	1.984	1.98	5.7	0.29	0.004354	206.413	8.13	**10**
Super 13Cr	5.811	5.81	4.6	0.08	0.001416	67.134	2.64	**7**
17-4 PH	4.84	4.82	17.6	0.36	0.007352	348.490	13.72	**12**
397(25Cr-15Ni)	5.086	5.06	30.1	0.59	0.010287	487.634	19.20	**15**
Duplex 25Cr (2507)	4.94	4.93	5.8	0.12	0.002227	105.582	4.16	**9**
Duplex 32Cr (3207)	9.665	9.66	9.3	0.10	0.004581	217.165	8.55	**11**
DS9 w/ N	6.864	6.84	23.7	0.35	0.001498	71.014	2.80	**8**

Sample E is the best than any of the commercial downhole materials studied

Project Status

- **To Continue Casting Production**
  - Optimize alloying content
  - Investigation of Grain Refinement Additions
- **To Continue Corrosion Resistance Assessment**
  - Chlorides at Elevated Temperatures ($\leq$ 200 ^{o}C)
  - Aggressive Environments
    - CO_2 gas (carbonic acid)
    - Sour (H_2S present)
- **To perform Mechanical Performance Evaluation**
  - Tensile Strength
  - Impact Toughness
- **To perform Wear Rate Evaluation**

Conclusions and Summary

Stainless Steel Alloy for Drill Collars has been identified which can achieve

- Reduced Cost Material
  - Mn replaces Ni
  - Air Casting instead of High Pressure Process
  - Mechanical Properties without Forging
- Outstanding Corrosion Resistance
- Work Continues
  - Corrosion testing with increasing aggressivity
  - Assessment of wear resistance, strength, toughness

SCC Susceptibility of High Strength Low Alloy Steels in CO_2-Containing Corrosive Oil and Gas Wells Environments

CSM: **Arshad Bajvani Gavanluei**
Brajendra Mishra & David L. Olson

1st Annual PI Partner Schools Research Workshop
The Petroleum Institute, Abu Dhabi, U.A.E.
January 6-7, 2010

PI Partners

PI Sponsors

Presentation Outline

- Background
- Objectives
- Experimental Setup
- Results and Discussions
- Project Status
- Conclusions and Summary

Background

- Bare steel corrosion rate, R is:

$$logR = 7.96 - \frac{2320}{T + 273} - \frac{5.55T}{1000} + 0.67logp_{CO_2}$$

[C. Dewaard and D.E. Milliams 1975]

- With a quick calculation of corrosion rate

At T= 65°C, and P_{CO2} =10 atm, R=25mm/yr,

At T=82°C, andP_{CO2} =160 atm, R=250mm/y

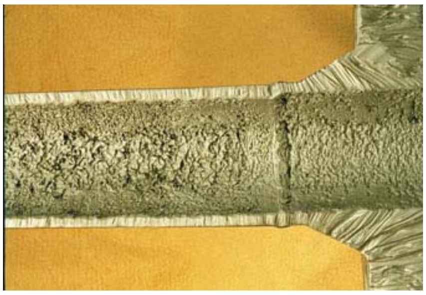

In practice, buildup of corrosion product scale on the surface take place, and

Passivating effect of scales decreases corrosion rate, R, significantly

$Fe^{2+}+ CO_2^{2-} \rightarrow FeCO_{3\ (s)}\downarrow$

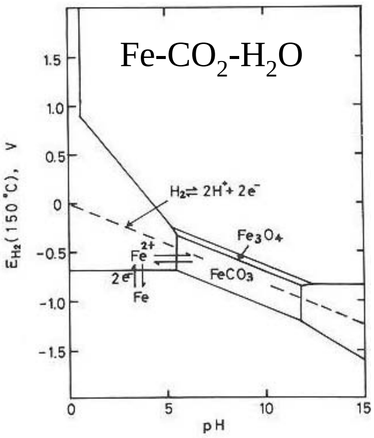

Project Objectives

Establish an analytical expression for CO_2 –SCC Corrosion Prediction of Downhole Materials

- Determine the SCC susceptibility behavior based on our matrix of experiments determine the activation energy of the environmental enhanced fracture mechanism
- Perform weight loss experiments inside the autoclave to obtain corrosion rate at higher temperature and pressure (determine the find the corrosion rate and nature of the corrosion products)
- Perform electrochemical study of these material (to achieve insight of the atomic processes at corroding interface)
- To analyze these interdisciplinary results to offer a better insight into the selection of the downhole materials

Experimental Setup

Slow Strain Rate Test

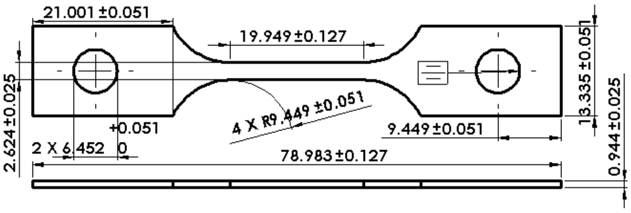

Autoclave Isothermal Test

Slow strain rate test by changing variables :

- Temperature
- Partial pressure of CO_2
- Yield Strength of steel

Results and Discussions

Plastic strain to failure

$$E_P R(\%) = \frac{E_{PE}}{E_{PA}} \times 100$$

Some of the broken SSRT specimens at different temperatures

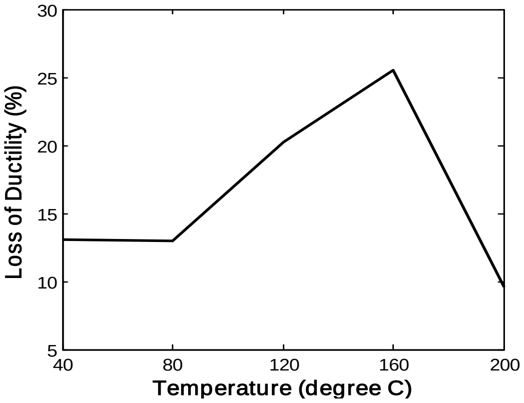

Loss of ductility of S-135 drill pipe steel at different Temperatures and CO_2 saturated solution

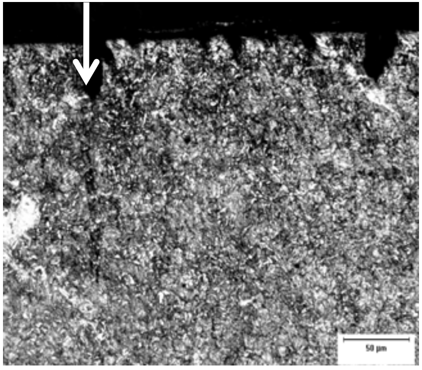

SEM of CO_2 corrosion and SCC damage at 160 ˚C

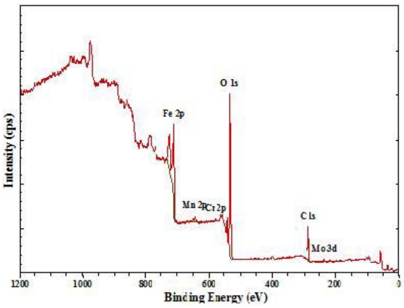

XPS of surface layer of the steel tested at 120 °C.

Interdisciplinary results achieving a basic ability to predict CO_2–SCC corrosion of downhole materials

Project Status

- Continuing the SCC susceptibility measurements based on our matrix of experiments (attempts to obtain activation energy of fracture)
- Weight loss experiments inside the autoclave to obtain corrosion rate at higher temperature and pressure (attempts to find the corrosion rate and nature of the corrosion products)
- Electrochemical study including impedance measurements of these material

---

Conclusions and Summary

- **Interdisciplinary results achieving a basic ability to predict CO_2–SCC corrosion of downhole materials are being obtained**
- **Experimental and analytical practice to achieve a quantitative understanding rate controlling mechanism of CO_2 – SCC.**
- **Results will achieve a rate expression which will allow comparison and selection of downhole materials.**

Investigation of Microbiologically Influenced Corrosion (MIC) in Ethanol Fuel Environments

CSM: David L. Olson, Brajendra Mishra, John R. Spear,
Shaily Bhola, Luke Jain, Chase Williamson

1st Annual PI Partner Schools Research Workshop
The Petroleum Institute, Abu Dhabi, U.A.E.
January 6-7, 2010

PI Partners

PI Sponsors

Presentation Outline

- Background
- Objectives
- Experimental Setup
- Results and Discussions
- Project Status
- Conclusions and Summary

Background

Corroded pipe from an ethanol contact water system

ASTM A36 steel coupon after exposure to a mixture of 1 pct water and 99 pct E10 fuel

The highly corroded portion of the coupon with visible slime was in the aqueous Layer that forms under the organic (gasoline) layer. The less corroded portion of the Coupon remained in the gasoline layer.

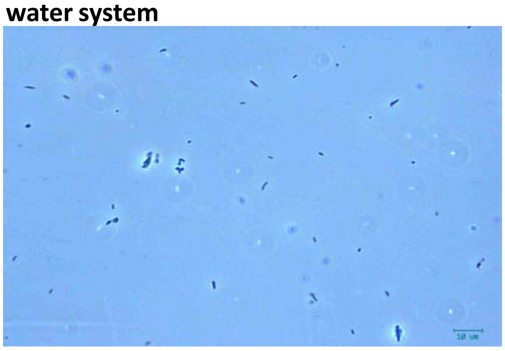

Light micrograph of ethanol contact water tank bottoms indicating the presence of microbes

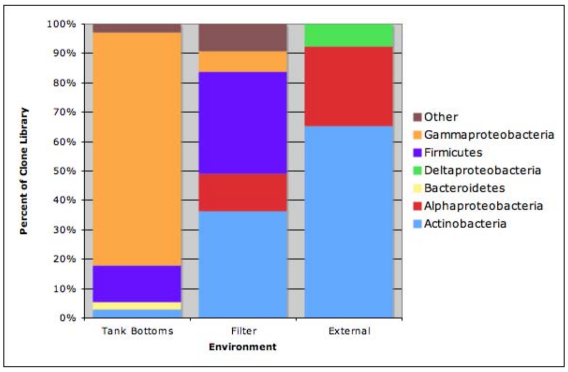

Source of microbes

Project Objectives

- Determine whether microorganisms can exist in ethanol and ethanol gasoline mixtures
- Determine the type of microbes
- Determining the electrochemical nature to ethanol water corrosion of linepipe steel
- Determine whether microbiological corrosion can assist ethanol cracking of linepipe steel
- Determine mitigation methods for microbiologically enhanced corrosion and cracking of linepipe steel

Experimental Setup

3-electrode system used

A36 steel U-bend specimen-
W.E.Ag/AgCl/EtOH/LiCl Electrode-
R.E.
(Potential: 0.097 V w.r.t. SHE)
Platinum wire- C.E.

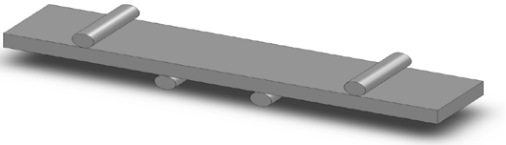

Four point bend fatigue testing arrangement for assessing susceptibility of ethanol cracking

- **DNA**

Fuel grade

ethanol filter

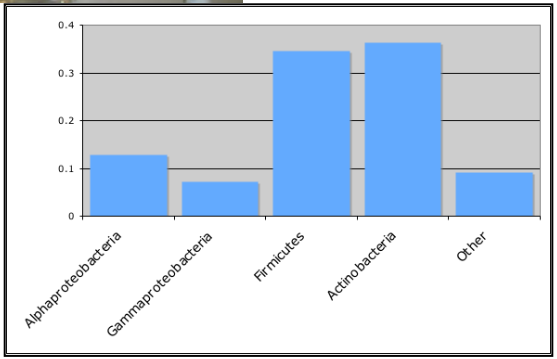

Bacillus	Spore-formers, Mn Oxidation
Actinobacteria	Common in soils, various metabolisms
Gammaproteobacteria	Ethanol metabolism, iron reduction

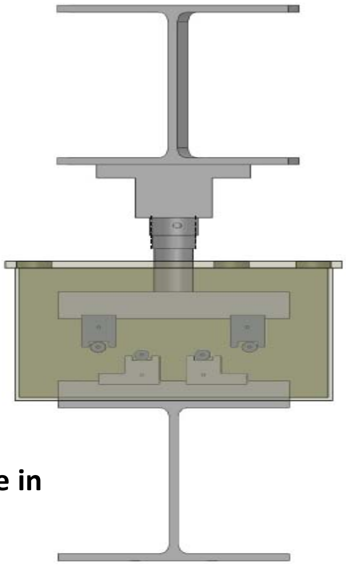

Test frame in fuel tank

Results and Discussions

Steel coupon in water-gasoline environment

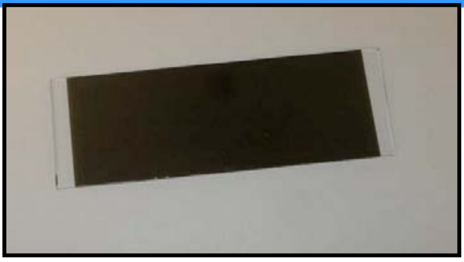

~20 nm layer of iron on a glass microscope slide

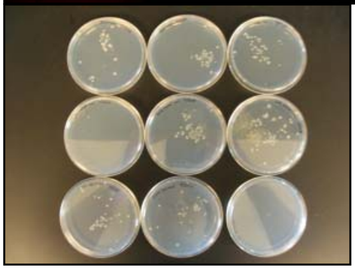

Microbes cultivated after exposure to a range of ethanol fuel blends

Solution	Survival?
E10	Yes
E50	Yes
E85	Yes
E100	Yes
70% Ethanol	Yes
50% Ethanol	Yes
10% Ethanol	Yes

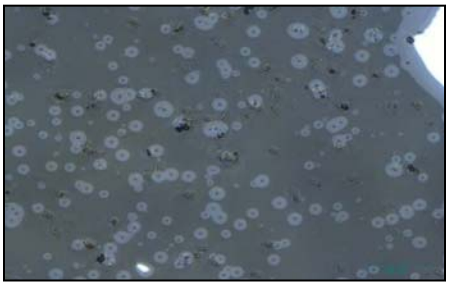

Avrami equations for kinetics

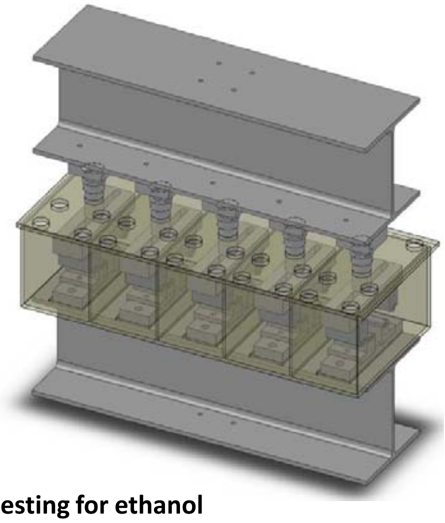

Mechanical testing for ethanol cracking during cyclic loading

Project Status

- Continue the microbiological experiments to characterize the role of microbes on ethanol corrosion and cracking of the linepipe steels.
- Apply advanced analytical tools (DNA, potentiostatic, impedance, microscopic analysis) to offer deeper insight to the nature of microbes in alcohol associated with linepipe steel.
- Perform low frequency fatigue loading on four point bend linepipe steel specimens to assess the susceptibility of ethanol cracking in ethanol-gasoline fuels

Conclusions and Summary

- Microbes can exist in ethanol-gasoline-water mixtures
- Microbes are spore formers and attack iron
- Ethanol related damage is found in the field at the facilities that process ethanol at the beginning (tanks to pipe) and the end (pipe to truck) of pipeline
- Mechanical system to assess the ethanol cracking susceptibility has been built and will soon initiate testing

Understanding the Role of Alternating Current on Corrosion of Pipeline Steels under Sacrificial Anode Cathodic Protection

CSM: Tatiana Reyes, Shaily Bhola
David Olson & Brajendra Mishra
Colorado School of Mines

1st Annual PI Partner Schools Research Workshop
The Petroleum Institute, Abu Dhabi, U.A.E.
January 6-7, 2010

PI Partners

PI Sponsors

Presentation Outline

- Background
- Objectives
- Experimental Setup
- Results and Discussions
- Project Status
- Conclusions and Summary

Background

Asymmetry Model

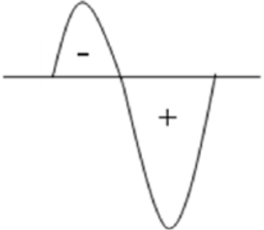

Anodic Asymmetry

More activity in the anodic region :

Pitting

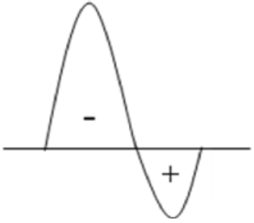

Cathodic Asymetry

More activity in the cathodic region :

Hydrogen charging and cracking

- AC current superimposed produces a bias potential shift not only in the electrode but also in equilibrium lines of Pourbaix diagram:

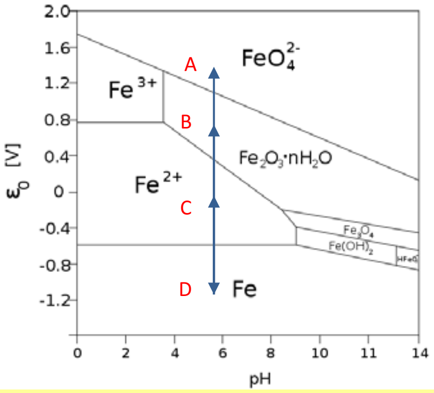

$$dG = -dW_{ext} + VdP - SdT + d\Sigma m_i n_i$$

Under isothermal and isobaric conditions:

$$\Delta G = 0 = -nFE - nF\Delta V_{bias} + RT \ln(\Pi\text{activity of prod} / \Pi\text{activity of react})$$

$$\mathbf{E = E^o - \Delta V_{bias} + (RT/nF) \ln[\Pi\text{activity of prod} / \Pi\text{activity of react}]}$$

Project Objectives

- To achieve an accurate and thorough understanding of the mechanisms and severity of applied AC currents on corrosion of 13Cr supermartensitic stainless steels in sea water.

- To assess the change in susceptibility to localized corrosion with and without AC current.

Experimental Setup

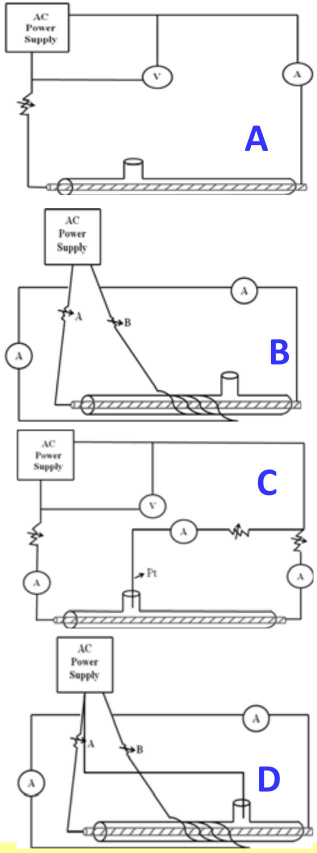

A. AC current in conduction,
B. AC current with induction,
C. AC current through metal (conduction) and through the water (stray current)
D. AC current through water in presence of induction (conduction is optional)

No.	Arrangement (C = conduction, L = induction & W = through water)	Induction current density (i_L) (A/m²)	Conduction current density (i_C) (A/m²)	Current density through water (i_W)(A/m²)	Pitting
1	C, L (done before)	1900	3860	-	Pits in 10 days
2	C	-	40	-	No Pits in 30 days
3	C	-	3860	-	No Pits in 30 days
4	C, L (repeated exactly as 1)	1900	3860	-	No Pits in 30 days
5	C, W	-	2584	478	Pits in 5 hrs.
6	W, L	222	-	42	Pits in 5hrs.
6 and on	W, L	Study of combined effect and different current ratios			In progress

Results and Discussions

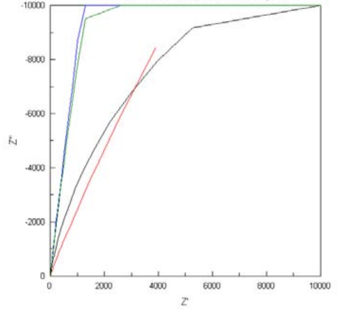

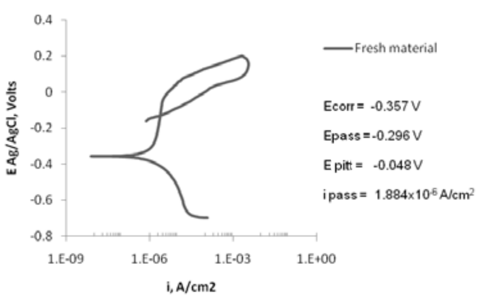

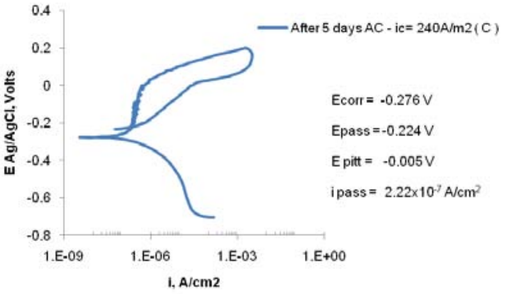

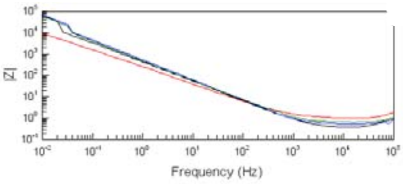

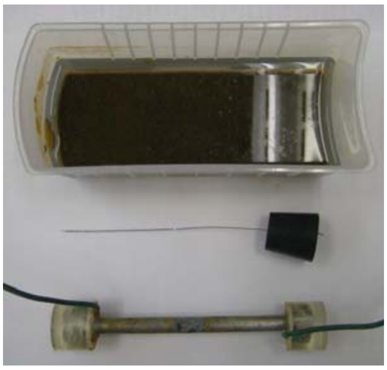

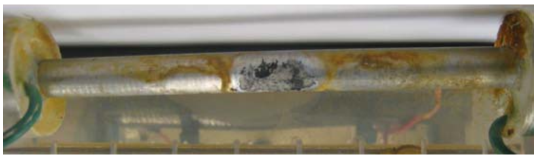

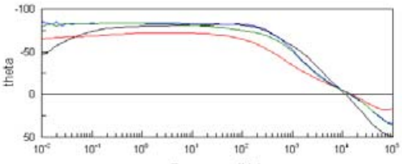

	R_s (ohms)	R_p (ohms cm²)	C_{dl} (F cm^{-2})
Fresh material	0.5248	13,141	3.33x10^{-4}
After 5 days AC - ic= 240A/m² (C)	0.5426	49,809	2.62x10^{-4}
After 5 days AC - ic= 240A/m² (C + L)	0.6842	37,866	2.77x10^{-4}
After 1day AC - iw = 42 A/m² (W + L)	1.161	8137	4.56x10-4

Project Status

- Study of asymmetry corrosion is in progress model with
  - – AC/DC circuit
  - – Wave form function generator
  - – SEM: characterization of surface (pitting)
  - – Leco: hydrogen charging
- Asymmetry model will continue be verified to explain the observed behavior of AC corrosion

Conclusions and Summary

- Evidence of asymmetrical current during AC corrosion has been obtained.
- Thorough characterization of AC corrosion will continue.
- Use of waveform generator to alter the AC current will be used to quantify the observed behavior.
- Electrochemical potentiostatic measurements and impedance spectroscopy will be used to assess the atomic processes at the corroding interface.

Advanced Materials for Industrial Applications

Synthesis and Processing of Functionalized Polyolefins

UMN Team: Marc Hillmyer, Shingo Kobayashi, and Chris Macosko
PI Team: Ahmed Abdala and Sulafudin Vukusic

1st Annual PI Partner Schools Research Workshop
The Petroleum Institute, Abu Dhabi, U.A.E.
January 6-7, 2010

PI Partners

PI Sponsors

Presentation Outline

- Background
- Objectives
- Results and Discussions
- Conclusions and Summary
- Future Plans

Polyethylenes

Polyethylene properties

Excellent	Chemical resistance, Waterproofness, Weatherability, Cost
Good	Plasticity, Flexibility, Impact Strength
Fair	Toughness, Stiffness, Rigidity
Poor	Recyclability, Compatibility, Wettability, Printability, Reactivity

---

Project Objectives

General objective

The goal of our research is to improve the adhesion of polyolefins to other materials (e.g., metals, paints) and render polyolefins compatible with a variety of polar/functionalized dispersants (e.g., graphene)
– adhesion to metal, ceramic , polymer substrates, to paint and inks.

Specific Objectives

Synthesis of model LLDPE materials to study and clarify structure- property relationships

ROMP of functionalized cyclooctenes to incorporate functional groups into model LLDPE

Synthesis of functionalized LLDPEs using ROMP and catalytic hydrogenation to study adhesion and graphene dispersions

Synthesis of LLDPE

Commercial

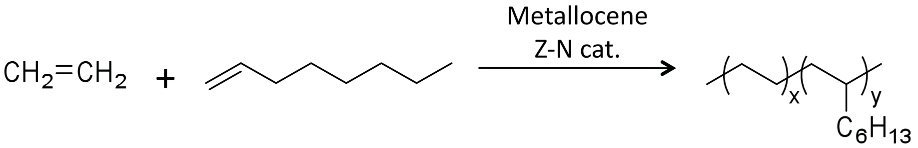

Model synthesis

Anionic polymerization

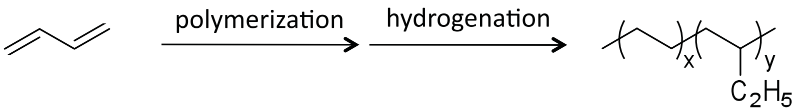

ADMET polymerization

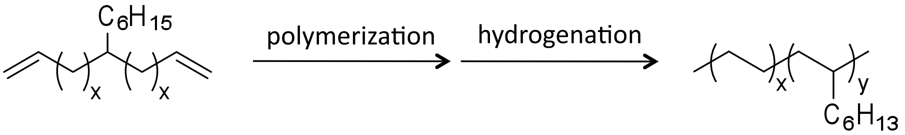

Rojas, G.; Wagener, K. B. *Macromolecules*, **2009**, *42*, 1934–1947.
Sworen, J. C.; Wagener, K. B. *Macromolecules*, **2007**, *40*, 4414–4423.

This Study

Synthesis of C8-LLDPE via Ring-Opening Metathesis Polymerization (ROMP)

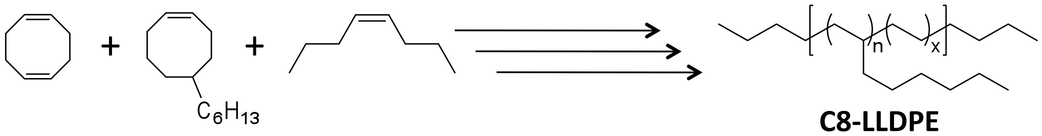

C8-LLDPE

with controls on molecular weight
number of Hex branches

Synthesis of functionalized C8-LLDPE via ROMP

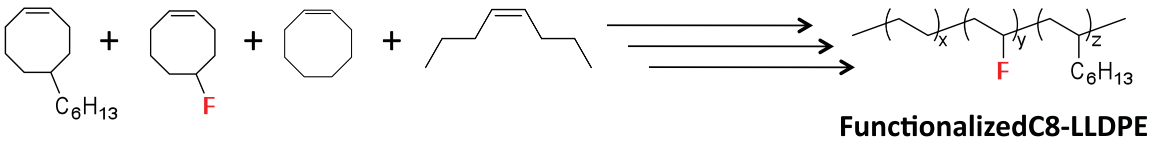

FunctionalizedC8-LLDPE
F= functional groups

with controls on molecular weight
number of functional groups
number of Hex branches

Synthesis of Model C8-LLDPE

Monomer Synthesis

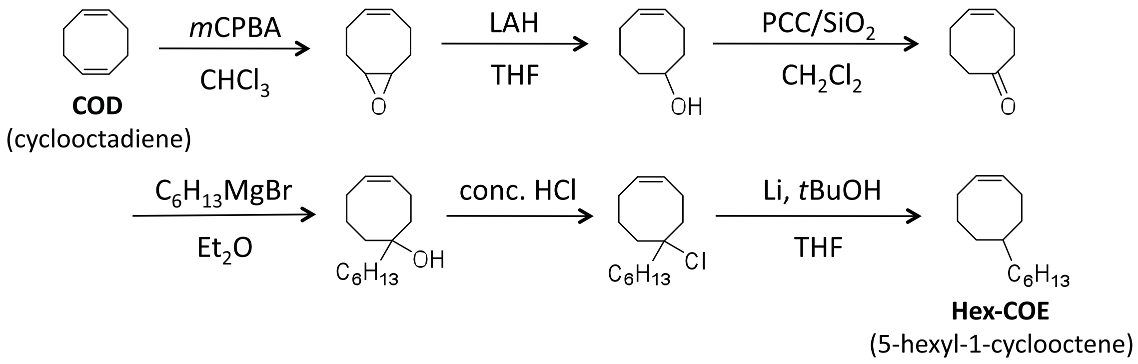

Synthesis of C8-LLDPE

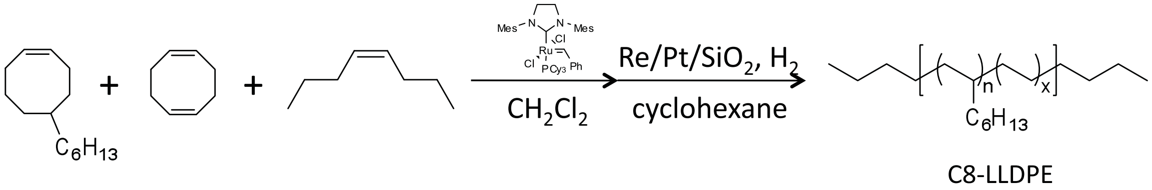

with controls on number of –Hex branches (= density)

molecular weight of the polymer

ROMP of Hex-COE and COD

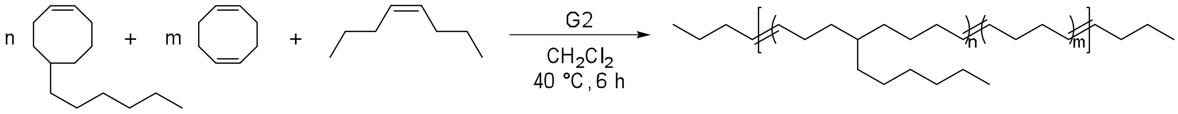

Monomer		*f*		Yield	M_n x 10^{-3}			M_w/M_n
Hex-COE	COD				calcd	GPC	LSGPC	
mol%	mol%	calcd	obsd	%	k	k	k	
100	0	0.761	0.759	92	18.9	11.0	10.7	1.70
32	68	0.152	0.155	94	13.3	10.8	10.2	1.69
16	74	0.073	0.072	86	12.2	11.3	12.5	1.77
8	92	0.039	0.039	87	11.5	15.4	13.7	1.74
4	96	0.023	0.024	89	11.2	15.9	13.1	1.72
2	98	0.015	0.017	90	11.0	17.1	12.0	1.77
1	99	0.011	0.011	94	10.9	19.7	12.5	1.76
0	100	0.007	0.009	93	10.9	18.3	12.5	1.71

M/CTA=100. M/G2=2700-4600. G2/CTA=2.2%-3.6%. Conversion=100% in all cases.

f: The integral area ratio of methyl signal/allyl signal in ^1H NMR spectra.

Hexyl branches were successfully incorporated into the polymer with control.

^{13}C NMR Spectrum of C8-LLDPE

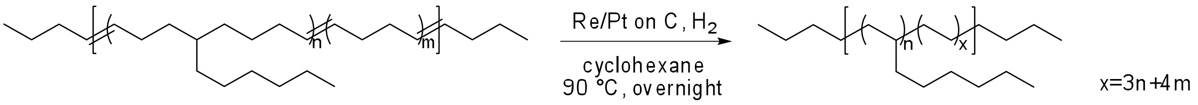

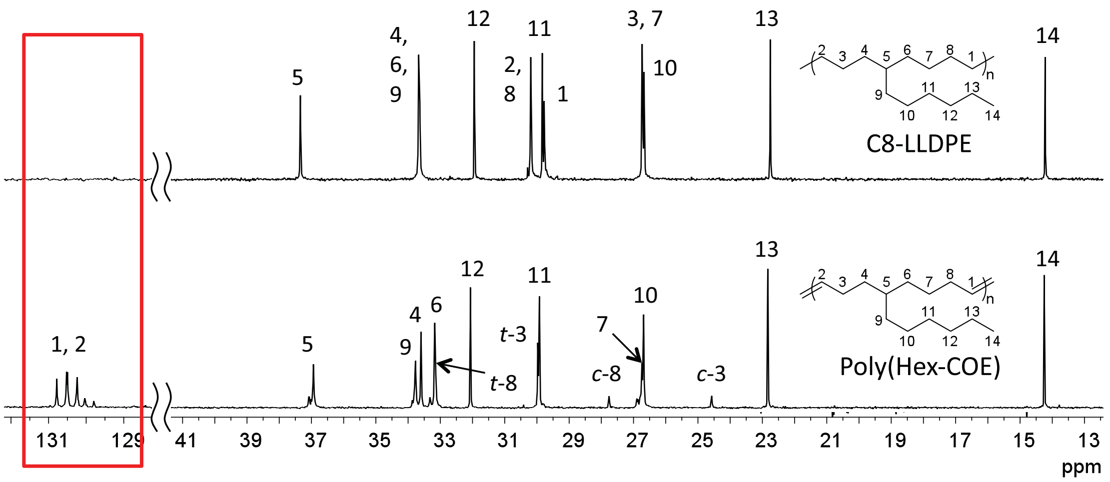

C8-LLDPE was obtained via ROMP of Hex-COE, followed by hydrogenation.

Physical Properties of C8-LLDPE

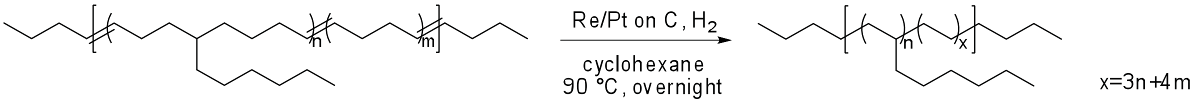

content of Hex-COE	hexyl branches per 1000 backbone carbons	$M_n \times 10^{-3}$	M_w/M_n	T_m °C	Δh_m J/g	T_c °C	Δh_c J/g	density g/cm^3
100	125.0	10.7	1.83	-	-	-	-	-
32	40.0	10.2	2.20	80.6	57	68.1	62	0.888
16	20.0	10.3	2.11	104.4	104	95.4	101	0.917
8	10.0	10.3	2.69	114.1	151	105.1	155	0.936
4	5.0	12.2	2.44	121.8	169	111.0	178	0.949
2	2.5	12.4	2.64	125.2	170	114.2	176	0.958
1	1.3	13.6	2.74	127.1	212	114.7	217	0.962
0	0.0	13.8	2.60	129.7	240	117.6	245	0.968

Thermal properties and density were tunable by changing the content of Hex-COE.

Physical Properties of Model C8-LLDPE

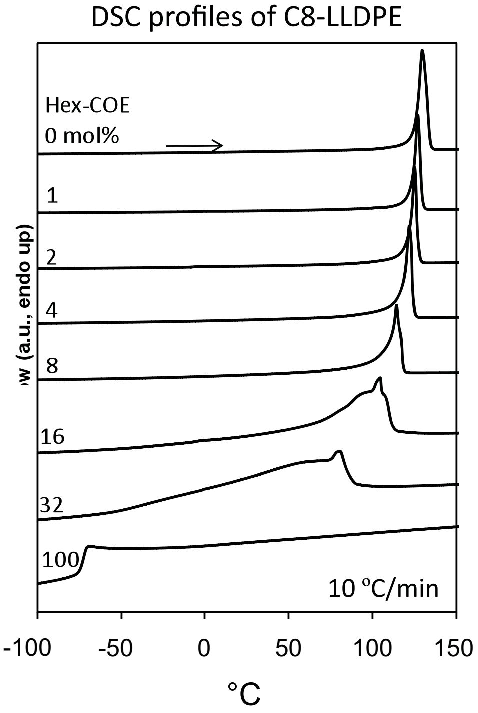

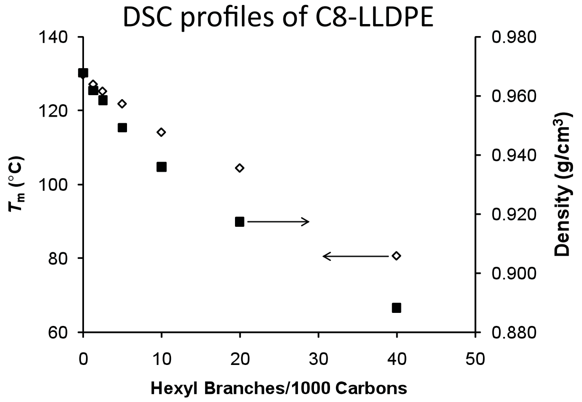

Melting temperature and density are tunable by changing the feed molar ratio of monomers.

⇩

Model C8-LLDPE was successfully synthesized by ROMP of Hex-COE and COE, followed by hydrogenation of polymer backbone.

Synthesis of Functionalized C8-LLDPE

Synthesis of functionalized C8-LLDPE using ROM copolymerization

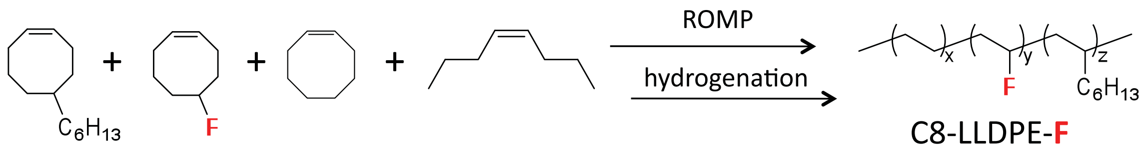

with controls on number of functional groups
number of hexyl branches
molecular weight of the polymer

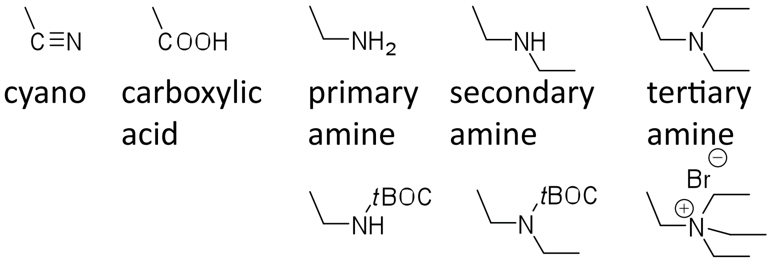

Functional groups (**F**)

cyano

carboxylic acid

primary amine

secondary amine

tertiary amine

Synthesis of Functionalized Cyclooctenes

Monomer Synthesis

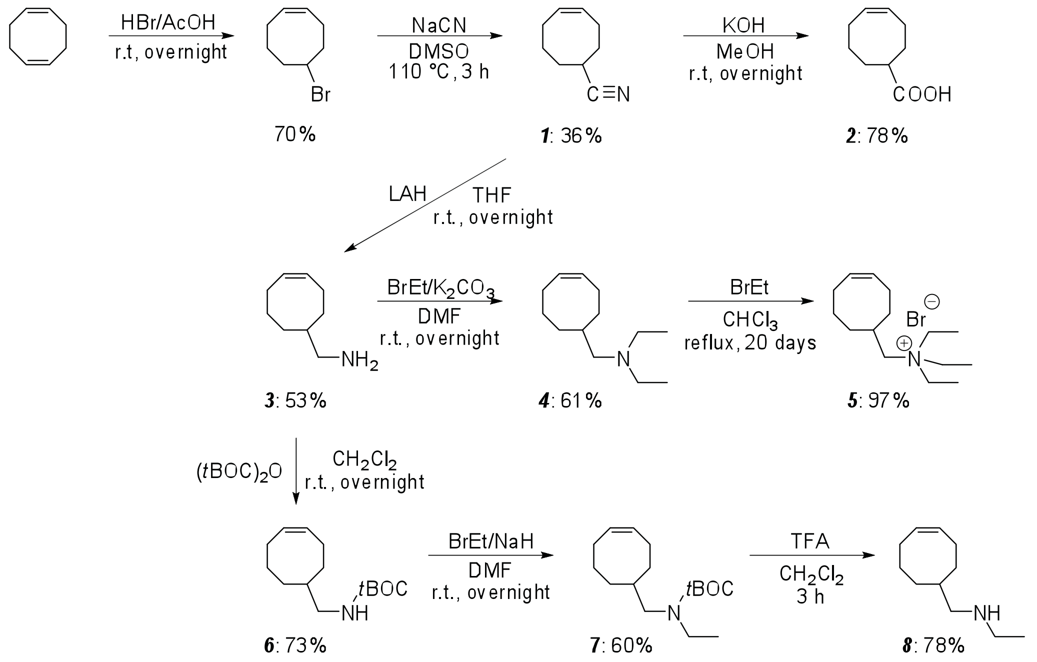

ROMP of COE, Hex-COE, and Functionalized COE

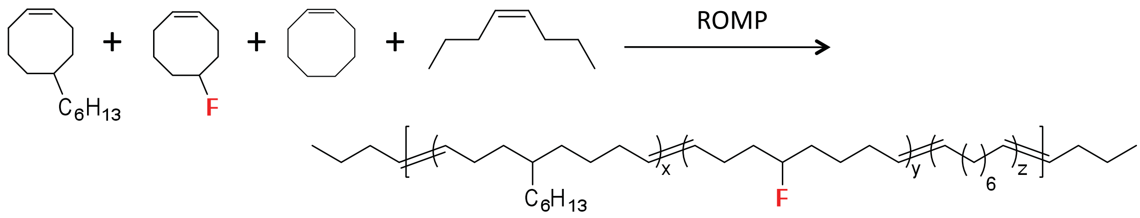

F	M/(CTA+cat)	COE	F-COE		Hex-COE		conv.	Yield	M_n		M_w/M_n
			feed	NMR	feed	NMR			calc	GPC	
		mol%	mol%	mol%	mol%	mol%		%	k	k	
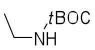	526	69.8	1.0	0.69	29.2	27.3	>99	92	70.8	36.1	1.63
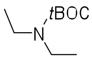	526	69.8	1.0	0.81	29.2	27.2	>99	92	71.0	34.7	1.58
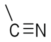	525	69.8	1.0	1.0	29.2	28.5	>99	91	70.2	32.6	1.60
none	527	69.8	0.0	0.0	29.2	29.7	>99	93	70.3	35.8	1.61

Hexyl branches and functional group are successfully incorporated.

Hydrogenation of Polymer Backbone

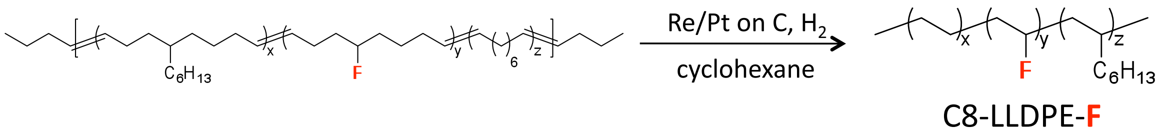

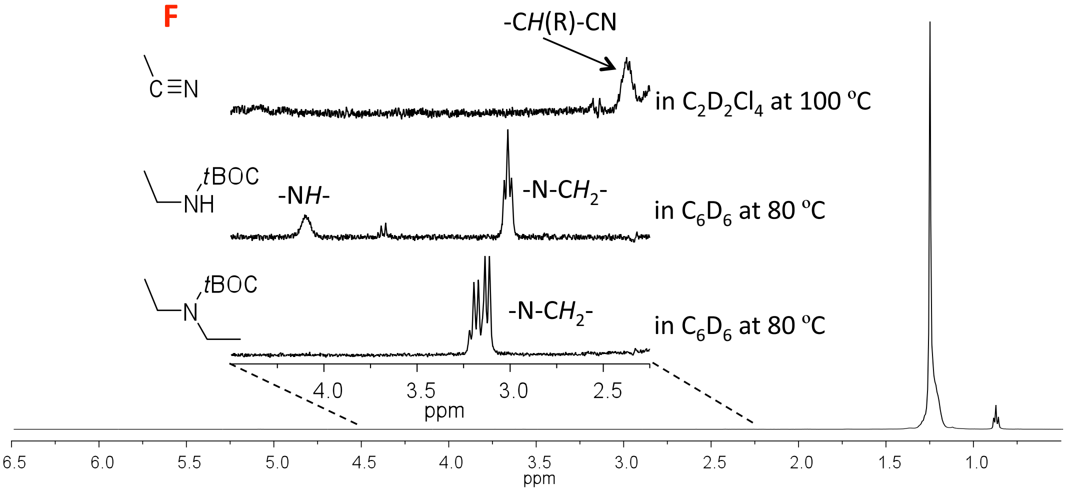

Polymer backbone was hydrogenated without decomposition of functional groups.

Deprotection of *t*BOC

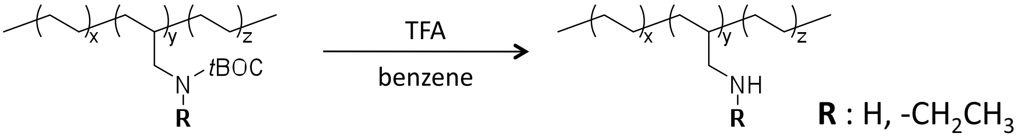

R : H, $-CH_2CH_3$

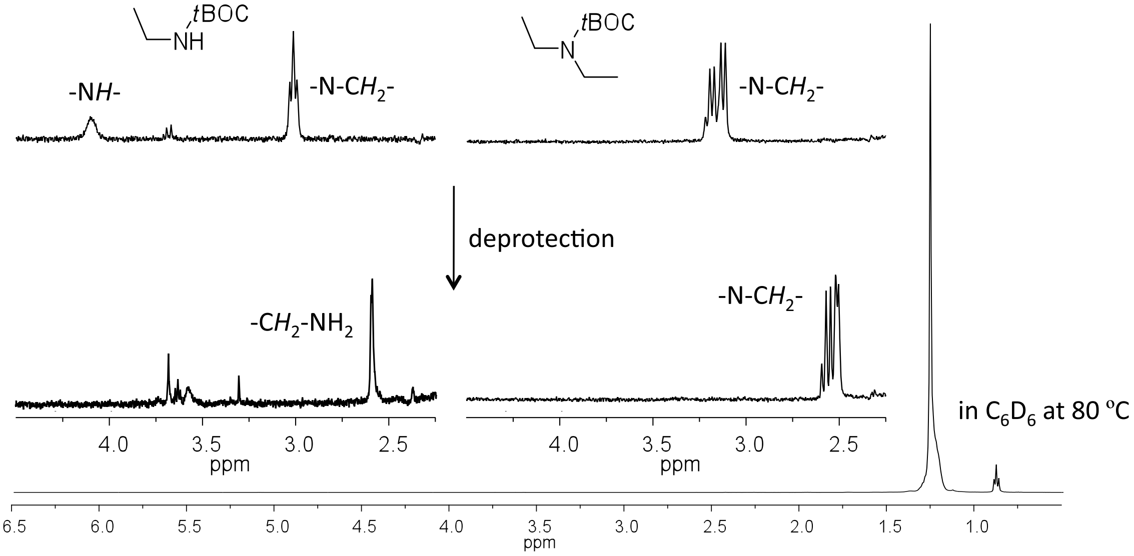

*t*BOC protected groups were successfully converted into primary and secondary amines.

Conclusions and Summary

Synthesis of C8-LLDPE

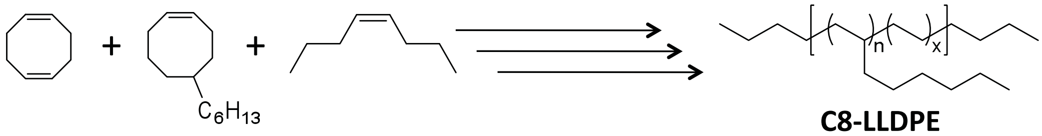

C8-LLDPE

with controls on molecular weight
number of Hex branches

Synthesis of functionalized C8-LLDPE

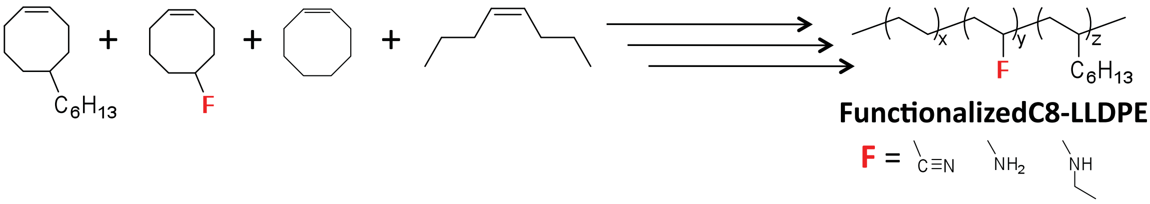

FunctionalizedC8-LLDPE

with controls on molecular weight
number of functional groups
number of hexyl branches

Future Plans

Synthesis of C8-LLDPE-F

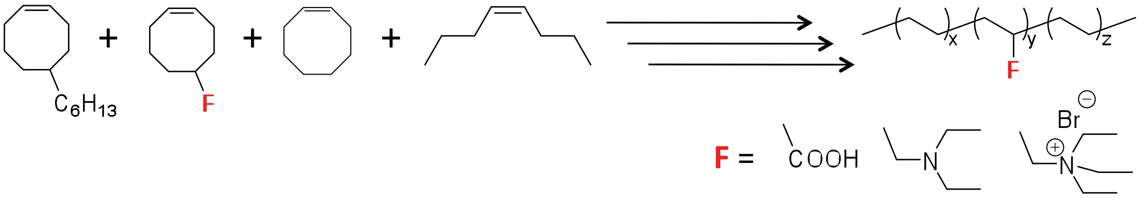

Solvent blending of C8-LLDPE-F/FGS

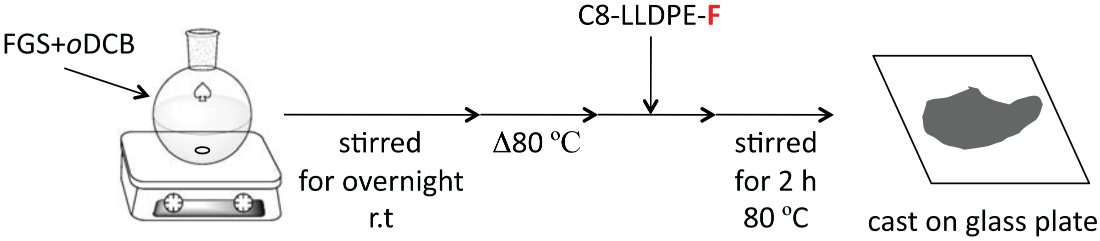

Characterization of C8-LLDPE-F/FGS blended films
mechanical properties, thermal properties, FGS dispersion, etc.

Graphene Reinforced Polyolefin Nanocomposites

UMN Team: Hyunwoo Kim, Kirby Liao, Frank Bates
and Chris Macosko
PI Team: Ahmed Abdala

1st Annual PI Partner Schools Research Workshop
The Petroleum Institute, Abu Dhabi, U.A.E.
January 6-7, 2010

PI Partners

PI Sponsors

Background

- Polyethylene (PE) is the largest commodity polymer
  - Global demand*
    - 65.4 million tons/year (2008)
    - 104 million tons/year (2020)
- Borouge is the one of the leading Polyethylene producers
  - 0.6 million tons/year (current)
  - 1.1 million tons/year (2010)
  - 4.5 million tons/year of combined PE and PP (2014)

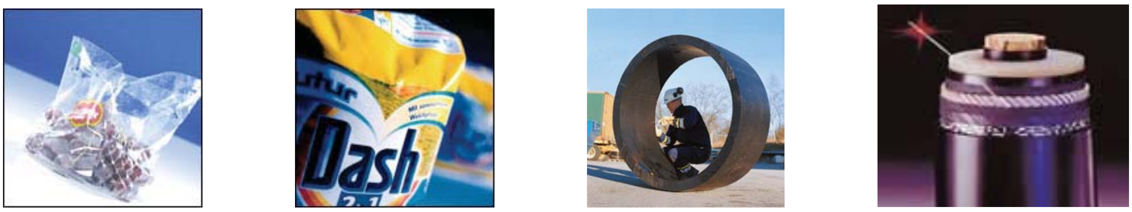

Project Objectives and Approach

- Objective
  - Production of electrically conductive PE with improved mechanical properties
- Approach
  - Reinforcing PE with electrically conductive filler (Functionalized Graphene Sheets) using different dispersion processes

---

Applications of Electrically Conductive PE

- Semiconductor layers for high-voltage cables
- Electrostatic dissipation (ESD) material
- Electromagnetic shielding
- Automotive parts

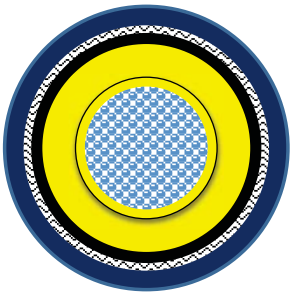

■ HDPE
▨ Corrugated metal
🟨 Semiconductor
■ Insulator
▦ Conductor

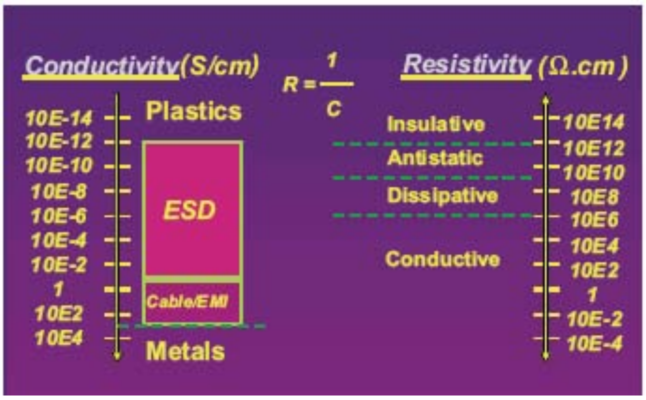

Challenges

- Dispersing fillers into hydrophobic PE is more challenging than mixing other (polar) polymers
- PE is a semicrystalline polymer
  - Crystallinity could be affected by the filler
    - Fillers may act as nucleating agent
- PE is very chemically resistant and therefore few solvents are available for solution mixing

Rewards

- Mixing of PE with graphene sheets can lead to:
  - Increase the electrical conductivity
  - Increased stiffness
  - Decrease the coefficient of thermal expansion
  - Reduce gas/water permeability
  - Reduce UV degradation

Graphene

- A 2-D honeycomb lattice of carbon
- The "Mother" of all carbon based materials
- The basic building block of carbon based materials

Graphene Properties	
Modulus, GPa	10^3
Strength, MPa	$140\text{x}10^3$
Electrical Conductivity, S/cm	10^4
Thermal Conductivity, W/m.°K	3000

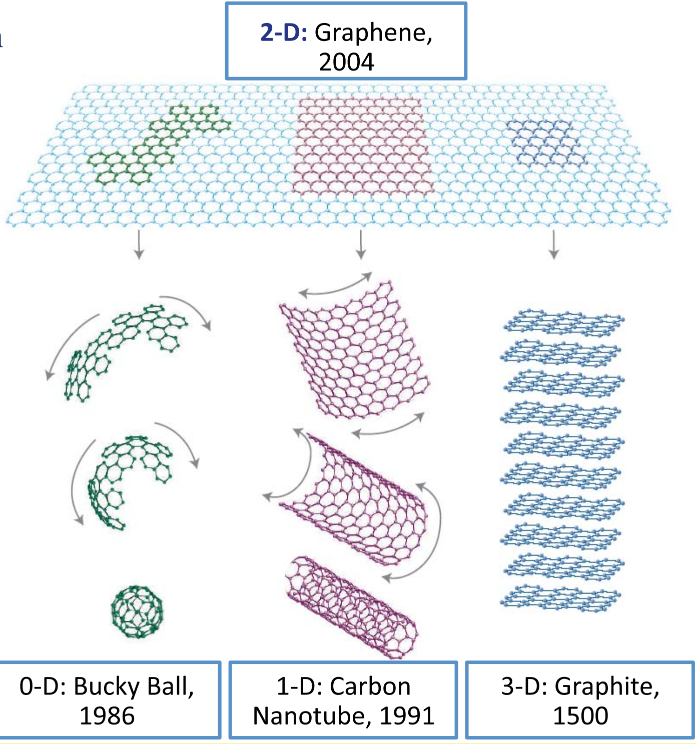

2-D: Graphene, 2004

0-D: Bucky Ball, 1986

1-D: Carbon Nanotube, 1991

3-D: Graphite, 1500

Geim, A. K. and Novoselov, K. S. (2007). *Nature Materials* **6** (3): 183-191

Graphene Production

- 2004: Manchester University[1]
  - Mechanical cleavage of graphene sheets from synthetic graphite
- 2006: Northwestern University[2]
  - Solution based exfoliation of graphite oxides treated with organic isocyanate
- 2006: Princeton University[3]
  - "Mass" production of functionalized graphene sheets (FGS) based on thermal exfoliation of graphite oxide
- 2008- 2009: Other methods
  - CVD, spatial growth of SiC, electrolytic, supercritical fluid, liquid phase exfoliation

1. Novoselov, *et. al.*, *Science*, 306, 666–669 (2004)
2. Stankovich *et. al.*, Nature, *442, 282–286 (2006)*
3. Schniepp *et. al.*, *Chemistry of Materials*, 19(18), 4396-4404 (2007)

Production of Functionalized Graphene Sheets (FGS)

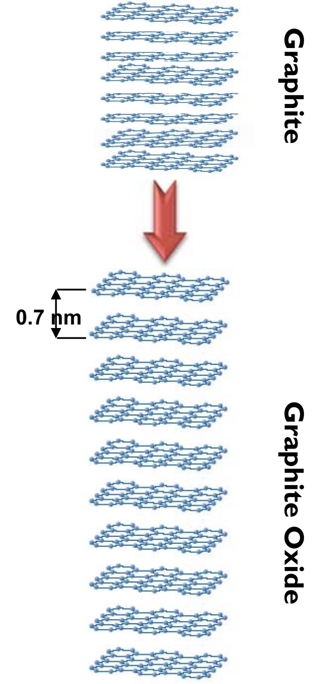

- Solution based oxidation
  - Mixture of concentrated H_2SO_4 and HNO_3
  - Oxidizing agent such as $KClO_3$, $KMNO_4$, etc…
- Oxidation leads to:
  - Expansion of the spacing between the graphene sheets
    - ~ 2-fold volume increase
  - Smaller “flake” size
- Chemical composition
  - 60% C, 2% H, 38% O (by weight)
- Molecular Formula
  - $C_8O_{3.8}H_3$

FGS Production: Thermal Exfoliation

- Rapid heating (2000°C/min) under inert gas
- Large volume expansion 100-300 times
- Complete loss of the layered structured
- Surface area ~ 1000 m^2/g
- Composition
  - 77.6% C, 21.6% O, 0.8% H
  - Molecular formula: $C_8O_{1.7}H$

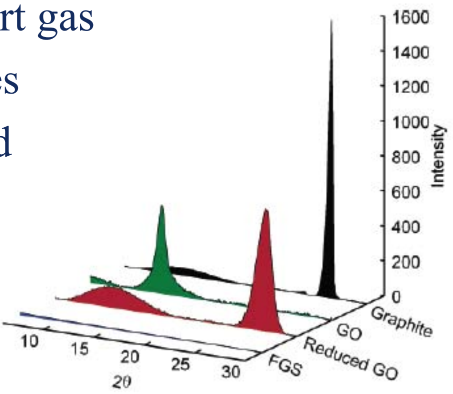

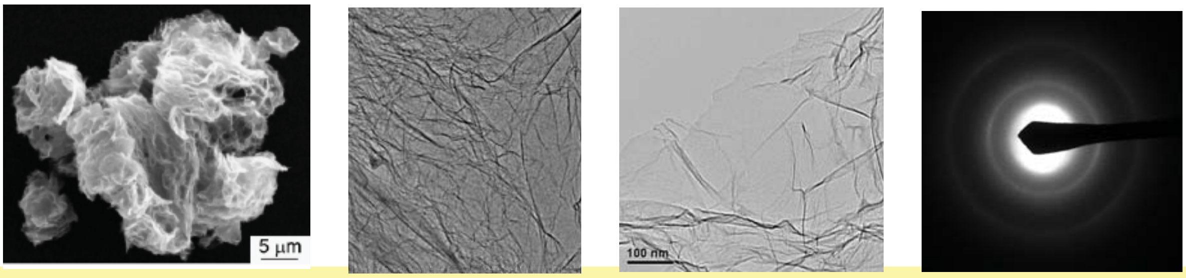

Composite Properties versus Processing Conditions for Polyurethane Composite

- Thermoplastic polyurethane composites

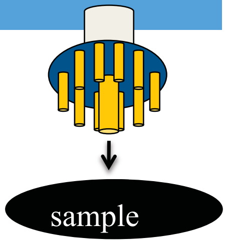

Solvent Blending

- Stirring in dimethylformamide
- Film casting at 50 °C

In-situ Polymerization

- Solution polymerization in DMF
- Surface functionalization by TPU

Melt Blending

- DACA Micro Compounder
- 180 °C, 6 min, 360 rpm

Electrical Conductivity

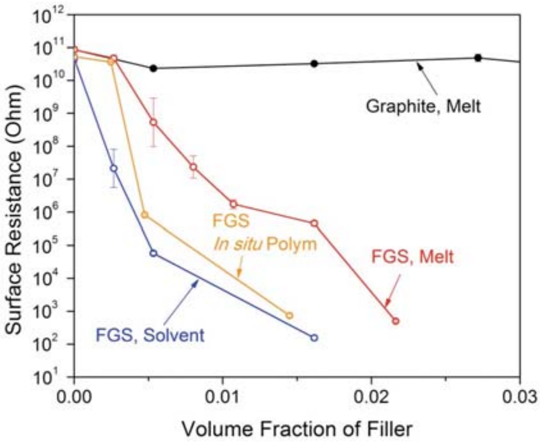

FGS:
solvent blend > in-situ polymerization > melt blend

Dispersion of FGS in PEN

- Poly(ethylene-2,6-naphthalate) (PEN) composites

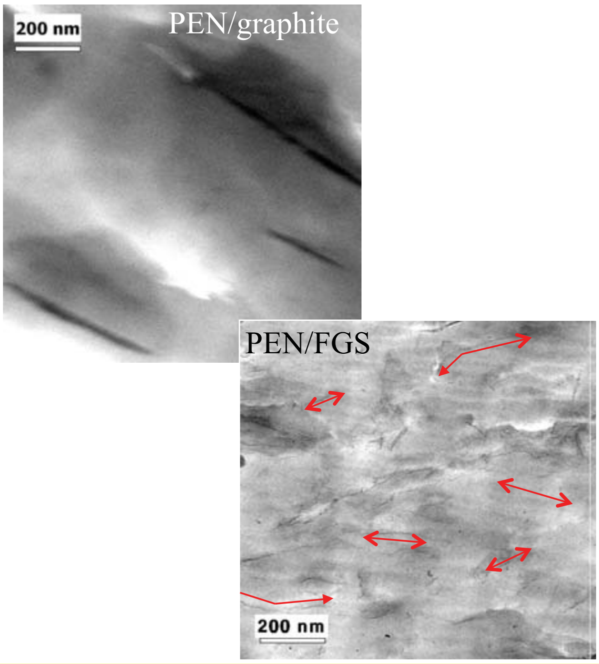

Size distribution from TEM

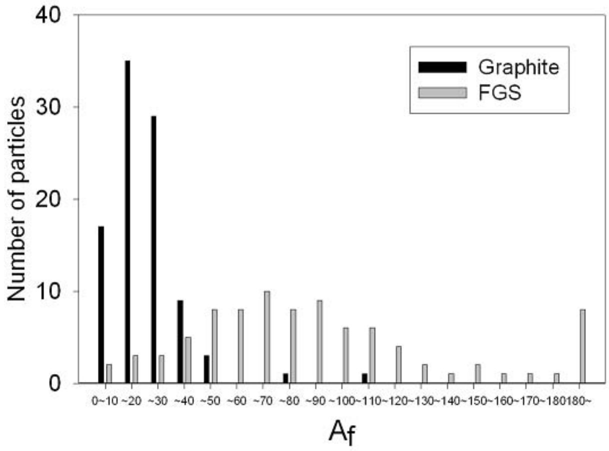

Average A_f of graphite: 21
FGS : 88

Experimental Setup: Blending Methods

Matrix: LLDPE, Dow Affinity EG-8200 (Mw = 201k, Mn = 67k) and EG-8200-MA (PE-f-0.8 wt% MA)

Melt blending

- DACA Micro Compounder
  : 180 °C, 8 min, 200 rpm

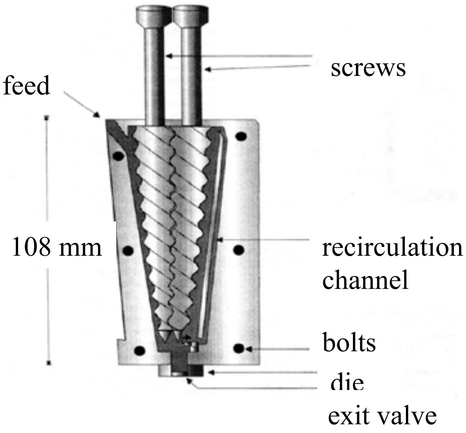

Solvent blending

- Toluene (reflux) at 110 °C
  or 1,2-dichlorobenzene (DCB) at 70-80 °C
- Cast films on heated glass plate

Dispersion of FGS: Melt Blending

TEM

1 wt% FGS EG8200
Melt blend

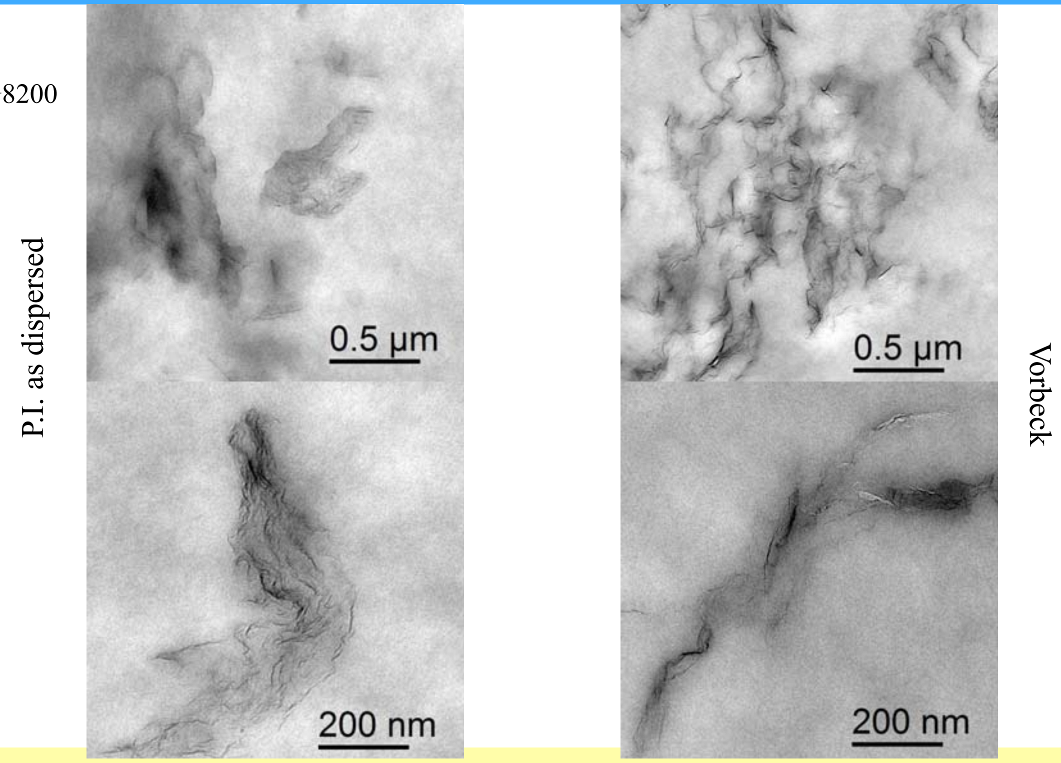

Rheology of Melt Blended Composite

Melt rheology at 200 °C

- Melt blended EG-8200/FGS P.I. (as densified)

Strain sweep

- Non-linearity sets in at smaller strain

Frequency sweep

- φ_{perc} between 2 and 3 wt.%
- $A_f = 40 \sim 50$

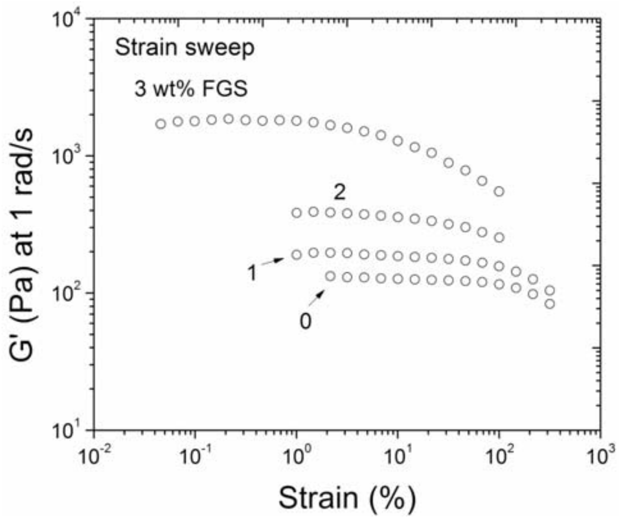

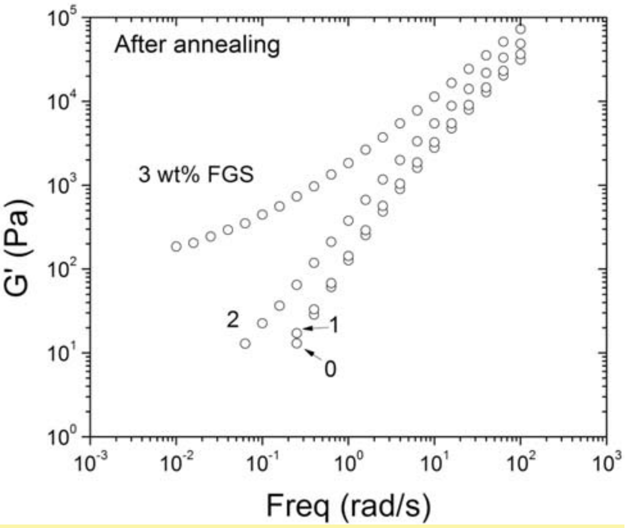

Electrical Conductivity of Melt Blended Composite

- DC surface resistance measurements with PRS-801, Prostat
- Melt blend FGS/EG-8200

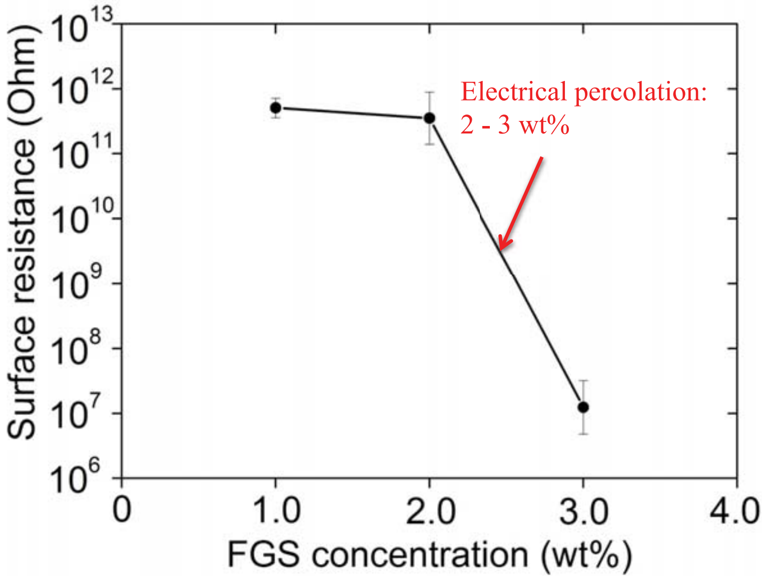

Electrical percolation: 2 - 3 wt%

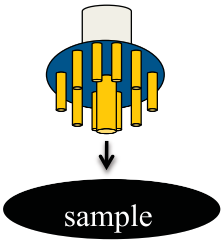

LLDPE-FGS: Mechanical Properties

- FGS loading
  - 1.0, 1.5, 2.0, 3.0 wt.%
- Ultimate strength and toughness with Minmat tensile tester
- Modulus measured using DMA (RSA1)
  - 4 specimens per sample

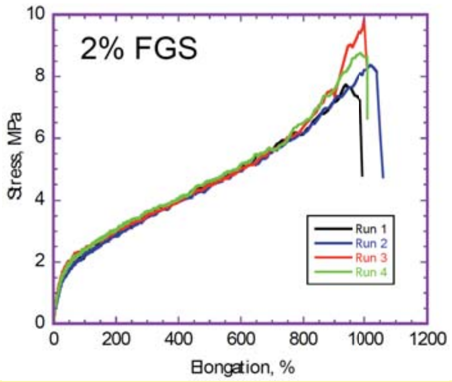

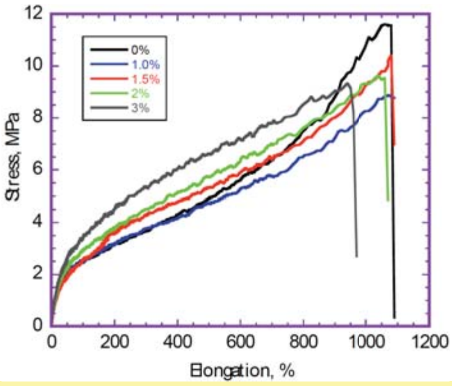

FGS-LDPE: Mechanical Properties

- With FGS loading
  - Modulus increases
  - Ultimate stress decreases
  - No significant change in toughness

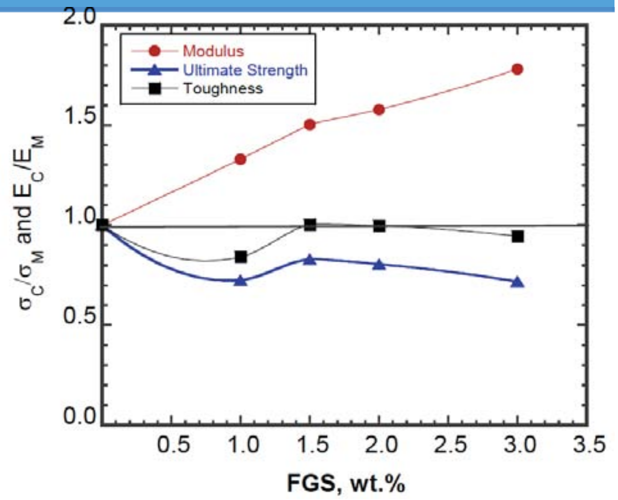

Properties of Neat LLPE	
Modulus, MPa	6.40
Ultimate Strength, MPa	11.4 ± 1.7
Toughness, J/mm^3	60.3 ± 7.5

FGS-LLDPE: Functionalized PE

- LLDPE functionalized with 0.8% maleic anhydride
- Moderate modulus increase (25%)
- Increased ultimate strength (31%)
- 98% Increase in toughness

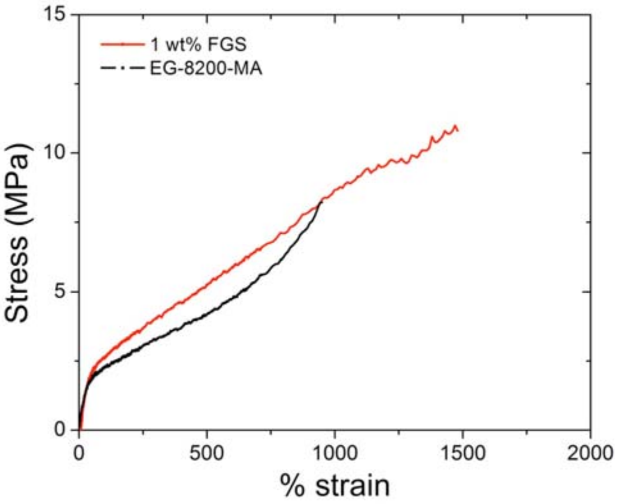

- ***Samples remain non-conductive with 1% FGS***

Barrier Properties

Sample	He Permeation in Barrer
LDPE	19.0
1 wt% FGS LDPE	20.7
1 wt% FGS -LDPE-MA	20.2

1 wt% FGS LDPE

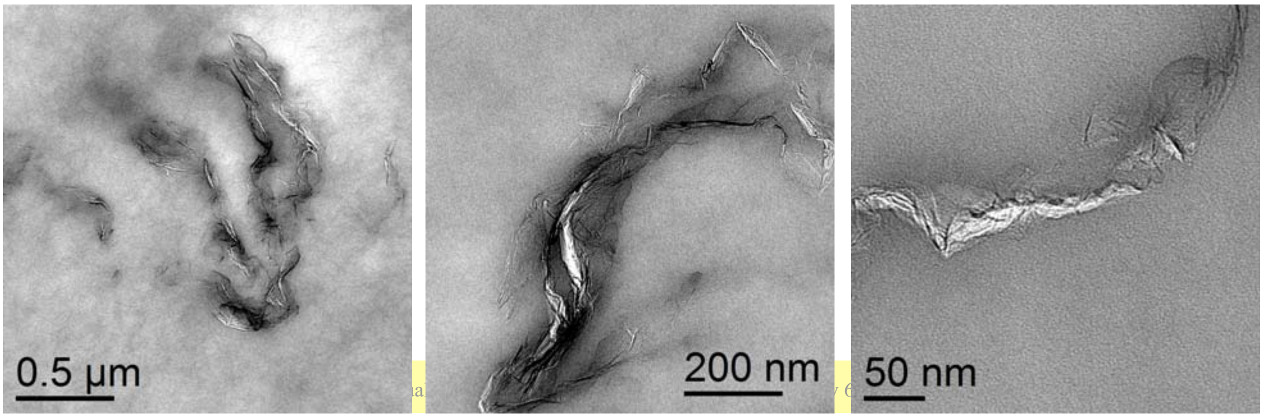

Solution Blended Composite

- Modulus
  - – 100% increase with 1% FGS and DCB as solvent
  - – 80% increase with 1% FGS with toluene as solvent
- Electrical Conductivity
  - – Percolation threshold for conductivity < 1%
  - – Resistance 10^{-4} ohm.cm compared to 10^{-12} for LLDPE

Conclusions and Summary

- LLPE-FGS composites were prepared via melt and solution Belding
- Impact of FGS addition to LLPE
  - Rheological percolation at 2-3 wt% (melt blended)
  - Conductivity percolation at 2-3 (melt) or 1 wt% (solution blended)
  - Moderate (melt) to good (solvent) enhancement in tensile modulus
  - Good ultimate strength and toughness retained after FGS addition
- Functionalization of polyolefin can improved graphene dispersion
  - Toughness of PE-MA doubled after FGS dispersion

Project Status

- Progress
  - Results presented at the AICHE Annual Meeting, Nov 2009
  - 2 publications underway:
    - Review paper on graphene/polymer nanocomposites
    - Graphene reinforced polyethylene
- Interaction
  - Weekly conference call
  - Visits:
    - UMN: Macosko (Feb 09), Kim (Jan 10)
    - PI: Abdala (Jul and Nov 09), Adnan (Jul 09)

Polymeric Membranes for Advanced Process Engineering

UMN Team: Frank Bates, Ed Cussler, Yuanyan Gu, Brian Habersberger,
Marc Hillmyer, Timothy Lodge, and Ligeng Yin
PI Team: Ahmed Abdala, Ioannis Economou, Sulafudin Vukusic

1st Annual PI Partner Schools Research Workshop
The Petroleum Institute, Abu Dhabi, U.A.E.
January 6-7, 2010

PI Partners

PI Sponsors

Presentation Outline

- Vision
- Project 1: Ionic liquid membranes
- Project 2: Nanoporous polymeric membranes
- Conclusions and Summary

Vision

- We aim to design, prepare and develop next generation gas and liquid separation membranes through precision macromolecular engineering
- Main application targets
  - Water purification
  - Gas separations (emphasis on CO_2/CH_4)
  - Polymer electrolytes for fuel cells

Background: Ionic Liquids

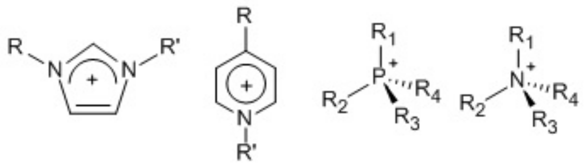

Large radii and asymmetric shapes

PF_6^-, BF_4^-, NO_3^-, Br^-, $[(CF_3SO_2)_2N]^-$

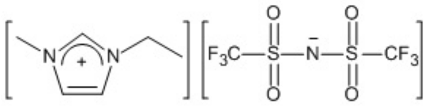

[EMIM][TFSI]

Unique combinations of properties:
- *Negligible vapor pressure*
- *Exceptional chemical & thermal stability*
- *Selective gas solubility*
- *Tunable solvation properties*
- *High ionic conductivity*
- *Wide electrochemical windows*

Applications:
- *Synthesis and catalysis*
- *Gas separation*
- *Electrochemical devices*

Polymer Membranes for Gas Separation

Robeson Plot

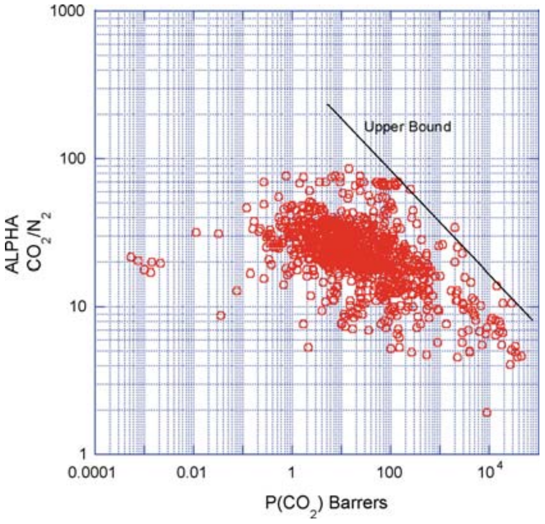

L. M. Robeson, *J. Membr. Sci.* (2008) 320, 390

- Polymer membranes represent an inexpensive, low energy route to gas separation;
- Almost all systems exhibit the "Robeson Upper Bound": a trade-off of selectivity vs. flux;
- Ionic liquids show excellent selectivity in terms of solubility and high diffusivity;
  - Bara, et al., *Ind. Eng. Chem. Res.* (2009) 48, 2739
- Ionic liquids might overcome "real" vs "ideal" selectivity bottleneck and lack the necessary mechanical integrity

$$P = SD$$

$$\alpha_{ij} = \frac{P_i}{P_j} = \frac{S_i}{S_j} \times \frac{D_i}{D_j}$$

Polymeric Ionic Liquid Materials

Ion gels: polymer networks swollen with ionic liquids

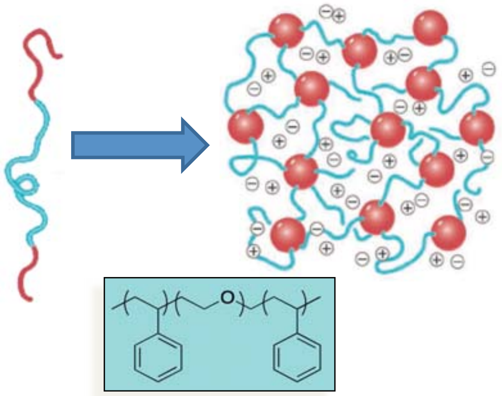

- Low polymer fraction: 5-10%
- Large mesh size: 10-100 nm
- Tunable mechanical properties

He, et al., *J. Phys. Chem. B* (2007) 111, 4645
He and Lodge, *Chem. Commun.* (2007), 2732

Polymerized ionic liquids: synthesized by polymerization of ionic liquid monomers

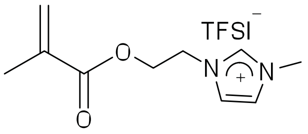

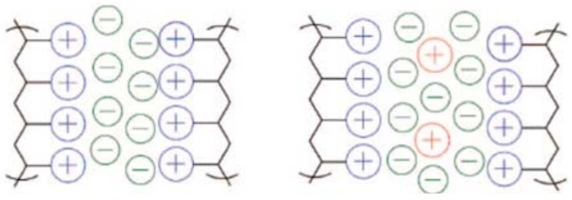

- Strong interaction between immobilized cations and free anions
- Membrane robustness to sustain higher pressure drop

Project Objectives

- Develop controlled polymerization routes to polymerized ionic liquids (PILs) and PIL-containing block copolymers
- Compare gas separation performance of ion gels, polymerized ionic liquids, and PIL-ion gels
- Optimize system performance for CO_2 based separations
- Extend to other systems such as alkanes/olefins via ionic doping

Recent Experimental Progress: PIL by RAFT

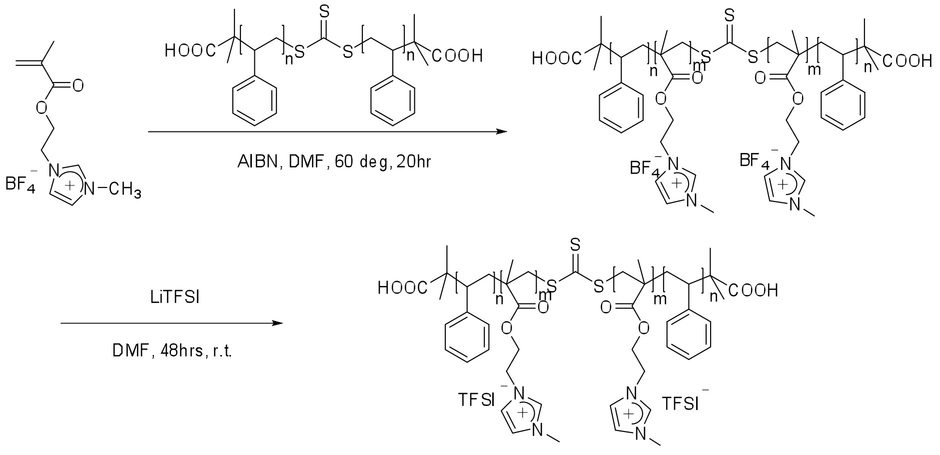

	Mn	PDI
PS-CTA-PS	8,400	1.14
PS-PIL-PS	104,000	1.24

Thermal Properties

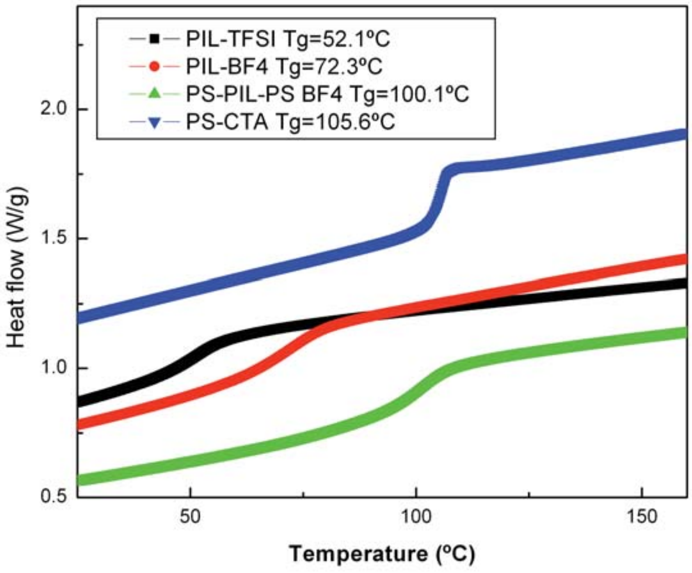

Nanoporous polymeric membranes

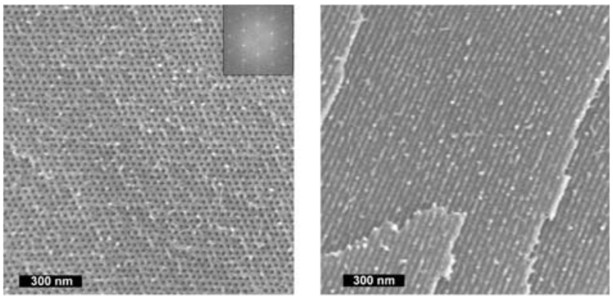

- 10^{11} pores cm^{-2}
- Simple etching chemistry
- Various systems demonstrated

Tremendous untapped potential
in separation technologies

Ultrafiltration membranes

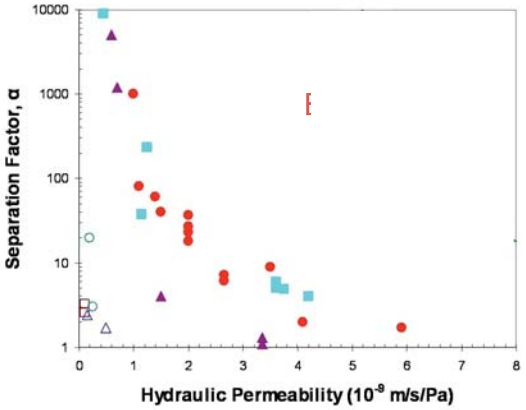

Philip *et al. J. Membrane. Sci.* 2006
Mehta *et al. J. Membrane Sci.* 2005

Grand challenges:

Avoid alignment: Networks

Mechanically integrity: Multiblocks

Nanoporous Membranes from Bicontinuous Microemulsions

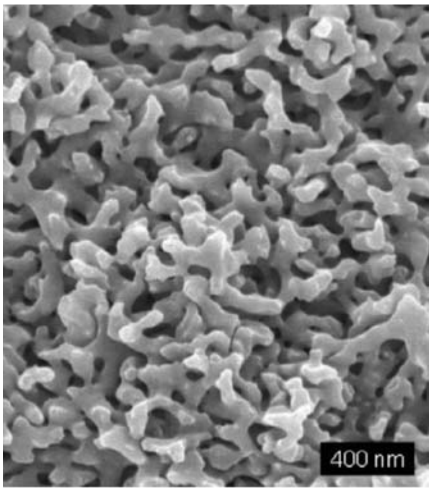

- Controlled pore structure
  50 < d < 300 nm
- 3-dimensionally connected pores
- Versatile design
- Generally brittle

Zhou, N. *et al.* *Nano Letters* **2006**, *6*, 2354-2357.

AB diblock + polyA + polyB Generalized Phase Diagram

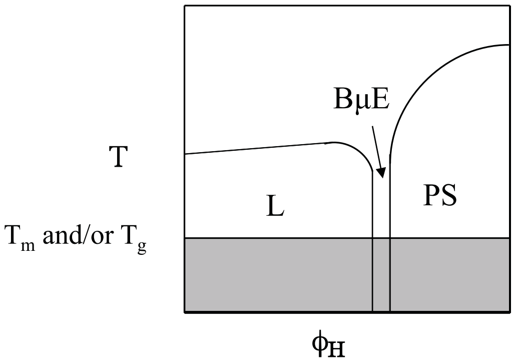

- Equal volume fractions of each homopolymer reduces the system to two variables
- Ordered at low ϕ_H, phase separated at high ϕ_H
- Bicontinuous microemulsion in a narrow channel between these regions

Towards mechanically tough bicontinuous membranes

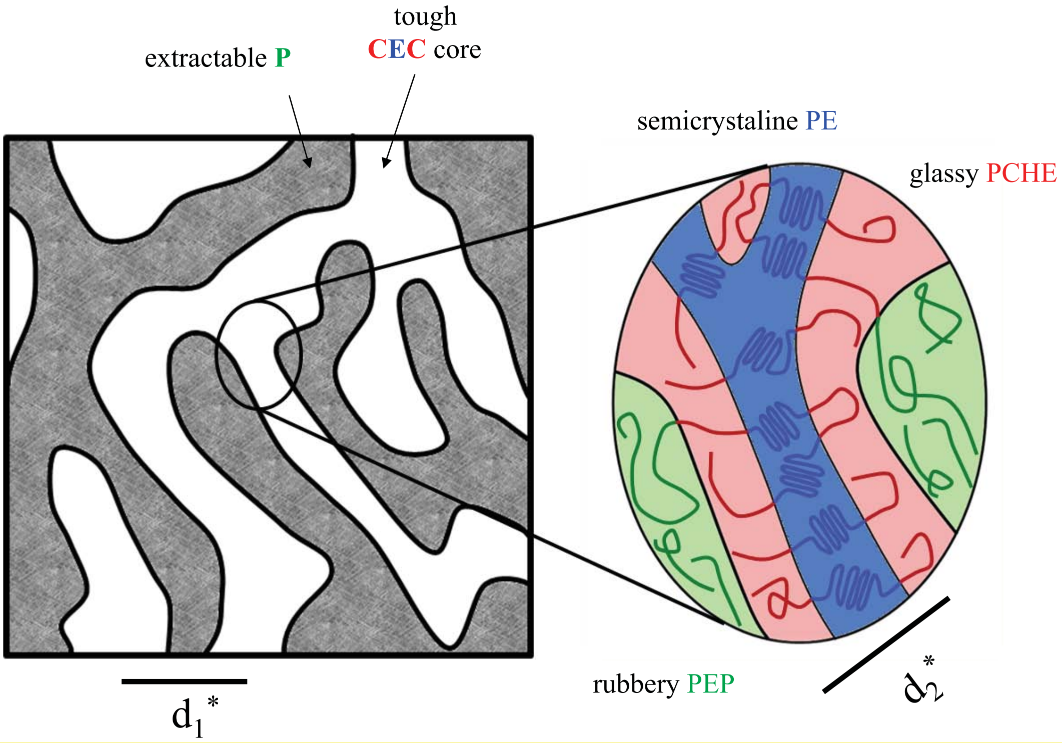

tough

CEC core

extractable **P**

semicrystaline PE

glassy PCHE

rubbery PEP

Hierarchical heptablock copolymer

Combine anionic polymerization and catalytic hydrogenation

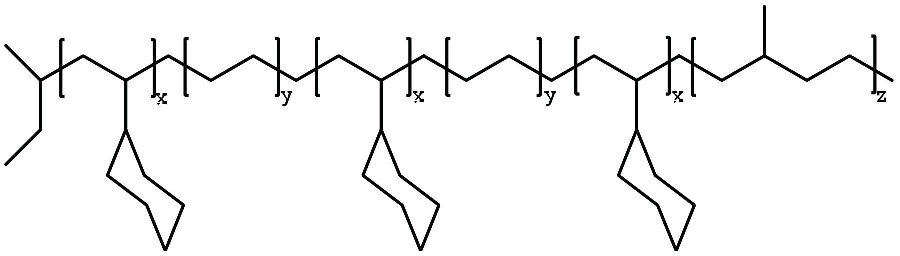

CECEC-P

Symmetric and asymmetric: 25% **C**, 25% **E**, 50% **P**

Perpendicular lamellae in parallel lamellae

CECEC-P

M_n = 120,000 g/mol

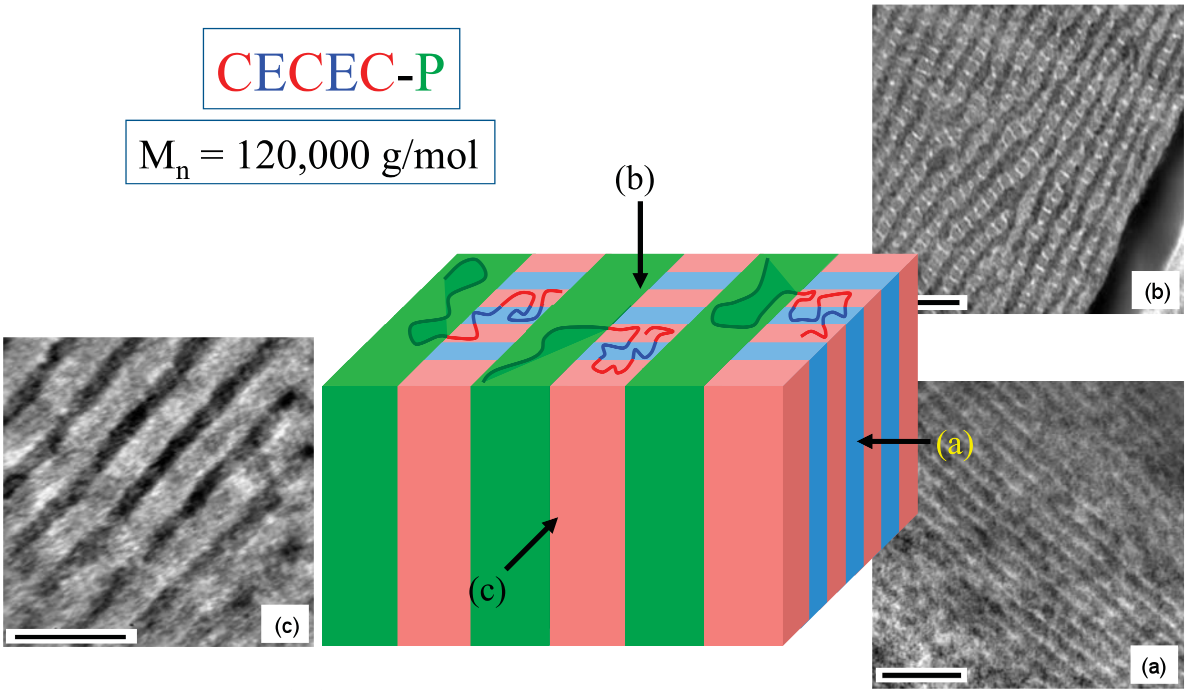

scale bars = 100 nm

Small-angle X-ray scattering (synchrotron)

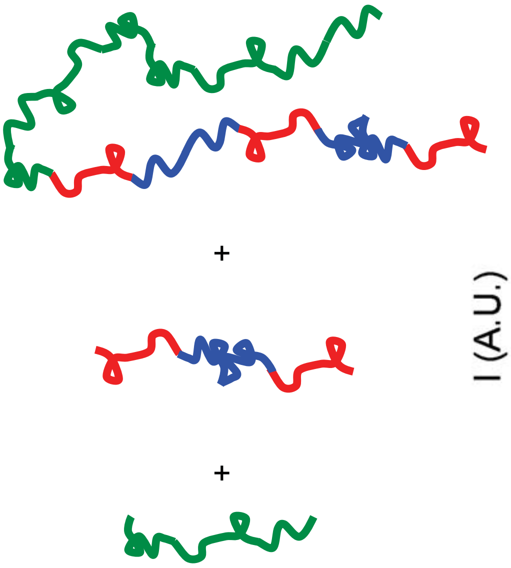

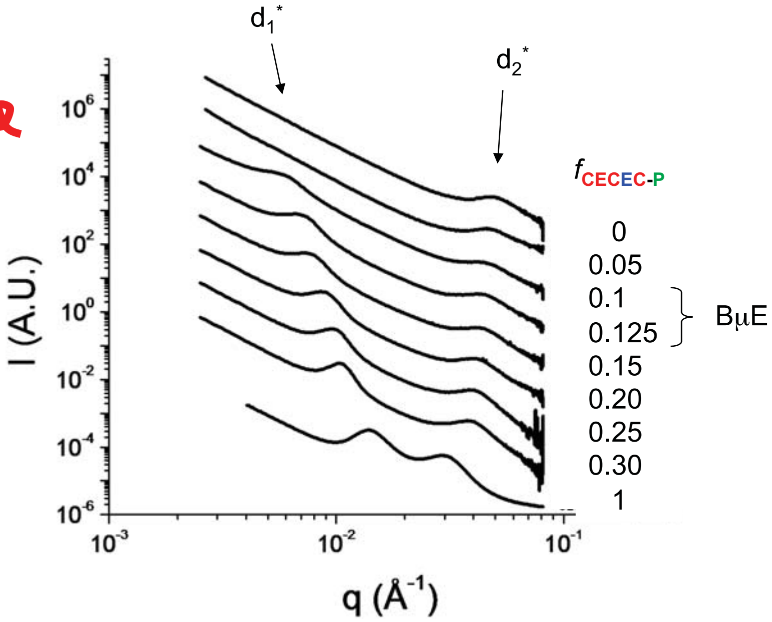

G. Fleury, F.S. Bates, "Hierarchically Structured Bicontinuous Polymeric Microemulsions," Soft Matter, submitted.

Hexablock concentration controls scale of morphology

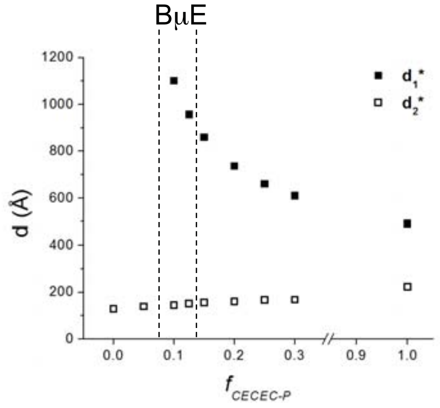

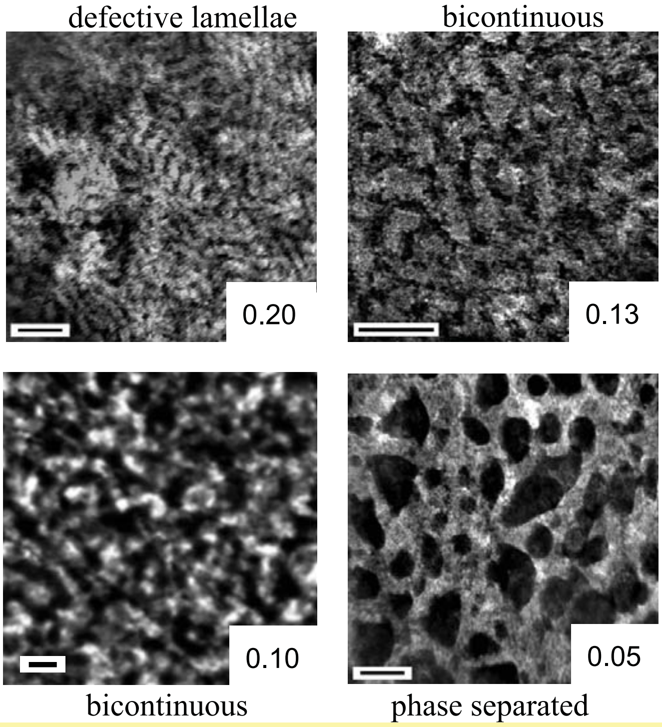

Next steps

- Evaluate mechanical properties of CECEC-P/CEC/P blends
- Optimize component molecular weights
- Develop process to extract P homopolymer

Other recent efforts

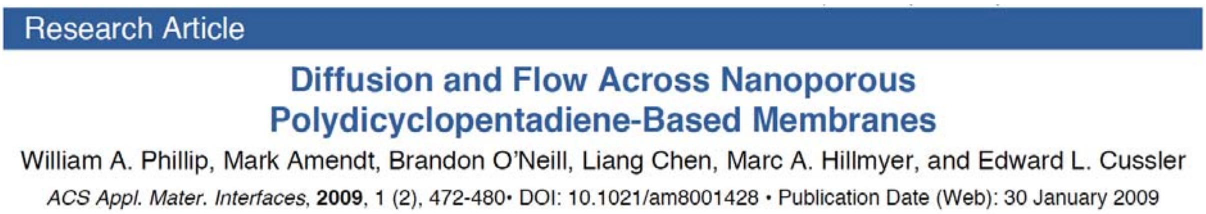
Research Article

Diffusion and Flow Across Nanoporous Polydicyclopentadiene-Based Membranes

William A. Phillip, Mark Amendt, Brandon O'Neill, Liang Chen, Marc A. Hillmyer, and Edward L. Cussler

ACS Appl. Mater. Interfaces, **2009**, 1 (2), 472-480• DOI: 10.1021/am8001428 • Publication Date (Web): 30 January 2009

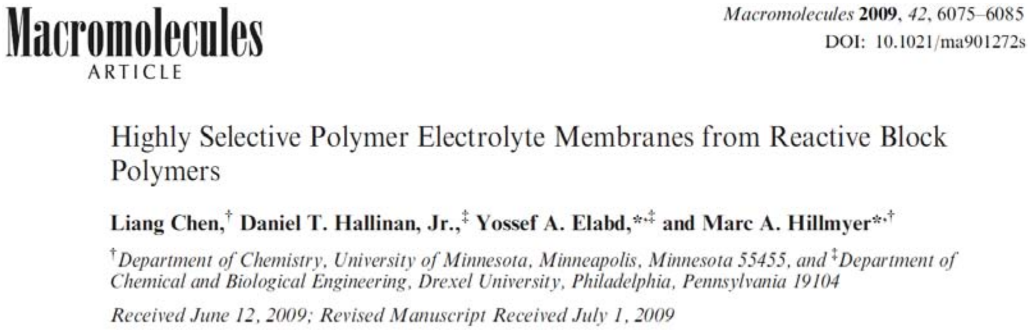
Macromolecules
ARTICLE

Macromolecules **2009**, *42*, 6075–6085
DOI: 10.1021/ma901272s

Highly Selective Polymer Electrolyte Membranes from Reactive Block Polymers

Liang Chen,[†] Daniel T. Hallinan, Jr.,[‡] Yossef A. Elabd,*[‡] and Marc A. Hillmyer*[†]

[†]*Department of Chemistry, University of Minnesota, Minneapolis, Minnesota 55455, and* [‡]*Department of Chemical and Biological Engineering, Drexel University, Philadelphia, Pennsylvania 19104*

Received June 12, 2009; Revised Manuscript Received July 1, 2009

Reservoir Characterization and Simulation

Characterization and Simulation of Abu Dhabi Fractured Carbonate Reservoirs

CSM Team:
A. Al-Sumaiti (PI), PhD candidate, B. Barzegar, PhD student
Dr. M. Kazemi, Dr. E. Ozkan, Dr. E. Graves and Dr. Miskimins

PI Team: Dr. Ghedan

1st Annual PI Partner Schools Research Workshop
The Petroleum Institute, Abu Dhabi, U.A.E.
January 6-7, 2010

PI Partners

PI Sponsors

CSM GEOSCIENCE/ ENGINEERING TEAM

Dr. Rick Sarg (GE)

Dr. Hossein Kazemi (PE)

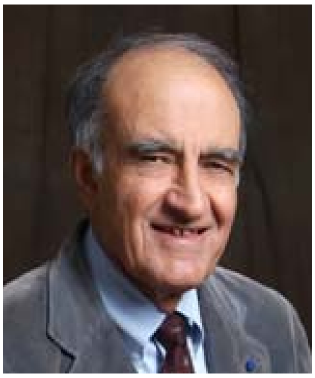

Dr. Manika Prasad (PE)

Dr. Mike Batzle (GP)

Dr. Ramona Graves (PE)

Dr. Erdal Ozkan (PE)

MISSION

- The research projects reported in the following slides were designed to produce the greatest amount of oil from Zakum field.

- In addition, these projects were designed as part of an educational process for the UAE graduate students studying at CSM, and a means for collaboration and technology transfer to the Petroleum Institute.

Background

- Thamama 1A Research Program consists of **FIVE** CSM/PI projects.

- The **research group** is an **integrated team** of petroleum engineers, geologists, petrophysicists, and geophysicists from CSM and PI.

Presentation Outline

- Background
- Objectives
- Results and Discussions
- Project Status
- Conclusions and Summary

Project Objectives

Characterization and Simulation of Abu Dhabi Fractured Carbonate Reservoirs

(Kazemi, Ozkan, Graves, Miskimins and Ghedan)

Primary graduate students

Ali Al-Sumaiti (PI), PhD candidate

Baharak Barzegar, PhD student

“The role of wettability on waterflood and subsequent gas injection (double displacement) in fractured carbonate reservoirs”

Results and Discussions

- Numerical modeling - computer code being developed
- Simulation cases being developed.
- Ultra-fast (high speed) centrifuge purchased to evaluate double displacement process in an artificially fractured core.
- Specifically the role of wettability on waterflood and subsequent gas injection in fractured carbonate reservoirs will be evaluated.

Results and Discussions

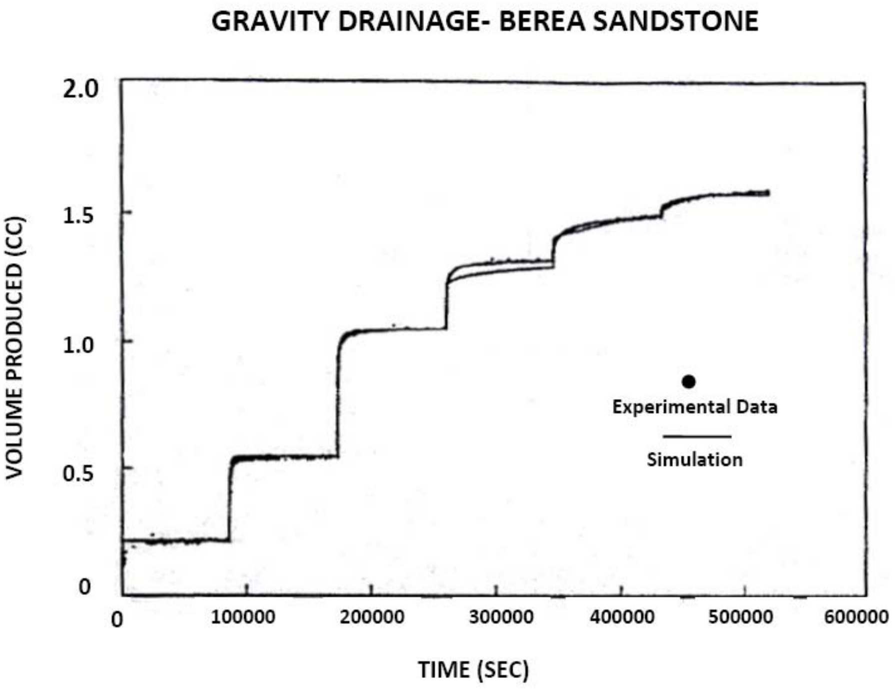

Results and Discussions

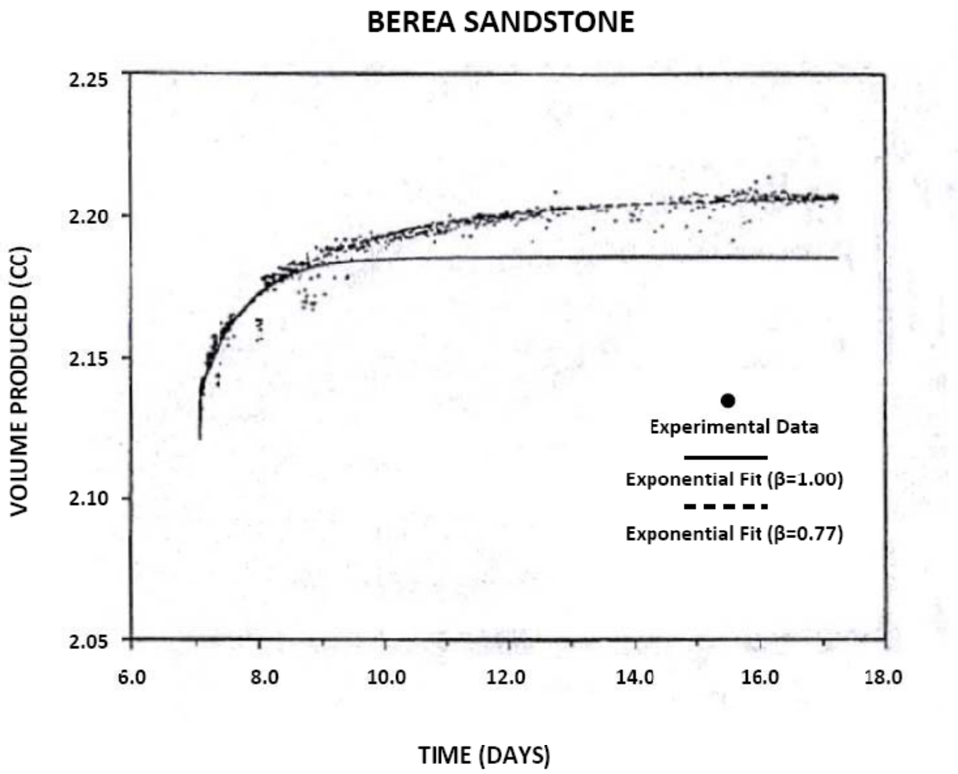

Exponential Fit to Long Time Production Data (M. J. King, et al, 1990 SCA 9011)

Conclusions and Summary

- From the results of the centrifuge experiments – examples shown in previous slides – capillary pressure, wettability, and relative permeability can be calculated for the zones of study in Thamama 1A.
- These results will be used in the simulation study. Sensitivity analysis will be done to determine next phase of experimental testing.

Project Status

- Ultra-high speed centifuge to be delivered in early January
- Centifuge training completed by Al-Sumaiti, Barak, Al-Ameri, and CSM Laboratory Coordinator at Core Lab facilities in Houston.
- Awaiting Thamama 1A core plugs to begin testing.

Questions and Discussion

Fluid Sensitivity of Seismic Properties in Carbonate Reservoirs

CSM Team:
Ravi Sharma (PhD candidate), Dr. Batzle, & Dr. Prasad

PI Team: Dr. Vega

1st Annual PI Partner Schools Research Workshop
The Petroleum Institute, Abu Dhabi, U.A.E.
January 6-7, 2010

PI Partners

PI Sponsors

Project Objectives

Fluid Sensitivity of Seismic Properties in Carbonate Reservoirs

(Batzle, Prasad, Vaga)

Primary graduate student

Ravi Sharma, PhD student

“Low frequency seismic experiments to quantify the variation in texture and heterogeneity in organic rich shale (ORS)”

RockPhysics Component

Core No.	Cut & Polished	CT Scan	LFM	Thin Section	XRD	ESEM	SAM	Porosity & Permeability	Elastic Properties	Remarks
SB-1*	X	X	X	X	^	^		X	X*	Currently Under LFM observation
SB-2		X					^			With Gypsum
SB-3									X	Broken during pressure expt.
SB-4										Broken during pressure expt.
SB-5									X	With Gypsum
SB-6										With Gypsum
SB-7										With Gypsum, Transition zone
SB-8							^		X (pressure)	seismic m/s done
SB-9*	X	X	X	X	^	^		X	X	Currently Under LFM observation
SB-10										With Gypsum
SB-11										With Gypsum, Transition zone
SB-12	X	X		X	^	^		X	X	Backup
SB-13	X	X		X	^	^		X	X	Backup
SB-14							^			With Gypsum
SB-15	X	X		X	^	^		X	X	backup
SB-16*	X	X	X	X	^	^		X	X	Currently Under LFM observation
SB-17	X	X		X	^	^		X	X	backup

CT scans

Xradia Micro –CT Scanner
Table Top Size

Homogeneous sample

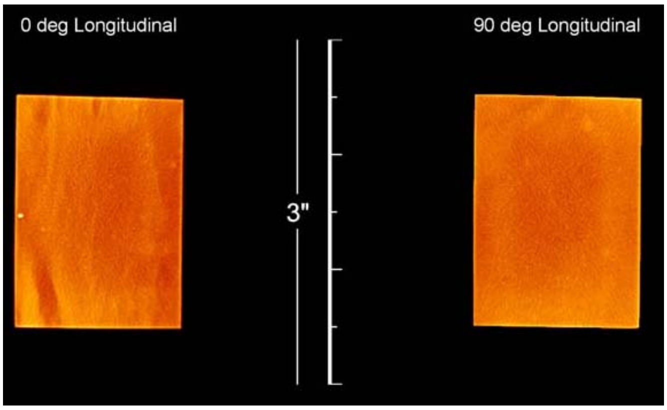

Heterogeneous sample

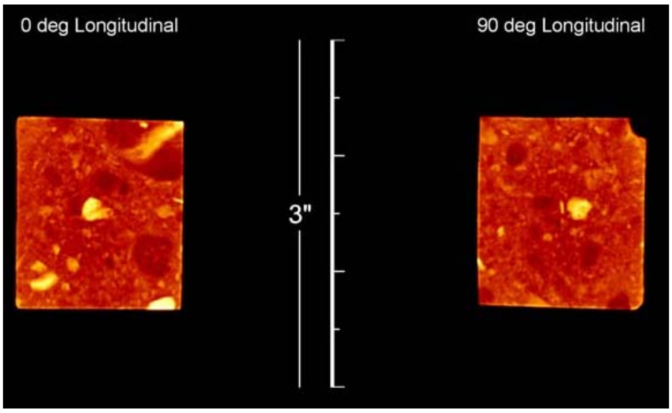

Porosity and Permeability

Homogeneous sample

Heterogeneous sample

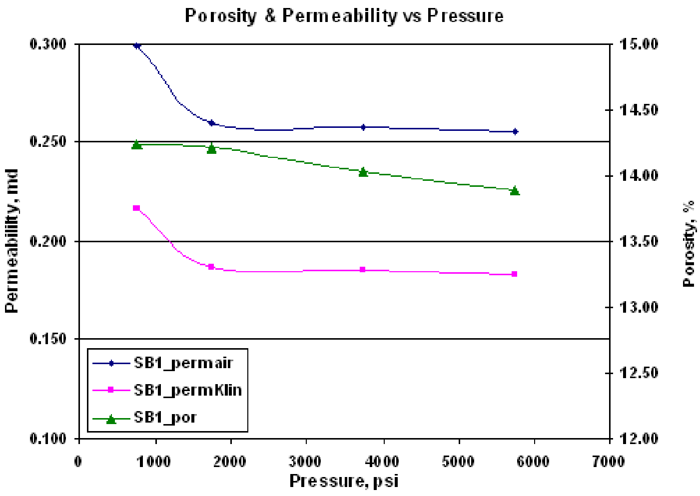

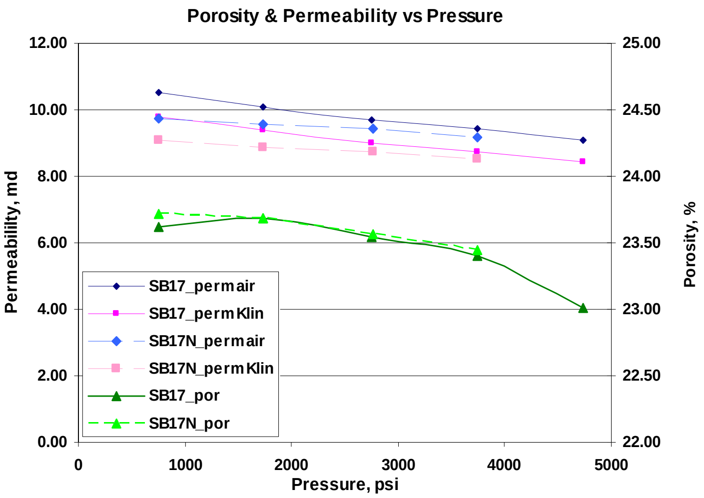

Effect of Heterogeneity

Homogeneous sample

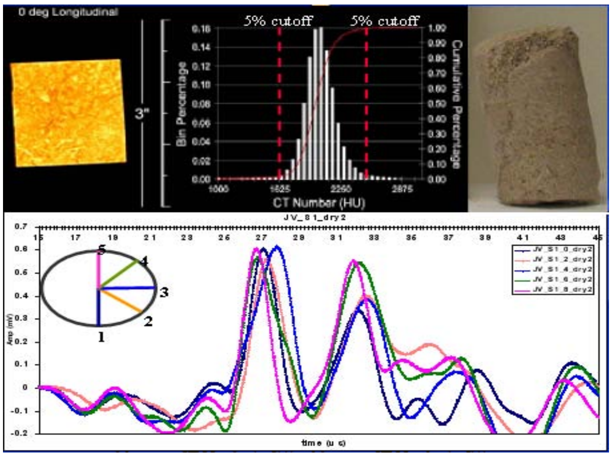

CT scan and shear wave signals showing effect of homogeneity on wave propagation

SEM image showing dual porosity

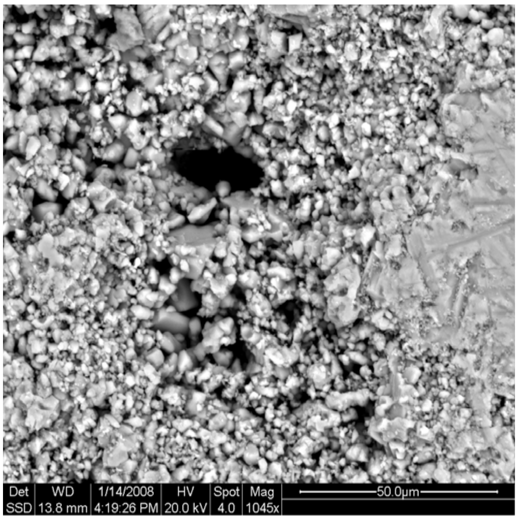

Effect of Heterogeneity

Heterogeneous sample

SEM image showing dual porosity

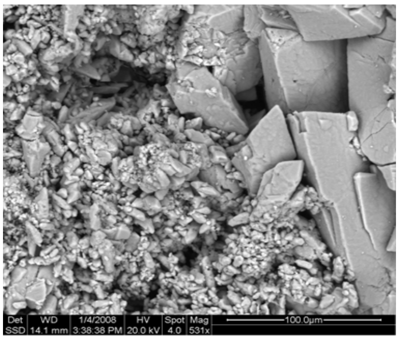

Acoustic image showing reflections from heterogeneities

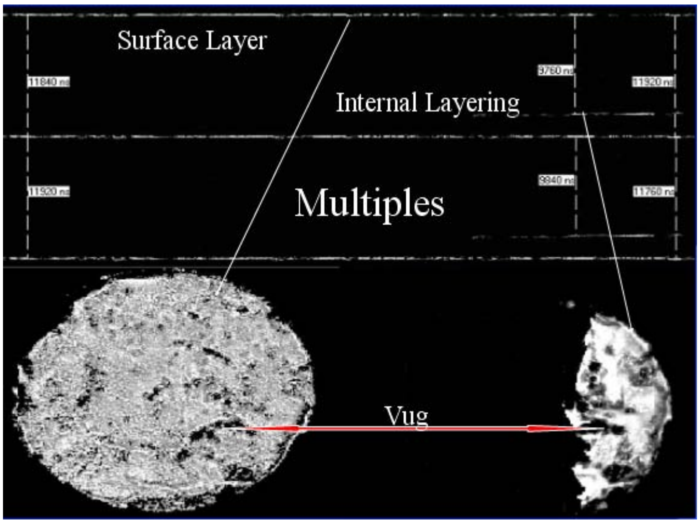

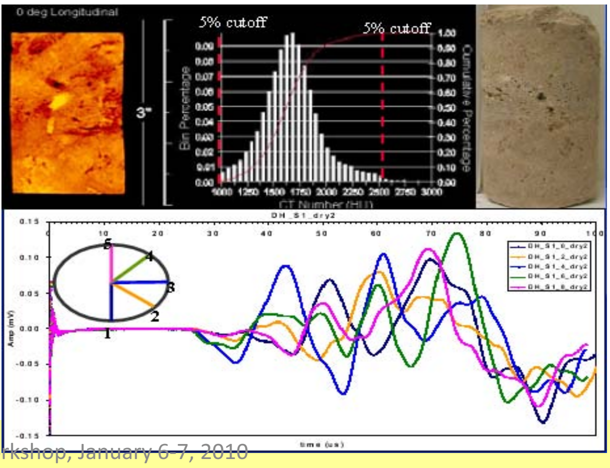

CT scan and shear wave signals showing effect of heterogeneities on wave propagation

---

Effect of Capillary Pressures

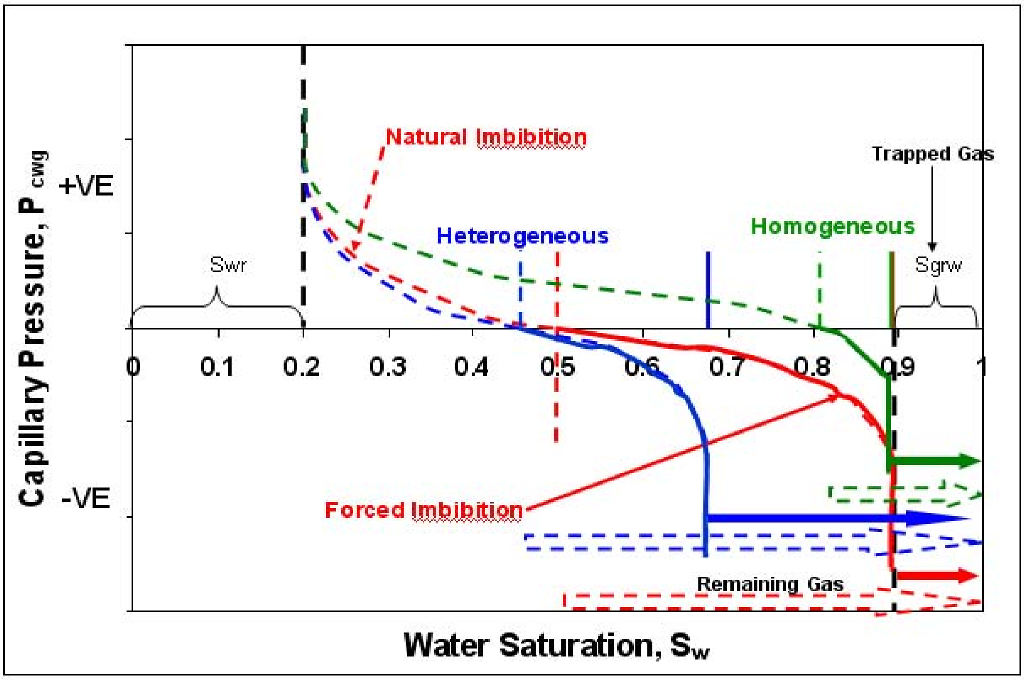

Changing wettability with change in imbibition type and changing capillary pressure. Note the hypothetical difference in amount of bypassed hydrocarbon for a changes from homogeneous to heterogeneous rock type.

Seismic Measurements

Velocity measurements

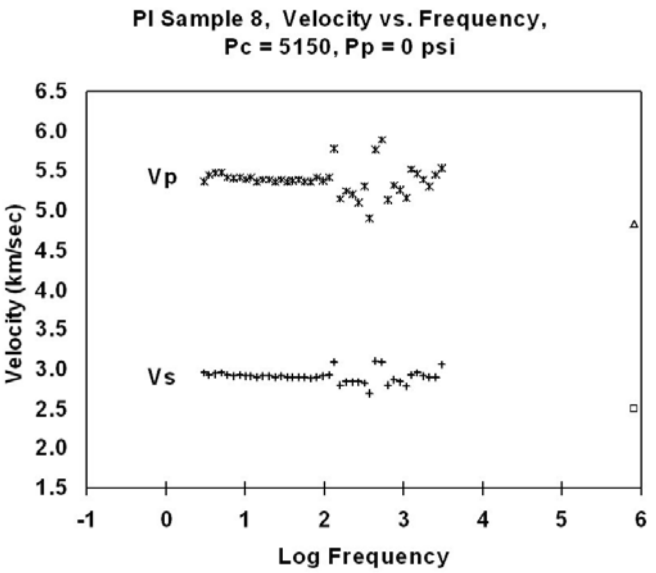

Strain measurements

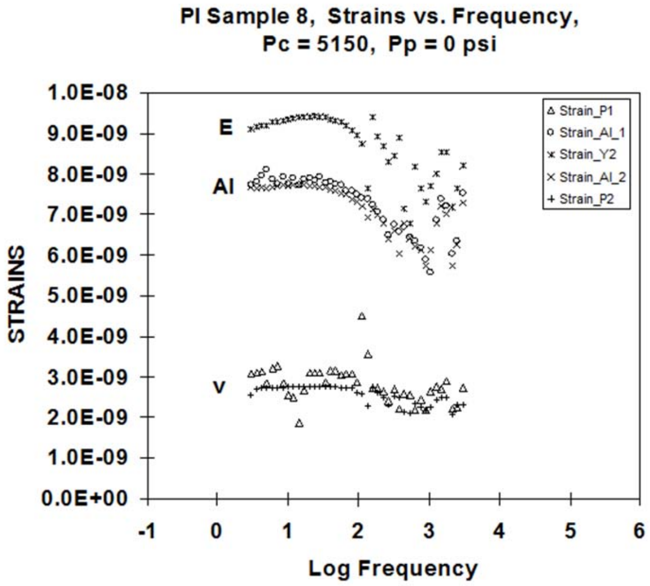

Project Status

- Micro-CT scanner purchased and calibrated. Experiments run on analogous cores.
- Experiments on-going on Acoustic Microscope.
- Awaiting Thamama 1A core plugs to begin testing and comparing to experimental data from analogous cores.
- Laboratory coordinator hired to manage new laboratory equipment: Acoustic microscope, CT Scanner, CMS -300, hand-help acoustic probe, and profile permeameter.

Questions and Discussion

Integrated Carbonate Reservoir Characterization

CSM Team:
Dr. Sarg, Dr. Lokier, & Dr. Steuber

PI Team: Dr. Vaga

1st Annual PI Partner Schools Research Workshop
The Petroleum Institute, Abu Dhabi, U.A.E.
January 6-7, 2010

PI Partners

PI Sponsors

Project Objectives

Integrated Carbonate Reservoir Characterization

(Sarg, Lokier, Steuber, Vega)

"Characterize carbonate reservoirs in 3-D space, to improve our ability to predict effective reservoir flow units, reservoir connectivity , and the dynamic fluid flow within them. Develop an integrated geoscience and engineering work flow that will utilize a new generation of numerical simulation tools, and an array of geoscience, engineering and completion technologies."

Current Research – 3D Natih E Reservoir Model

Jebel Madar - salt-cored dome

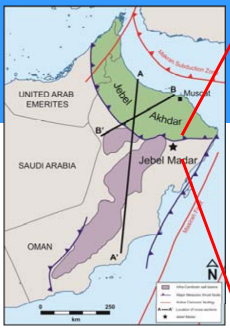

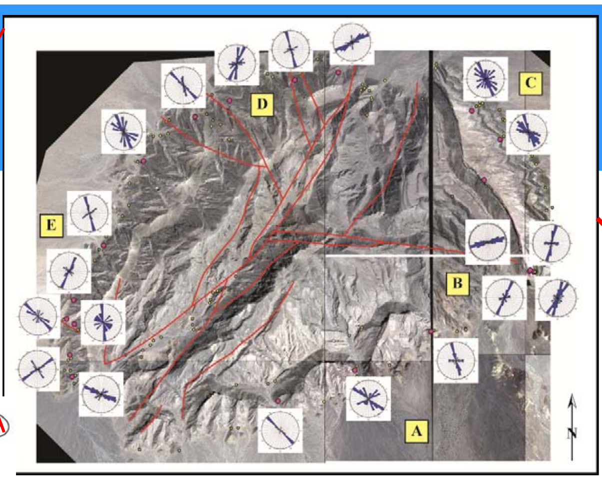

Radial & Concentric Fracture System

Gocad model will be populated with outcrop-based fracture, lithofacies and porosity data to construct Petrel reservoir geomodel

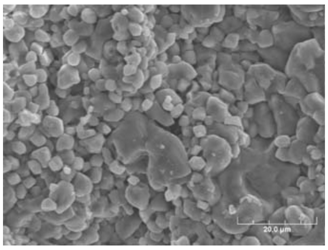

Lime Mudstone micro-porosity dominant matrix porosity

3D Gocad model draped on DEM

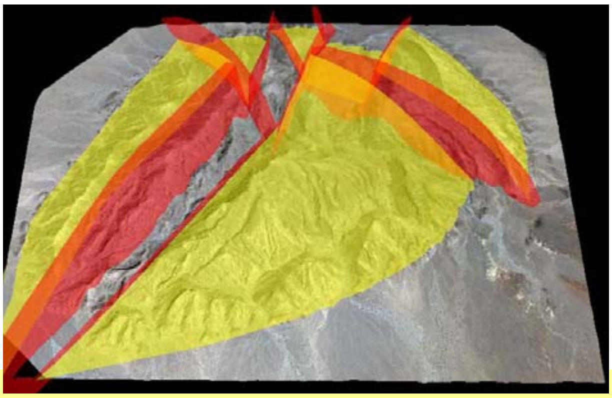

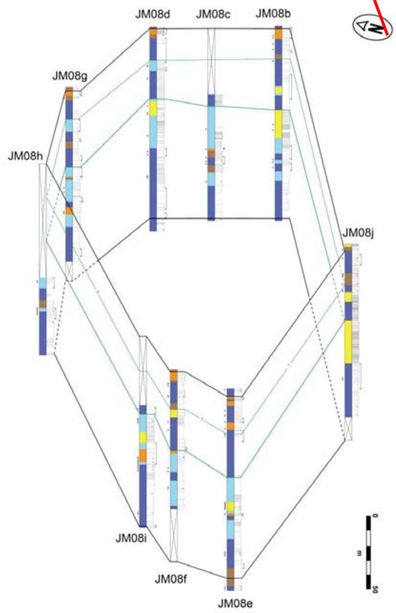

🟫 Bioturbated skeletal mudstone
🟦 Bioturbated wackestone
🟦 Bioturbated packstone
🟧 Rudist/stromatoporoid floatstone
🟨 Peloid grainstone

Three Shallowing Upward, Outer Ramp Cycles

Project Status

- Selected test reservoir – Thamama 1A reservoir at Upper Zakum.
- Joint CSM-PI planning workshop.
- Identified test area within Upper Zakum field & requested subsurface data.
- Identifying a list of cored wells in the central study area
- Continued “proof of concept” work with Natih E reservoir study in Oman outcrop.

Project Status

Tasks	YEAR 1	YEAR 2	YEAR 3
Joint CSM-PI planning workshop	■		
Compile data, select test reservoir and appropriate outcrop analog	■		
Joint PI/CSM field trips and on-site workshops		■	
Outcrop mapping & sampling of analog reservoir, incl C, O, Sr analyses		■	■
Core description & sampling		■	
Collect & interpret hi-resolution seismic data		■	
Preliminary QEMSCAN® porosity analysis of core samples			■
Develop 3-D fracture and matrix pore distribution model using image analysis		■	
Build 3-D integrated outcrop geomodel			■
Build 3-D simulation model from outcrop geomodel			■

Plan Forward

- Onsite in Abu Dhabi workshop on carbonate reservoirs.
- Core description.
- Initial interpretation of seismic data.
- Initial outcrop sampling of analog reservoir.

Questions and Discussion